

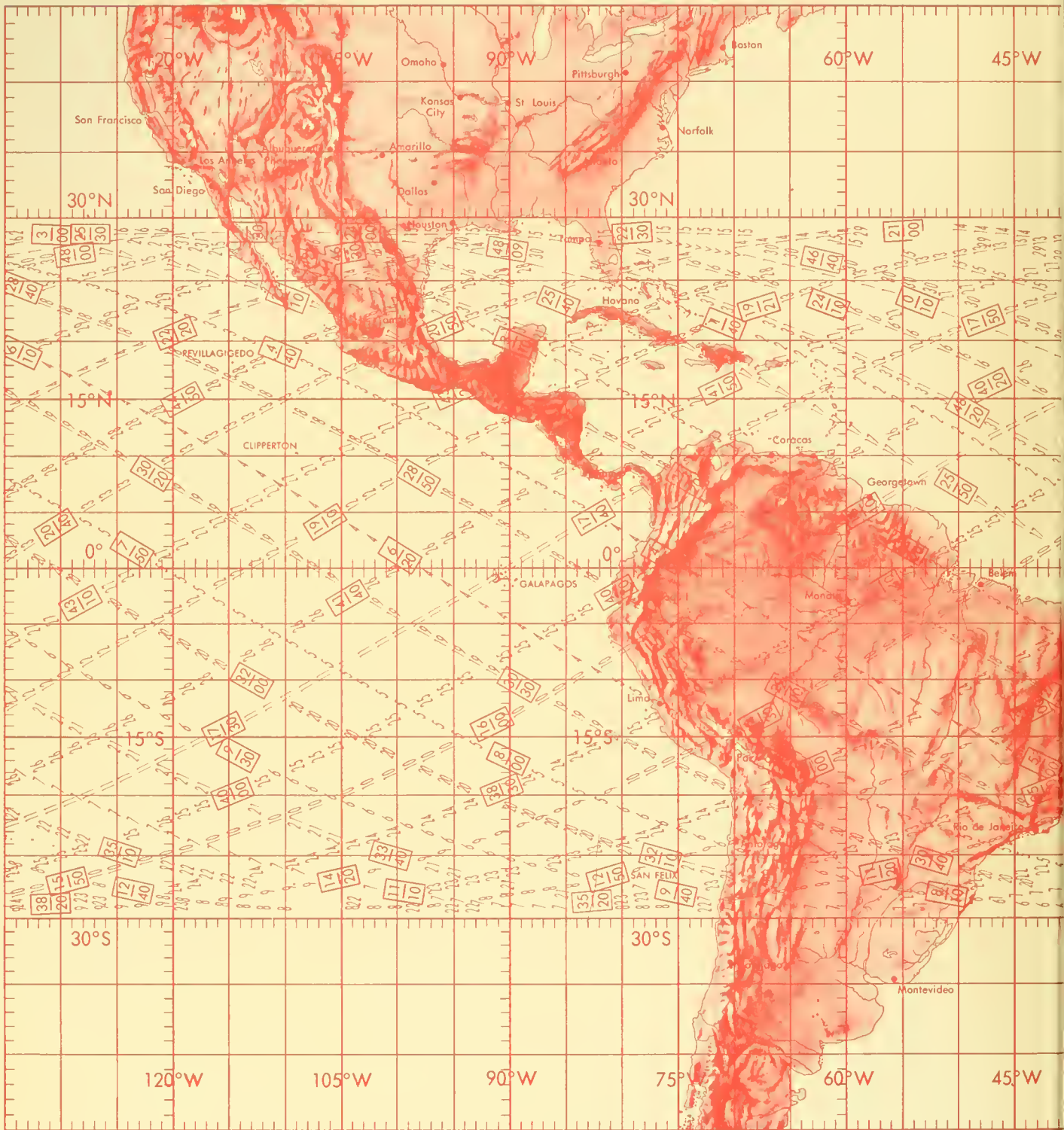
qQB
637
U55

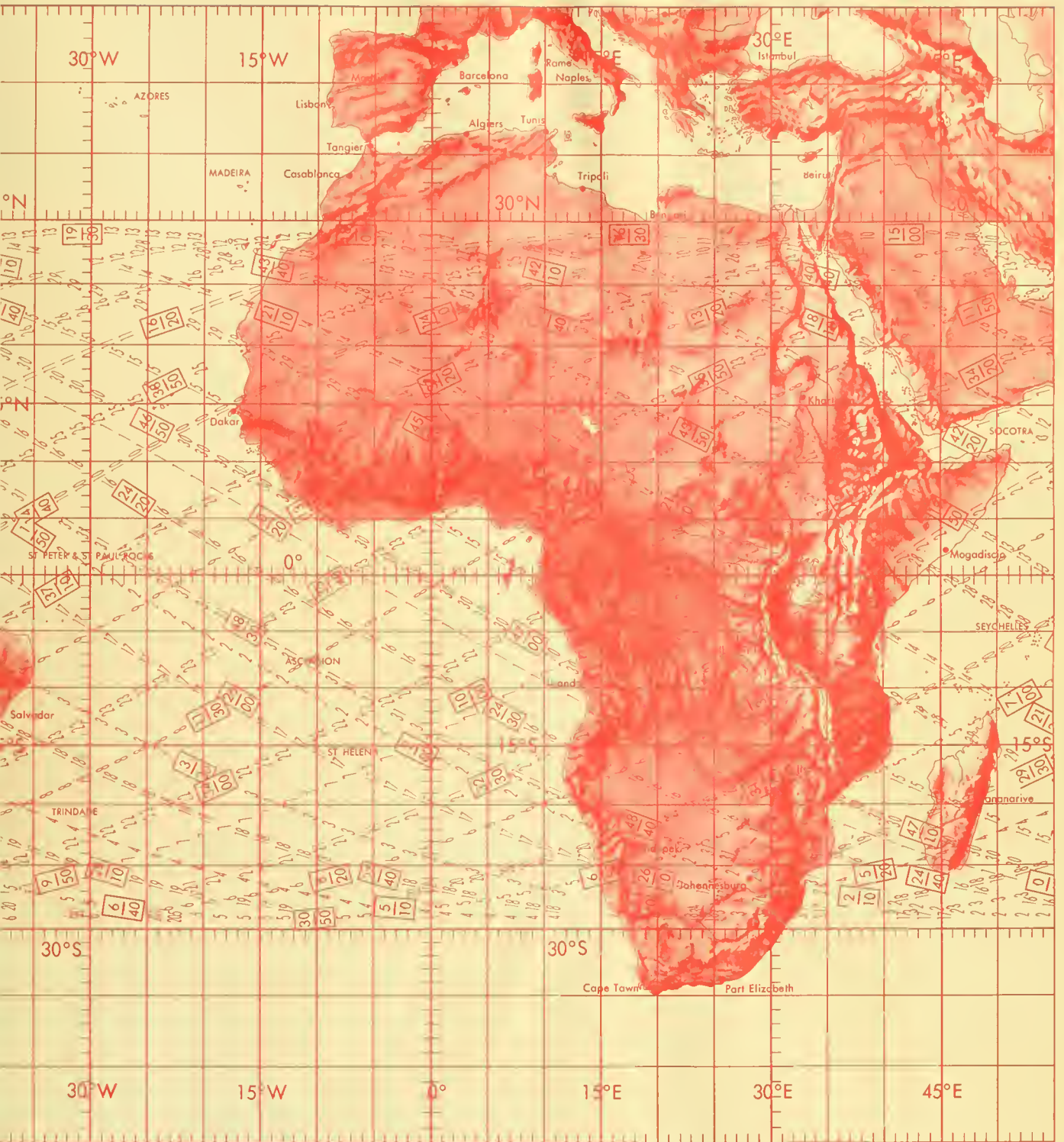
NASA SP-129



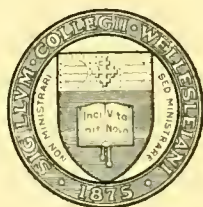
EARTH PHOTOGRAPHS from Gemini III, IV, and V

NATIONAL AERONAUTICS AND SPACE ADMINISTRATION





LIBRARY OF
WELLESLEY COLLEGE



PURCHASED FROM
LIBRARY FUNDS

EARTH PHOTOGRAPHS from Gemini III, IV, and V



Scientific and Technical Information Division

OFFICE OF TECHNOLOGY UTILIZATION

NATIONAL AERONAUTICS AND SPACE ADMINISTRATION

Washington, D.C.

1967

7

100
100
100
100
100

FOREWORD

IN 1962, preparations for space-science investigations on manned missions were undertaken by NASA on the assumption that man's flexibility, judgment, sensory perceptions, and manipulative abilities would be useful in performing a variety of experiments. The soundness of this assumption has been borne out by the early two-man Gemini flights when man's unique ability to control, modify, and reschedule contributed greatly to the success of the scientific portion of the missions.

The Gemini flight program has shown that man can operate and perform in the space environment. Beyond that, it has demonstrated that man's unique talents and capabilities are of tremendous value to the conduct of scientific investigations in space. Not only have astronauts been able to perform scientific tests during the operational missions, perfecting the techniques of space maneuvers, but in at least one instance the success of an experiment came from the astronaut's ability to repair a delicate instrument during flight.

The experiments conducted during manned flight have derived from a variety of disciplines, including aeronomy, astronomy, biology, physiology, geography, geology, meteorology, and space physics. As a result of Gemini photographs major geological features, hitherto unrecognized, have been identified, including a fault structure in Baja California and an extinct volcanic field in northern Mexico. Other results from these experiments include photographs of the gegenschein—the reflection of light off interplanetary particles beyond the orbital path of Earth—and photographs of twilight bands. Excellent photographs have also been obtained of the zodiacal light, the reflection of light from interplanetary particles between the sun and earth's orbital path.

The early Gemini flights have shown that man is particularly well suited to perform the scientific investigations conducted in space. He can act as a sensor to observe, monitor, and adapt his own observations. He can also evaluate data and manipulate instruments and equipment. He is able to respond creatively to unexpected phenomena and to improvise.

Although earth-science photographs were not formally scheduled on Gemini III, the astronauts did take 25 pictures, most of which showed cloud formations. On Gemini IV, two scientific experiments, Synoptic Terrain Photography (S-5) and Synoptic Weather Photography (S-6), were notably successful. More than 200 useful pictures were taken, the most significant of which are reproduced here. In Gemini V, terrain and weather photography was included in a schedule of 17 medical, engineering, and scientific investigations. Guided by the principal investigators of the S-5 and S-6 experiments, Paul Lowman of NASA's Goddard Space Flight Center and Kenneth Nagler of the U.S. Weather Bureau, the astronauts obtained almost 250 pictures.

The advances that have been made in the Nation's manned space-science program to date will contribute directly to future efforts. Many of the experiments in the Gemini missions, including photography, will be incorporated into the early Apollo earth-orbital flights, generally in a more sophisticated form. It is a goal of NASA to provide an integrated program of scientific investigation that uses both manned and unmanned spacecraft to complement each other in the important task of gaining knowledge of our universe.

GEORGE E. MUELLER,
Associate Administrator
for Manned Space Flight

HOMER E. NEWELL,
Associate Administrator
for Space Science and Applications

PREFACE

THE OVERALL AIMS of the Gemini program have been to exploit and extend the capabilities developed in the pioneering Mercury earth-orbital flights and to provide a vital link for the operating capability, the supporting technology, and astronaut proficiency in space that are so necessary to the Apollo program and to other future national efforts in space.

Specific Gemini objectives were (1) to determine how man performs in the space environment on flights of as much as 2 weeks; (2) to develop the capability to rendezvous with another craft and dock with it; (3) to maneuver the combined vehicles; (4) to provide a platform for scientific, engineering, and medical experiments; (5) to develop methods of controlling reentry flight paths to selected landing areas; and (6) to develop astronaut space-flight experience, including extravehicular activity. The Gemini III, IV, and V flights in 1965 made important contributions toward the accomplishment of these objectives.

The Gemini III two-man crew achieved the first change of orbital plane by a manned spacecraft and the first use of variable lift during reentry to "fly" to a selected landing area. The maneuvering of the spacecraft by the crew marked a major step toward rendezvous and docking objectives and set the stage for the 4-day Gemini IV mission.

Further assurance that the overall objectives of the Gemini program could be met was provided by Gemini IV, which scored success in virtually all areas of accomplishment: Station-keeping exercise associated with rendezvous, long-duration flight, extravehicular activity, and scientific experiments.

The most significant result of the Gemini V mission was to show that rendezvous and docking with another object in space should not pose a particularly difficult problem. Primary objectives met by Gemini V were crew capability for 8 days of flight with no adverse effects, spacecraft capability for long periods of flight, and evaluation of the onboard radar necessary for rendezvous and docking flights scheduled later.

In addition to accomplishing these major objectives, the three Gemini flights produced some significant experimental results, of which the photographs in this volume are a part. Most of them were obtained by Gemini IV and V in a series of synoptic weather and synoptic terrain photography experiments, formally scheduled to obtain high-quality color photos of terrain features and cloud systems for geological, geographical, and meteorological purposes. These experiments were under the direction of the Manned Flight Experiments Division of the Office of Space Science and Applications.

As can be seen in the pages that follow, the color in many of the pictures is outstanding and ground resolution remarkably high. Many small roads, canals, and similar features are clearly visible. Photos of shorelines, river courses, and details never before seen by man are included. Considerable bottom topography and water current structure is visible, making these pictures highly valuable in planning future photography for studies in oceanography and marine geology. These photographs and other Gemini experiments are the beginning of a vast increase in man's useful knowledge of Earth and its environment.

ROBERT R. GILRUTH, *Director*
Manned Spacecraft Center

ACKNOWLEDGMENTS

The material for this book grew out of the synoptic terrain and weather photography experiments which were significant parts of the Gemini science program. The idea of publishing a volume of color photographs originated with Robert R. Gilruth, Director of the Manned Spacecraft Center. Its publication is an effort to fulfill the part of NASA's charter that calls for full and prompt dissemination of scientific information. It is hoped that various scientific disciplines and other public interests will have a multitude of uses for these Gemini photographs.

The principal investigators for these two Gemini experiments, Paul Lowman, Jr., of the Goddard Space Flight Center, and Kenneth Nagler and Stanley Soules, of the U.S. Weather Bureau, contributed much of the material for the captions. They were aided in this task by Arthur Alexiou and L. V. Streeves of the U.S. Naval Oceanographic Office, and Herbert Tiedemann and Jose Toro of Goddard. Preliminary identification of the photographs was carried out by Richard W. Underwood, Manned Spacecraft Center, following each Gemini flight.

A technical panel with members from NASA and other agencies assisted in the original selection of the photographs. Panel members, in addition to Dr. Lowman, Mr. Soules, and Mr. Alexiou, were, Winston Siebert, W. D. Harris, and John T. Smith of the U.S. Coast and Geodetic Survey; Anthony Liccardi of NASA's Office of Manned Space Flight; and Jocelyn R. Gill, Gemini Science Manager. Dr. Gill was also responsible for the organization of the effort to produce the book and served as scientific editor.

WILLIS B. FOSTER, *Director*
Manned Flight Experiments Office



CONTENTS

	<i>Page</i>
Gemini III	5
Gemini IV	11
Stereoscopic coverage of southwest United States	57
Gemini V	109
Index	257
Appendix	259



INTRODUCTION

THE PURPOSE of this volume is to provide examples of the photographs obtained from the first three manned Gemini flights, and to make them available to scientific users in various disciplines. Most of the photographs selected are the result of the synoptic terrain photography and weather photography experiments formally scheduled for Gemini IV and V. In the case of Gemini III, photography was not a part of the scientific program, but the astronauts obtained 25 pictures during their flight, 3 of which are reproduced here.

The objective of the Synoptic Terrain Photography Experiment (S-5) in Gemini IV and V was to show major geologic structures, their form, color, and albedo. The astronauts of Gemini IV were requested to give priority to photography of east Africa, the Arabian Peninsula, Mexico, and the southwestern United States. For Gemini V, the selected land and near-shore areas were chosen not only for geologic study, but also for geographic and oceanographic investigations. The camera was a Hasselblad Model 500C modified by NASA, using a Zeiss Planar lens of 80-mm. focal length, F/2.8. The film was Ektachrome MS (S.O. 217). During the Gemini V flight, one roll of Anscochrome D-50 was taken. The film format is 55 mm. by 55 mm. on 70-mm. film rolls of over 60 exposures. A haze filter helped reduce the intensity of the ultraviolet scattering from the atmosphere.

Most of the photographs obtained on these Gemini missions were considered to be of excellent quality with respect to exposure, resolution, and orientation. Although fuel and power restrictions prevented the flight crew from always orienting the spacecraft vertically, as preferred for photography, a continuous series of 39 near-vertical views were obtained by Gemini IV covering the flight path on the 32d revolution from

the Pacific coast of Mexico to central Texas. The photographs are reproduced here.

The objective of the Synoptic Weather Photography Experiment (S-6) in Gemini IV and V was to provide a set of high-resolution pictures that would cover a broad range of meteorological phenomena, with emphasis on photographs of a number of cloud systems that could be used to verify and amplify information obtained from the unmanned weather satellites. Cloud cover over the same area was photographed on successive revolutions during the Gemini V mission to study the dynamic changes at 90-minute intervals. The camera was the same NASA-modified Hasselblad 500C used in the S-5 experiment.

Results of the two photographic experiments are of value to scientists in many disciplines. Of particular interest to geologists, oceanographers, geographers, and hydrographers are the Gemini IV terrain photographs which reveal a large amount of geologic detail. Photographs taken over Baja California, for instance, show the contact between quaternary alluvium and bedrock, identify aligned linear valleys as a fault zone, and make subsidiary faults apparent. Photographs taken over a section of Mexico identified the Sierra Carizarilla as volcanoes, probably of relatively young age, judging from the fresh-appearing topography. Geologic maps of Mexico, however, show only a few isolated outcrops of volcanic rock dated as more than 1 million years old. Another photograph shows an area in which two major tectonic provinces merge without marked change of direction. Such a relationship could until now be determined only by extensive mapping in two countries.

Other examples, of interest to oceanographers, hydrographers, and hydrologists: An ex-

cellent photograph of the mouth of the Colorado River entering the Gulf of California, giving a synoptic view of sediment distribution; details in shallow-water bottom topography revealed in photos of the Bahamas; Gemini V pictures of Rongelap Atoll in the Marshall Islands, making it possible to correct existing charts of reef areas; and pictures of the Odessa-Midland area of central Texas showing the terrain darkened by heavy rainfall on the previous day.

Orbital weather photos taken during the Gemini missions, by providing a higher resolution and contrast, have aided in interpreting data obtained from weather satellites. For example, photographs obtained over Florida on three successive revolutions show changes in, and movement of, clouds at approximately 90-minute intervals. Included are photos of tropical and extra-tropical cyclones and the intertropical zones of convergence, for comparison with lower resolution pictures made with the help of meteorological satellites.

In addition to the many photographs of cloud patterns, the Gemini missions yielded photographs of other features of interest to meteorology and related fields, such as smoke from forest fires or industrial sources that may indicate the low-level wind direction and may possibly provide information on the stability of the lower atmosphere. Similarly, photographs of various types of sand dunes in the world's great deserts are of help in determining the relationship between winds and deposition patterns.

The Gemini photographs are also of potential practical importance in agriculture, forestry, water and marine resources, cartography, and the study of air pollution. The use of orbital photography to depict geological formations may lead to applications in mining. The detection from space of faults, lineaments, folds, domes, basins, or haloes may indicate areas of potential mineral or petroleum deposits. Application in forestry and agricultural mapping is particularly promising because of the wide areal coverage possible with spacecraft.

Systematic photography of Earth from space

has only begun, but its feasibility and its usefulness in science, as well as for practical applications, have been demonstrated by the experiments performed by the Gemini astronauts.

Of the 550 photographs taken by the Gemini III, IV, and V flight crews, 244 have been selected for this book. They are arranged in orbital sequence within three sections, representing the three missions. Details concerning length of flight, apogee and perigee, crew, number of photos taken, and photographic equipment used preface each section. Captions accompanying the photographs identify political subdivisions, geographic features, and in some cases discuss geological and meteorological phenomena. Place names used follow the standard established by the National Geographic Atlas of the World. Following each caption is the color print number assigned by NASA as the films were developed.

The photographs are placed with the horizon at the top when applicable. In oblique angle views, the foreshortening—furthest point from the spacecraft—is at the top of the picture. When the viewing angle is nearly vertical, the pictures are often oriented with north at the top. For further reader guidance, the viewing direction is specified in many of the captions.

A geographic index and an appendix complete the volume. The index provides a guide, by page number, to photographs of major geographic areas. No subject index is included, but, in view of the large number of photographs taken of cloud formations, as a result of the S-6 experiment, these have been listed separately at the end of the geographic index.

The appendix lists, in orbital sequence, every photograph taken on the three flights. It also gives the magazine and frame number of the film; the color, as well as black and white, print number; the orbit; approximate Greenwich mean time; and geographic location. The photographs included in the book are marked by asterisks. All photographs, however, may be ordered from the National Aeronautics and Space Administration.

The map used on the inside covers represents a typical flight pattern for a Gemini mission. It was prepared by the Aeronautical Chart and Information Service, U.S. Air Force, St. Louis, Mo.

Persons interested in acquiring transparencies, color prints, or black and white prints of any of the photographs listed in the appendix may make inquiry to:

NASA Headquarters
Public Information Office
Washington, D.C. 20546

or

Manned Spacecraft Center
Public Affairs Office
Houston, Tex. 77058



GEMINI III

Gemini III was launched on March 23, 1965, and continued for three orbits or 4 hours and 52 minutes. A total of 25 pictures were taken. The camera used was a Hasselblad, Model 500C, modified by NASA. The F/2.8 lens was a Zeiss Planar, 80-mm. focal length. The 70-mm. film was Ektachrome MS (S.O.-217). Gemini III, piloted by Virgil I. Grissom and John W. Young, had an apogee of 140 miles and perigee of 100 miles. Three of the photographs taken on the mission are included in this section.



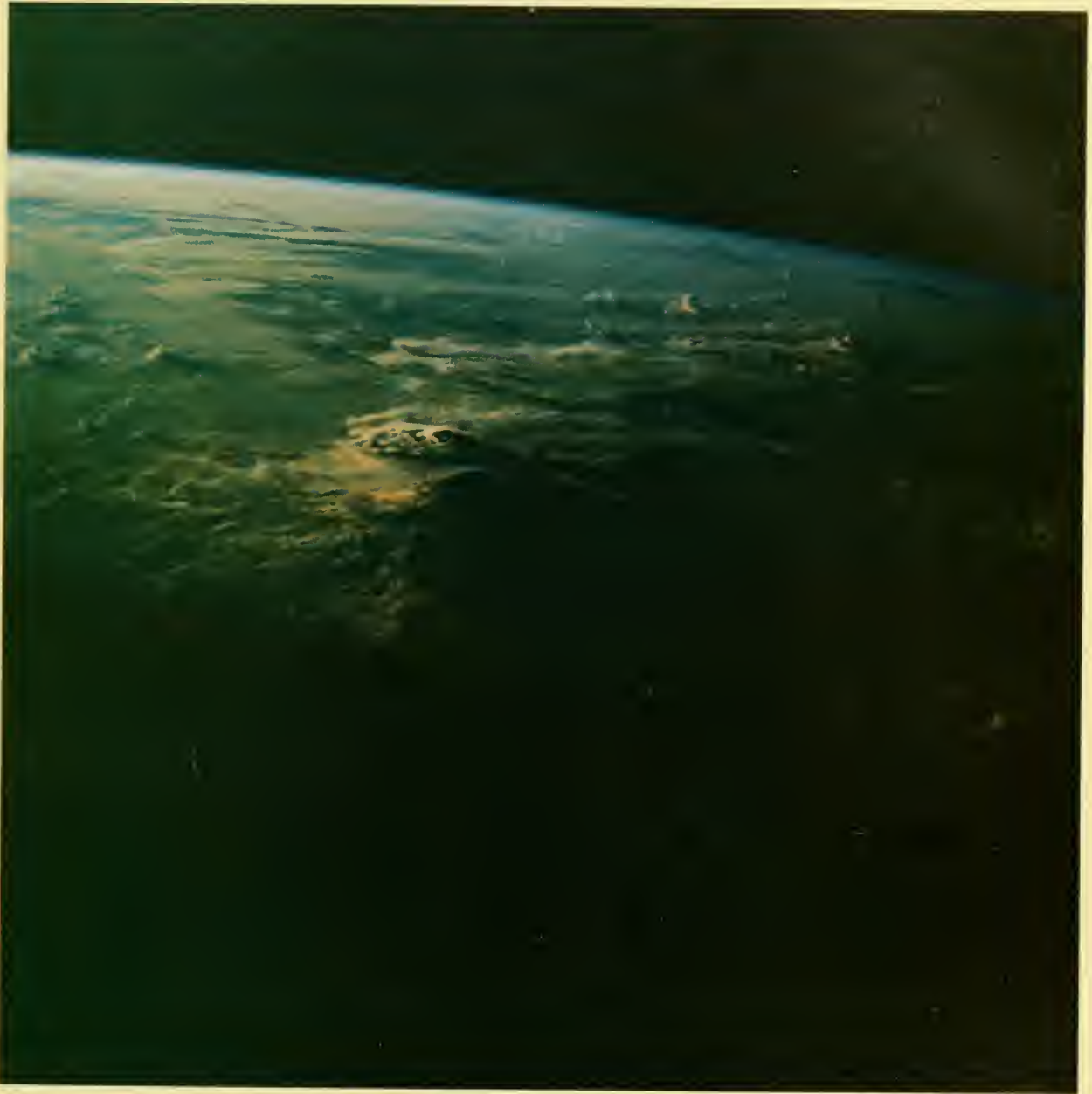
View to the northwest over northern Mexico and southern California in the vicinity of Mexicali (upper right) and El Centro, with the Pacific Ocean at upper left. The dark area in the middle foreground is cultivated land of the Imperial Valley around the delta of the Colorado River. Clouds at upper right hide the Salton Sea. The yellowish barren area in the lower right corner is the Great Sonora Desert.

S-65-18740



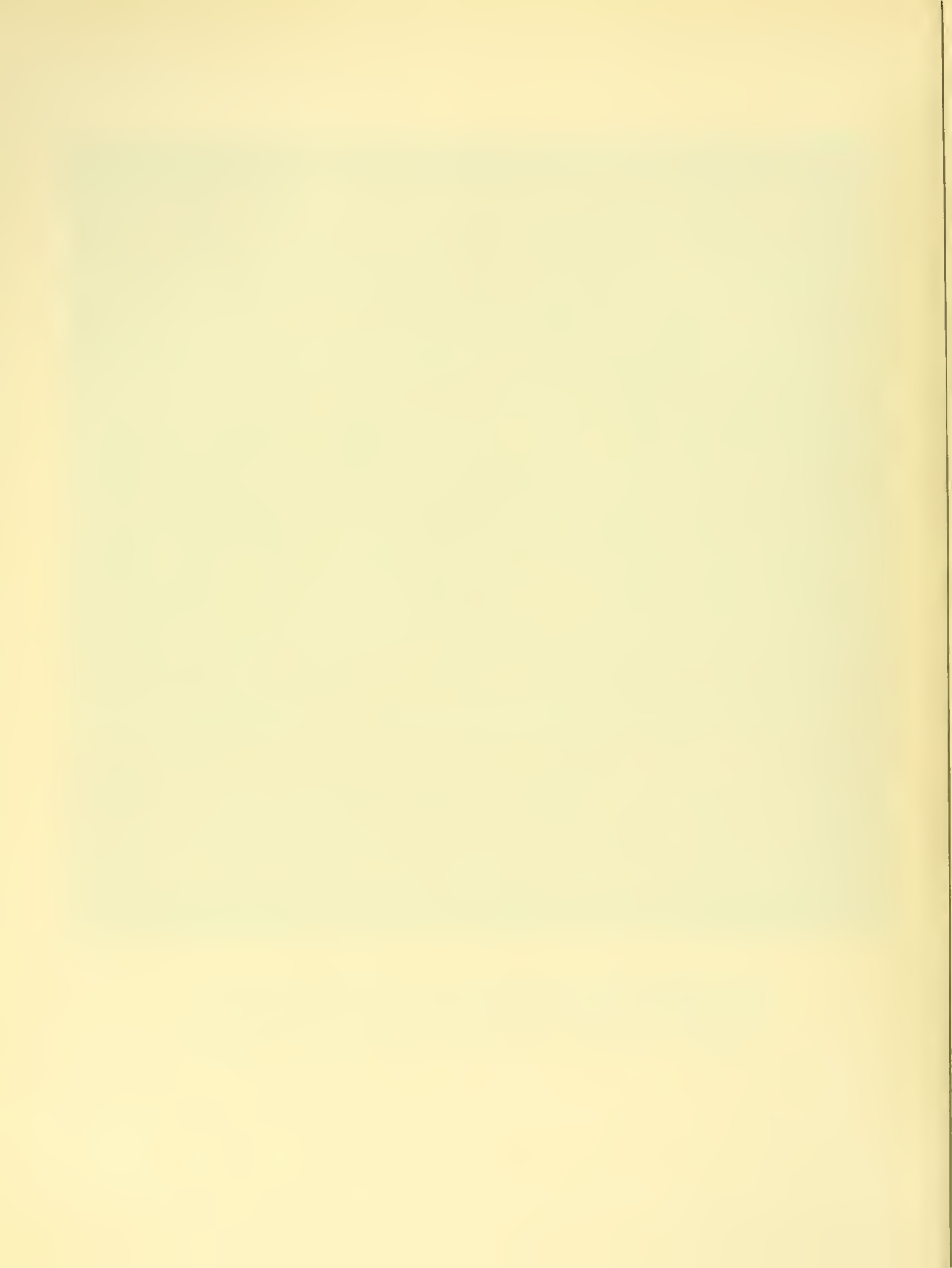
This view to the northwest shows Yuma, Arizona, and the Colorado River at upper center and the Great Sonora Desert at lower left. The dark area at the bottom of the photograph is Cerro del Pinacate, a large volcanic field in Sonora, Mexico.

S-65-18741



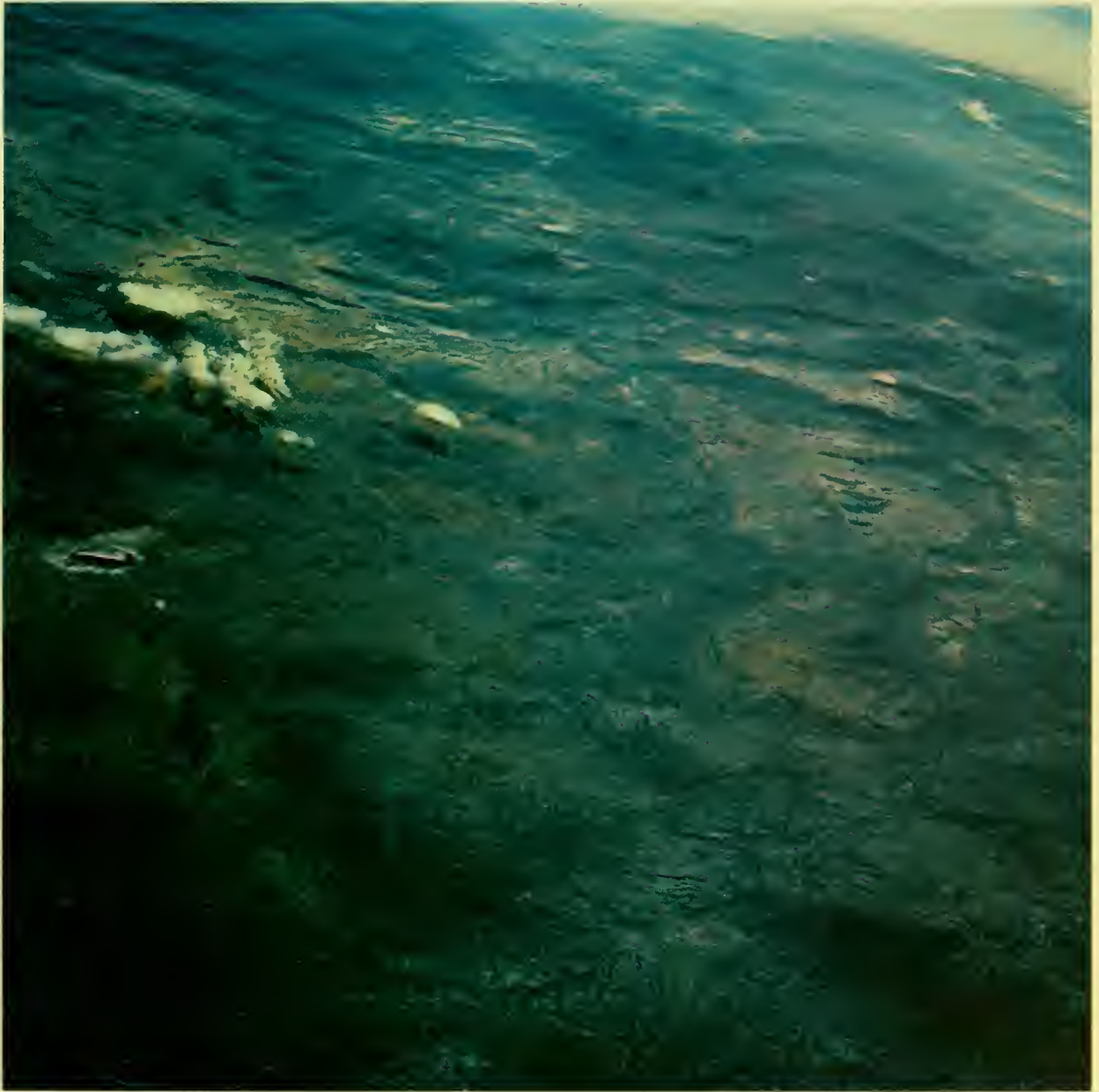
Long shadows emphasize the vertical development of cumuloform clouds over Madagascar Island near Tananarive. The sunset terminator line crosses the picture from upper right to lower left. Considerable cirrus cloudiness prevails as a result of numerous storms in the region. The sunlit top of a large thunderstorm is seen near the center.

S-65-18752



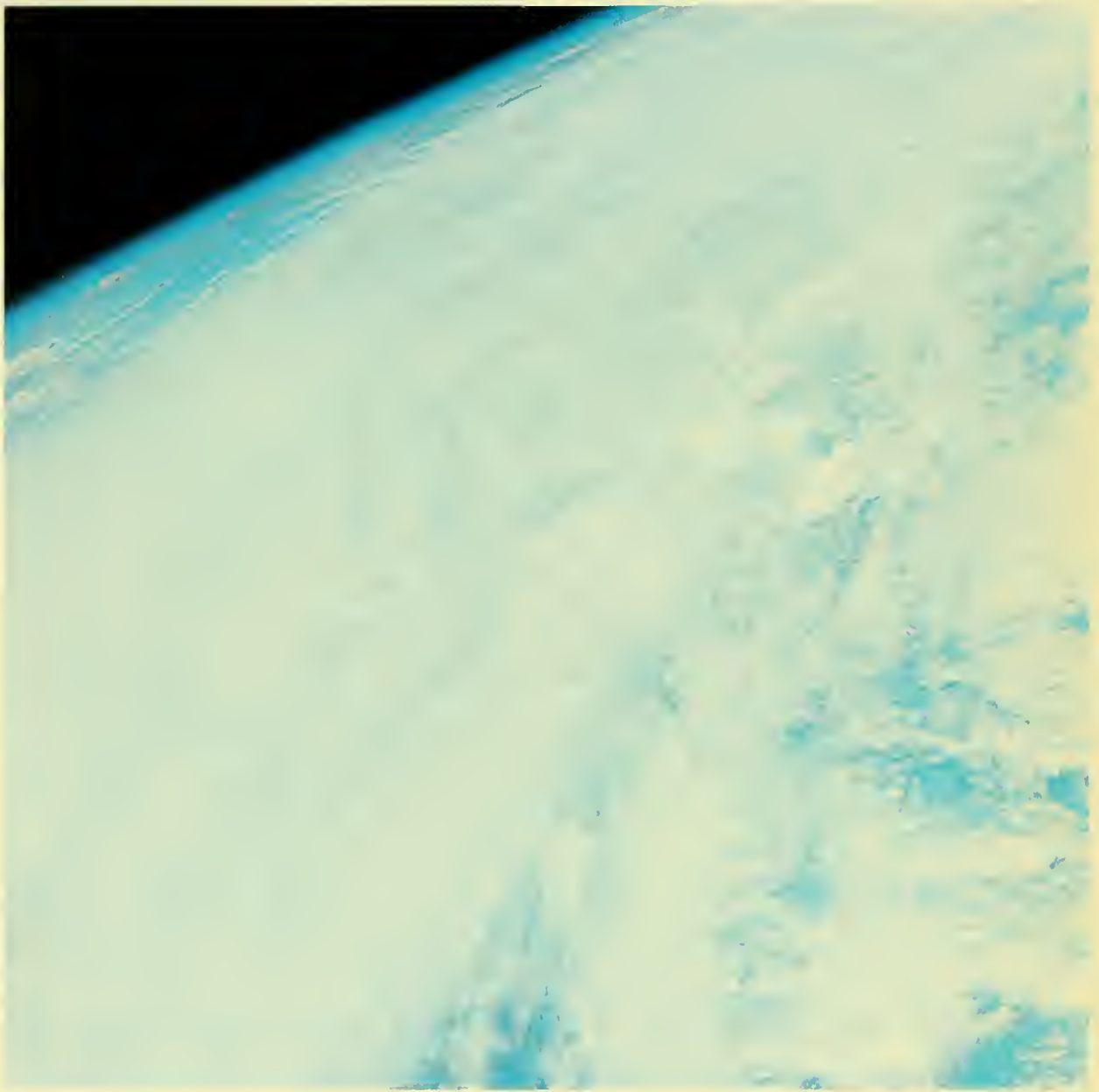
GEMINI IV

Gemini IV, launched on June 3, 1965, lasted 97 hours and 56 minutes. During that time the spacecraft made 62 orbits and 219 photographs were taken by the crew, James A. McDivitt and Edward H. White. This was the first flight in which the S-5 and S-6 photographic experiments were included. The camera used was a hand-held modified Hasselblad, Model 500C with a Zeiss Planar lens of 80-mm. focal length; the film was Ektachrome MS (S.O.-217). During the 4-day flight apogee reached was 175 miles, perigee was 100 miles. Included in this section are 96 of the photographs taken. A continuous series of 39 overlapping photographs of the southwestern United States is included in its entirety.



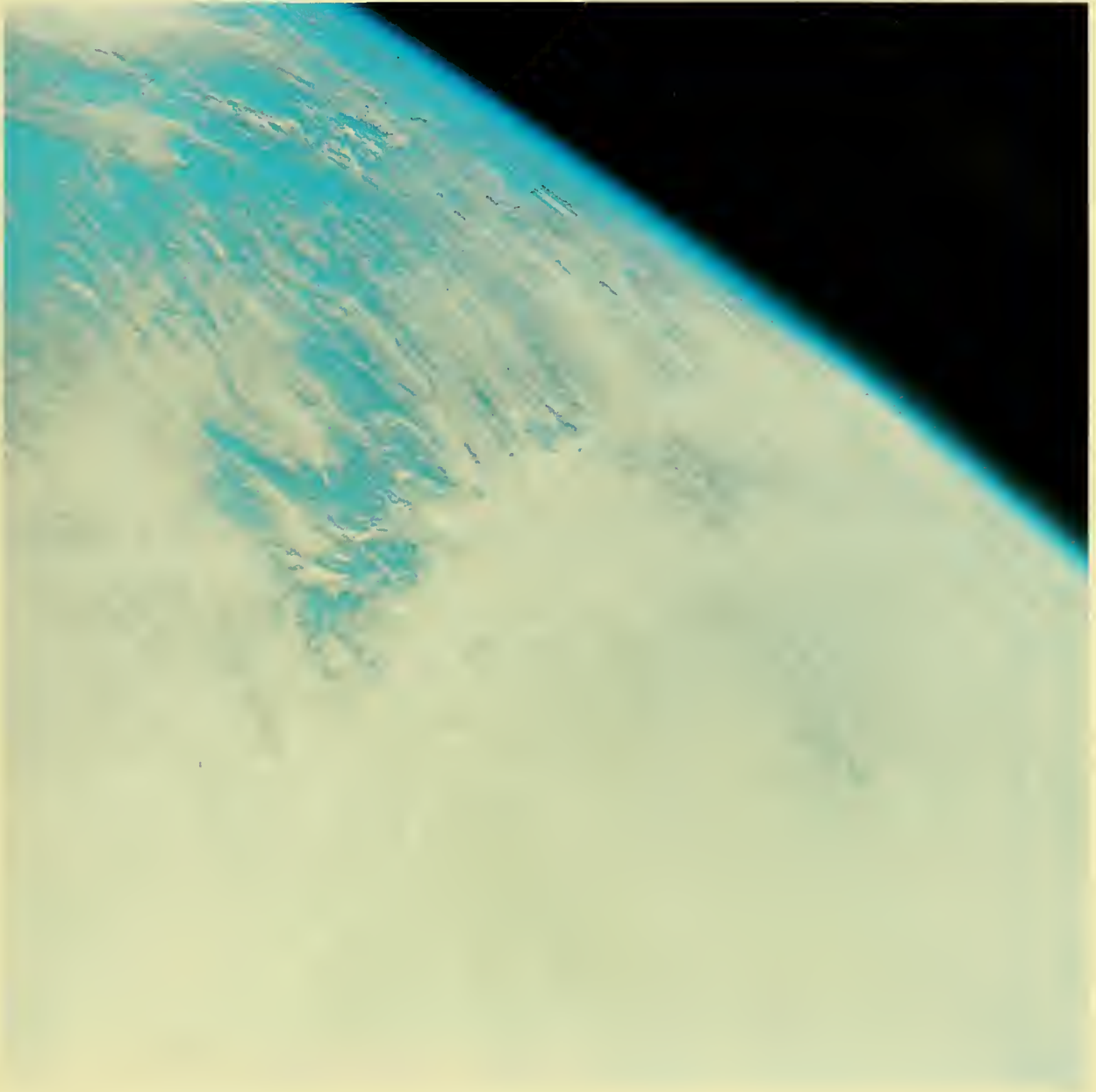
Northern Chihuahua, Mexico, viewed to the north with the Rio Grande at the top. The two lakes at left are Laguna Bustillos and, below, Laguna de los Mexicanos. The city of Chihuahua is in the cultivated valley at right center. The dark areas in the foreground are mid-Cenozoic volcanic rock of the Sierra Madre Occidental. Immediately behind lie linear ridges of folded sedimentary rock, chiefly of Cretaceous age and typical of the Sierra Madre Oriental.

S-65-34633



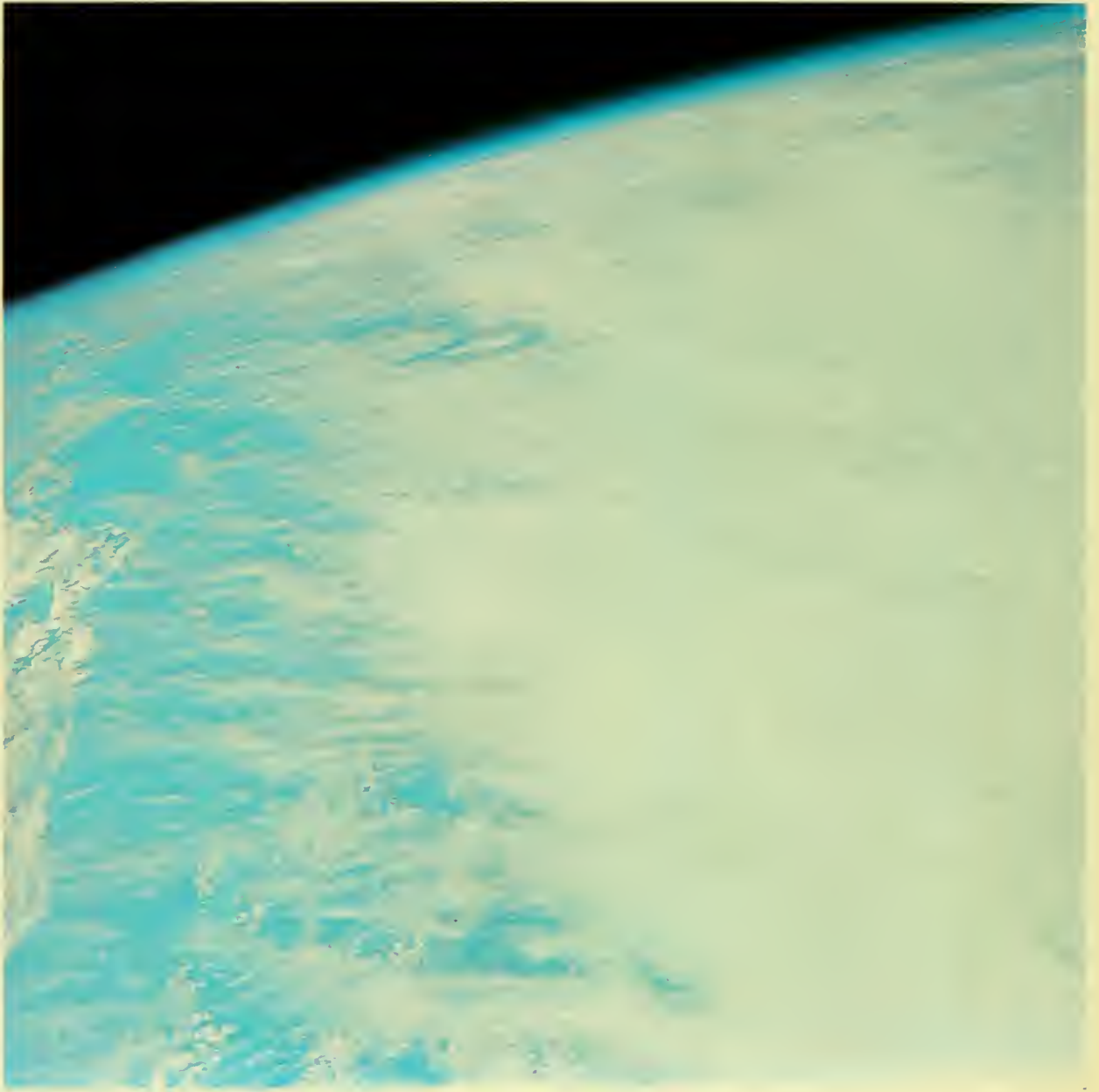
This photograph and the three that follow were taken over a cold front in the western Pacific Ocean about 200 miles southeast of Japan. The viewing direction is west-southwest.

S-65-34647



A second view, 3 minutes later, of a cold front over the western Pacific Ocean near Japan. The undercast is thickest in the vicinity of the frontal zone. Nearly all the lower cloud layers are obscured by cirrus clouds.

S-65-34650



The third photograph, taken 6 minutes later, shows the cold front east of Wake Island. Various cloud layers are visible to the left of the frontal zone. S-65-34651



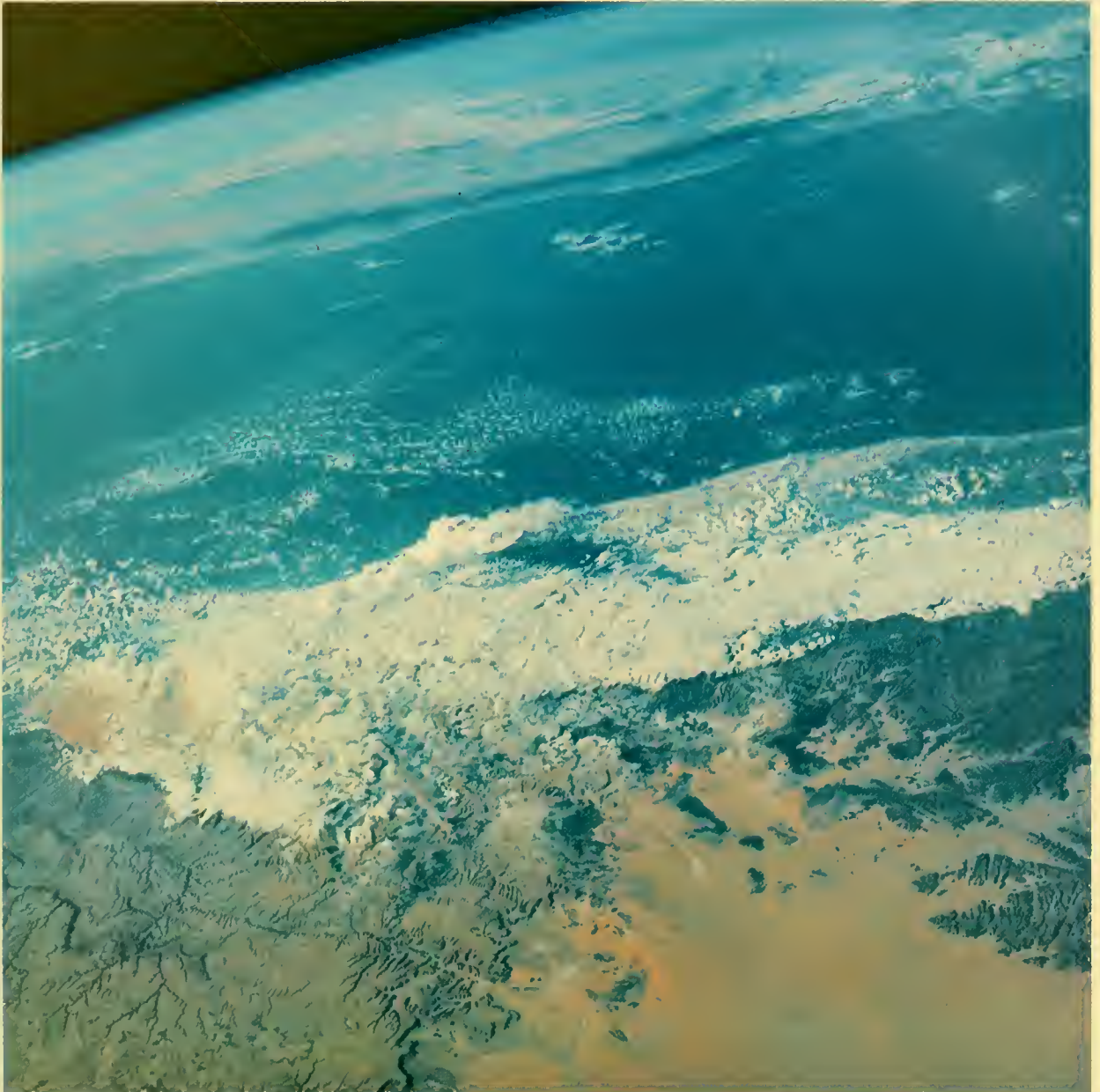
The cold front over the Pacific Ocean east of Wake Island a moment later. This fourth view shows a complex structure of major cloud bands, many of which are subdivided into lesser bands.

S-65-34652



The southern edge of the Arabian Peninsula with the Gulf of Aden and the Somali Republic in the background. The Port of Aden is in the lower right central portion of the picture.

S-65-34656



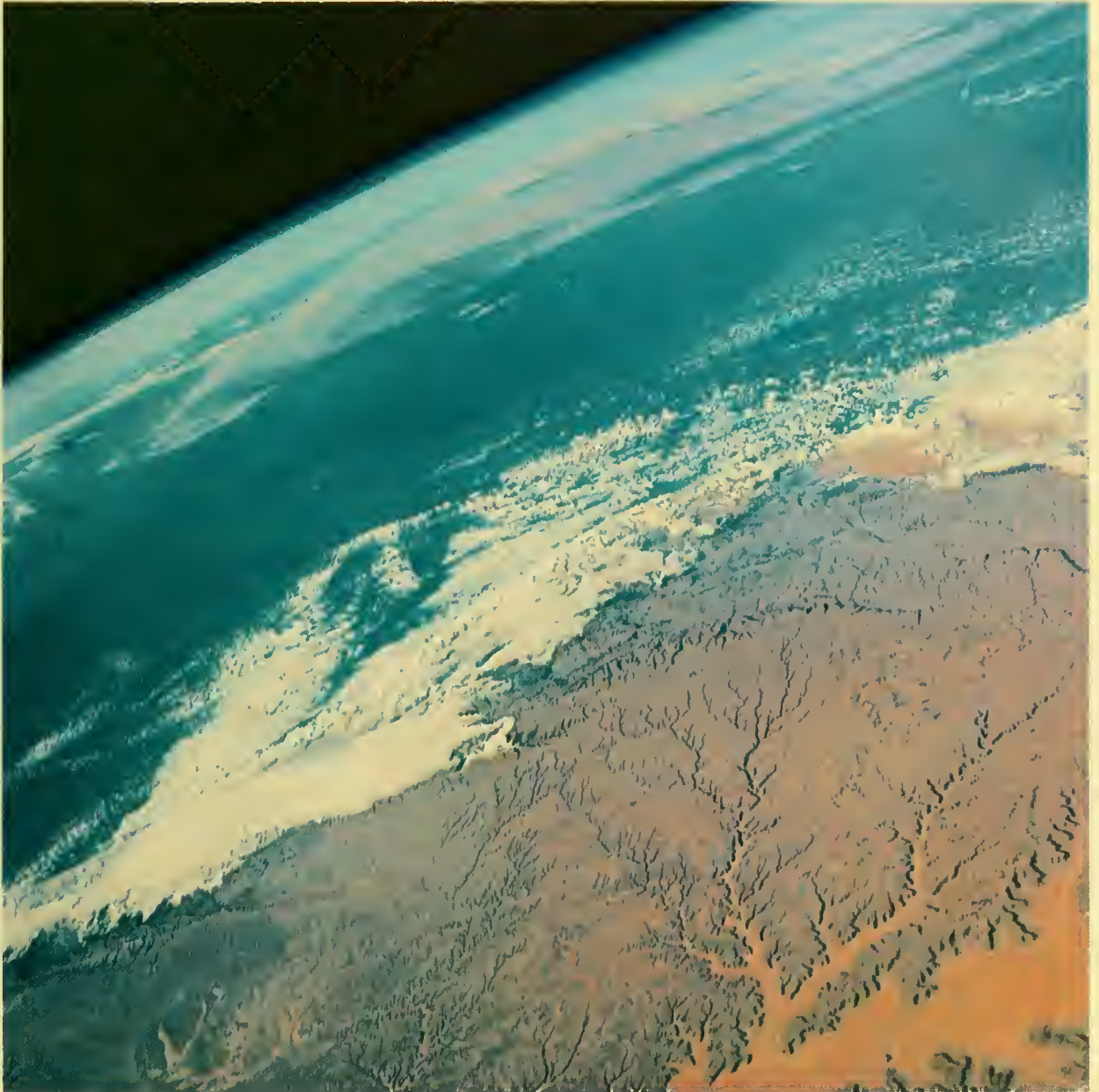
The southern tip of the Arabian Peninsula is seen in the foreground. The view looks south across the 200-mile wide Gulf of Aden to the Somali Republic in the background.

S-65-34657



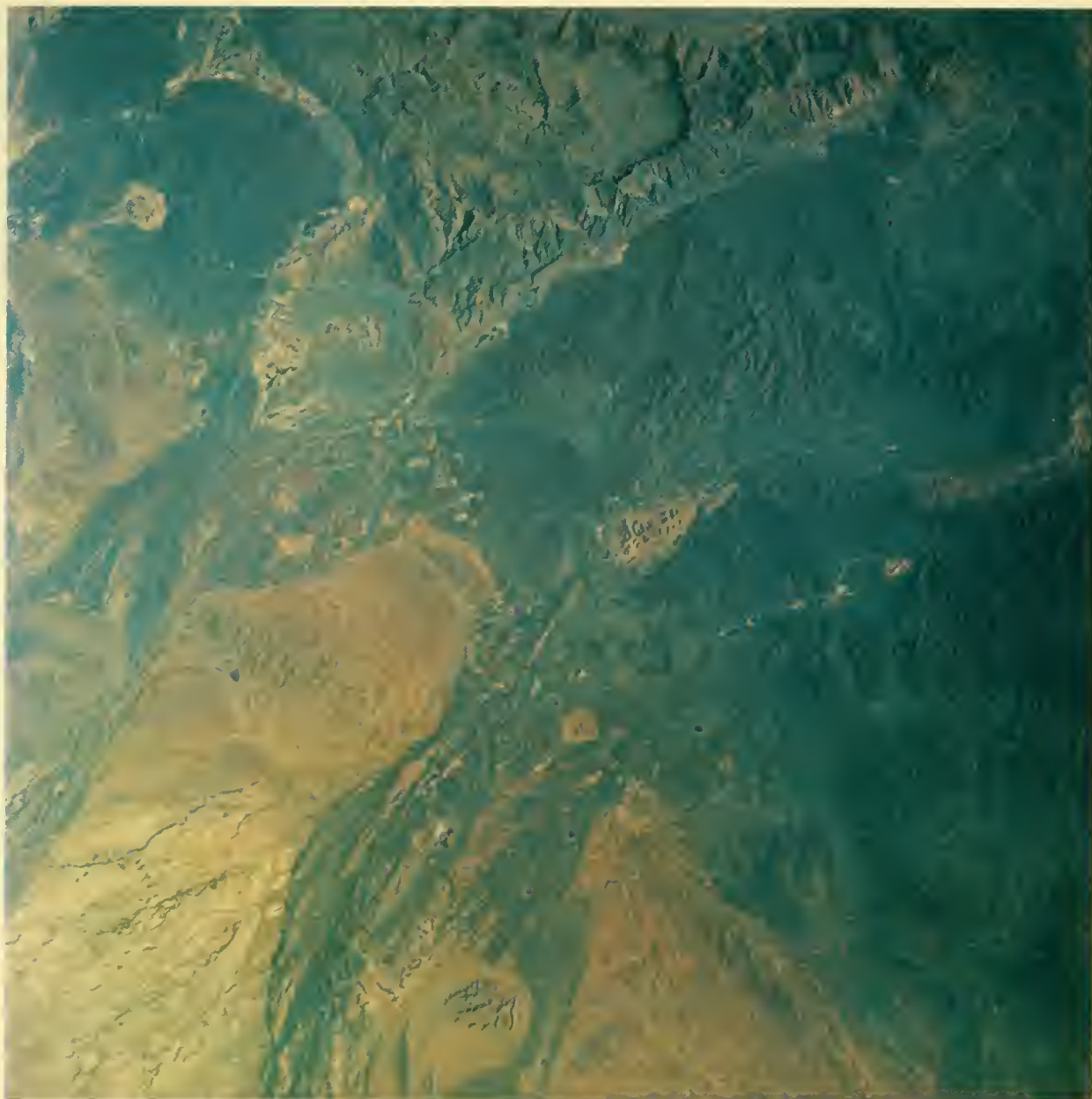
View to the southeast over the Hadramawt Plateau in southern Saudi Arabia. The Wadi Hadramawt, a dry river basin, shows classic dendritic drainage patterns. Note the prominent tributary (left center) which is beheading other tributaries in the background. The Hadramawt Plateau is underlain by gently dipping marine sediments.

S-65-34658



This frame overlaps the previous photograph of the Arabian Peninsula. The Hadramawt Plateau is in the lower half of the picture with the Wadi Hadramawt at lower right. The Ras Asir in the Somali Republic, the easternmost point of Africa, is visible in the upper left corner. In the center lies the Gulf of Aden, 100 fathoms deep near the shore and up to 1,000 fathoms in the middle.

S-65-34659



The southeastern part of the Arabian Peninsula in a near-vertical view, showing the Sultanate of Muscat and Oman. The center of the area is about 23° N., 58° E. The dark areas at the lower right are igneous rock in the highlands bordering the Gulf of Oman (out of view).

S-65-34660

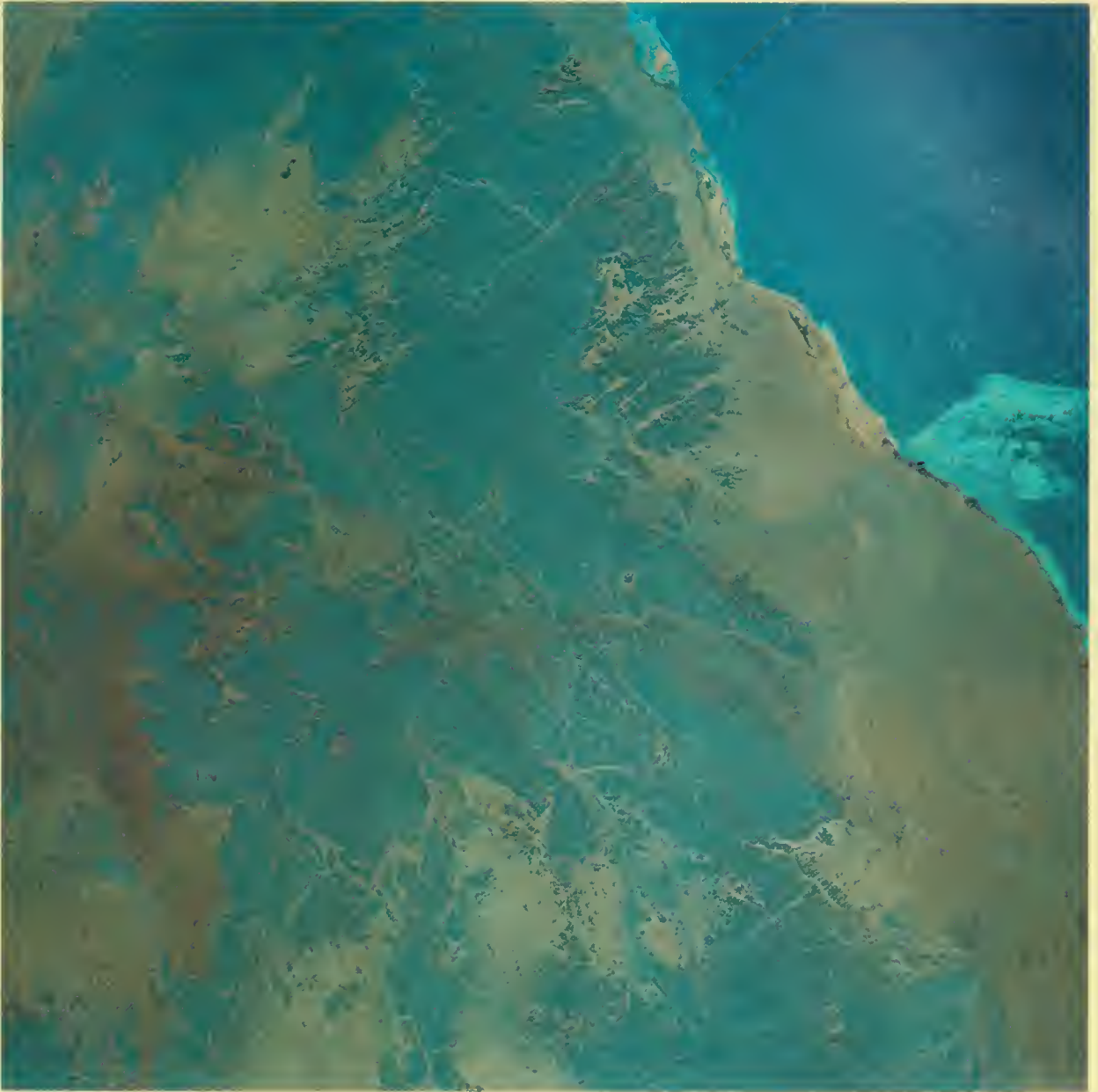


Ras al Hadd, a prominent cape at the southeastern tip of the Arabian Peninsula in a near-vertical view. The Gulf of Oman is at the top of the photo, the Arabian Sea at the bottom. Light area at lower left shows seif dunes in the Empty Quarter. Masqat, capital of Muscat and Oman, is out of view at top left. S-65-34661



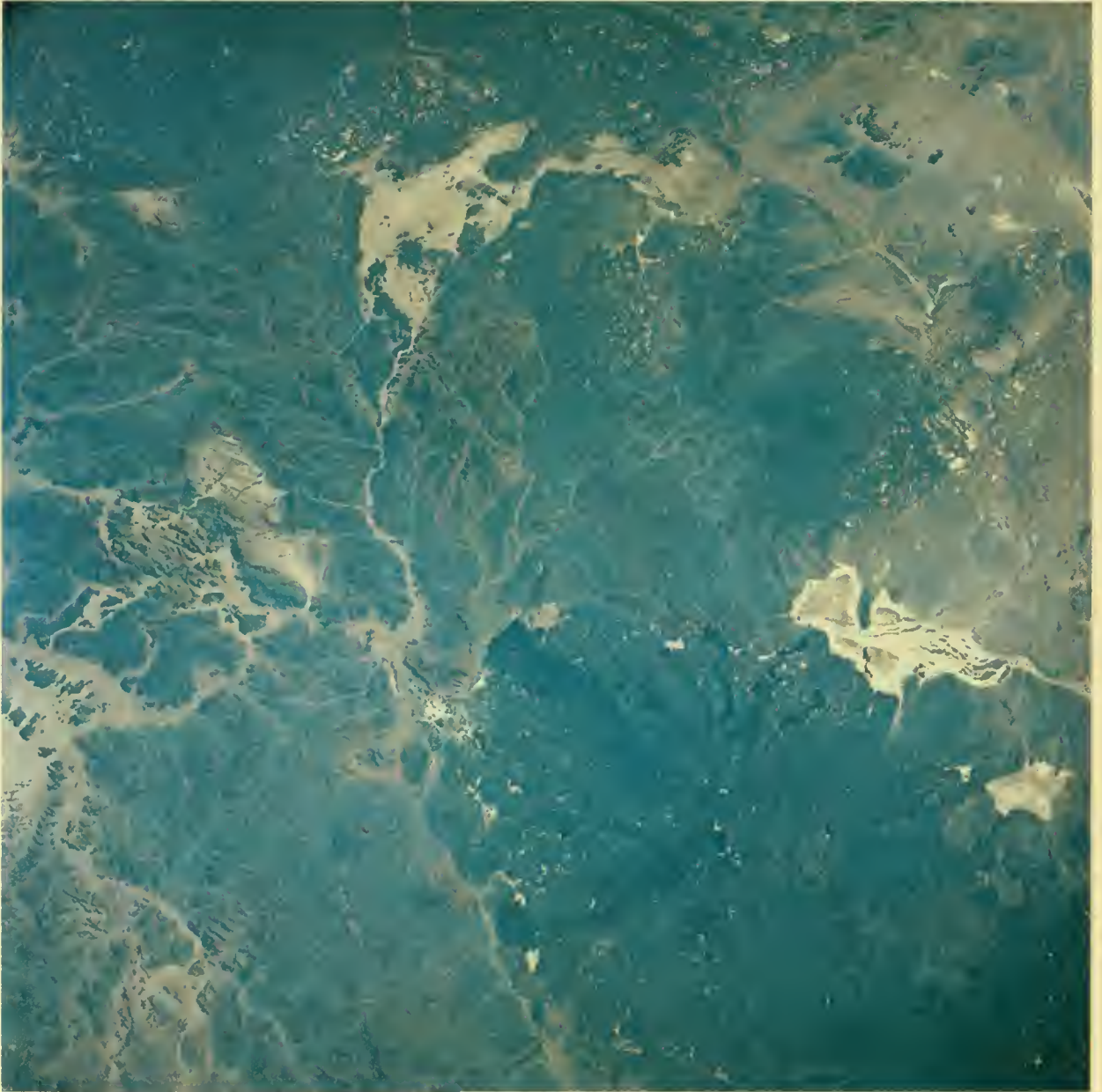
The Sahara Desert in northern Sudan with a near-vertical view of a sandstone plateau with dunes. The center of the picture is about 19° N. and 27° E. The ridges at lower left are the eastern end of the Ennedi Plateau.

S-65-34663



Border area of the United Arab Republic and Sudan on the west coast of the Red Sea just south of Foul Bay. The dark areas are exposed igneous and metamorphic rock cut by linear valleys following fractures. The viewing direction is nearly vertical.

S-65-34664

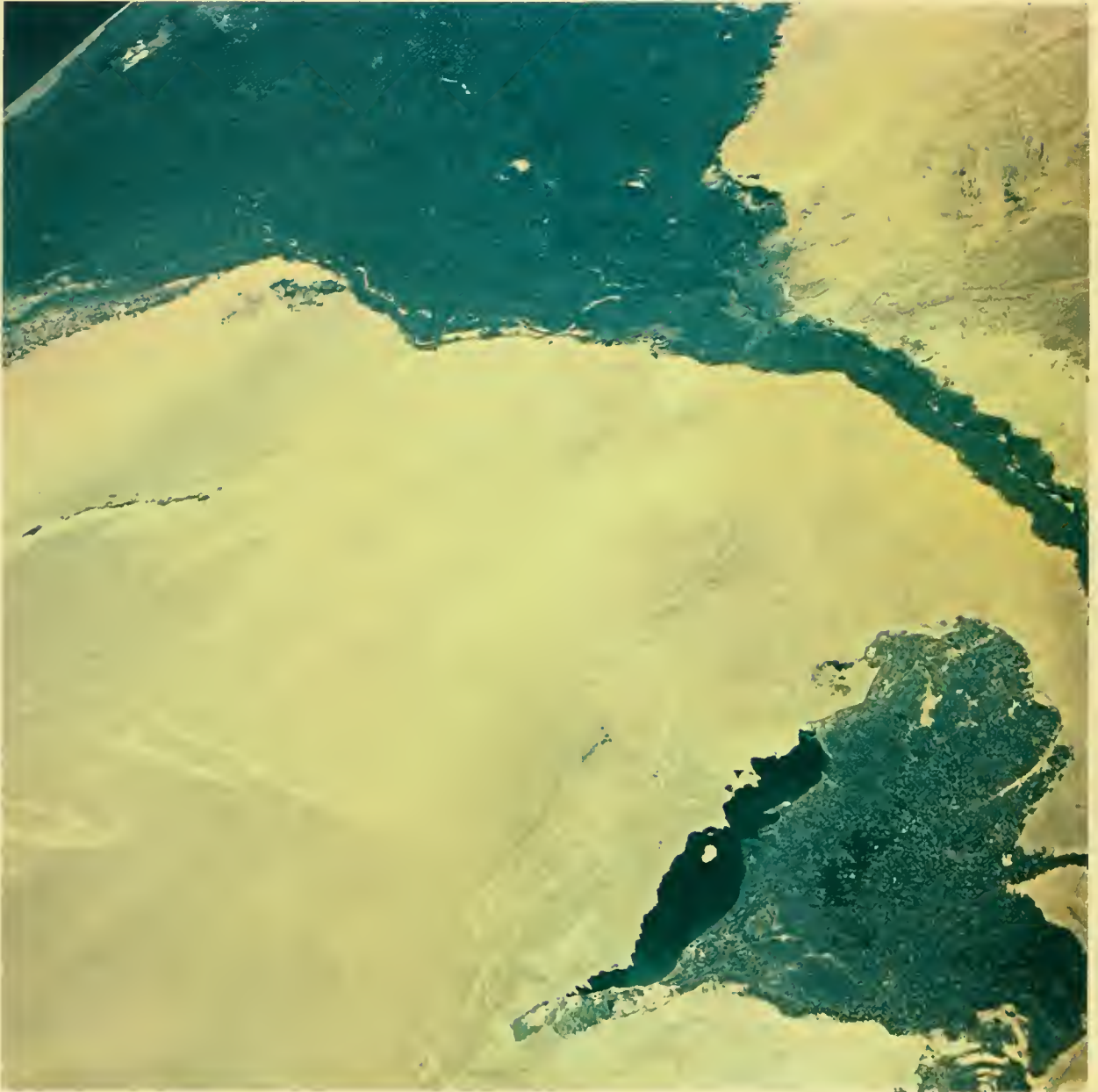


This photograph of the western Arabian Peninsula gives a clear view of the Harrat Rahat, a volcanic mountain range (dark area at lower center). The city of Medina, Saudi Arabia, lies immediately above the range. The river bed running north-south is the Wadi al Hamd.

S-65-34665



An oblique view of Iran over the Zagros Mountains. The Persian Gulf is clearly seen. Just visible at the top of the photograph are the Qatar Peninsula in Saudi Arabia (right) and the tip of the Trucial Coast (left). S-65-34666



The dark triangular area at the top is cultivated land of the Nile Delta in the United Arab Republic. The Mediterranean coast is seen in the upper left corner. The dark area at lower right is El Faiyum, a depression irrigated by the waters of the Nile and partially occupied by the Bohirat Quiron, a lake 148 feet below sea level. Cairo lies in the upper center to the right, at the beginning of the delta. S-65-34668



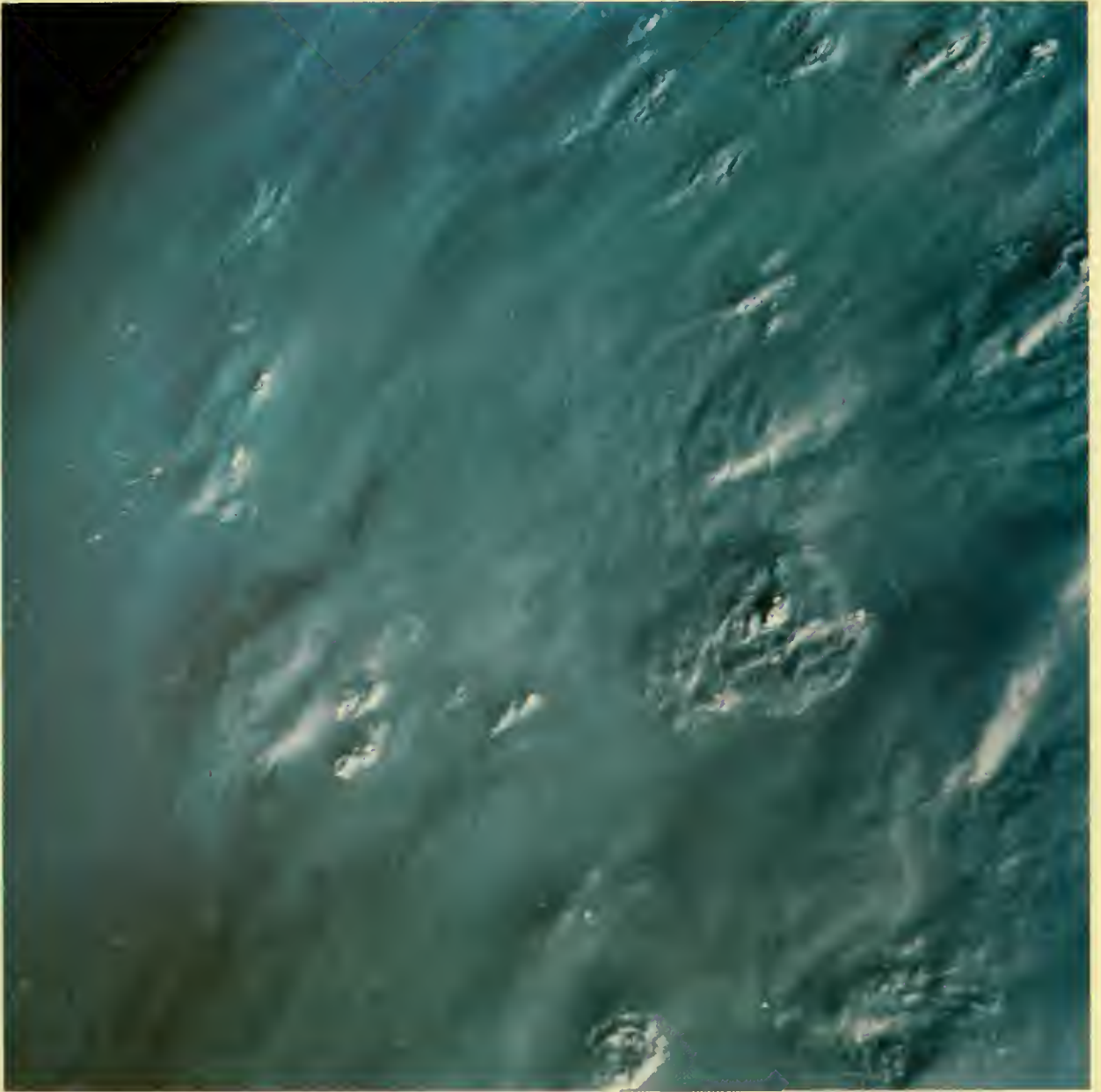
The view is to the southeast over the Dhar Adrar in Mauritania. In the center is the Richat Structure, a concentric series of ridges considered to be either an igneous intrusion or an impact feature.

S-65-34670



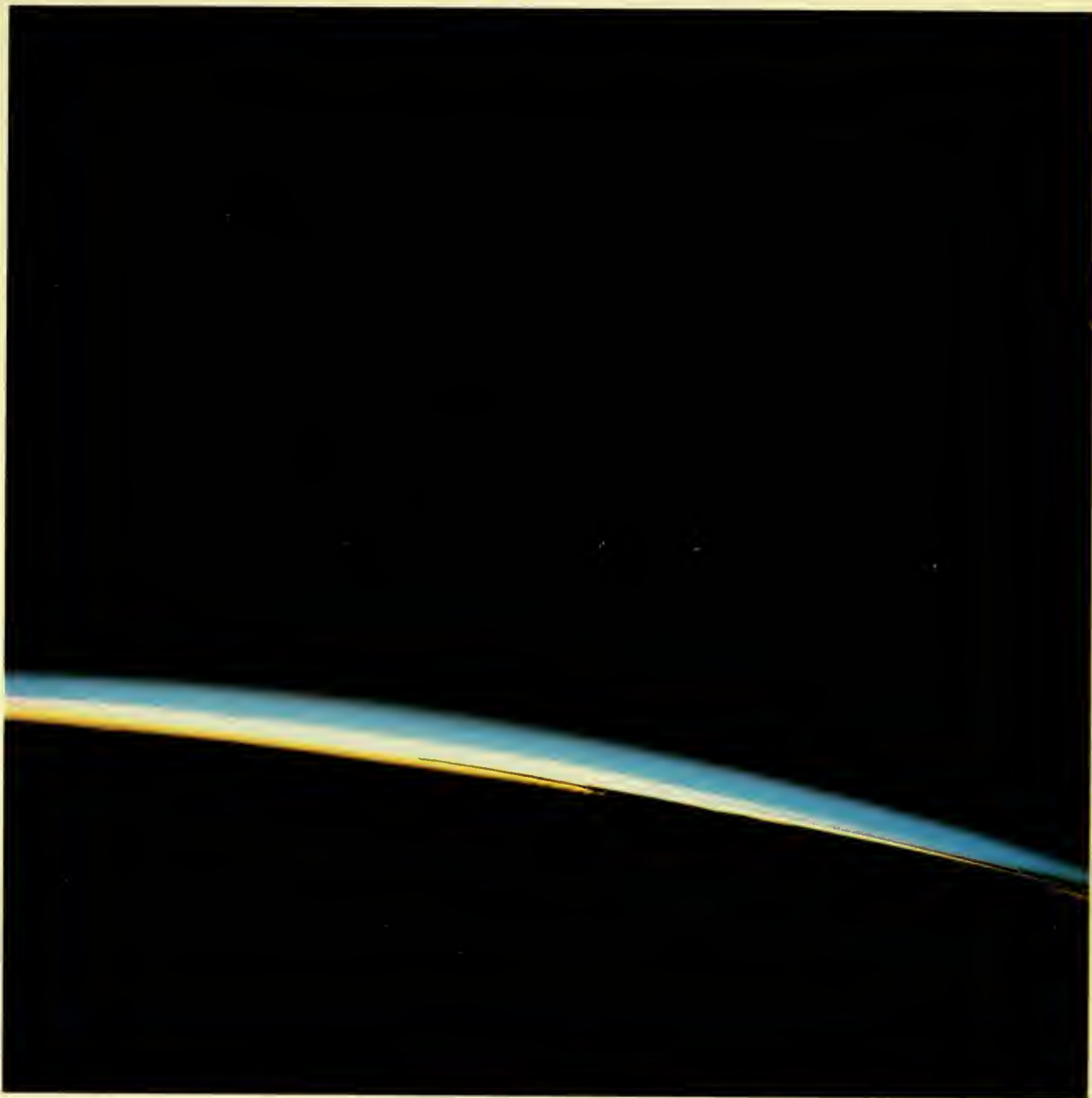
The Nile Delta and the Sinai Peninsula viewed to the southeast with the Mediterranean to the left. The Suez Canal and the Rosetta and Damietta branches of the Nile are seen clearly. The Dead Sea, 1,290 feet below sea level, is visible at the upper left. Parts of the United Arab Republic, Jordan, Saudi Arabia, Iraq, and Israel are shown.

S-65-34776



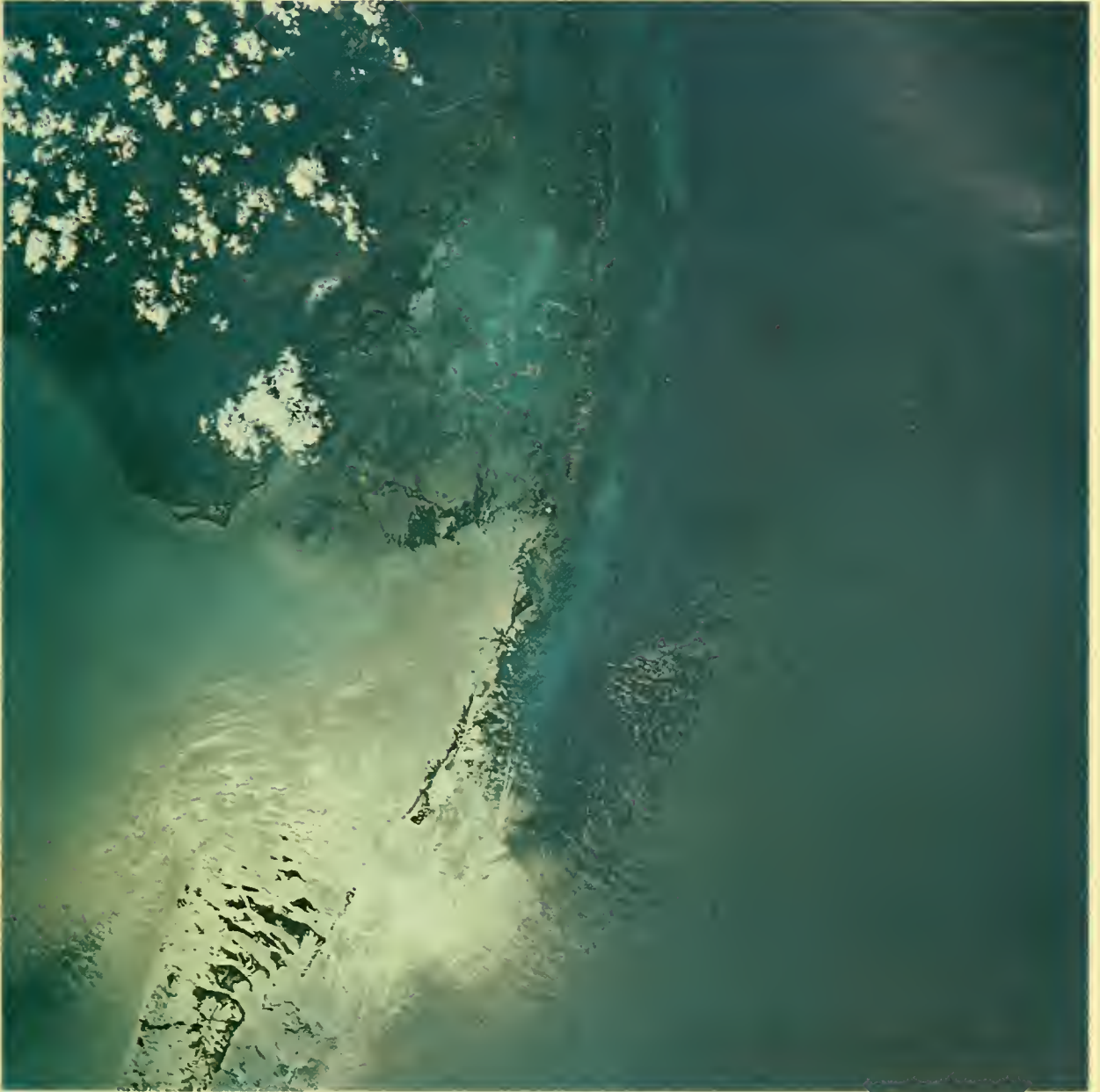
This cloudy region is located in the Pacific Ocean southwest of Panama. Weak light from the setting sun reflects from protuberances in the massive undercast. Such cover frequently extends 300 to 400 miles in tropical areas. Each bulge marks the top of one or more convective cells nearly hidden in the top layer of cirrus cloud.

S-65-34773



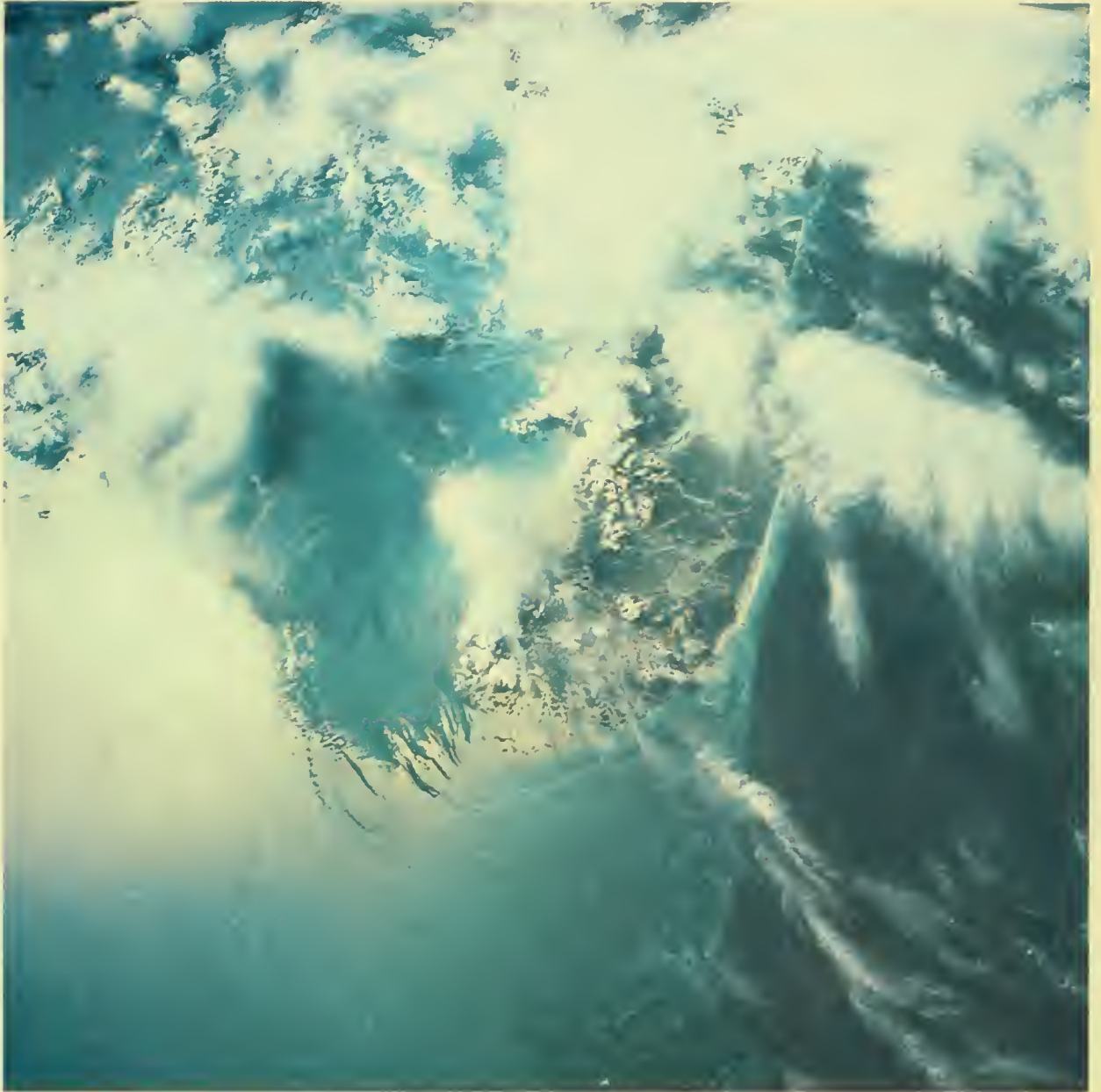
A photograph of Earth's limb—the edge of the planet seen at twilight. The silhouette shadow of cloud layers can be seen in the atmosphere (white), above which lies an airglow layer (blue).

S-65-34771

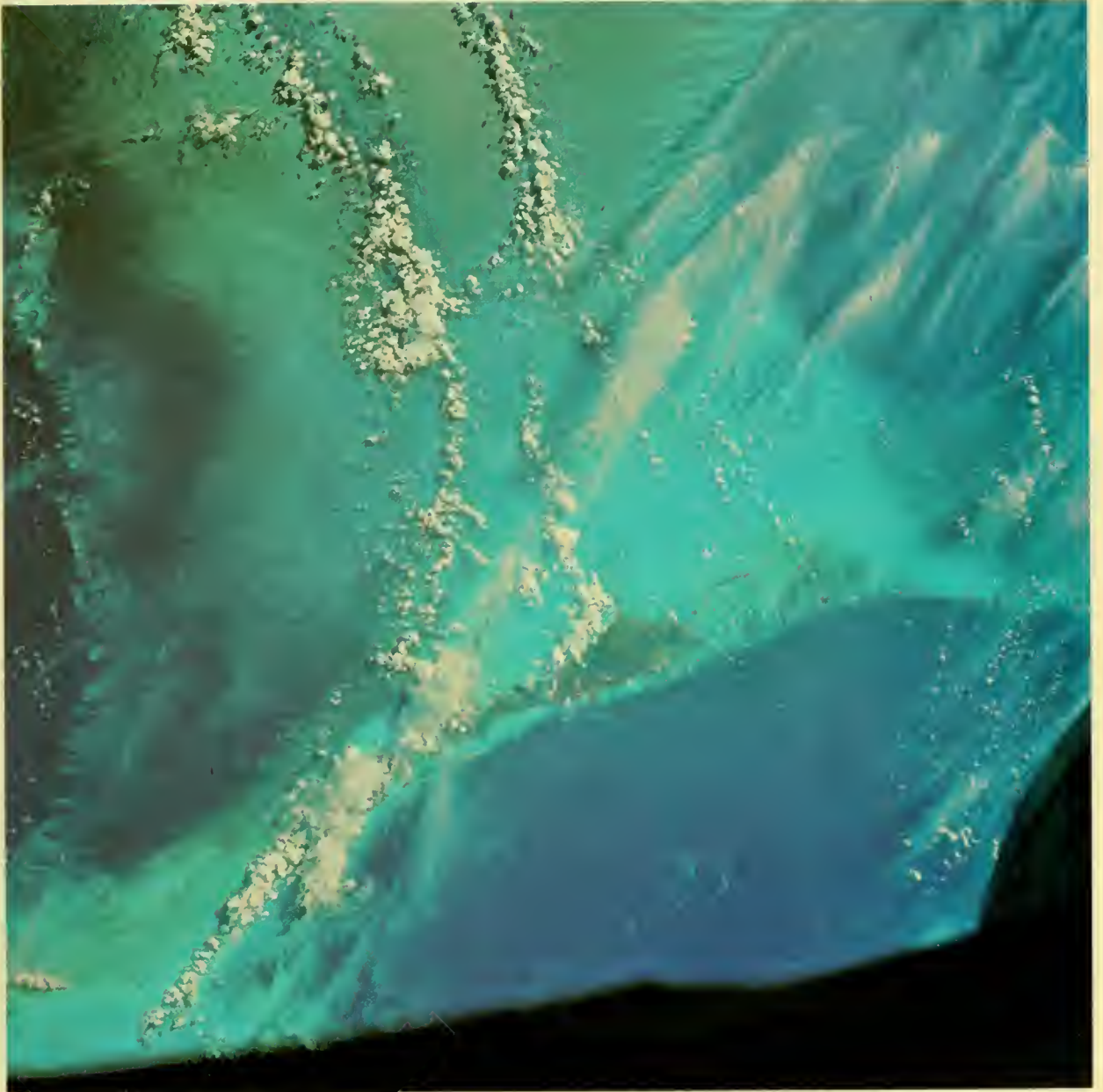


Vertical view of the Florida Keys with the Everglades National Park and Cape Sable visible at the top of the photograph. The shoal areas and underwater detail from Key Largo to Boca Chica Key are seen in the center. The structure in the pattern of sun glitter on the water (whitish area) is partially due to slicks.

S-65-34766

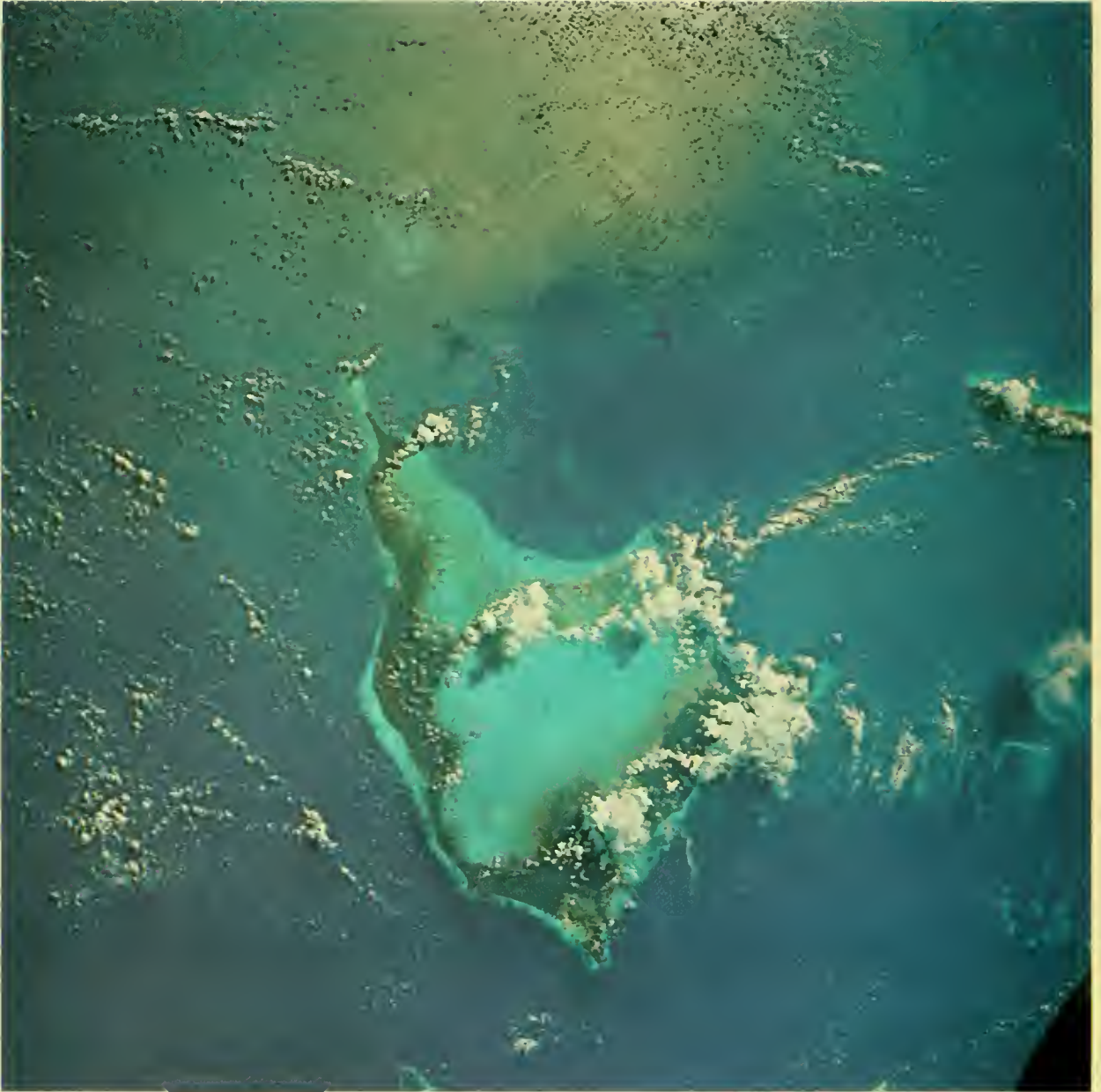


The southern portion of Andros Island in the Bahamas. The rest of the island and some adjacent sea areas are covered with clouds. Sea swells form a pattern in the sun glitter region to the left. The Tongue of the Ocean, where depths exceed 900 fathoms, is located on the right. The Great Bahama Bank is at left. S-65-34763



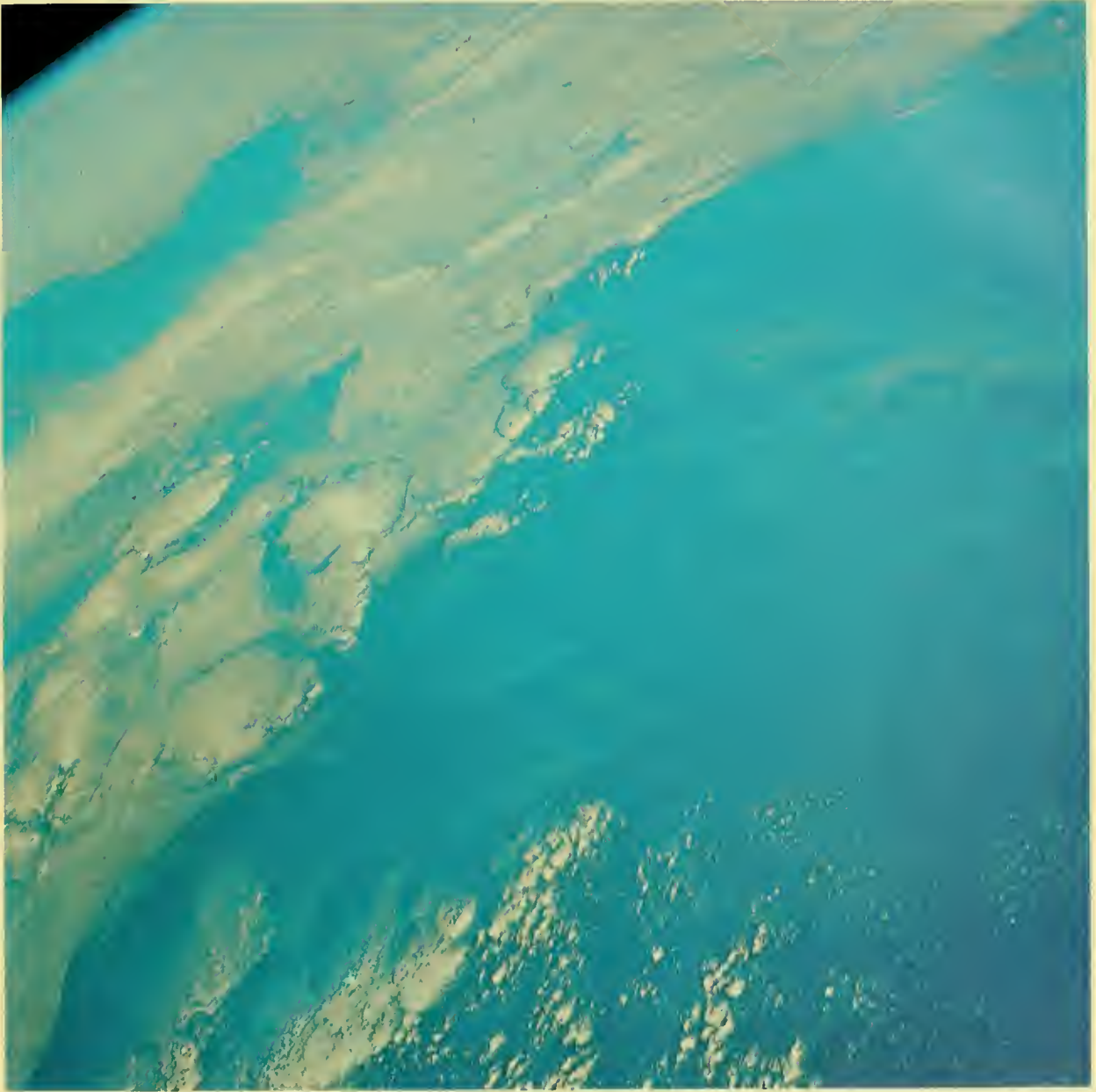
The shallow water of the Great Bahama Bank in the center has depths from 1 to 4 fathoms and bottom configurations are easily seen. Great Exuma Island with adjacent cays is perched at the edge of Exuma Sound (right), where depths exceed 1,000 fathoms. Cirrus clouds occasionally hide the puffy cumulus clouds which form lines in the lower atmosphere. Pictures such as these, showing over 7,000 square miles, are valuable to oceanographers in mapping shoal waters.

S-65-34762



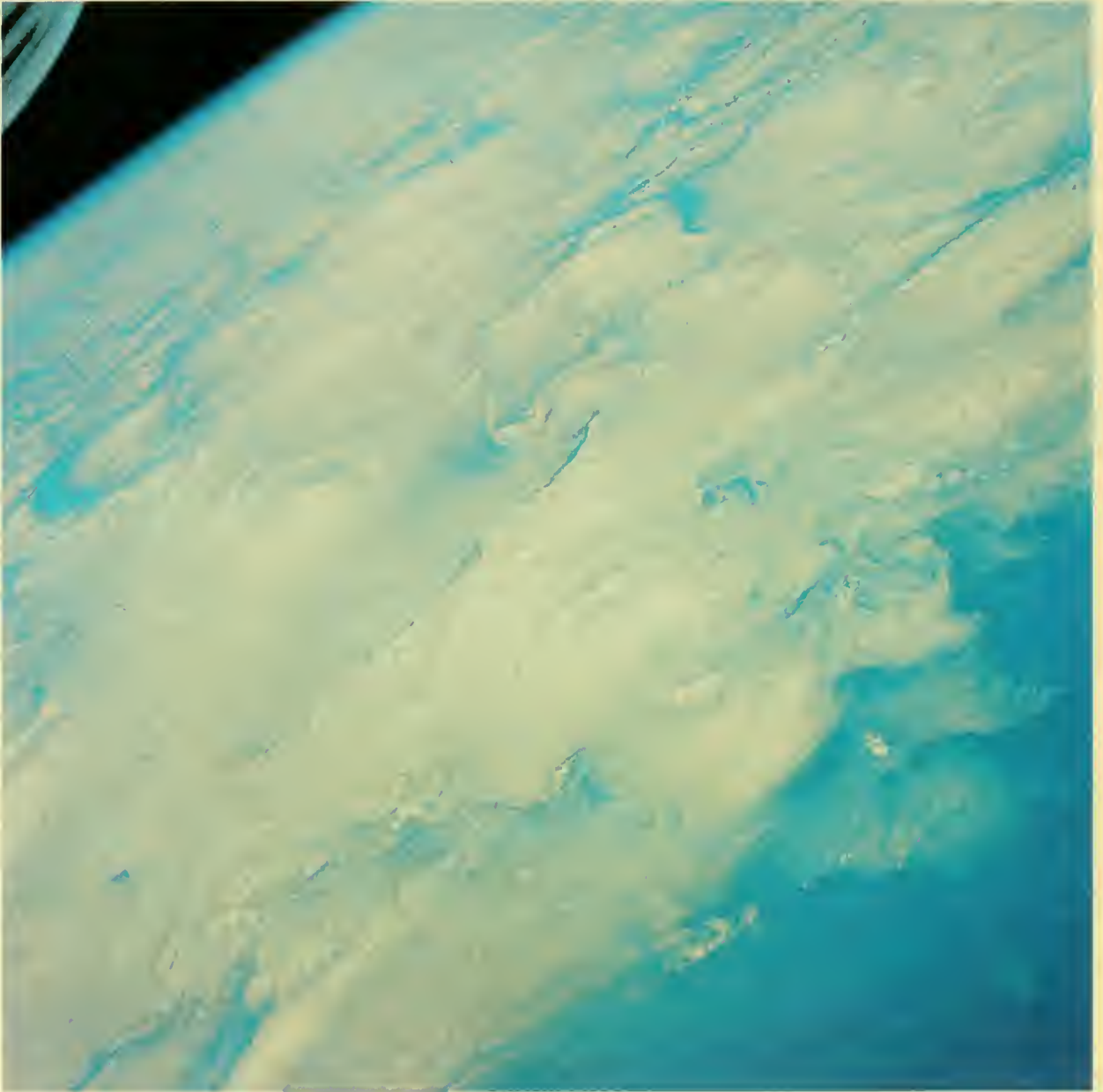
Acklins Island (center) and the adjacent Crooked Island in the Bahamas nearly enclose the Bight of Acklins, a shallow water lagoon, where the average depth is about 9 feet. Swampy areas in the northern part of the bight are seen as light green. The tall cumulus clouds are probably induced by surface heat. Shadows of many small cumulus clouds appear as black dots against the bright background. At the top of the picture, the sun glitter reflects irregularities in waves and swells on the sea surface.

S-65-34761



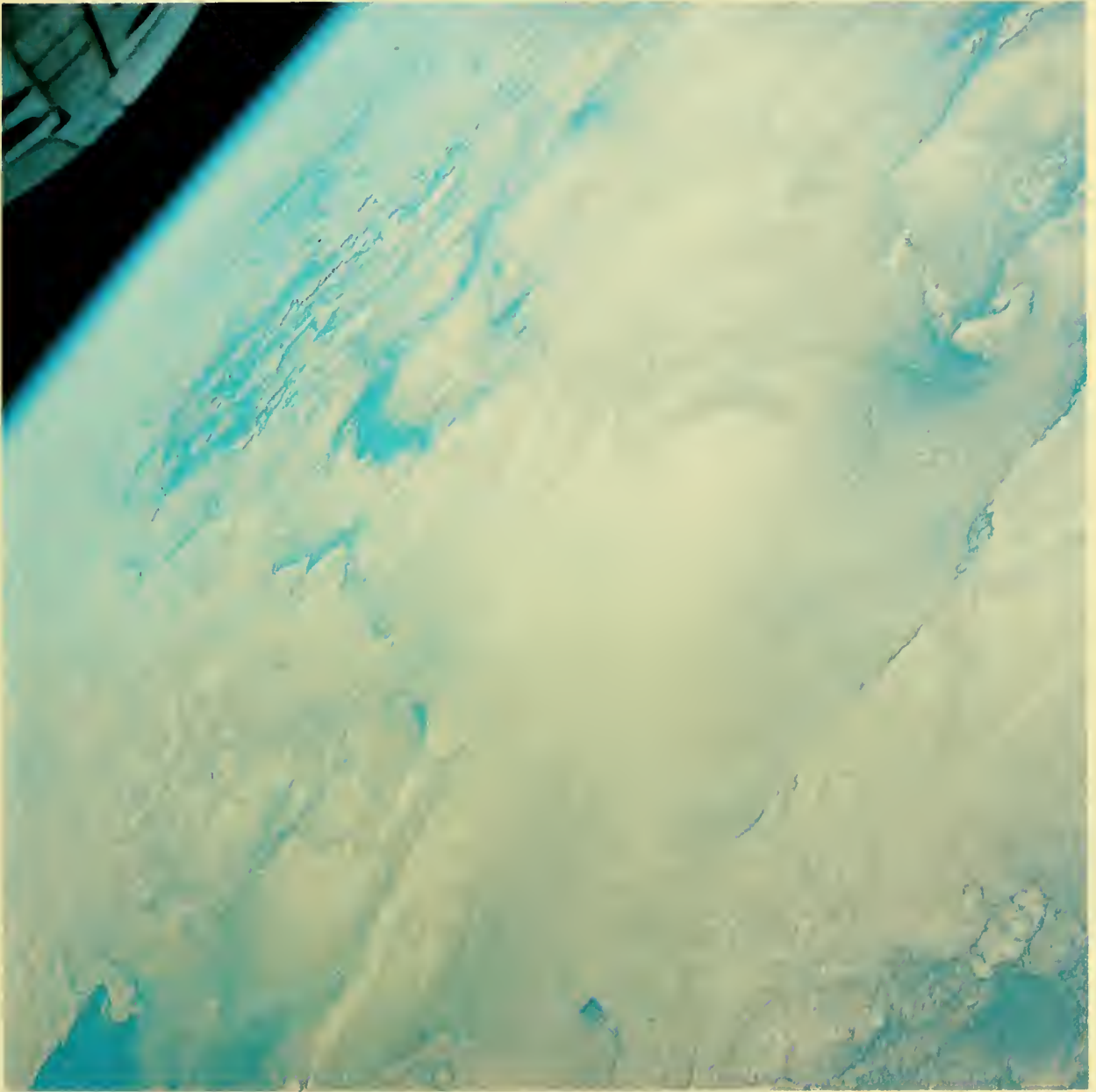
A high-pressure area frequently dominates the eastern North Pacific Ocean and stratocumulus clouds commonly occur in the eastern and southern regions of the anticyclone. This picture and the four that follow were taken in sequence and show similar cloud patterns.

S-65-34754



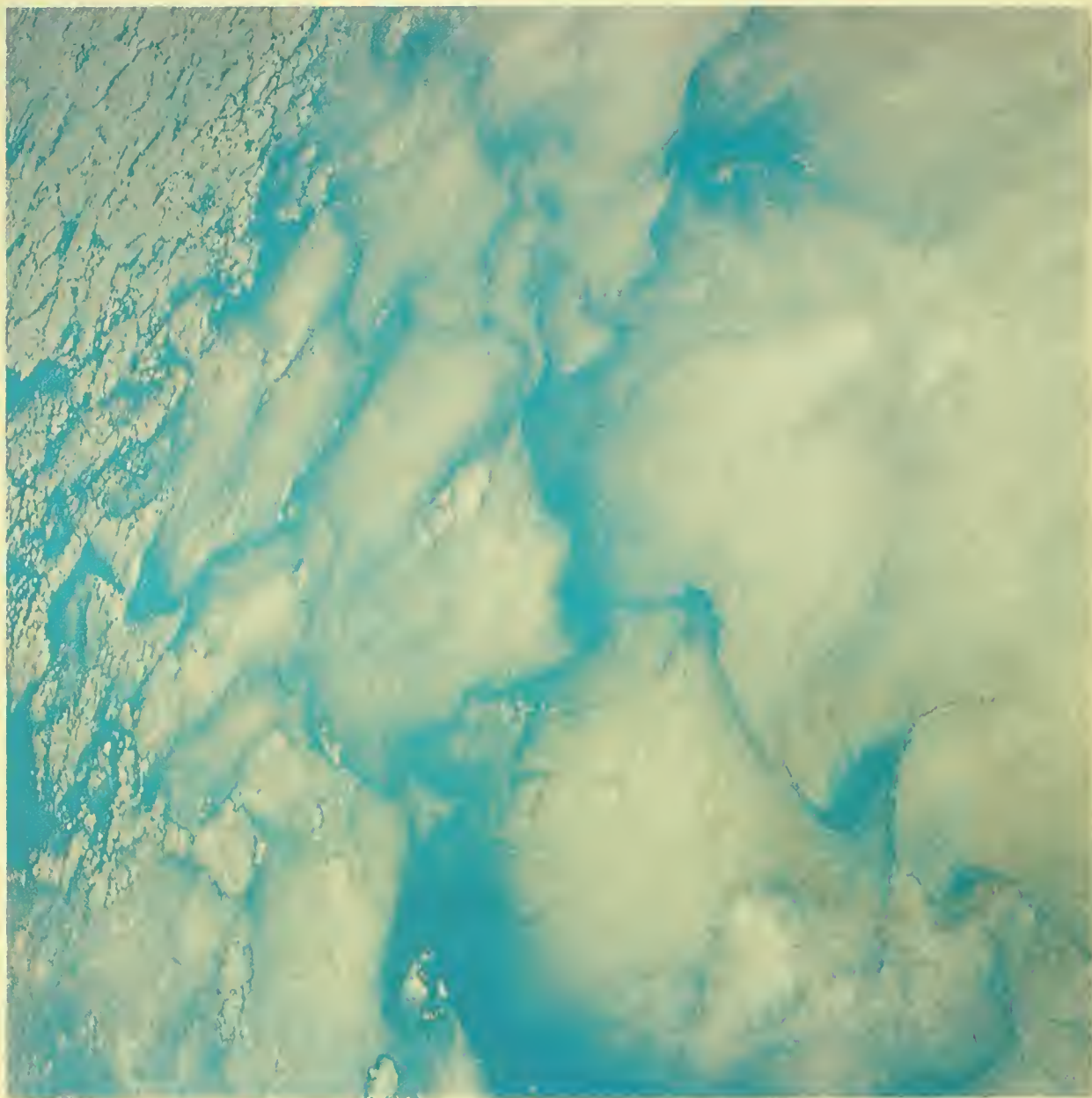
In this view, the stratocumulus clouds of the eastern North Pacific have formed irregular shaped cells whose thicknesses tend to decrease from the center outward to the perimeter.

S-65-34753



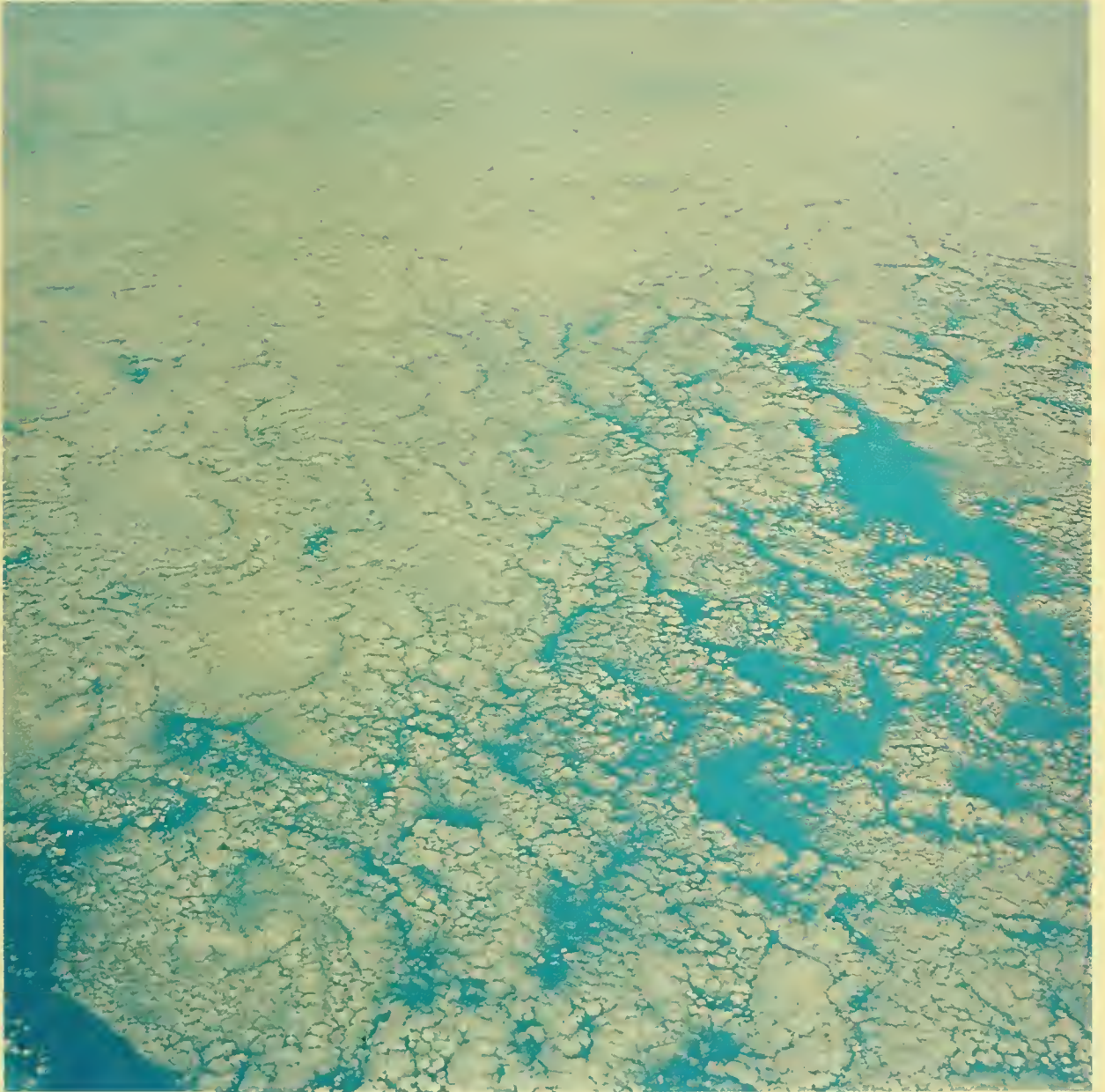
Another view of the stratocumulus clouds over the North Pacific Ocean, north of Marcus Island. The cellular patterns on the right are shown more clearly in the next frame.

S-65-34752



The cloud patterns shown here suggest that Benard cell circulation is occurring over this region of the Pacific Ocean. The pattern is probably a result of weak organized convection occurring in the absence of vertical wind shear. Spiral eddies have formed along the perimeters of the cells seen in the center of the photograph. An abrupt change in cell diameter can be observed at left. S-65-34751

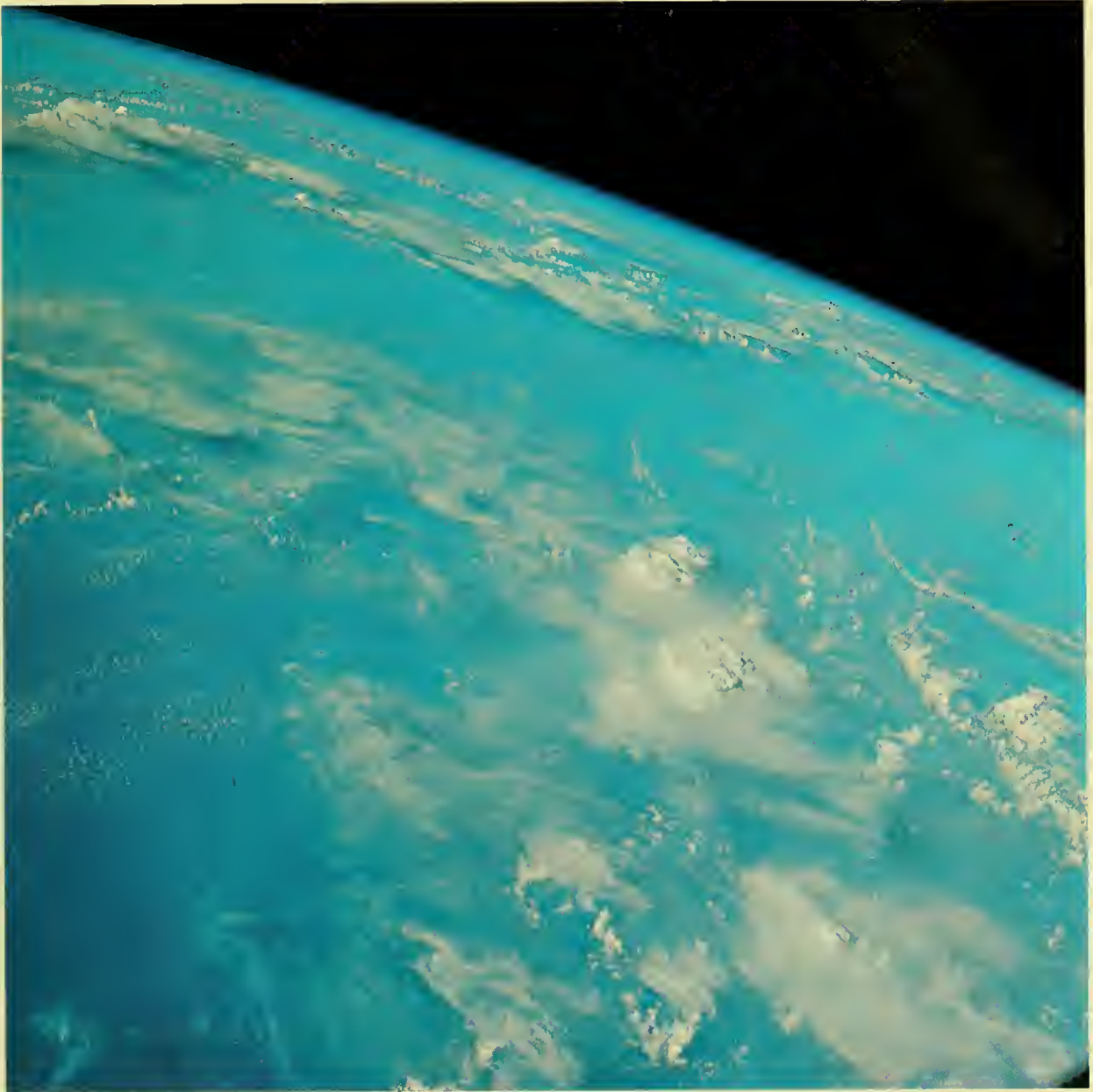
★



The small scale stratocumulus which were shown along the left edge of the previous frame are seen here covering a large area of the North Pacific Ocean. This photograph and the four preceding ones were taken during a 3-minute period. S-65-34750



Mexico's Pacific coastline in the vicinity of Jalisco and Colima appears across the center of this photo looking northeast. A line of thunderstorms over the mountains is seen at right. Other convective activity is found over broad areas of eastern Mexico near the horizon. Filaments and tufts of cirrus associated with the extreme outer fringes of tropical storm Victoria fill the foreground. S-65-34749



This photo, taken 2 minutes after the preceding one, shows a continuation of the thunderstorms over the Central American countries to the southeast. The two towers of dense clouds near the center are probably producing tropical showers below. The rest of the cloud cover consists of a mixture of low-level cirrus and cumulus clouds.

S-65-34747

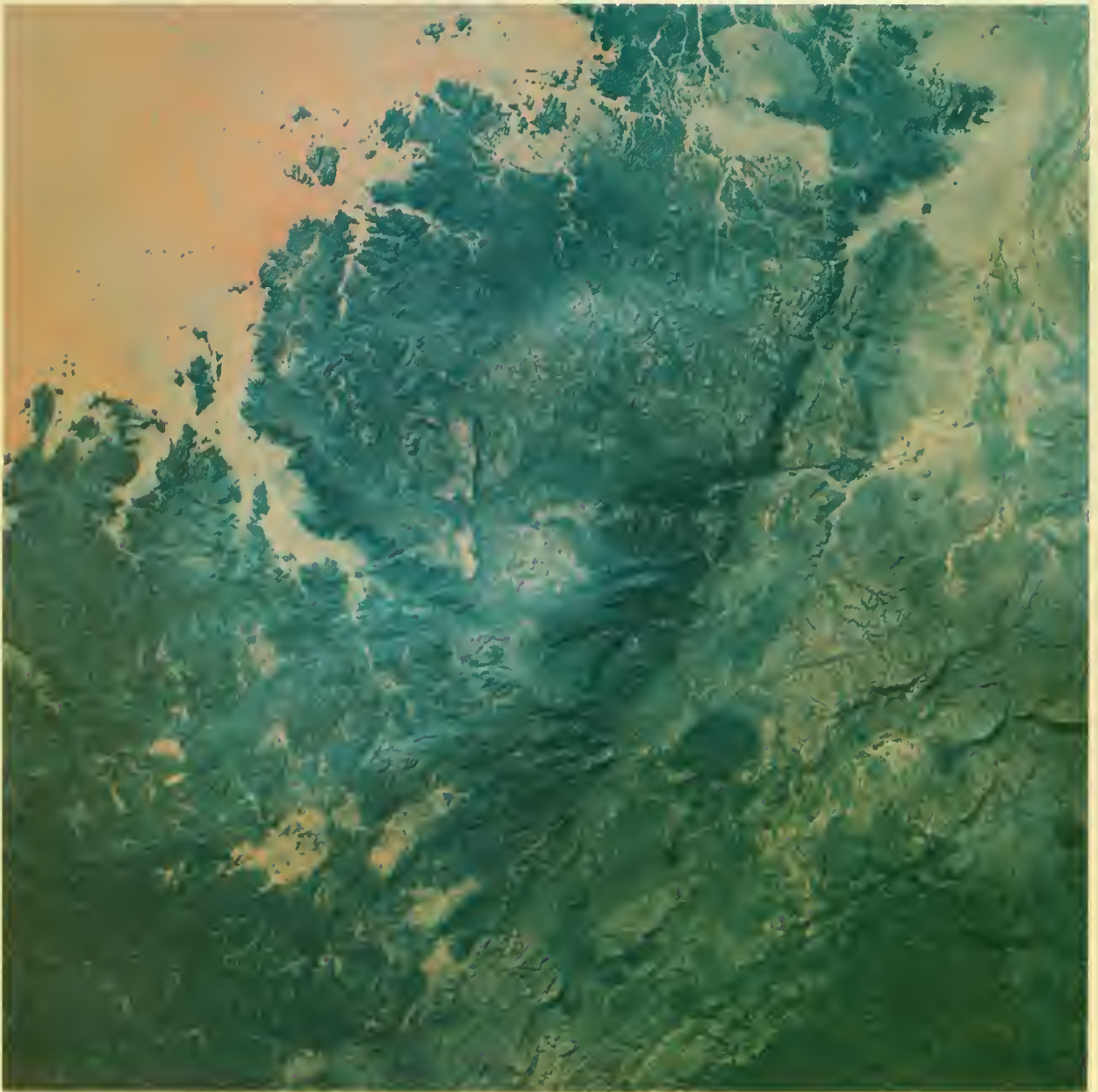


The Pacific Ocean west of Baja California, Mexico. The cool temperature of the sea surface helps to maintain stability in the lower atmosphere. A temperature inversion is found frequently near 2,000 feet and the layer of stratocumulus clouds with a partly banded or cellular structure, as seen here, may persist for days. S-65-34743



This picture was taken looking directly into the sun over the eastern Pacific Ocean. The light foglike area at top center is scattering resulting from a deposit on the spacecraft window. The pentagon-shaped reflection below it is caused by the camera diaphragm.

S-65-34737



A near-vertical view of Yemen in the southwestern part of the Arabian Peninsula between Al Kharab and Salamat. At top left is the western edge of the Empty Quarter, a sandy desert with complex longitudinal dunes. The dark area in the highlands is composed of faulted and jointed Precambrian igneous and metamorphic rock. The prominent scarp in the middle of the picture is probably a fault.

S-65-34726



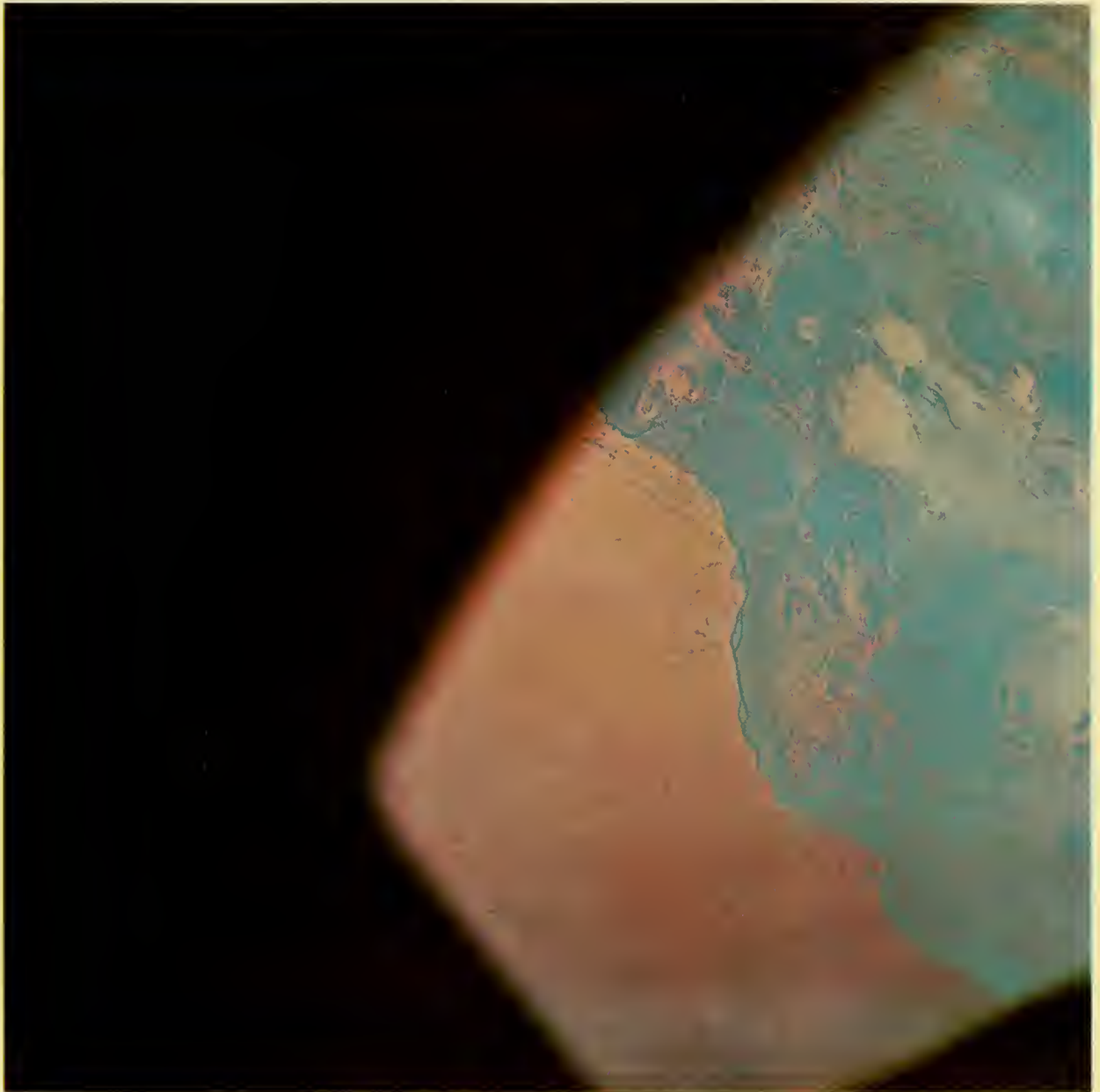
This photograph shows the Empty Quarter of southern Arabia, Yemen, and Saudi Arabia looking toward the Hadramawt Plateau. The longitudinal sand dunes in the foreground and center are clearly visible.

S-65-34765



This picture, although poorly exposed, shows interesting land patterns of northern Chad and Libya. Plateau d'Erdebe is in the center and the Tibesti Mountains at the left. The prominent crater to the near left center is Emi Koussi, an extinct volcano, 11,204 feet high. The arcuate pattern in the center is a combination of ridges and sand dunes. The horizontal streak is a light leak.

S-65-34778



Partially obscured by the spacecraft window, the Nile River winds through northern Sudan, south of Wadi Halfa. The dark area is composed of igneous and metamorphic rock. To the left are sand and gravel flats.

S-65-34779



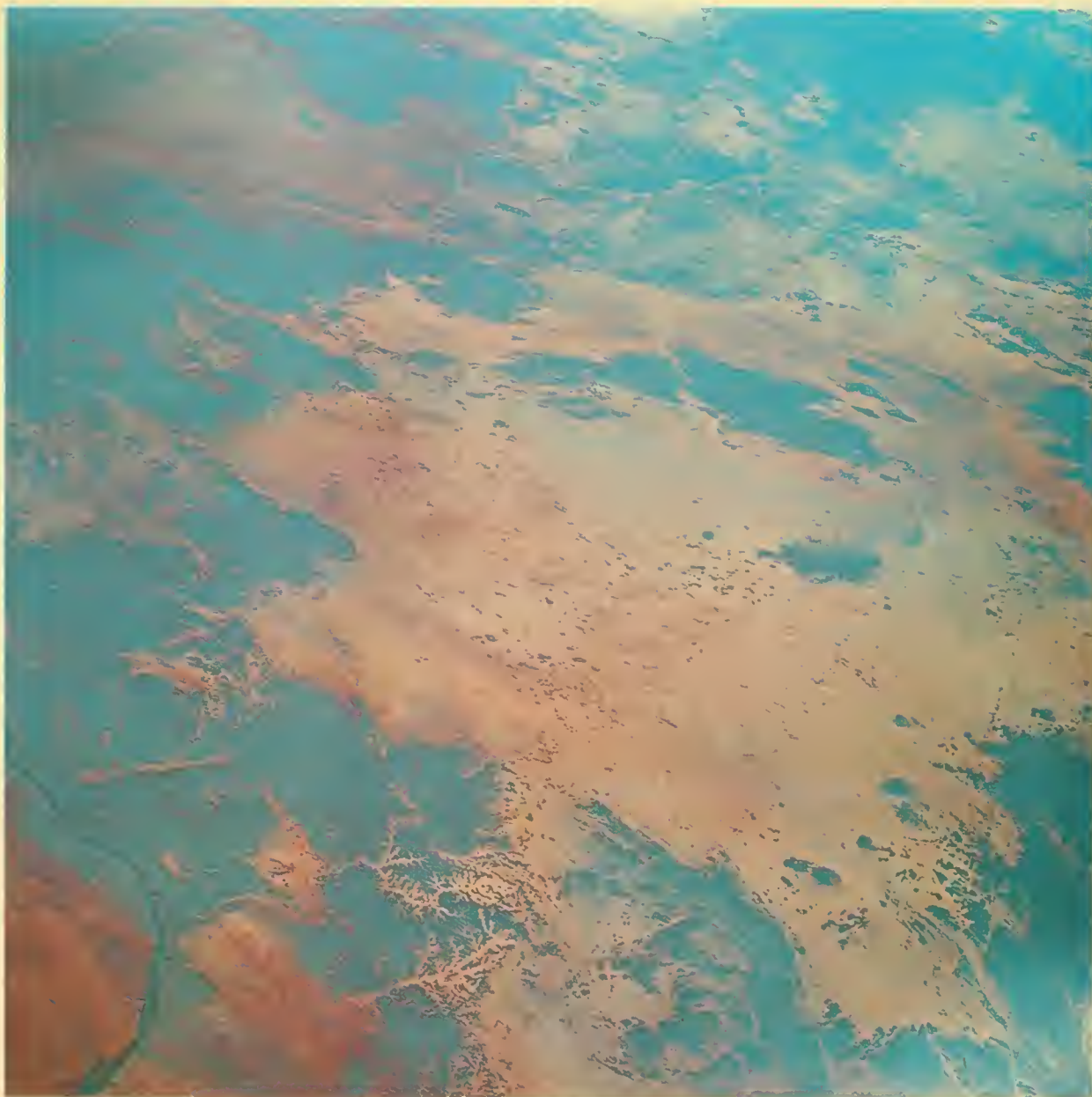
A view of the Nile River in the southern part of the United Arab Republic from the border of Sudan up to Wadi El'Allaqi. The dark areas consist of bare, igneous, metamorphic rock.

S-65-34780



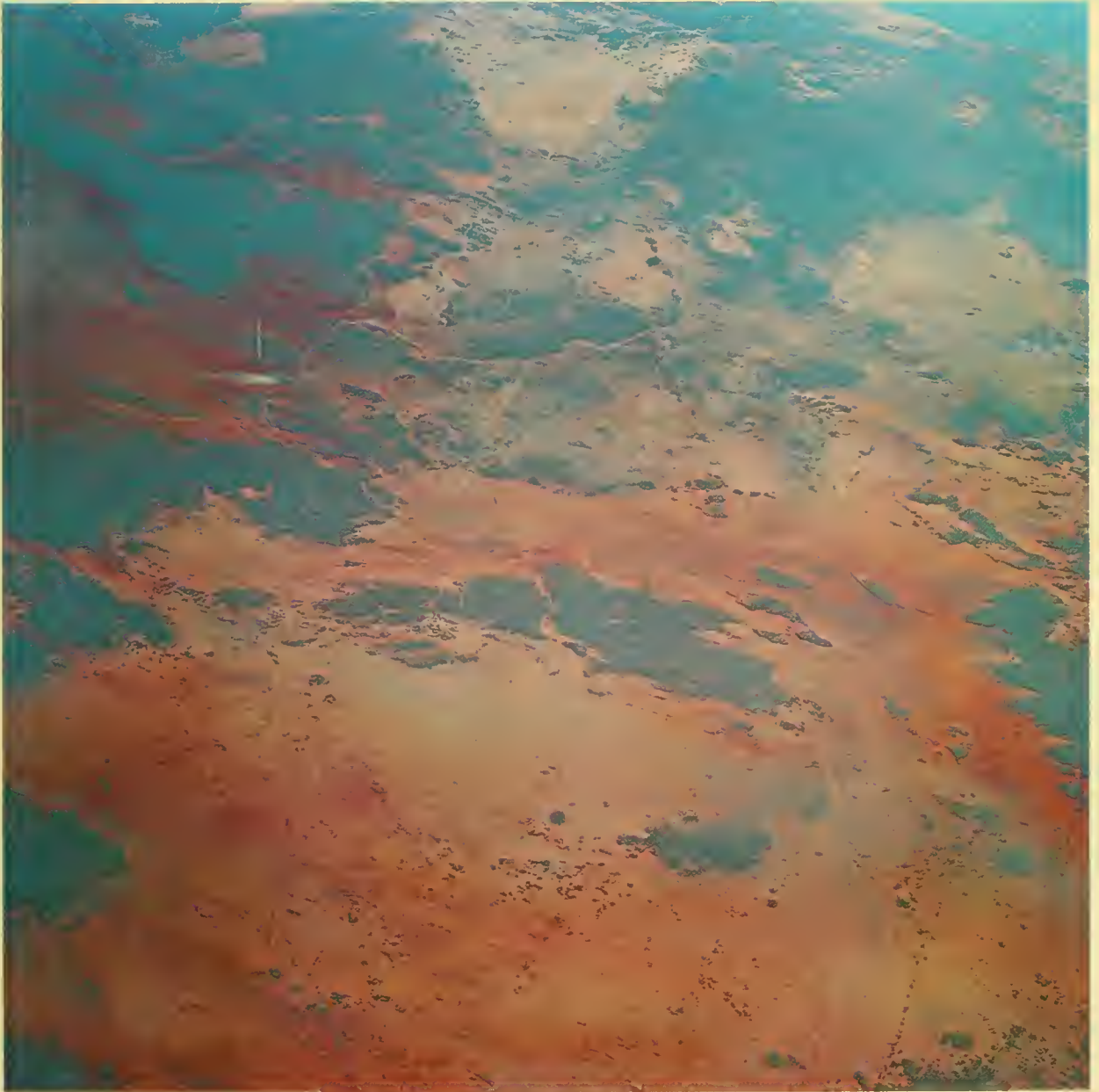
This photograph of the Nile River overlaps the preceding one, but extends further north. The Aswan Dam is visible at the top. Part of the area in the center will be covered by the future reservoir.

S-65-34781



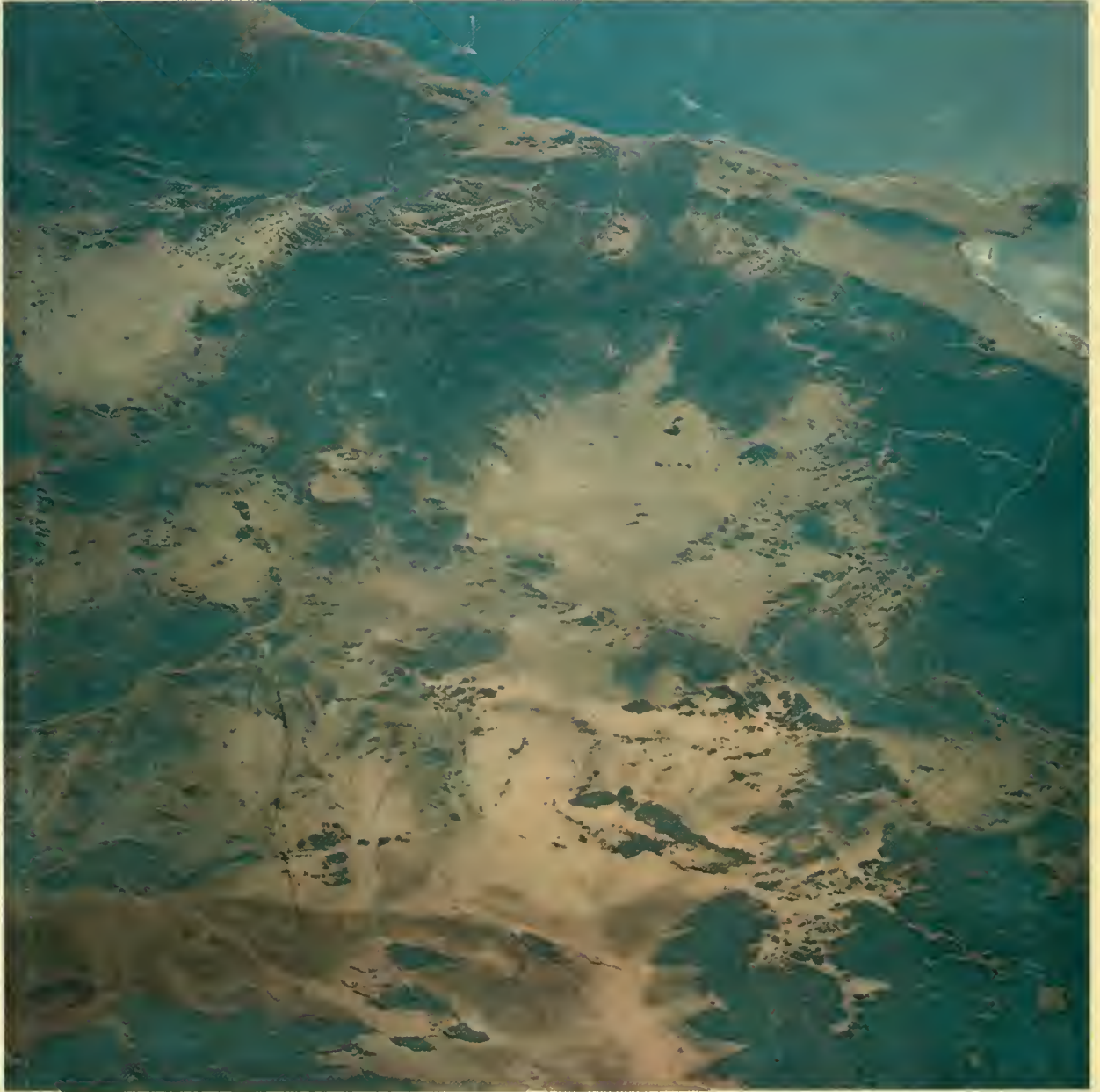
A view of the southeastern part of the United Arab Republic, looking into the Eastern Desert in the Red Sea Province. The Nile River, just north of El'Allaqi, is visible in the lower left corner. The Hamiata Range is at the top right of the photograph. The dark areas are igneous and metamorphic rock of the Nubian Ramp, highlands bordering the Red Sea.

S-65-34782



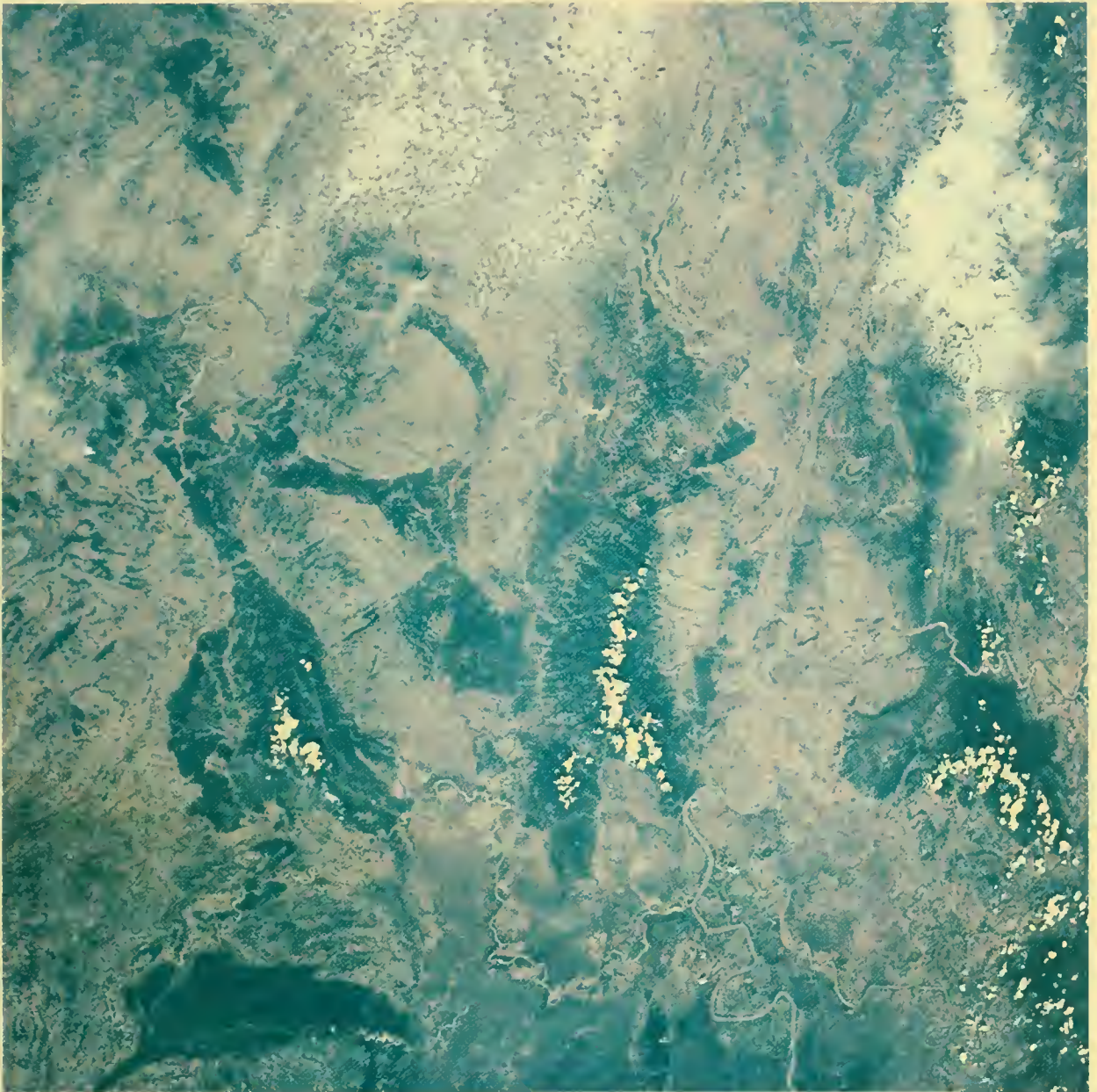
Overlapping the previous frame, this photo of the southeast portion of the United Arab Republic shows volcanic highlands with several large extinct craters. The coast of the Red Sea is visible in the upper right corner.

S-65-34783



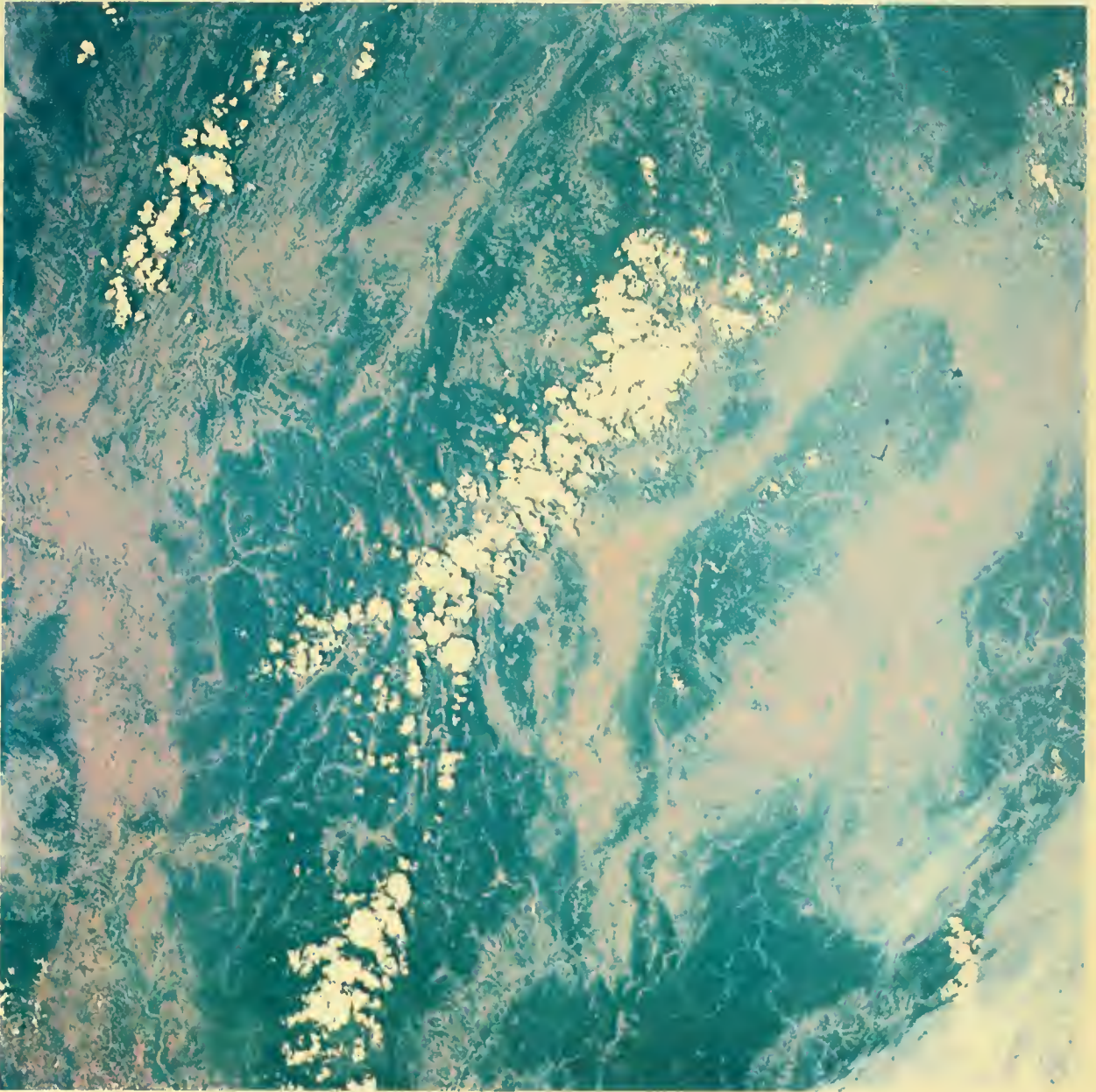
The coast of the United Arab Republic on the Red Sea viewed to the northeast. The peninsula at the right is Ras Banas, north of Foul Bay. At top left are the Hafafit Mountains. The drainage pattern is shown in the rectangular white lines to the right.

S-65-34784



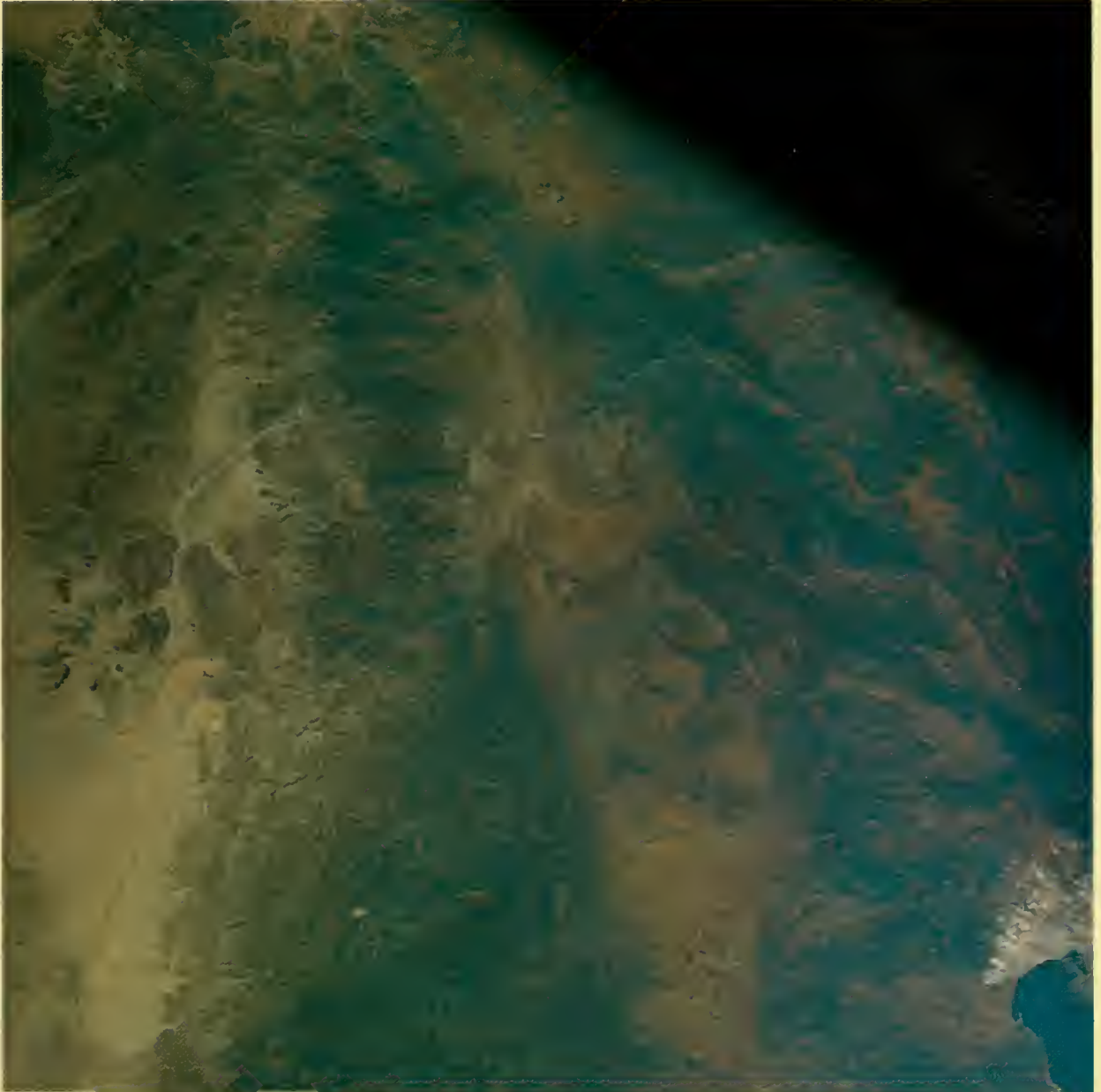
Hunan Province in mainland China, with the Hsiang River flowing north (right side of photo). The city of Hengyang is located at the triangular river junction in the lower right.

S-65-34786



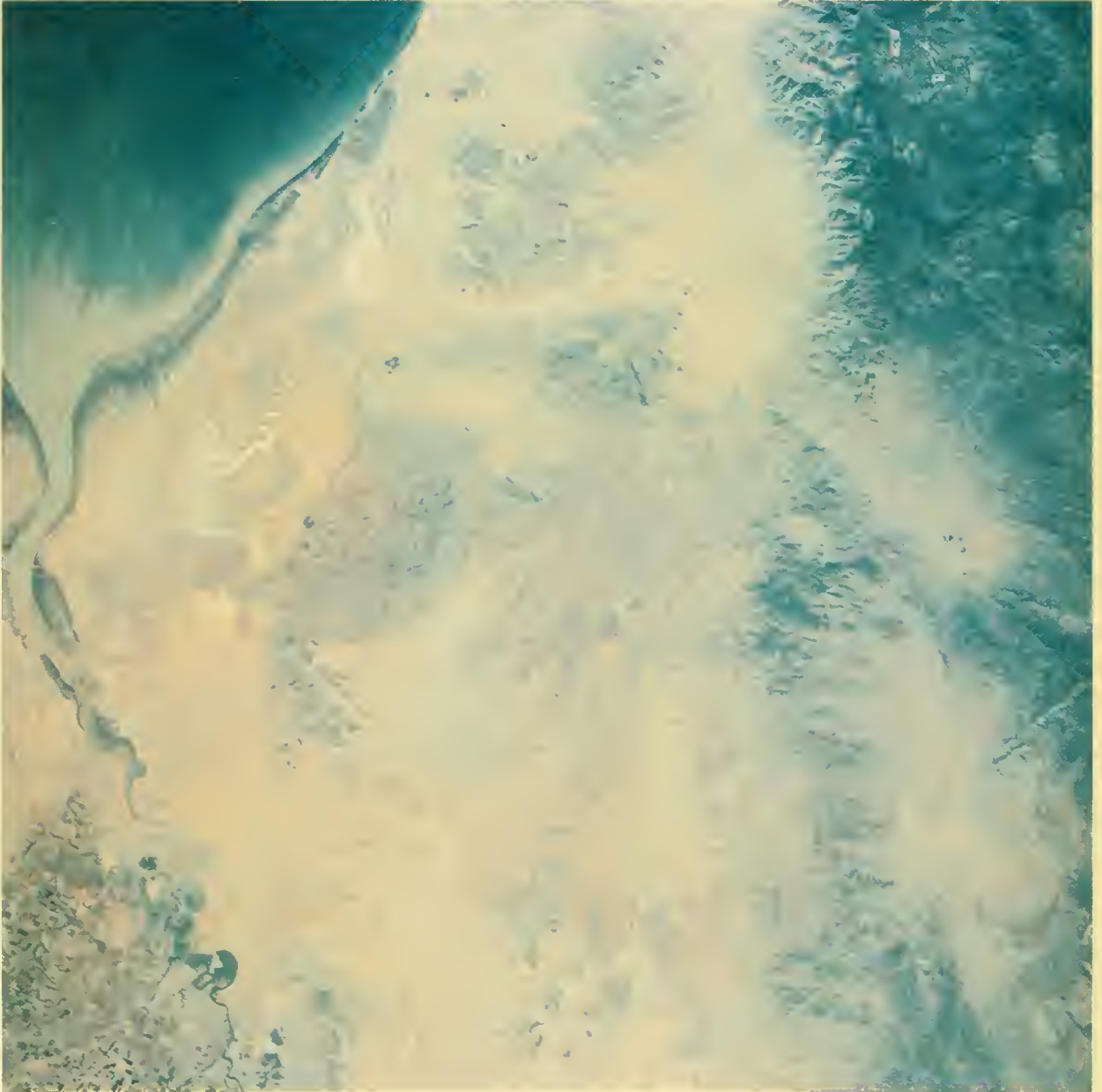
Another view of Hunan Province in mainland China just west of the area shown in the previous frame. The town of Yunghsin lies in the valley at right center. Yuhsien is in the valley at bottom left.

S-65-34787



A photograph of the Mexican State of Baja California just south of the United States border, showing the Sierra de Juarez and Sierra San Pedro Martir. Linear valleys at upper right follow the Agua Blanca fault zone. Bahia de Todos Santos on the Pacific Ocean is visible in the lower right corner. This picture is the first of 39 consecutive stereoscopic frames taken over the southwestern United States and Mexico.

S-65-34671

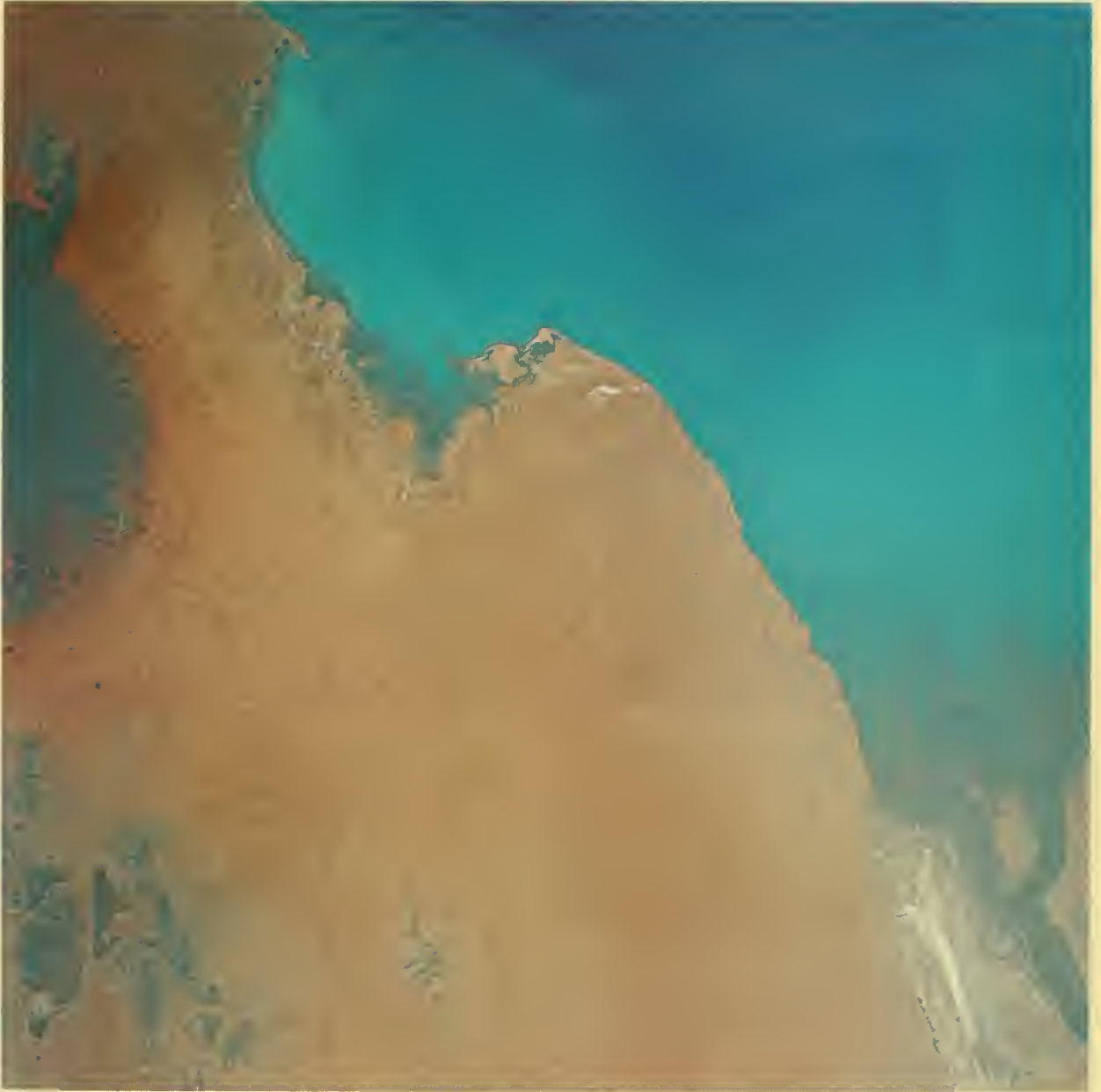


Moving eastward from the previous photograph, this view of northern Baja California just south of Mexicali shows the Sierra San Pedro Martir at the upper right. The Colorado River empties into the Gulf of California to the left. The white sinuous feature to the right of the gulf is a dry meandering stream. S-65-34762

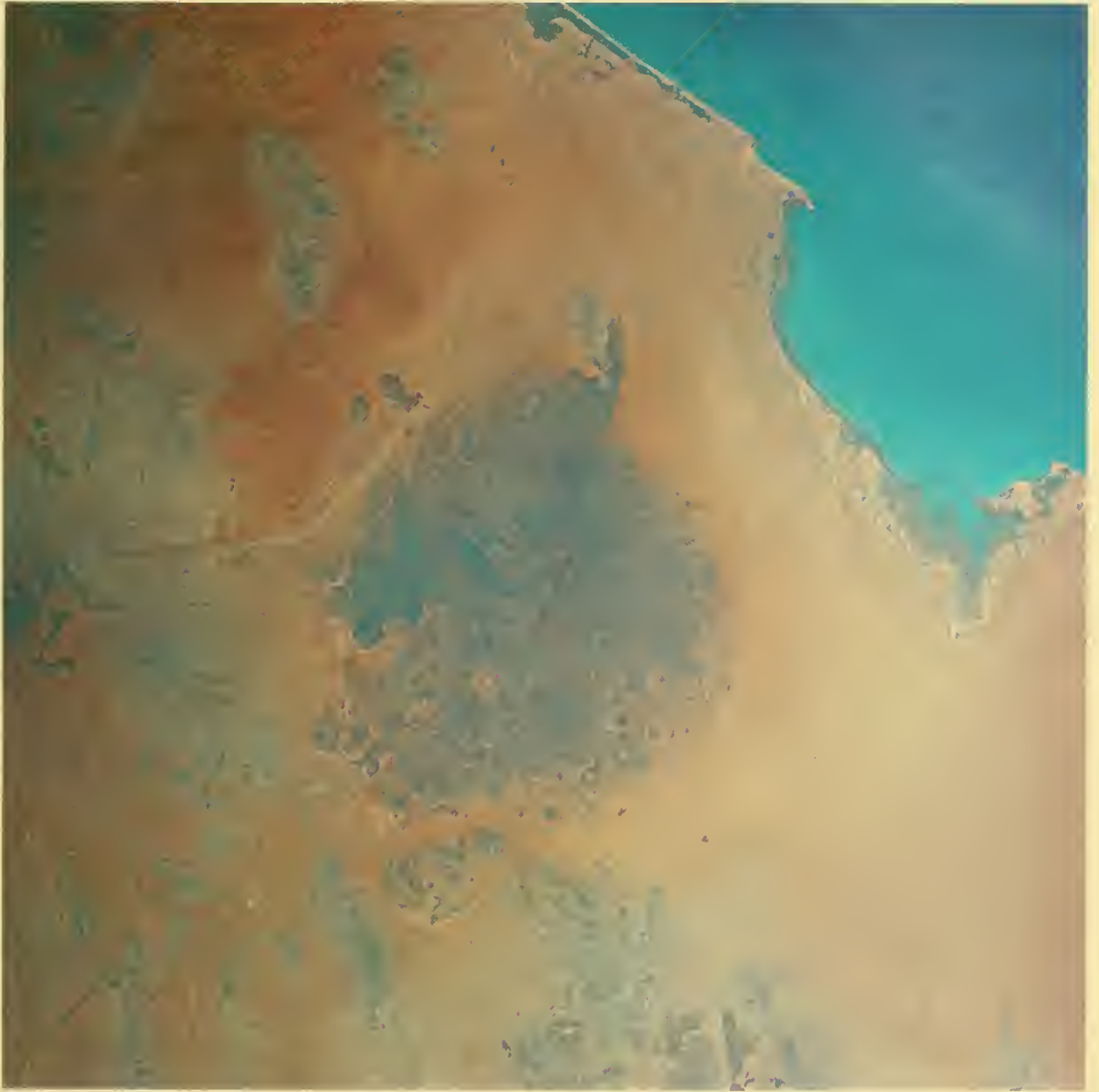


The northern end of the Gulf of California and the mouth of the Colorado River dominate this view. River deposits of silt and underwater detail can be seen clearly. Baja California, Mexico, is on the right; northwest Sonora, Mexico, on the left. The large reddish area is the Great Sonora Desert. The white feature left of the Colorado River is a fault of the San Andreas system.

S-65-34673

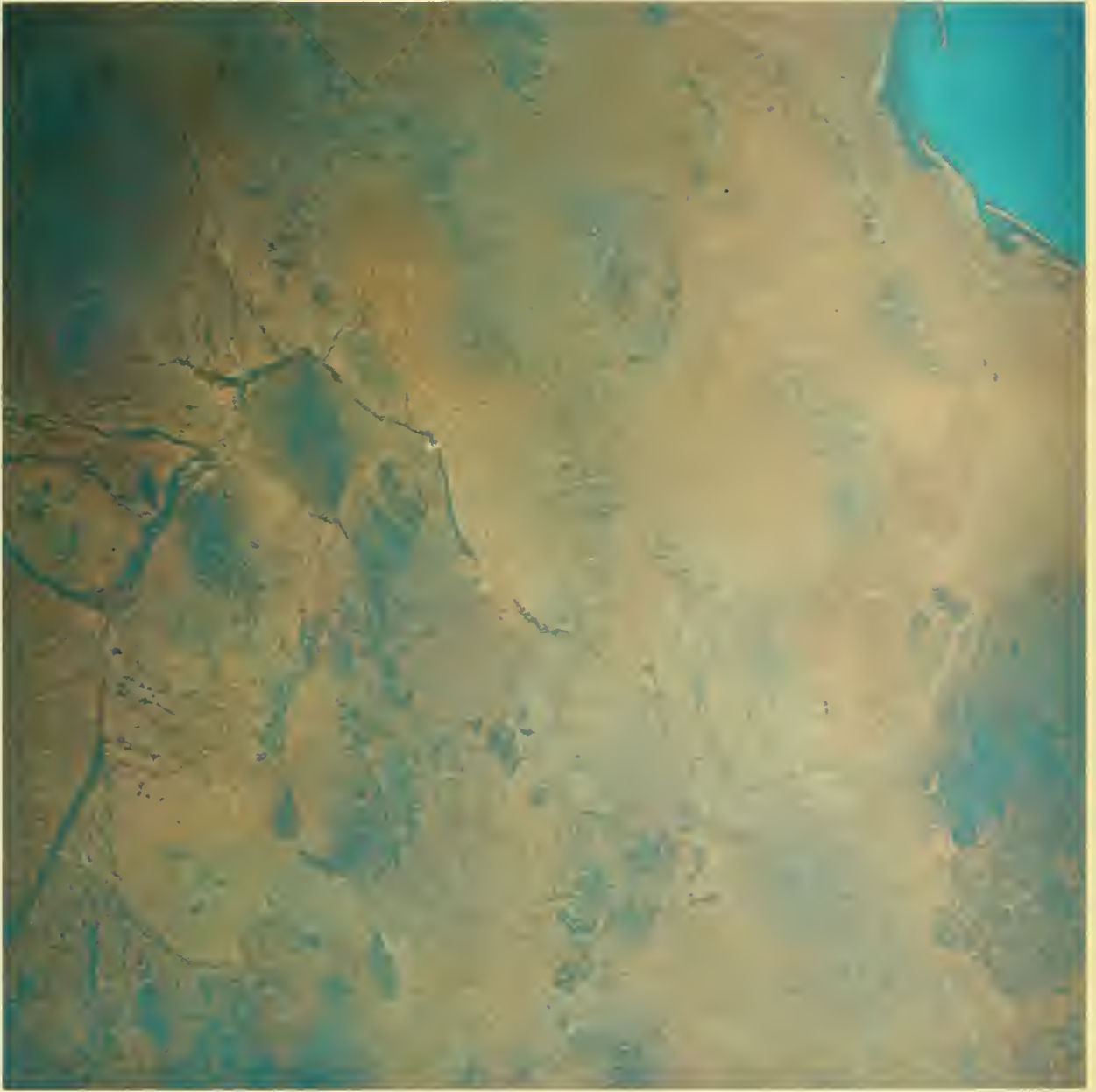


The Great Sonora Desert in Mexico with the Gulf of California to the right. The large dark area is Cerro del Pinacate, a large volcanic field. The bottom topography of Bahia de Adair in the upper left corner is clearly discernible. S-65-34674

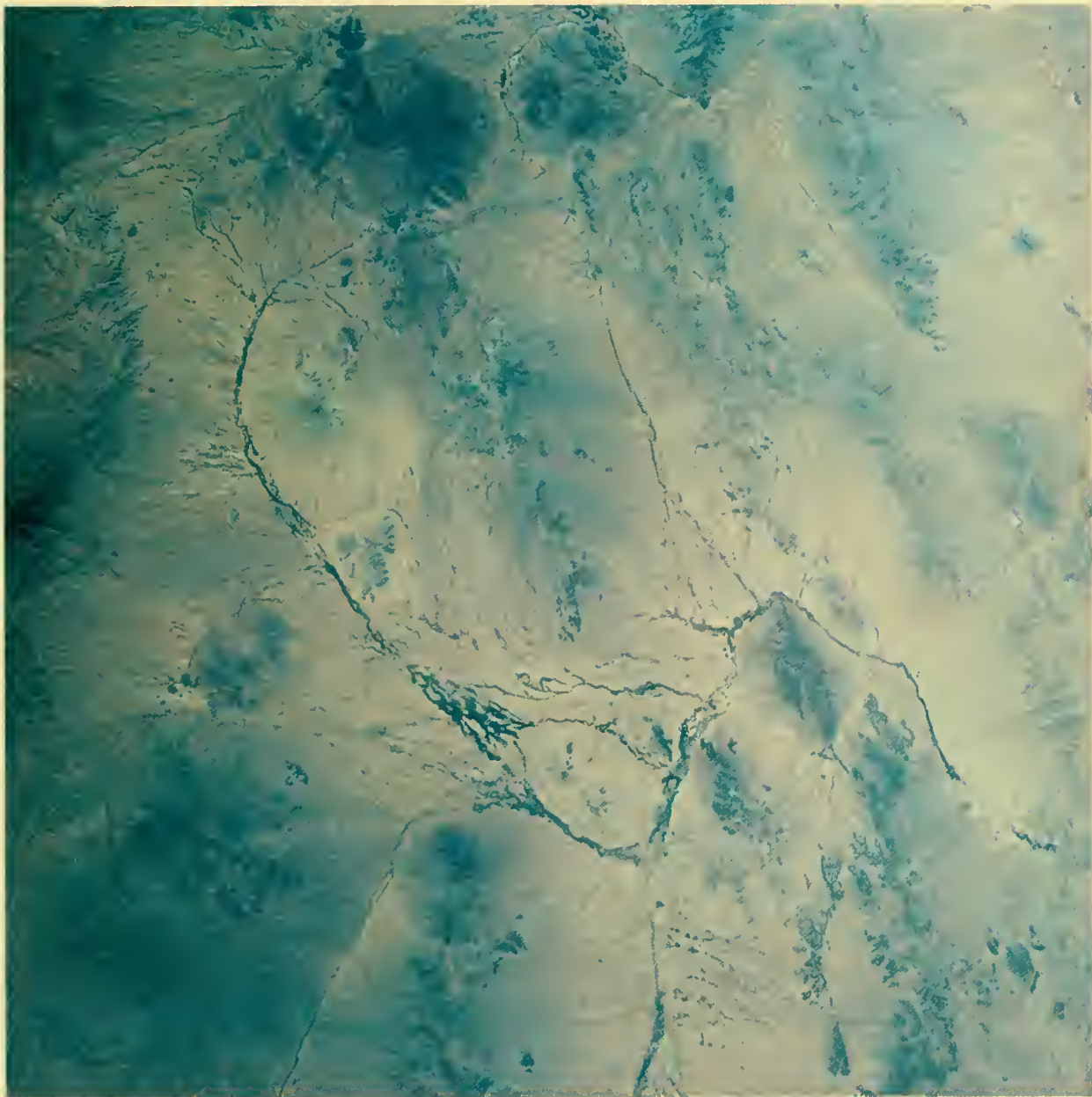


The border area between northwestern Sonora, Mexico, and southern Yuma County, Arizona. Cerro del Pinacate is in the center. The Great Sonora Desert lies at bottom.

S-65-34675

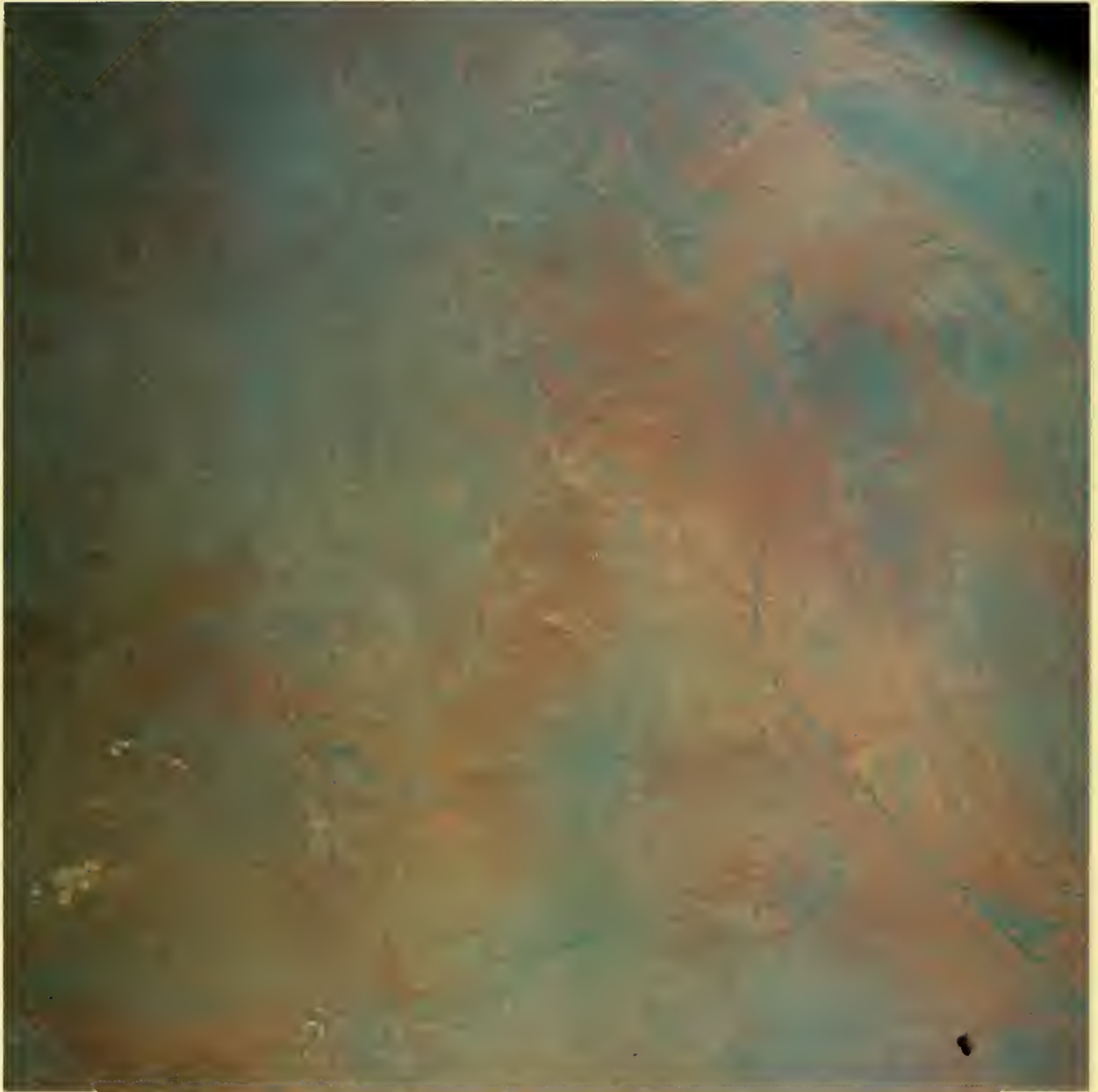


Another view of northern Sonora, Mexico, and southern Arizona, featuring the Sonoyta River. The Gulf of California and Cerro del Pinacate are visible on the right. The Mexico-United States border runs from upper left to lower right. S-65-34676



This frame showing north central Sonora, Mexico, and south central Arizona overlaps the preceding one. In the center is the Sonoyta River.

S-65-34677



Southern Arizona and northern Sonora, Mexico, with the Baboquivari mountain range at the bottom center and the Tucson Mountains to the lower left. The white patches are open pit mines. The Santa Cruz River, outlined by cultivated land, runs along the left edge of the picture. The site of Kitt Peak Observatory is in the lower center.

S-65-34678



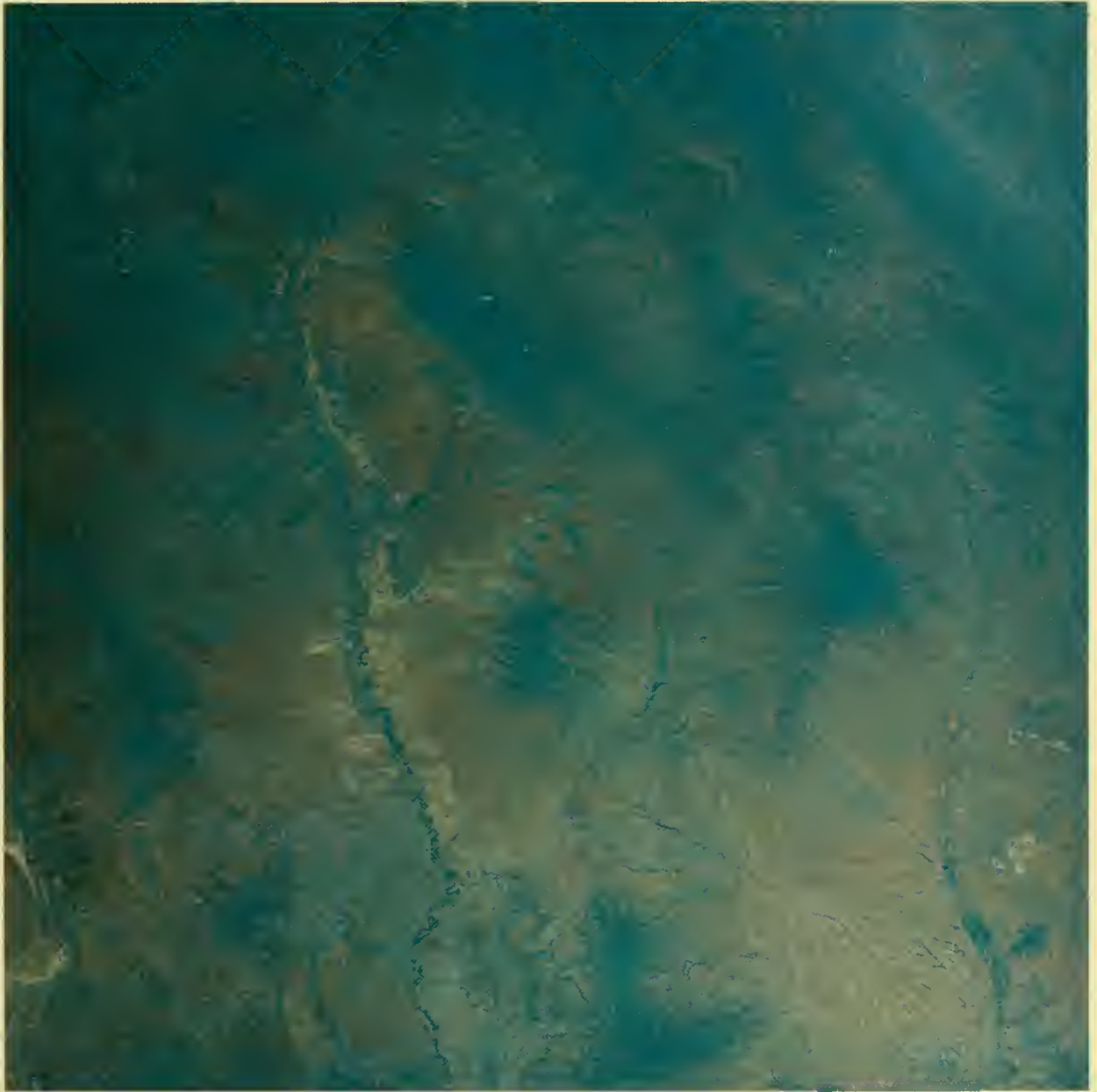
This view of southern Arizona overlaps the one in the preceding photograph. Tucson is at lower left. The Santa Cruz River bisects the picture. The broad, light area to the right of the river is a pediment, an erosional surface veneered with stream gravels, typical of deserts. The small dark patches within this area are lava flows of Quaternary age.

S-65-34679



Southern Arizona east of Tucson. The dark sickle-shaped area at lower left is the Rincon Mountain Range.

S-65-34680

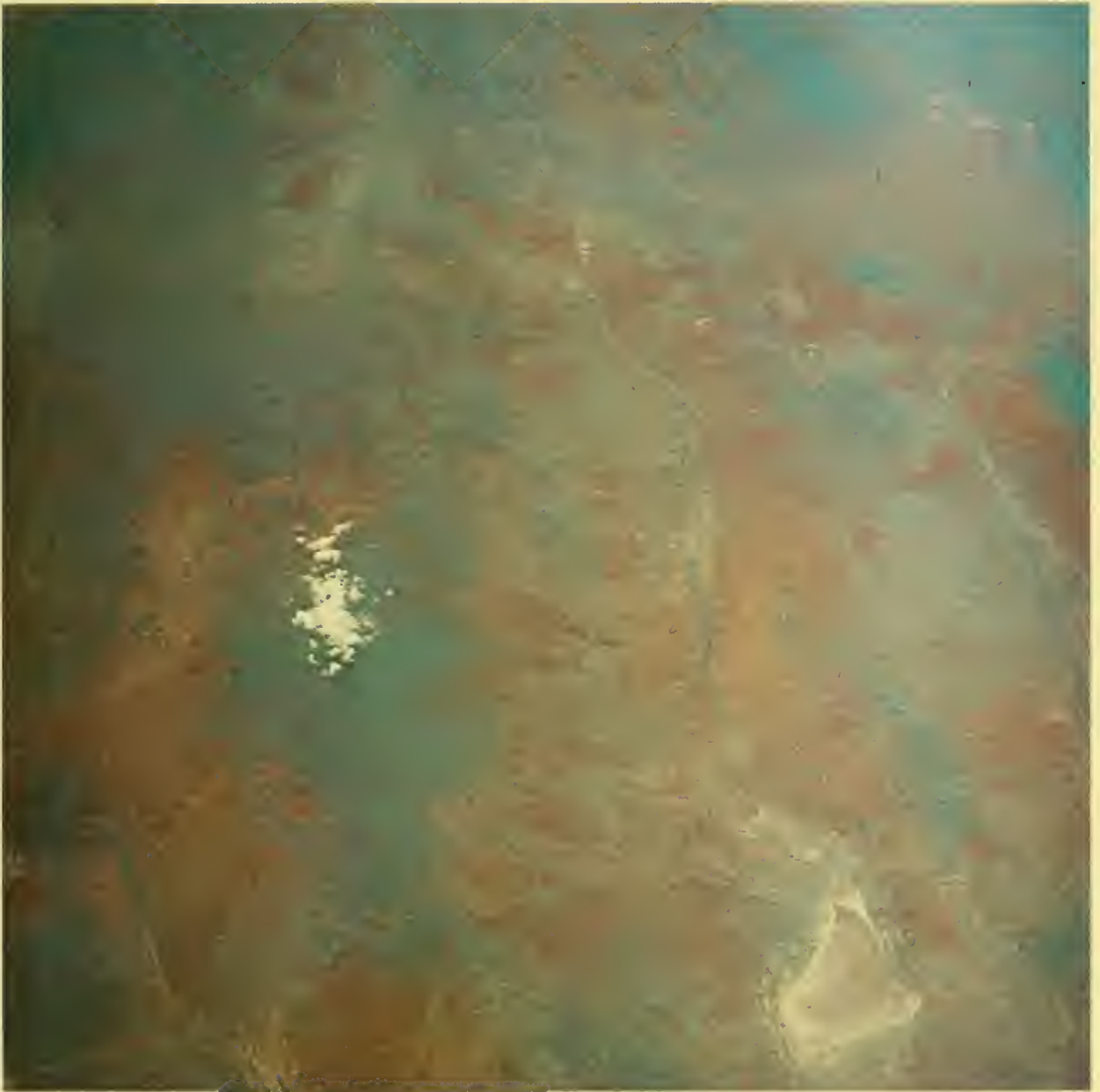


Another view of southeastern Arizona, showing the San Pedro Valley, dotted by farms, at left center. The Willcox Dry Lake is visible in the lower left corner. S-65-34681



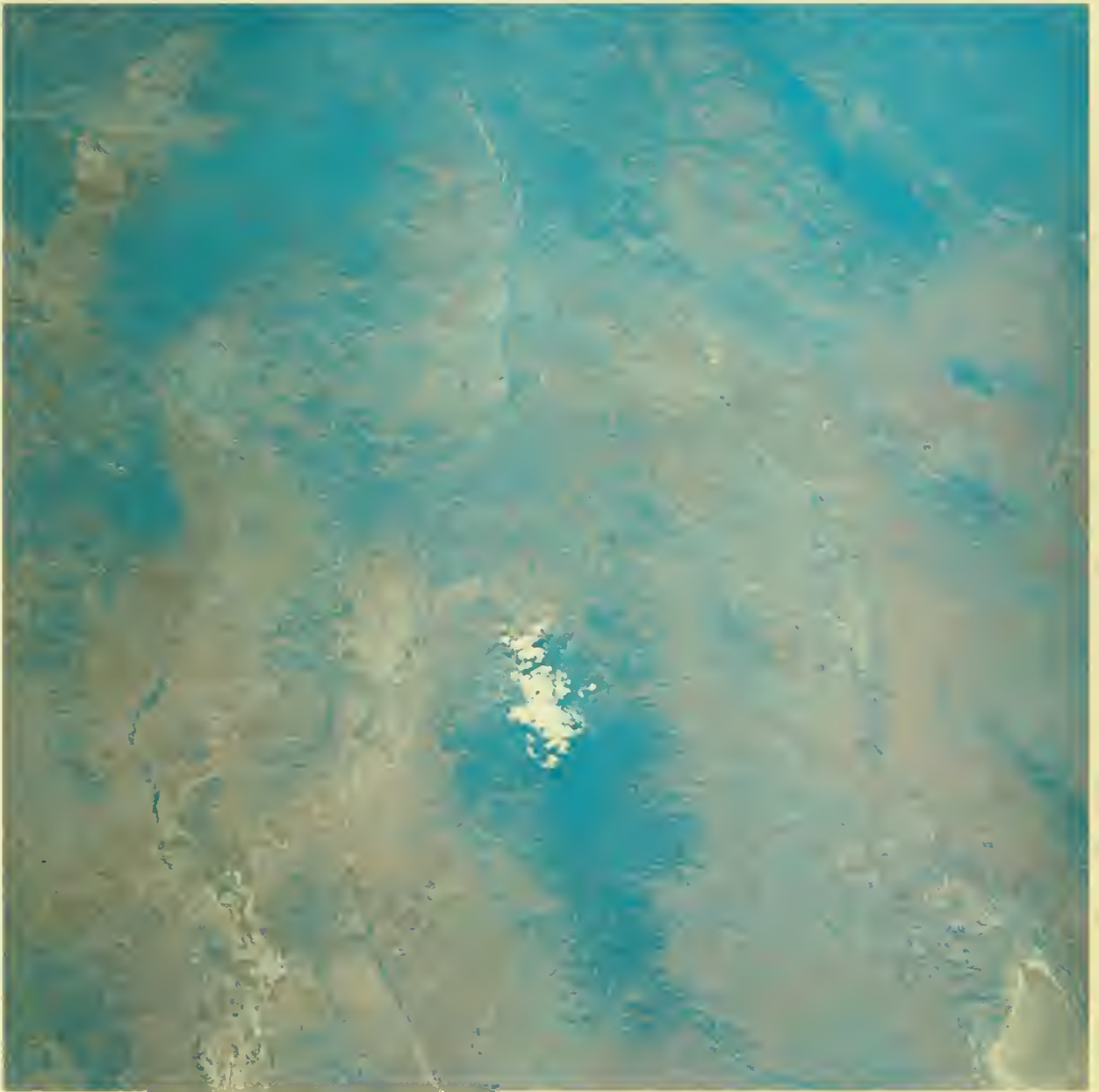
The prominent white feature at the bottom of this photograph is the Willcox Dry Lake in southeast Arizona. The San Pedro Valley is to the left and the Mule Mountains are in the upper center. The mines of Bisbee, Arizona, are visible south of the Mule Mountains.

S-65-34682



The Willcox Dry Lake (lower right) in Arizona with Sulpher Springs below it. The cloud-covered mountains are the Chiricahuas. The New Mexico-Arizona border is to the left.

S-65-34683



This photo largely overlaps the preceding one. The Chiricahua Mountains, under cloud cover, are at the bottom.

S-65-34684



The dark area at lower right is the Chiricahua Mountains in Arizona. In the center of the photograph, running north-south, are the Peloncillo Mountains. To the left of center are the Animas Mountains, including the 8,519-foot high Animas Peak. The Alamo Hueco Mountains are at upper left.

S-65-34685

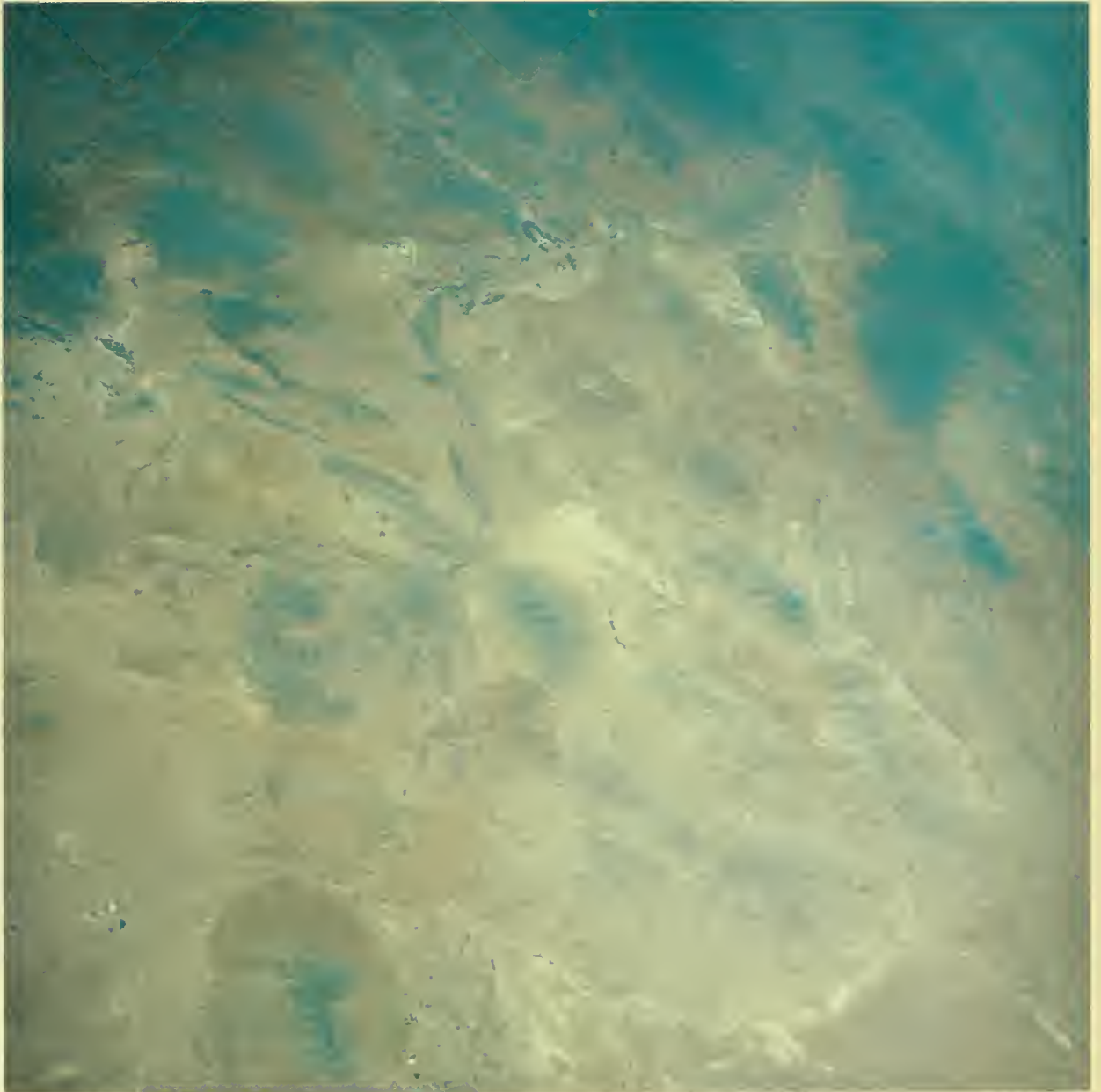


This photograph covers the entire New Mexican Panhandle, as well as parts of northwest Chihuahua and northeast Sonora in Mexico (top of photo). The view is to the southwest.

S-65-34686

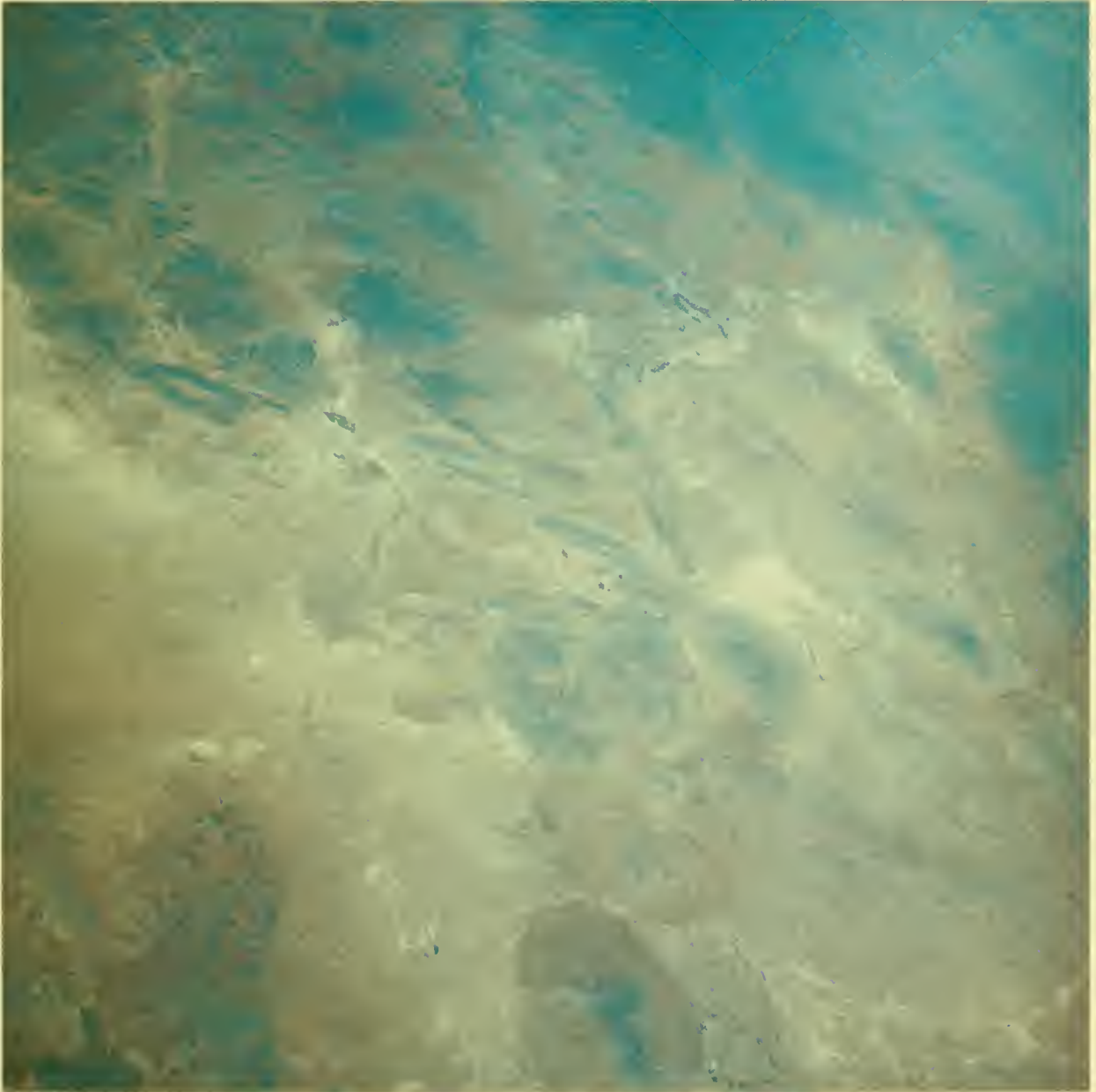


The light-colored linear range at the bottom center of the photograph is the Cedar Mountains in southwest New Mexico. The dark circular hills to the left of this range are the Sierra Carizarilla, a relatively unknown volcanic field of Quaternary age located in Mexico. This picture shows the transition from folded mountains typical of the Sierra Madre Oriental (dark sinuous ridges at upper left) to the block-faulted mountains such as the Cedar Range of the Basin and Range Province. S-65-34687



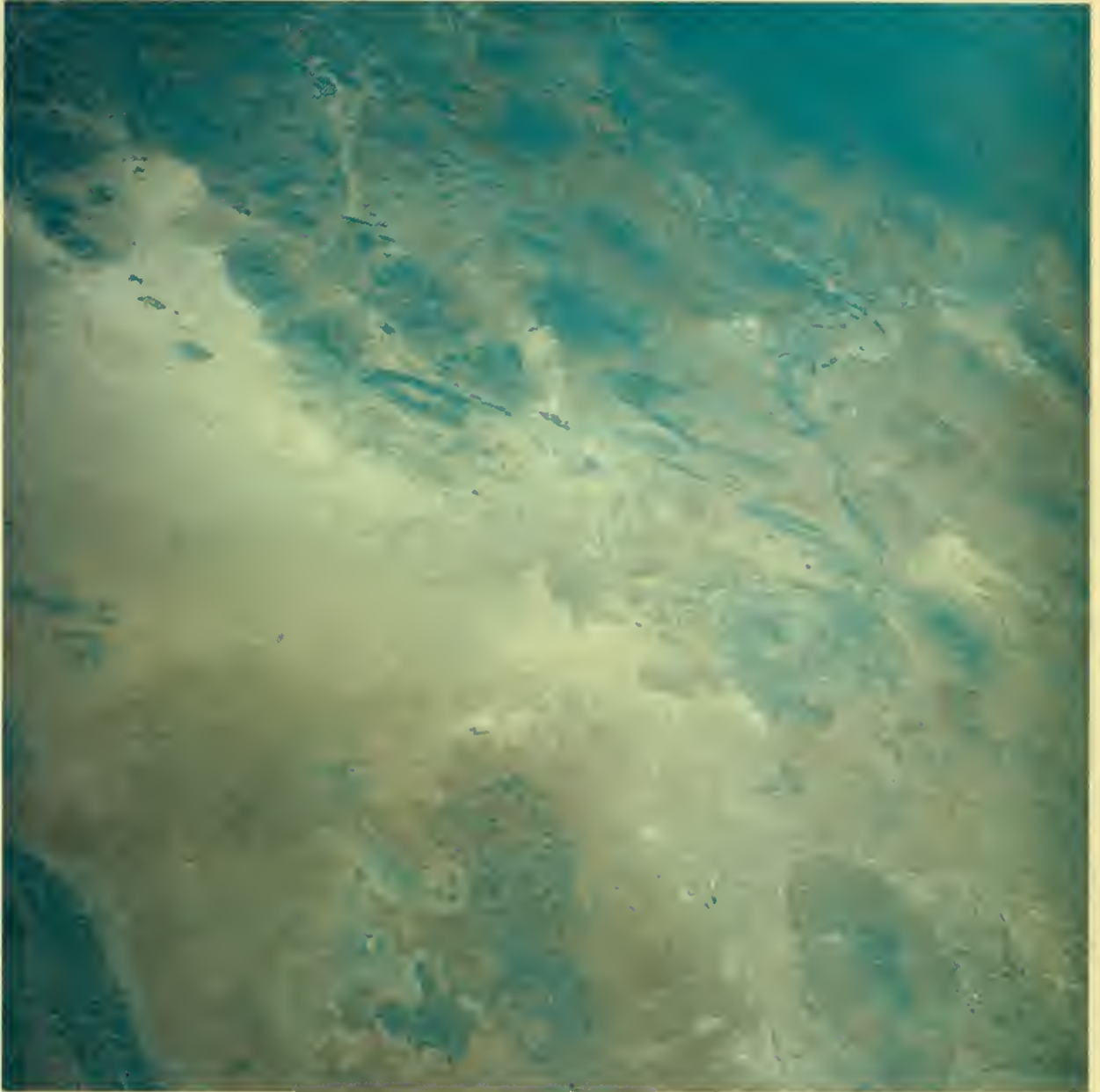
The Florida Mountains in southern New Mexico are at the lower left. The elliptical surfaces surrounding them are pediments. Most of the ranges in this area are folded Cretaceous sedimentary rock or Tertiary or Quaternary volcanic rock. Beginning with this picture the pronounced southward tilt of this series of photographs becomes apparent.

S-65-34688

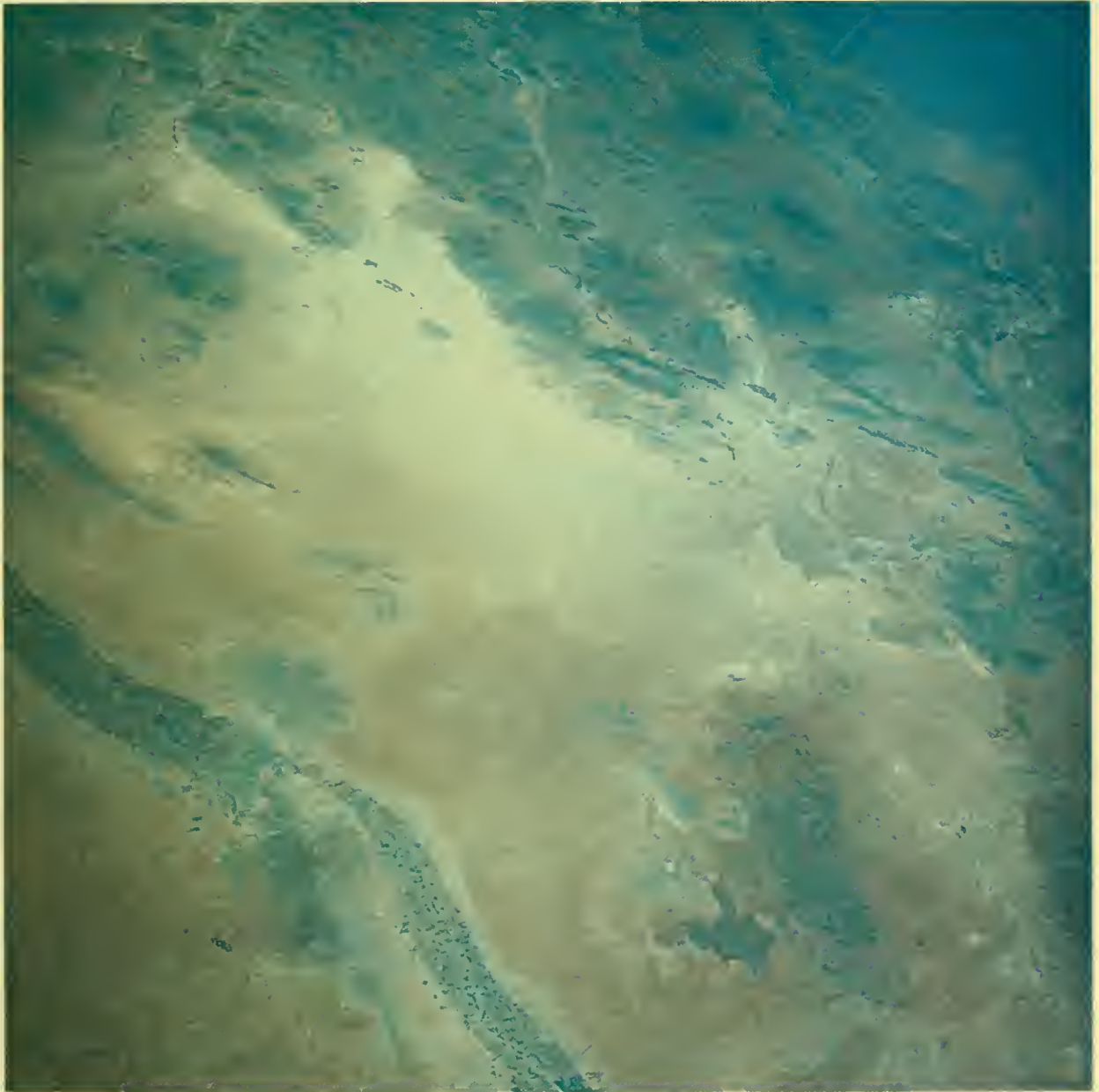


This photograph of south-central New Mexico and northern Chihuahua was taken as the spacecraft was at perigee of approximately 100 nautical miles. At lower left are Quaternary volcanoes of the West Potrillo Mountains. The black rimmed crater in the lower left corner is Kilborne Hole, a maar (explosive volcano) now extinct. The large array of black hills in the center is the Sierra Carizarilla in Chihuahua, Mexico.

S-65-34689



South-central New Mexico and northern Chihuahua, Mexico. The dark hills at bottom center are the West Potrillo Mountains with volcanoes and lava flows of Quaternary age. The Rio Grande is seen in the lower left corner. S-65-34690



Another view of south-central New Mexico, with the West Potrillo Mountains (bottom right). El Paso and Juarez are located at the bend in the Rio Grande where the area of cultivated land increases (lower left). The Franklin Mountains below El Paso are folded Paleozoic sedimentary and igneous rock. The linear ranges in Mexico (left, above the river) consist chiefly of folded Cretaceous sedimentary rock.

S-65-34691



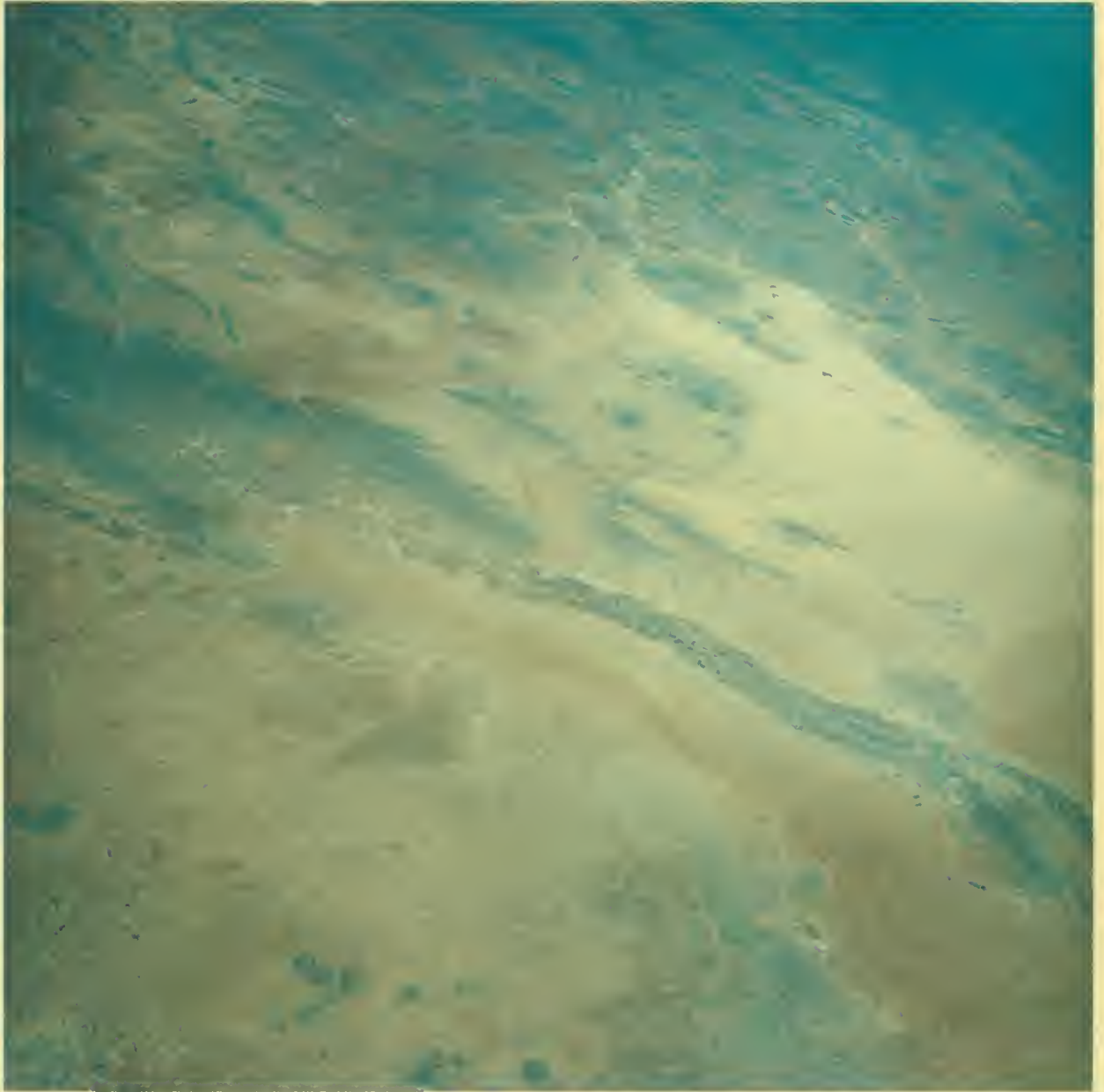
Chihuahua, Mexico, the valley of the Rio Grande, and south-central New Mexico with the Juarez-El Paso metropolitan area (below center). The Tulsa Rosa Valley is to the lower left of El Paso. The dark areas in the far left corner of the picture are the Hueco Mountains, underlain by upper Paleozoic limestone and other sedimentary rock. The Sierra de San Luis are seen at top right.

S-65-34692

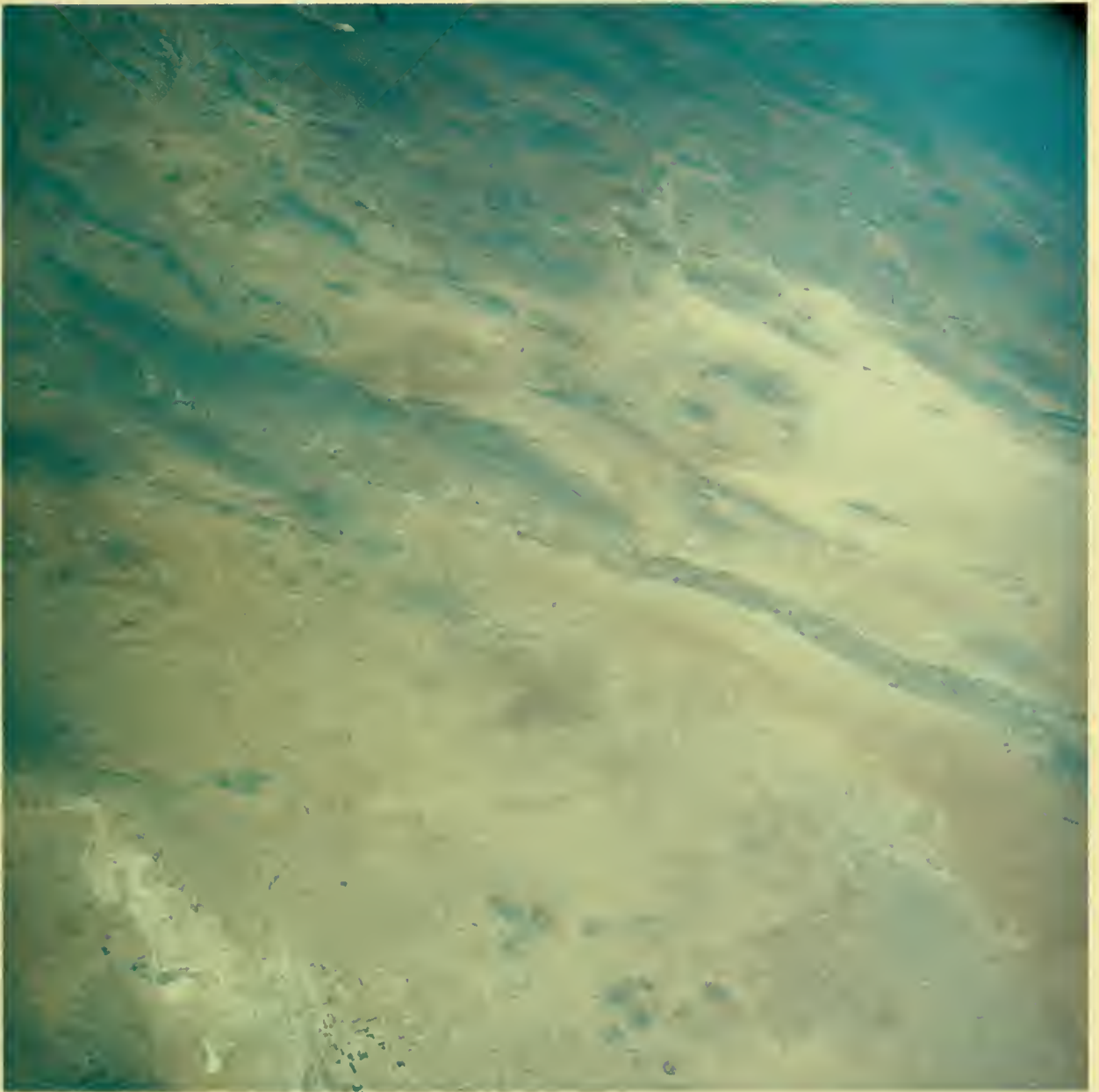


Parts of New Mexico, Texas, and Chihuahua, Mexico, are included in this photograph. The Rio Grande bisects the picture, occupying the Hueco Basin and following the trend of the folded mountains comprising the northwestern part of the Sierra Madre Oriental and the Quitman, Van Horn, and Chinati Ranges in Transpecos Texas.

S-65-34693



South-central New Mexico, northern Chihuahua, Mexico, and west Texas, overlapping the previous frame. The Diablo Plateau, top center, is underlain by upper Paleozoic sedimentary rock, chiefly sandstones and limestones. The Cornudas Mountains, small igneous intrusions of Tertiary age, are seen at the bottom of the photo. S-65-34694



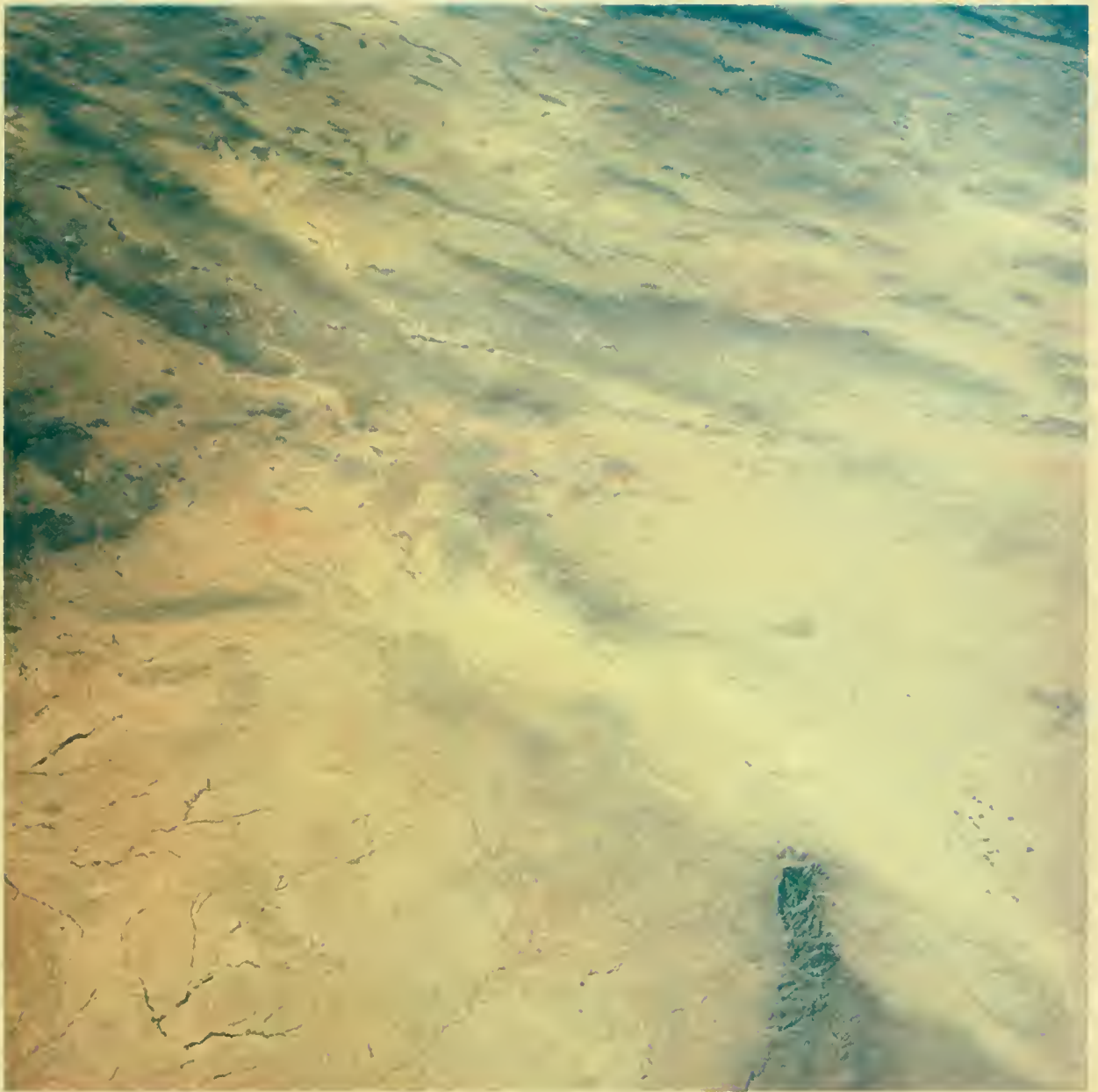
A view to the south with the Cornudas Mountains at bottom center. The foreshortening to the bottom of the picture is a result of camera tilt, which also accounts for the dark color. The white area in the lower left corner is the Salt Basin of west Texas and southern New Mexico.

S-65-34695

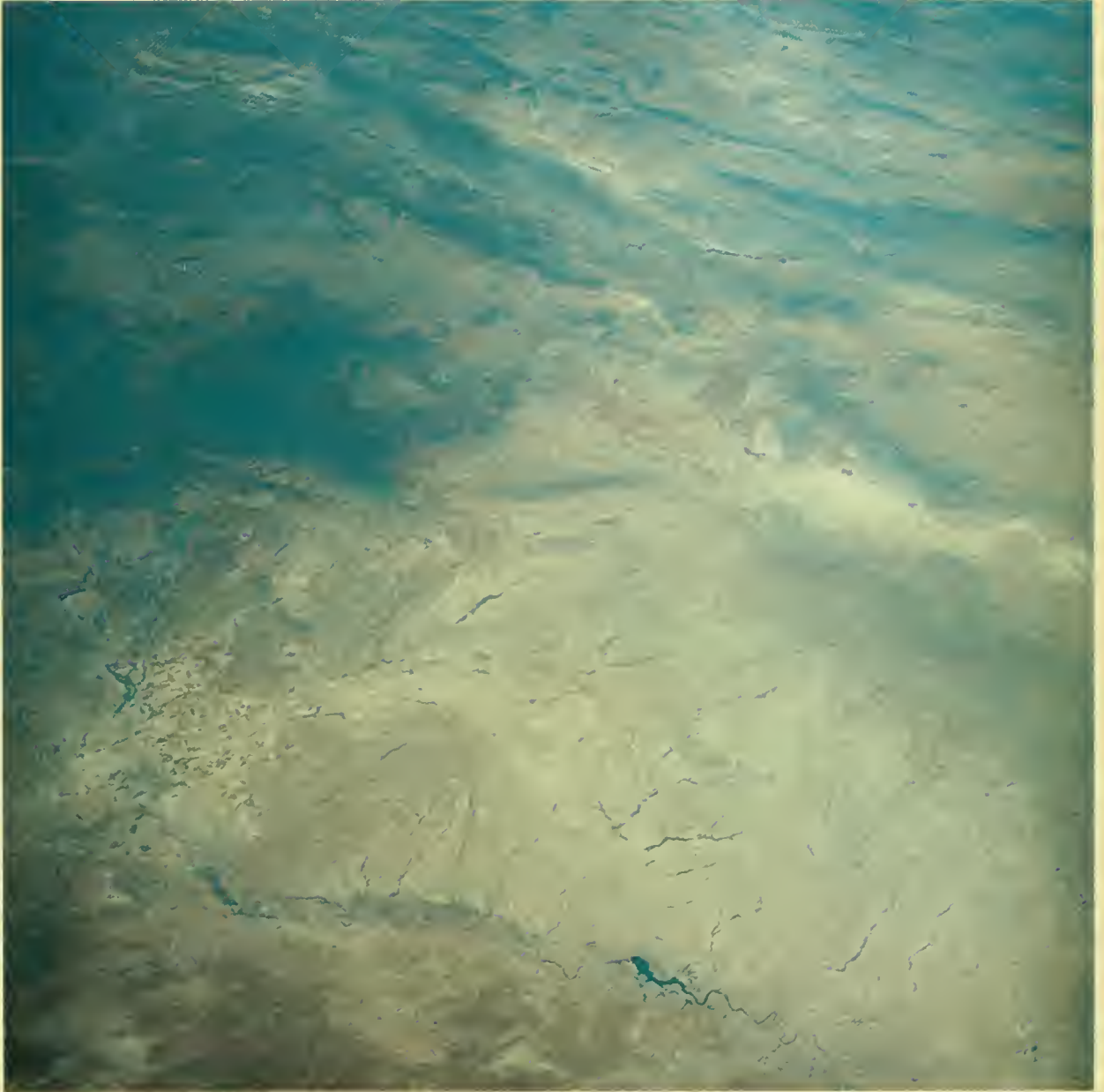


The area shown encompasses parts of southern New Mexico, western Texas, and northeastern Chihuahua, Mexico. The Salt Basin is at bottom center and contains playas. The Delaware Mountains are the dark linear range just northeast of the basin. Guadalupe Peak is visible at bottom center.

S-65-34696

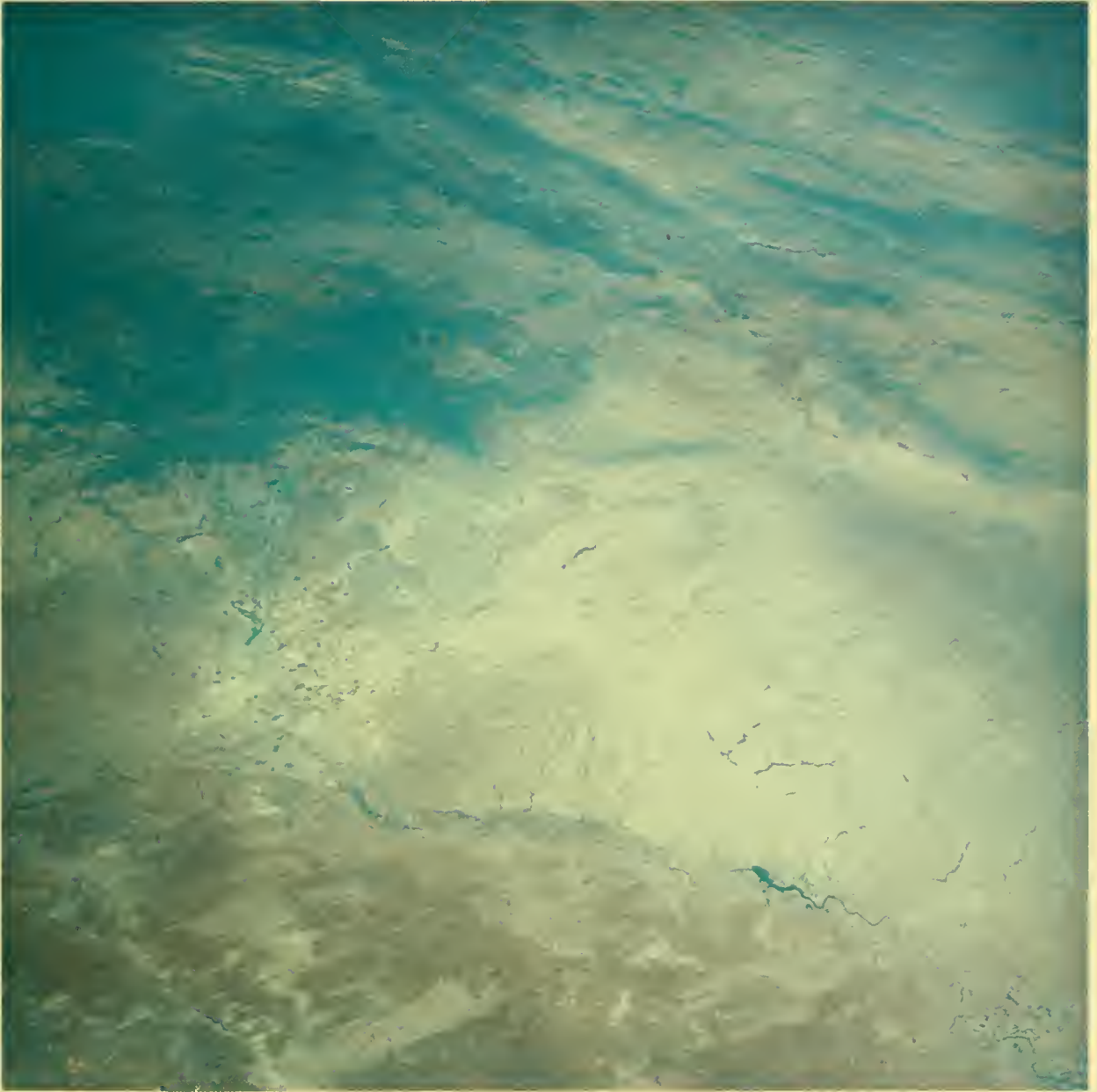


Southeast New Mexico and west Texas with Chihuahua, Mexico, in the background. The Guadalupe Mountains, at lower right, are composed of folded and faulted upper Paleozoic sedimentary rock. The dark northwest-trending range in the center of the photograph, bounding the Salt Basin, is Sierra Diablo. S-65-34697

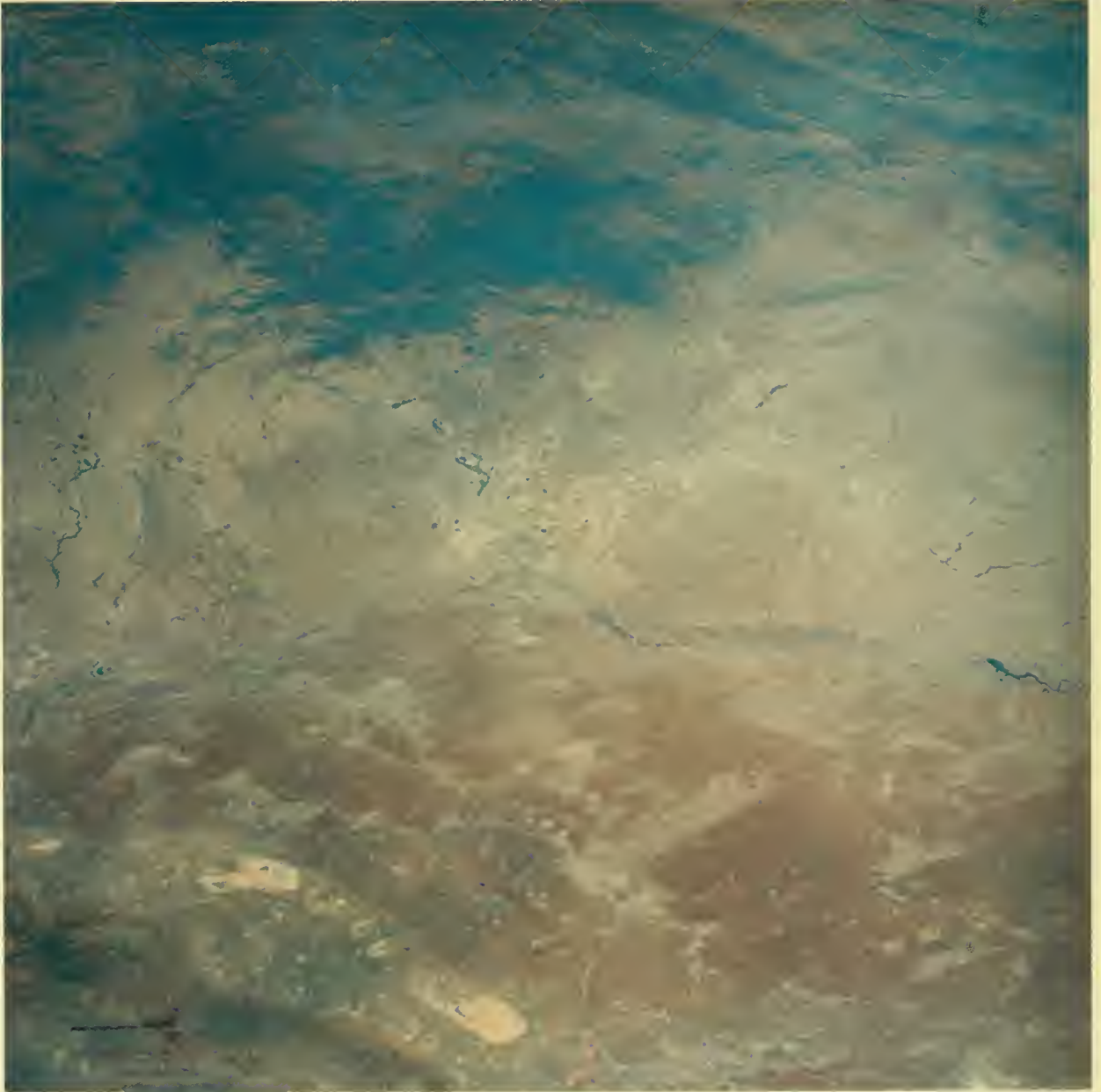


An oblique view to the southwest of New Mexico and Texas. The Rio Grande and the Sierra Madre Oriental are seen at the top of the photo. Red Bluff Lake, formed by a dam on the Pecos River, is at lower right. The dark range at left center is the Davis Mountains, a large volcanic field.

S-65-34698

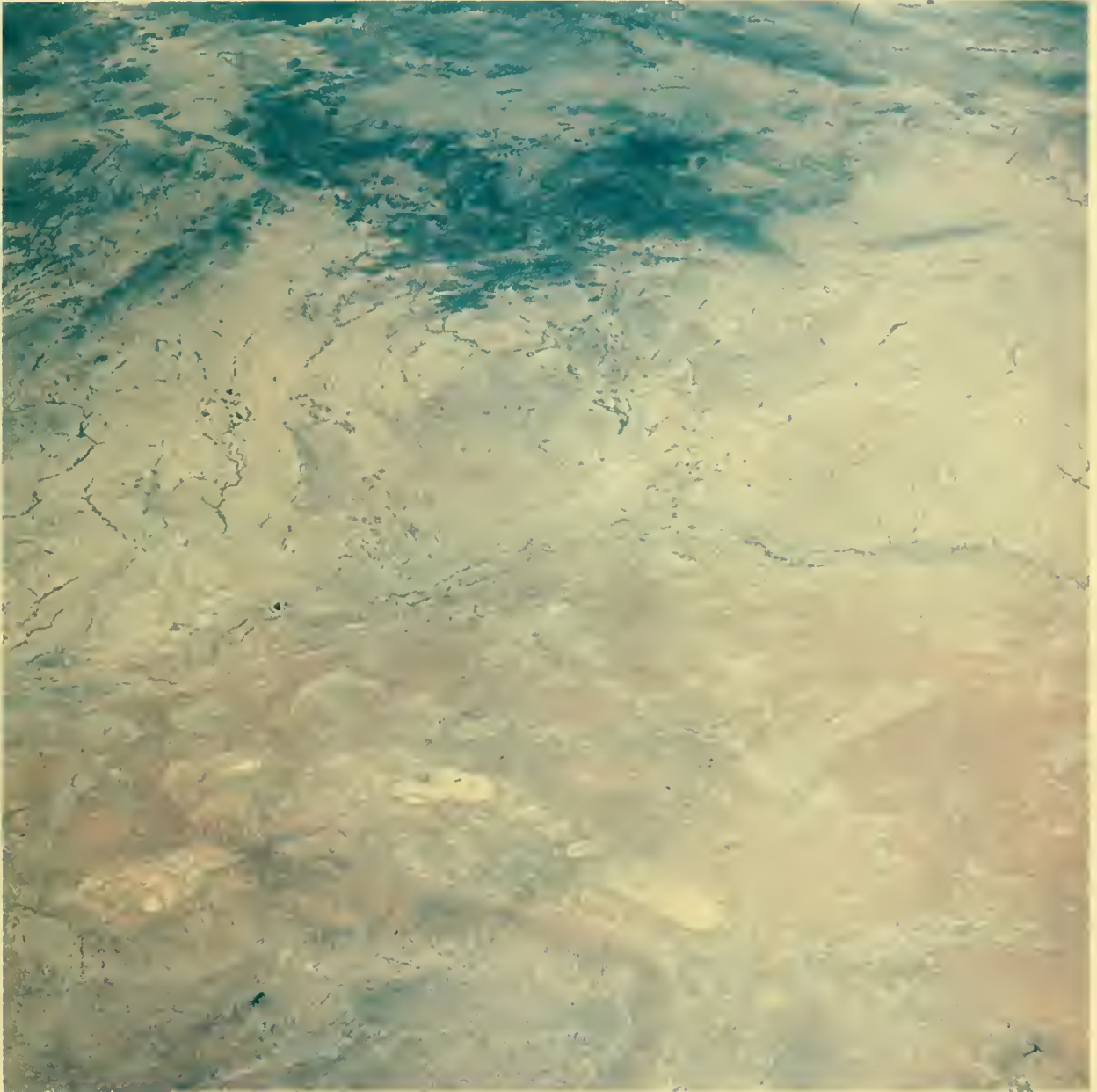


A second view of the Davis Mountains (left of center) and Red Bluff Lake (lower right) near the New Mexico-Texas border. The area above and to the right of the lake is underlain chiefly by gently dipping upper Paleozoic rock. S-65-34699



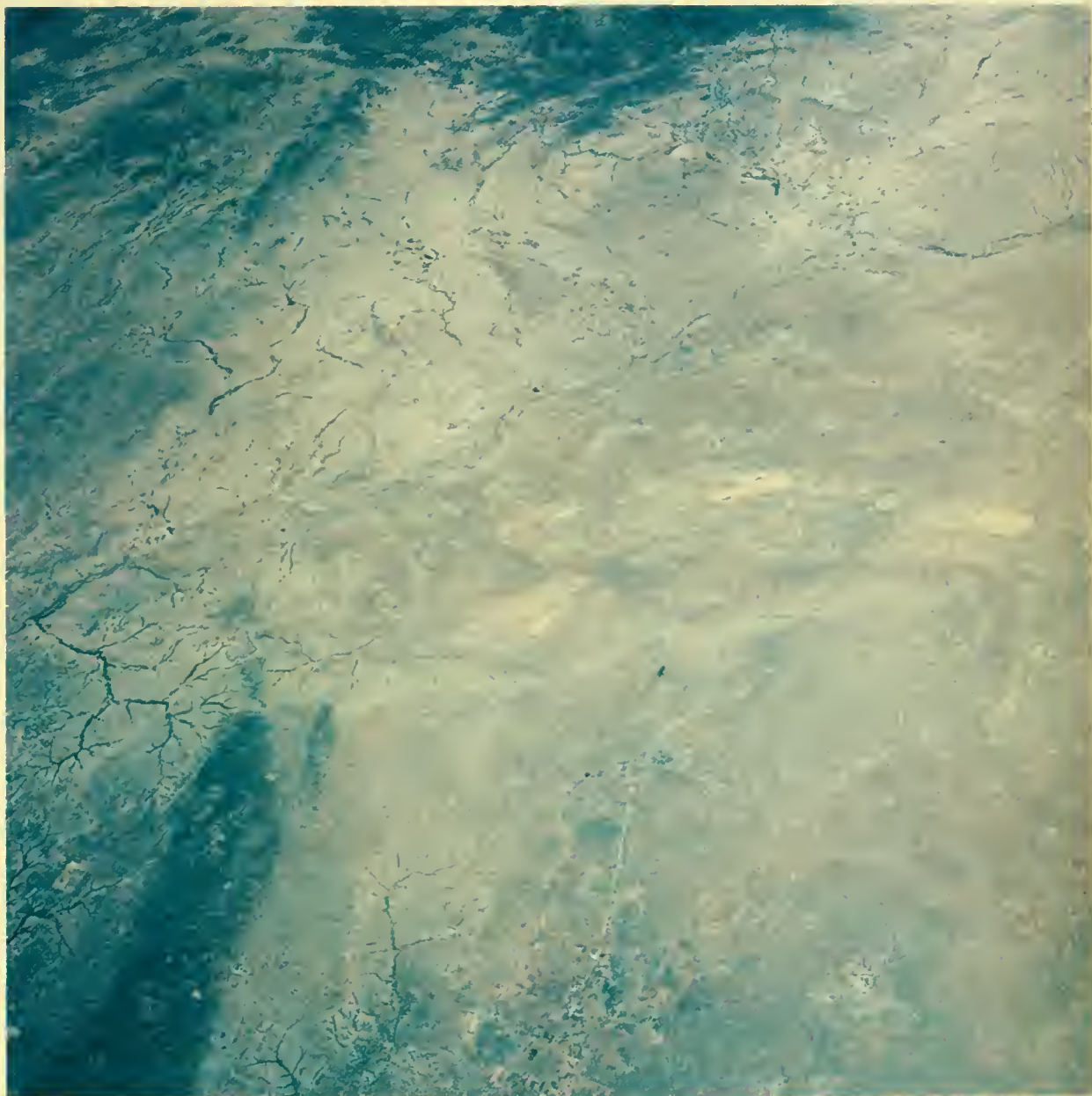
In this oblique view of west Texas, the Davis Mountains are seen at top center. Below them the Toyah Basin is outlined by the patchwork pattern typical of farm land. The white arcuate area to the lower left is a sand dune field. The Mescalero Escarpment at bottom center forms the western boundary of the Staked Plains.

S-65-34700



The rectangular grid array of dots along the bottom edge of this photograph are oil wells in the Permian Basin of west Texas. Smoke from a carbon black plant west of Odessa is visible as a small black smudge at lower left. The linear ridges to the upper left are the Glass Mountains, underlain by Upper Pennsylvanian sedimentary rock. Above and to the left of these ridges are the folded Paleozoic rock of the Marathon Basin, considered to be structurally an extension of the Appalachian Mountain Range.

S-65-34701



This photograph gives a clear view of Midland and Odessa in Texas (bottom and lower center, respectively) and the highways and railroads connecting the two cities. The dark patch at lower left is damp soil reflecting the path of heavy rain the previous day. The rectangular pattern and dots in the lower right corner are oil and gas wells of the Permian Basin.

S-65-34702



An oblique view to the southwest, with the Edwards Plateau area of west Texas to the lower left. A dendritic drainage pattern is accentuated by vegetation and valleys in this semi-arid region. The Stockton Plateau is at upper left. Both plateaus are underlain chiefly by flat-lying Cretaceous sedimentary rock. S-65-34703



The area of Texas covered in this photograph almost completely overlaps the previous frame. Reservoirs are visible in the lower right. The Concho River drainage system is to the lower left.

S-65-34704



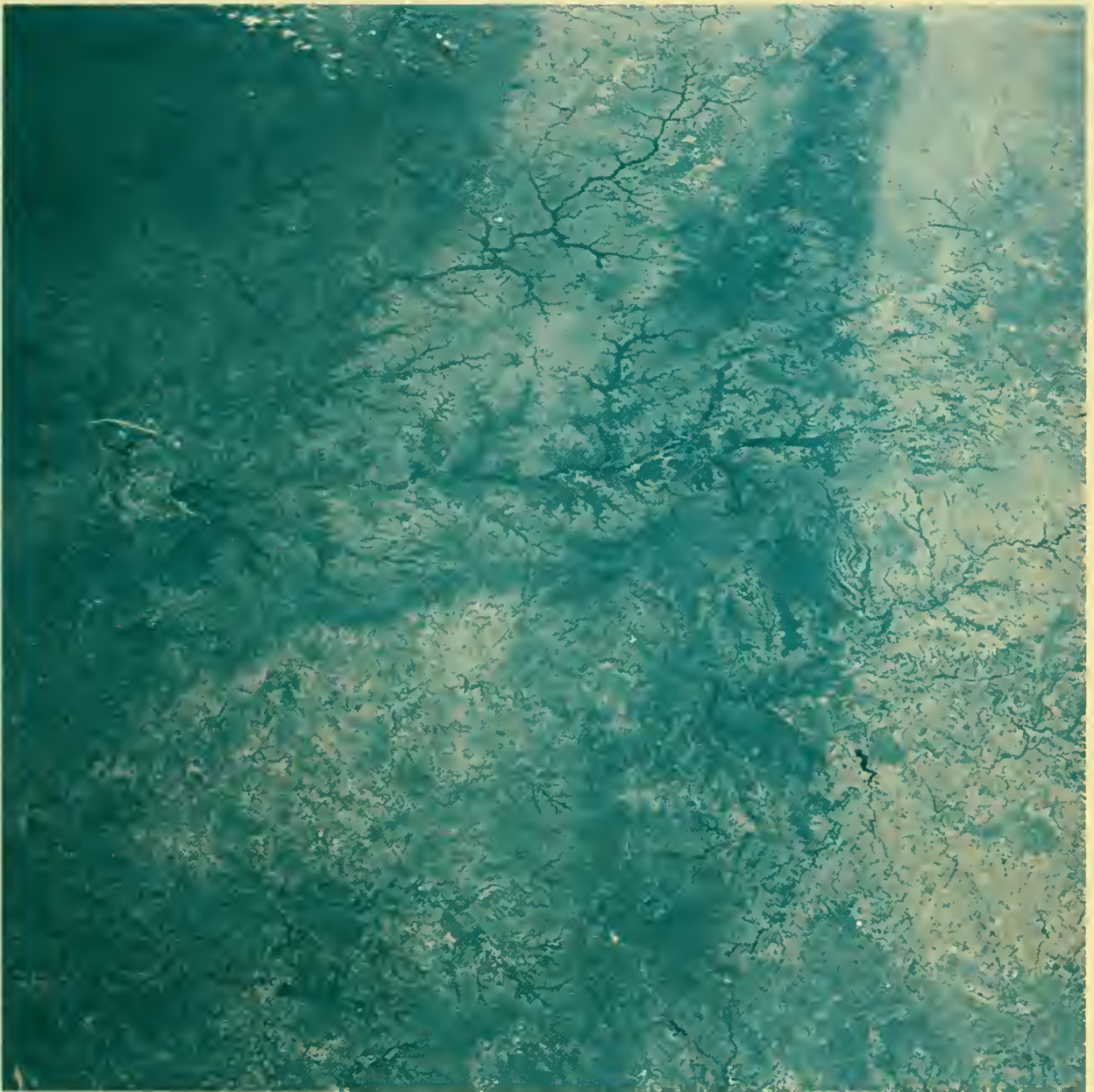
The Edwards Plateau region of west Texas. The dark area to the lower left is a continuation of rain-darkened ground shown in the preceding photographs.

S-65-34705



Another view of the Edwards Plateau in west Texas, moving toward San Angelo.

S-65-34706



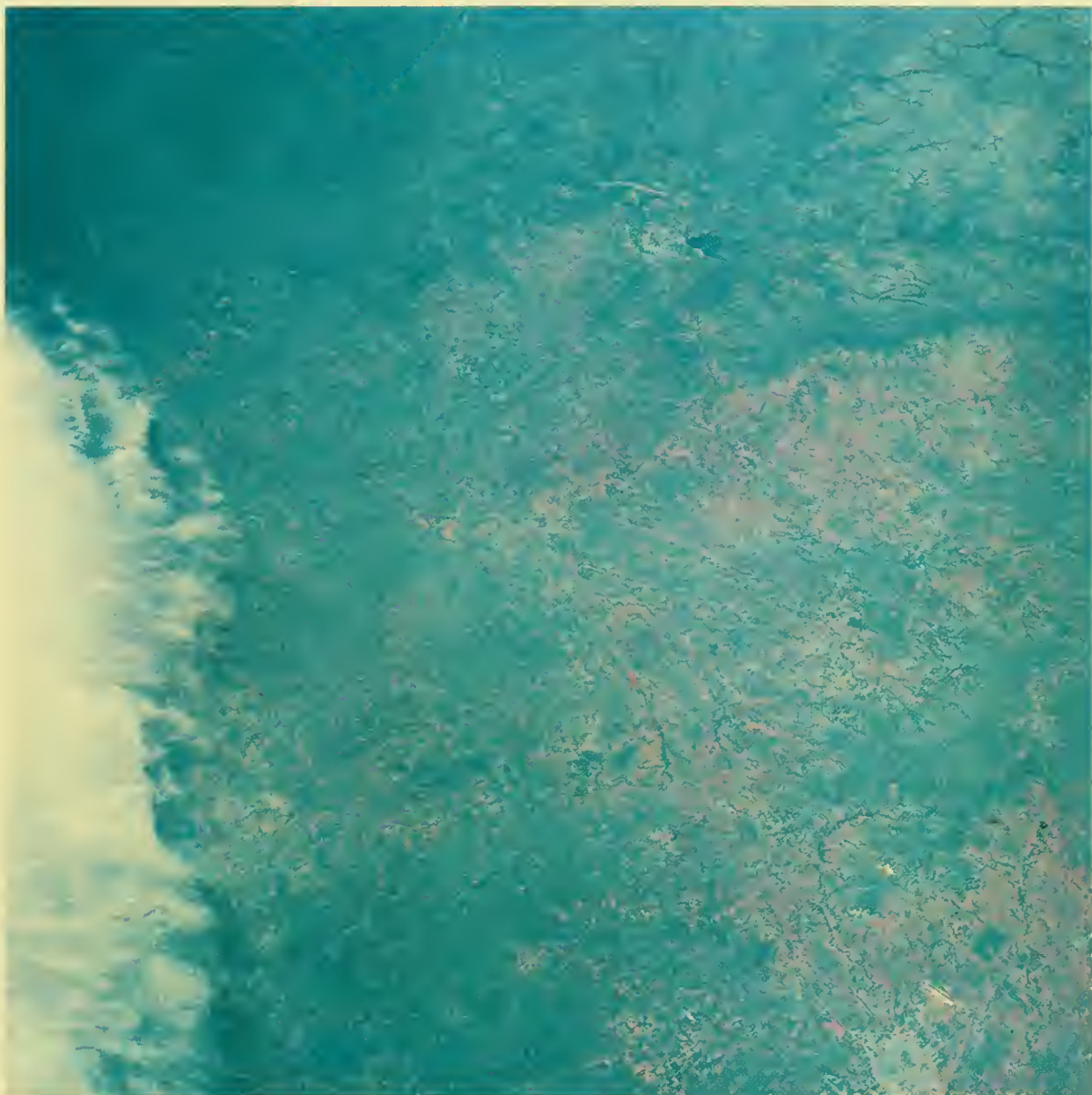
The city of San Angelo, Texas, is seen on the left. A flood control project (white line) at the junction of the North, Middle, and South Concho Rivers will form the San Angelo Reservoir. The circle shown below the city is a tire-testing track.

S-65-34707



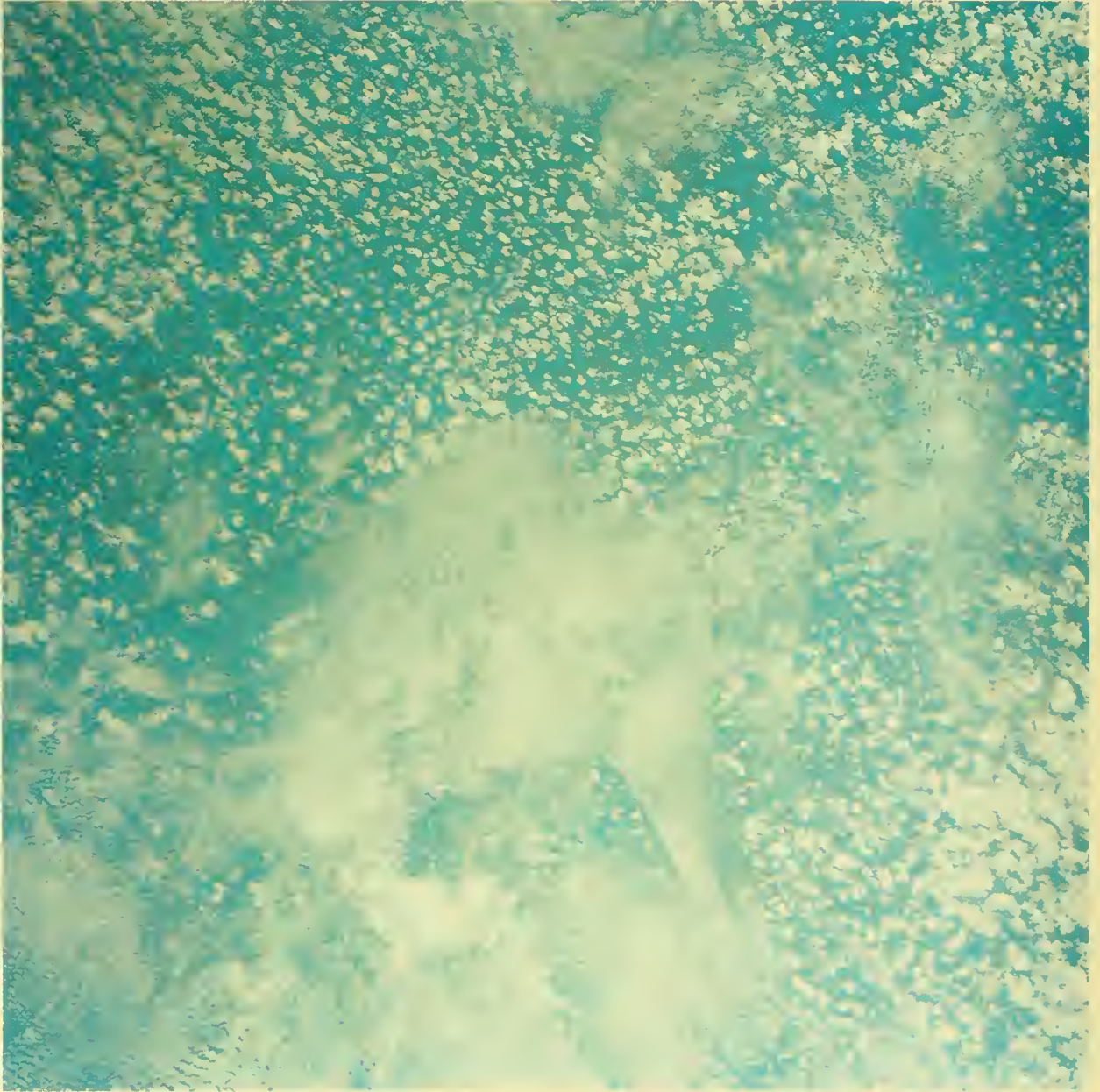
A second view of San Angelo, Texas, with numerous highways visible. The Concho River system, which joins at San Angelo, branches off in the upper half of the picture.

S-65-34708



Abilene, Texas, is seen in the lower right corner of this photograph, the last of a continuous series of 39 stereoscopic frames taken during a 4-minute time period. Further coverage of the southwestern United States was not possible because of intervening clouds, visible to the left.

S-65-34709

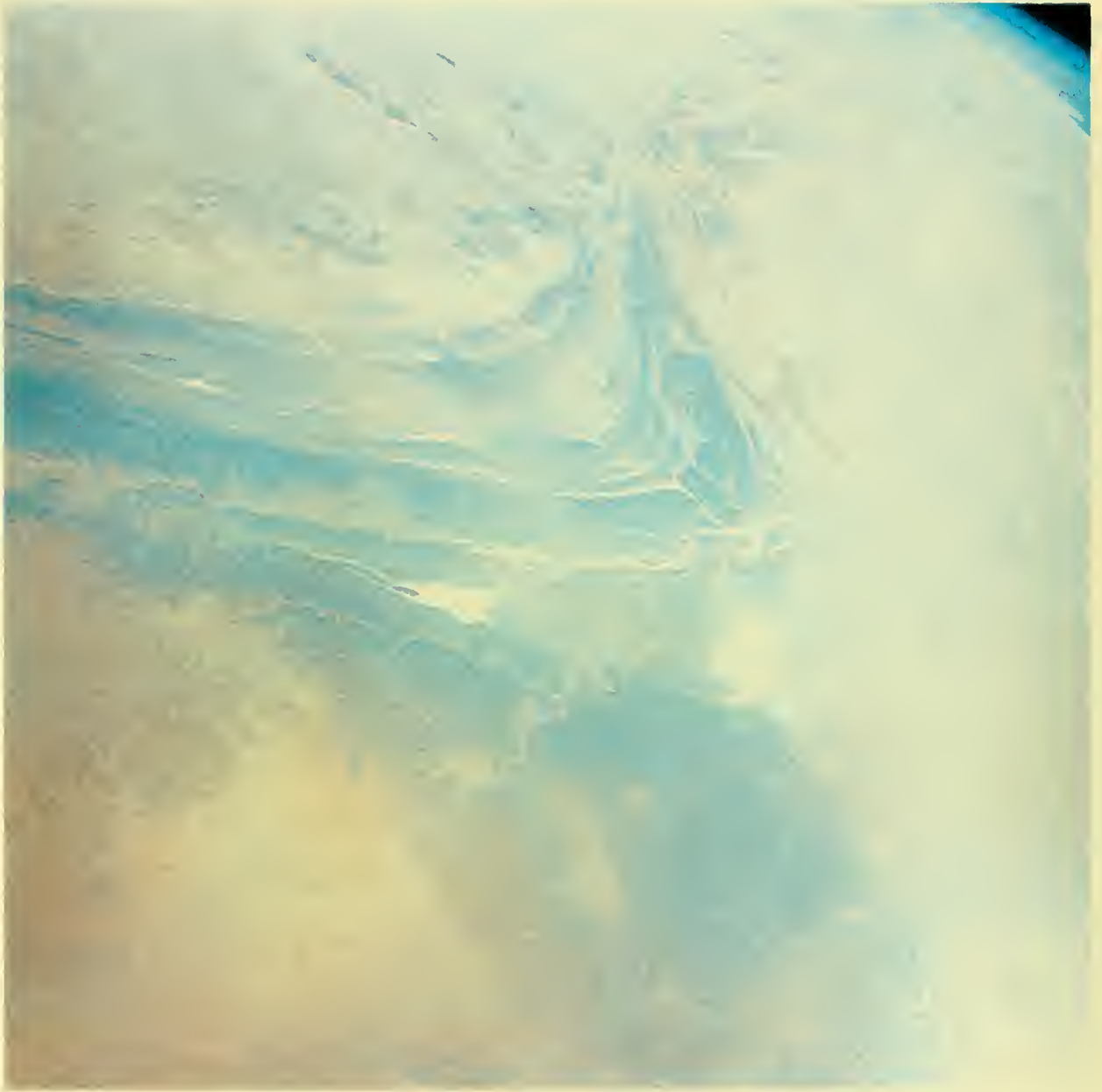


Layers of cumuloform clouds cover parts of western Florida, southern Alabama, and southwestern Georgia. The occasional banded structure of the higher cloud level is seen clearly. Part of the Jim Woodruff Reservoir is visible left of center. S-65-34712



This photograph of central Florida, with Cape Kennedy in the foreground, shows the development of convective clouds during the day. The alignment of the cumulus cloud rows in an east-west direction and the lack of extensive cloud development along the Atlantic coastline suggest that the low-level winds are easterly. The Lake Okeechobee area to the left is cloud-free because the underlying surface is relatively cool.

S-65-34717



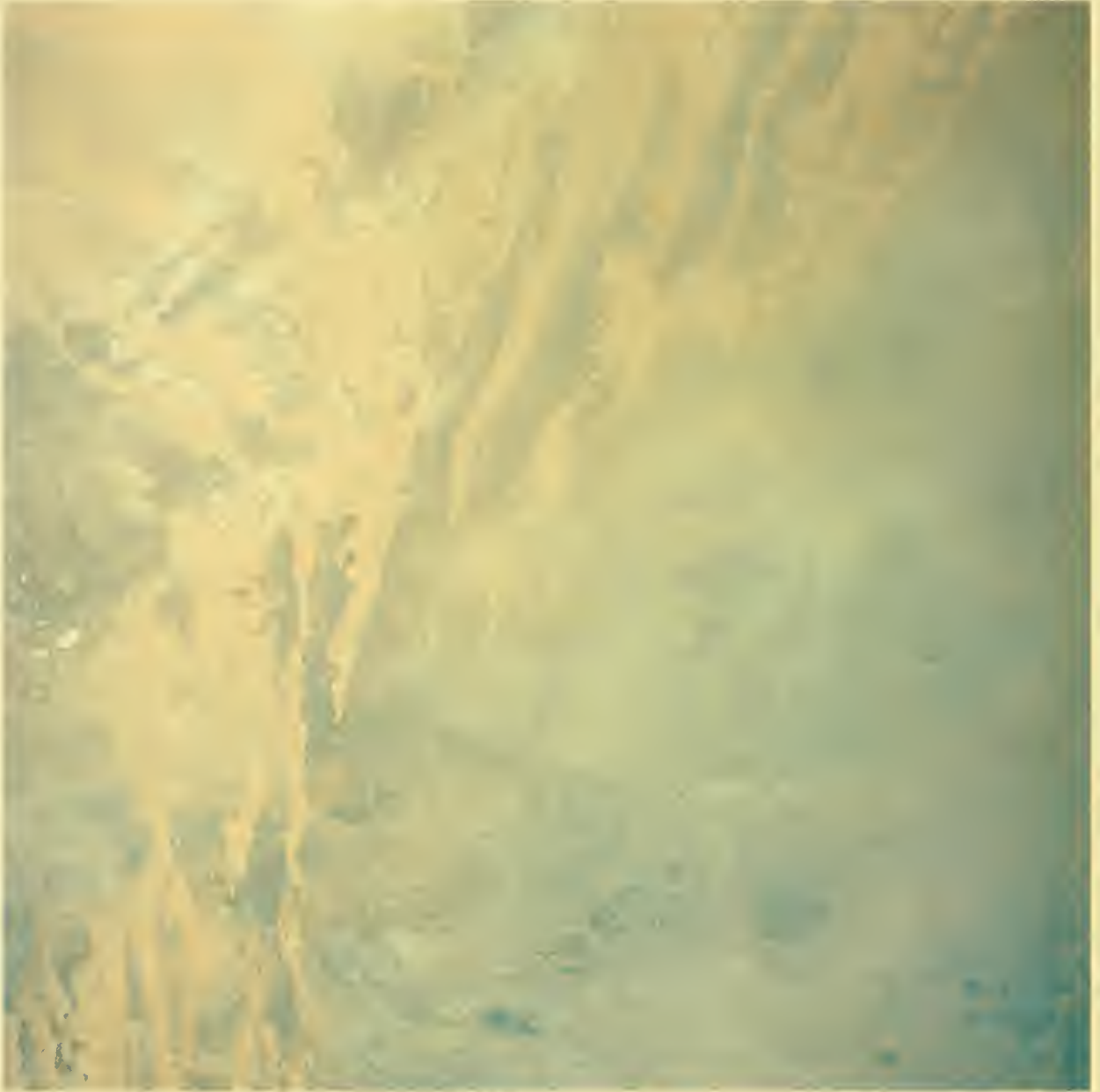
The southern Anti Atlas Mountains of Morocco. The photo shows the south limb of the Tindouf Basin, a large synclinal structure, overlain by sedimentary rock of the Hamada du Dra (foreground). The streamlike patterns are sandy, dry river beds.

S-65-34810

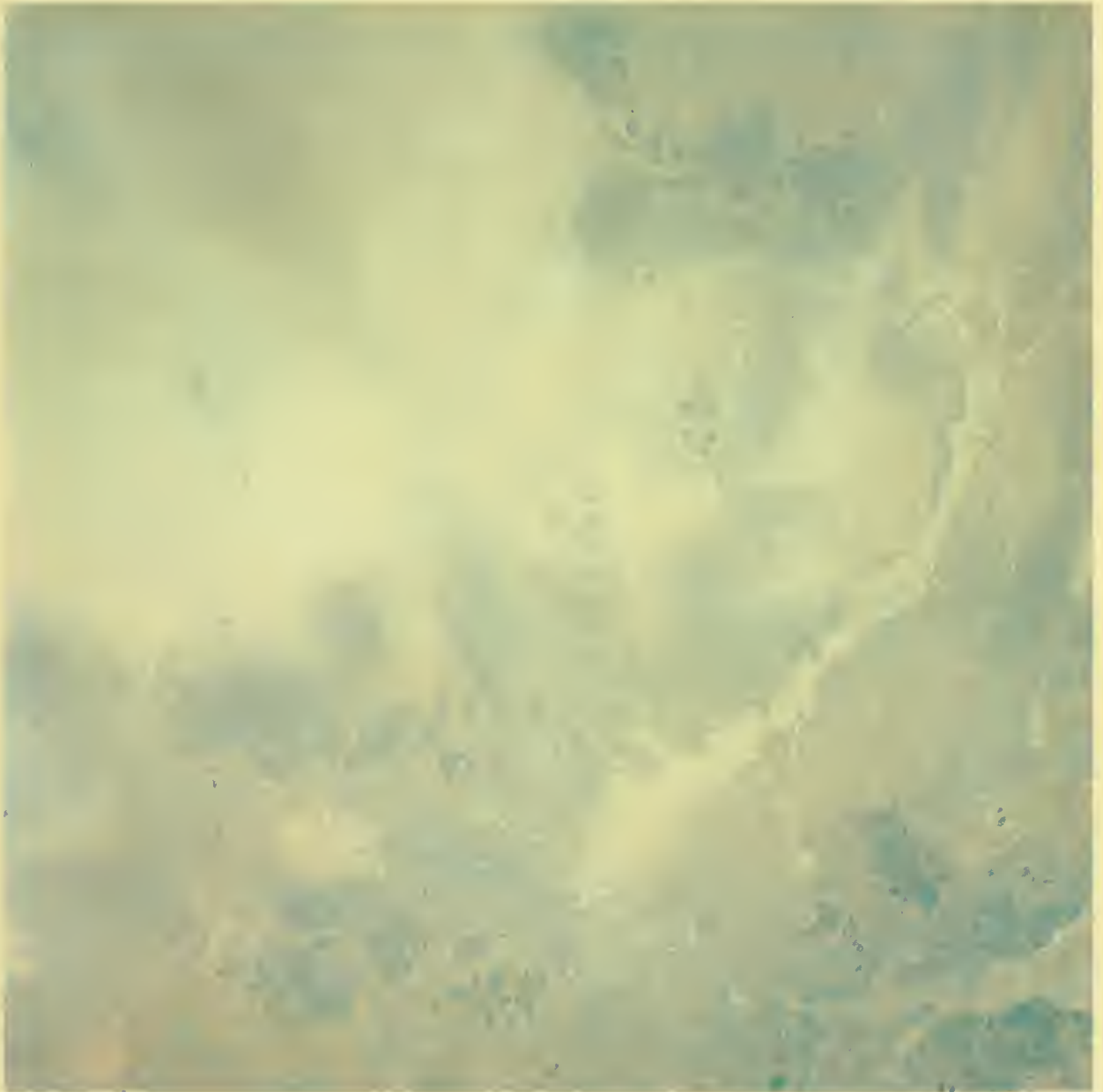


Hamada du Dra in Morocco and southwest Algeria. The linear pattern on the left is probably the topographical expression of fractures.

S-65-34809



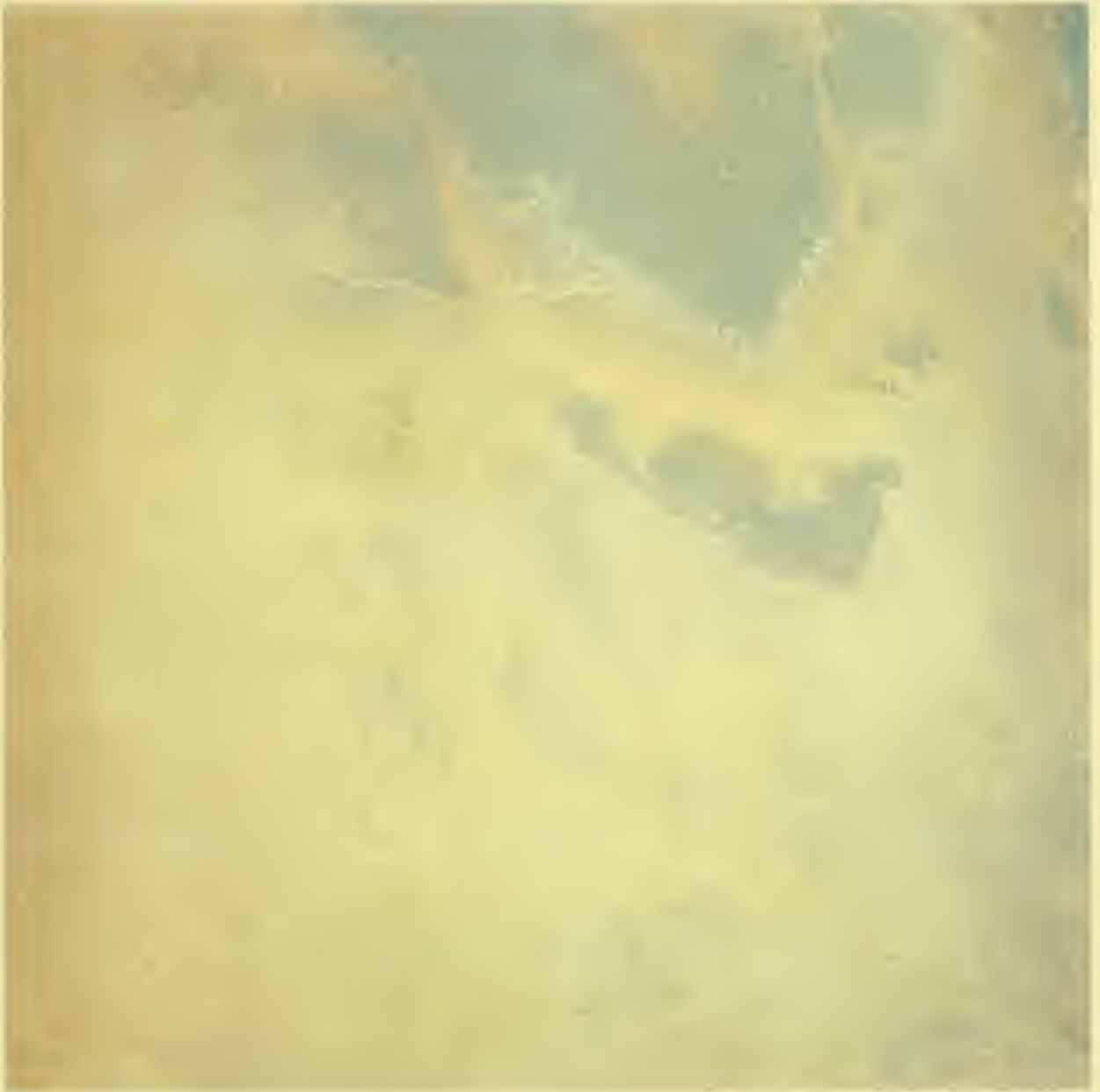
A near-vertical view of the Erg Iguidi in southwest Algeria, showing sand dune chains overlying Precambrian igneous and metamorphic rock. The dark areas are chiefly rhyolitic intrusives; the white areas are salt flats (playas). S-65-34807



Northern Mauritania and southwestern Algeria in the El Eglab-El Hank region, an area underlain by Precambrian igneous and metamorphic rock. The picture is obscured by sunlight striking debris on the spacecraft window. S-65-34806

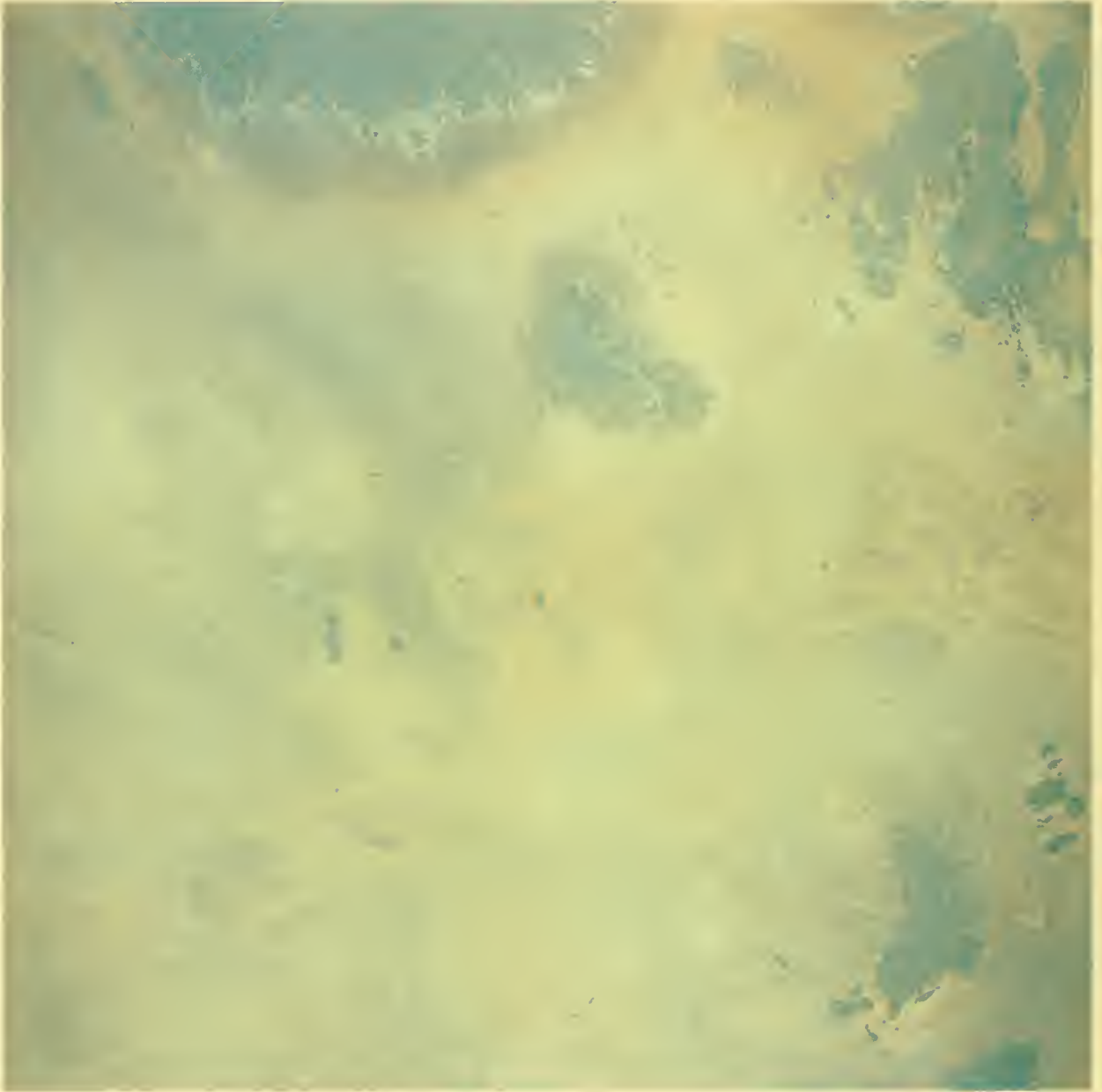


This view is to the northeast over the Assedjrad Escarpment in south central Algeria. The town of Ouallene is near the center of the picture. The dark areas at the upper right are cliffs and mountains of lower Paleozoic sedimentary rock. S-65-34803



Another frame of the Assedjrad Escarpment in south central Algeria, taken a few seconds after the preceding one.

S-65-34802



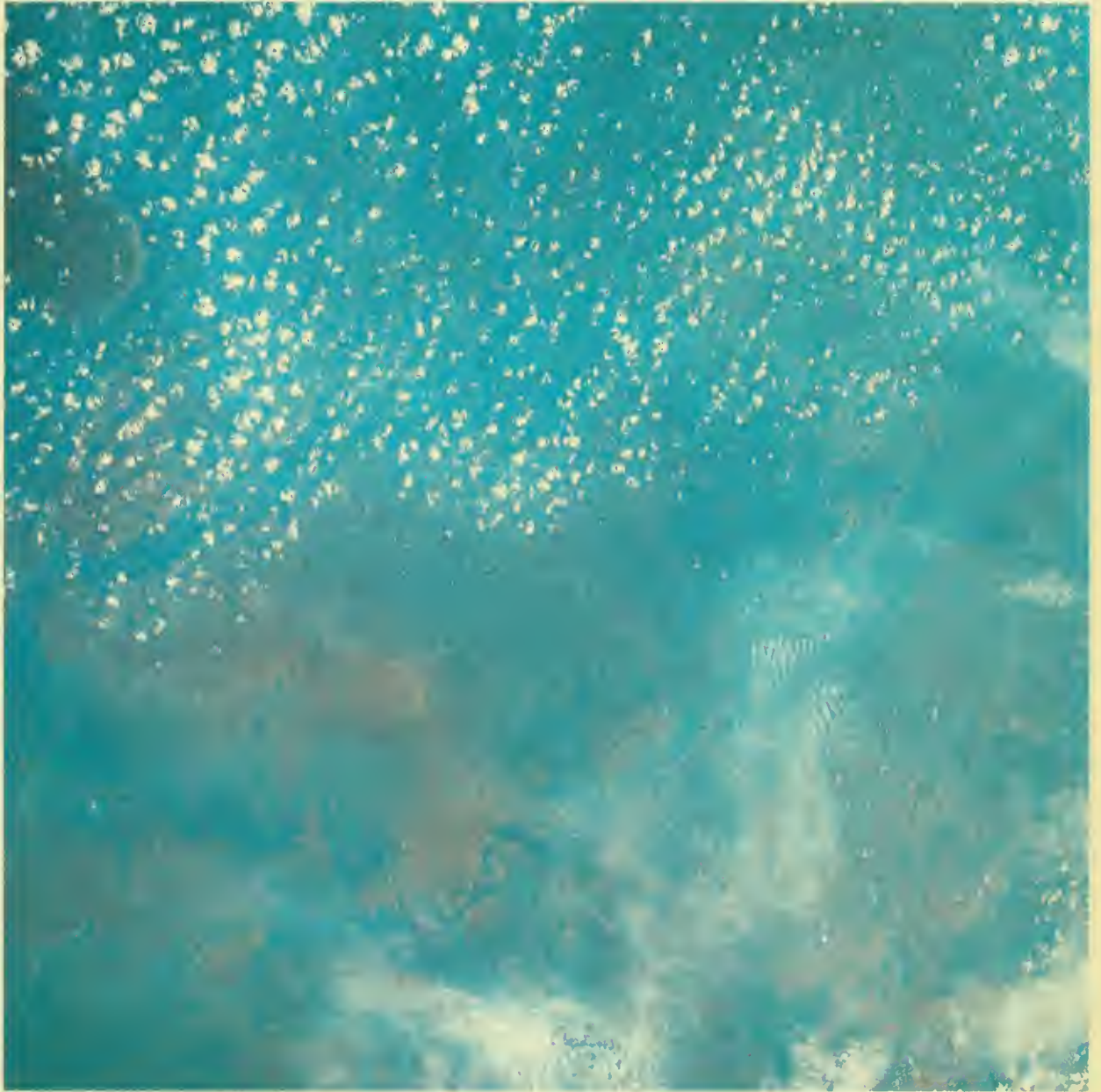
The Assedjrad Escarpment and the Erg Afarag in south central Algeria. The area overlaps that shown in the preceding photograph.

S-65-34801



The Ahaggar in south central Algeria, the major massif of the Sahara Desert, is underlain by intensely fractured Precambrian gneisses and schists, and by Quaternary volcanics.

S-65-34799



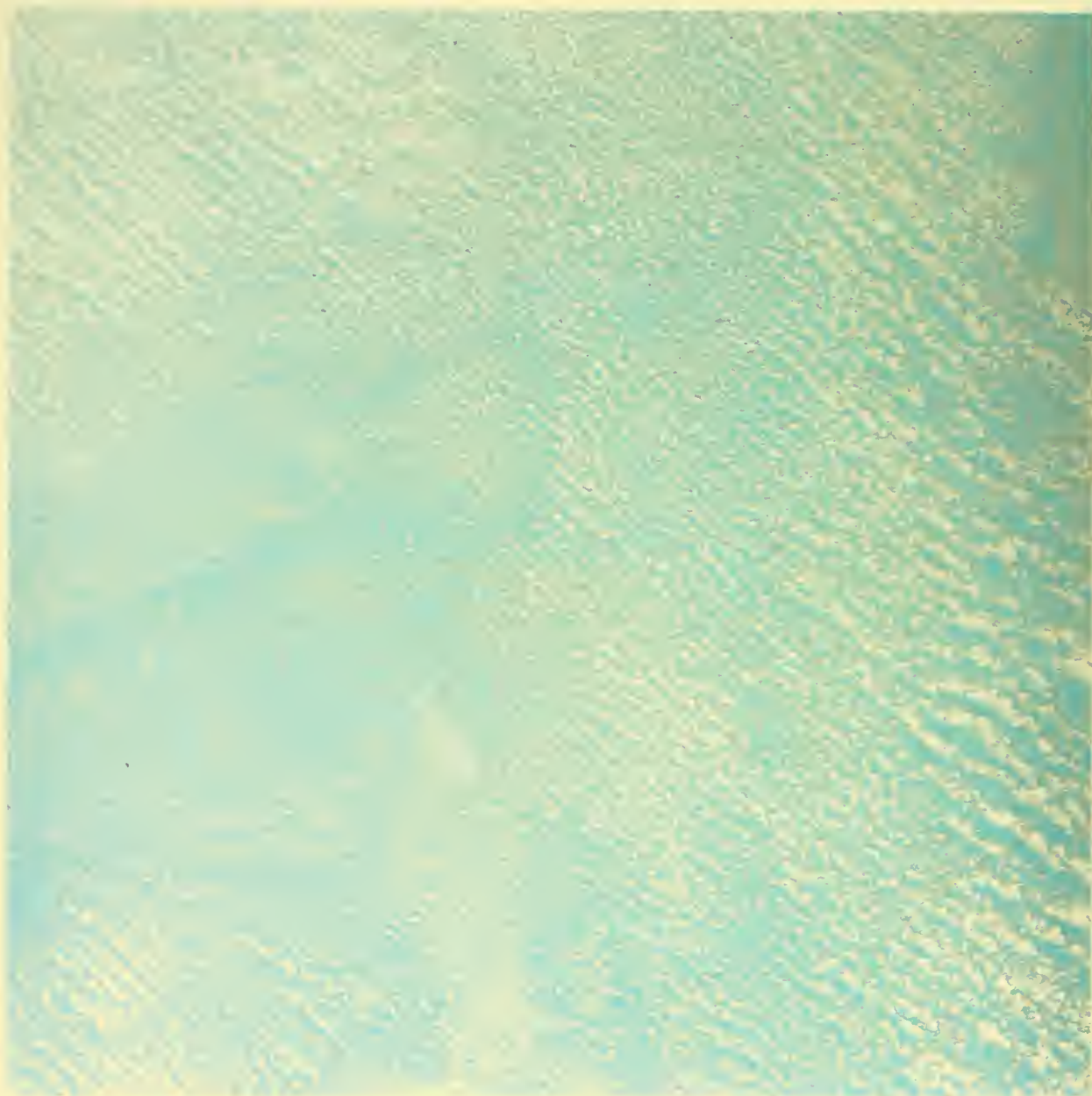
The eastern edge of the upper White Nile Basin in eastern Sudan and western Ethiopia.
The dark regions under the dotted clouds are swampy areas.

S-65-34798



The large narrow body of water in the middle of this photograph is Lake Rudolph, which borders the southeast edge of Sudan, the southwest edge of Ethiopia, and extends into northwest Kenya.

S-65-34796

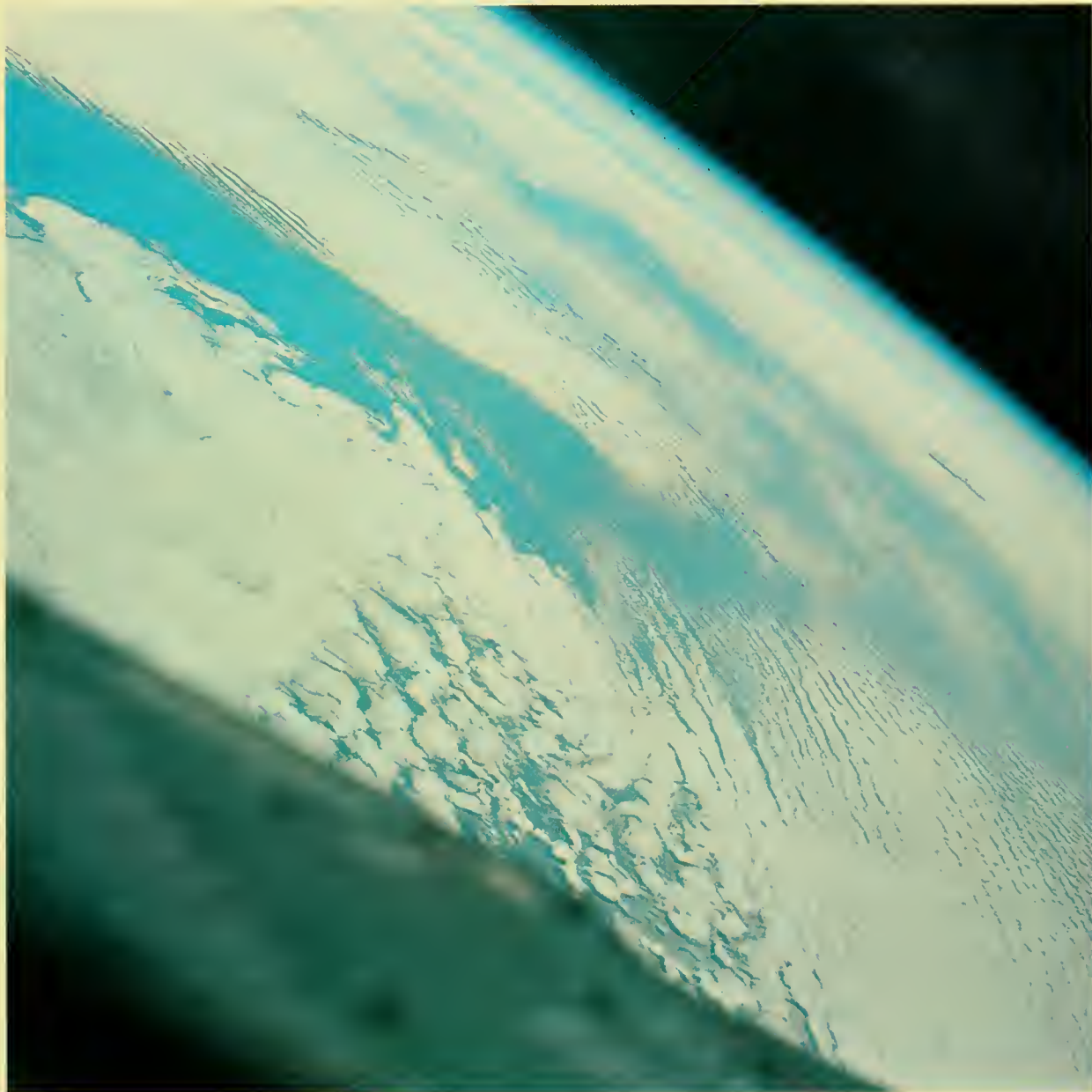


The Atlantic coastline southwest of Charleston, South Carolina, is visible in the upper right corner. Developing cumulus cloud lines are oriented southeast-northwest over eastern Georgia and southern South Carolina. They are about 1½ miles apart near the center of the picture.

S-65-34791

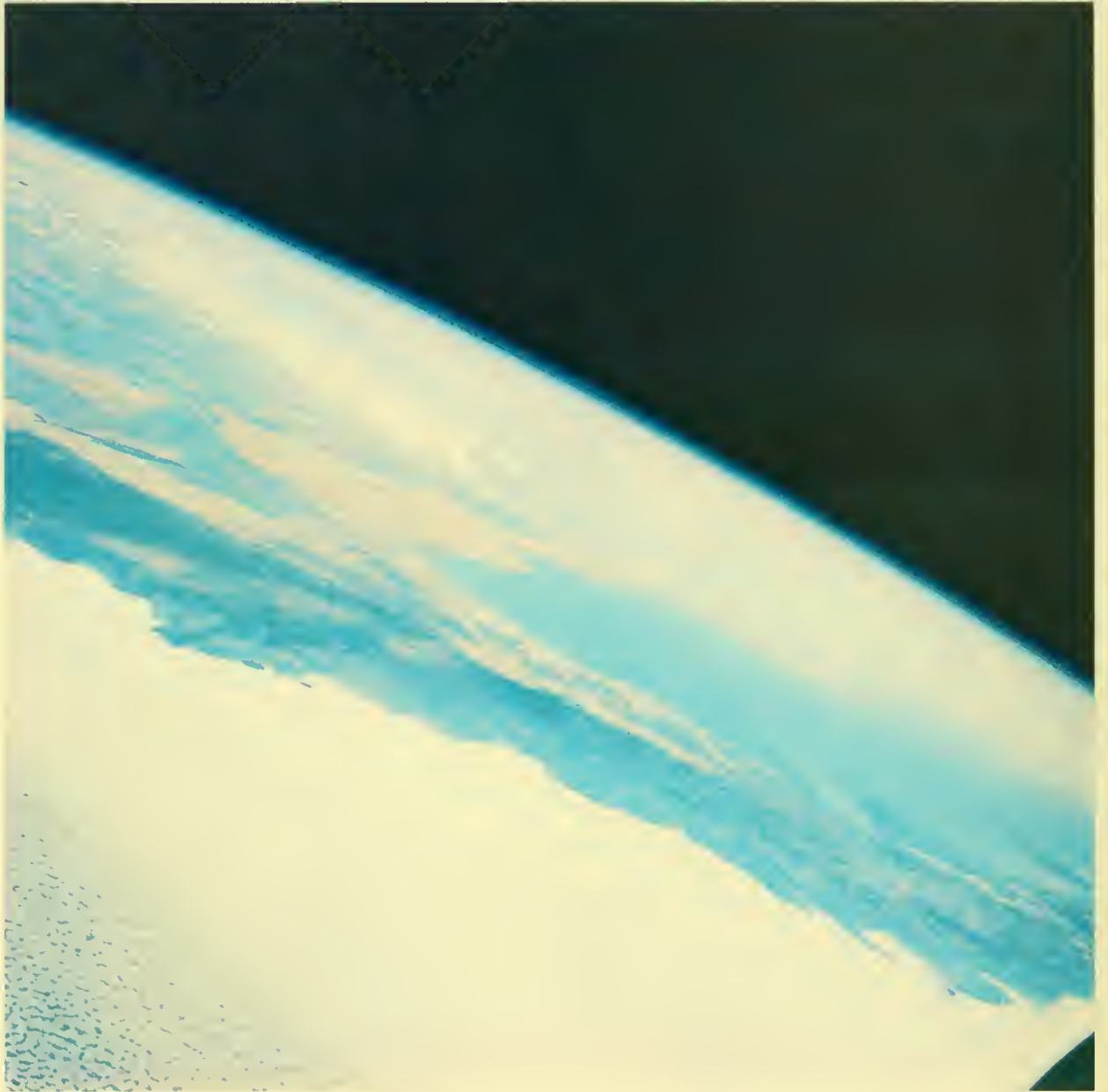
GEMINI V

On August 21, 1965, Gemini V was launched from Cape Kennedy at 1400 G.m.t. The flight, which ended August 29, took 190 hours and 55 minutes. During the 120 orbits Astronauts L. Gordon Cooper and Charles Conrad, Jr. took 250 photographs of the earth and clouds. On the following pages 145 of them are reproduced. The camera was a NASA-modified hand-held Hasselblad, Model 500C with a Zeiss Planar 80-mm. lens. Three of the films used were Ektachrome MS (S.O.-217); the fourth roll was Anscochrome D-50. Apogee was 215 miles and perigee 100 miles.



Stratocumulus clouds form a pattern of rows and individual cells in this view of the Pacific Ocean off the southern California coast. The shoreline of Baja California is near the horizon. The break in the cloud cover on the right marks the location of Guadalupe Island.

S-65-45674



A layer of stratocumulus clouds lies along the Pacific coast of Baja California. Across the Gulf of California, a thick haze covers much of northwestern Mexico. The band of convective clouds seen at top left stretch from Sonora, Mexico, into southwestern United States. At center left, in Baja California, the aligned valleys follow the Agua Blanca fault zone and the fault boundaries of the Sierra de Juarez. S-65-45676



The view looks eastward across central Alabama, Georgia, and South Carolina. The Atlantic coastline is marked by an abrupt end in the convective cloud pattern near the horizon. In the upper portion of the picture, well-defined cloud streets depict the airflow. This band structure is disrupted by the development of cumulus congestus and cumulonimbus (center and lower right). A major thunderstorm complex can be seen in the lower right corner.

S-65-45679



Thunderstorm activity southeast of Bermuda over the western Atlantic Ocean. Two cumulonimbus clouds are visible through the cirrus area in the center of the picture, as a third one develops nearby.

S-65-45681



A band of cirrus clouds extends diagonally across this picture of the western Atlantic Ocean, southeast of Bermuda. Composed of ice crystals, such clouds may be found as high as 12 miles in tropical regions. Also present are cumulus clouds, composed of water droplets suspended at heights up to several miles. Sea swells are noticeable in an area of sun glitter (left).

S-65-45682



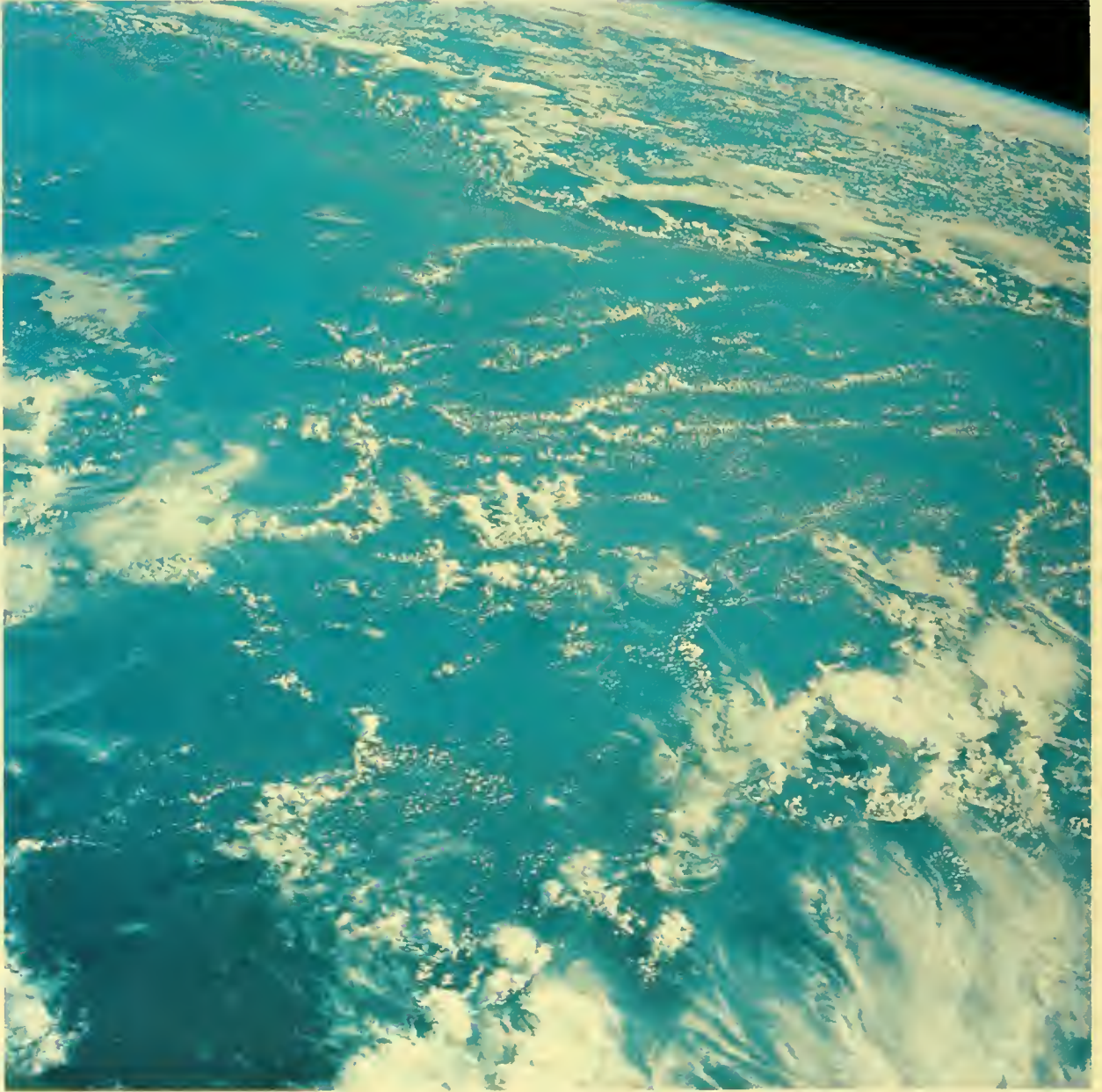
Trade wind cumuli are arranged in polygon-shaped cells, rows, and forked lines in this photograph east of the Lesser Antilles in the Atlantic.

S-65-45686



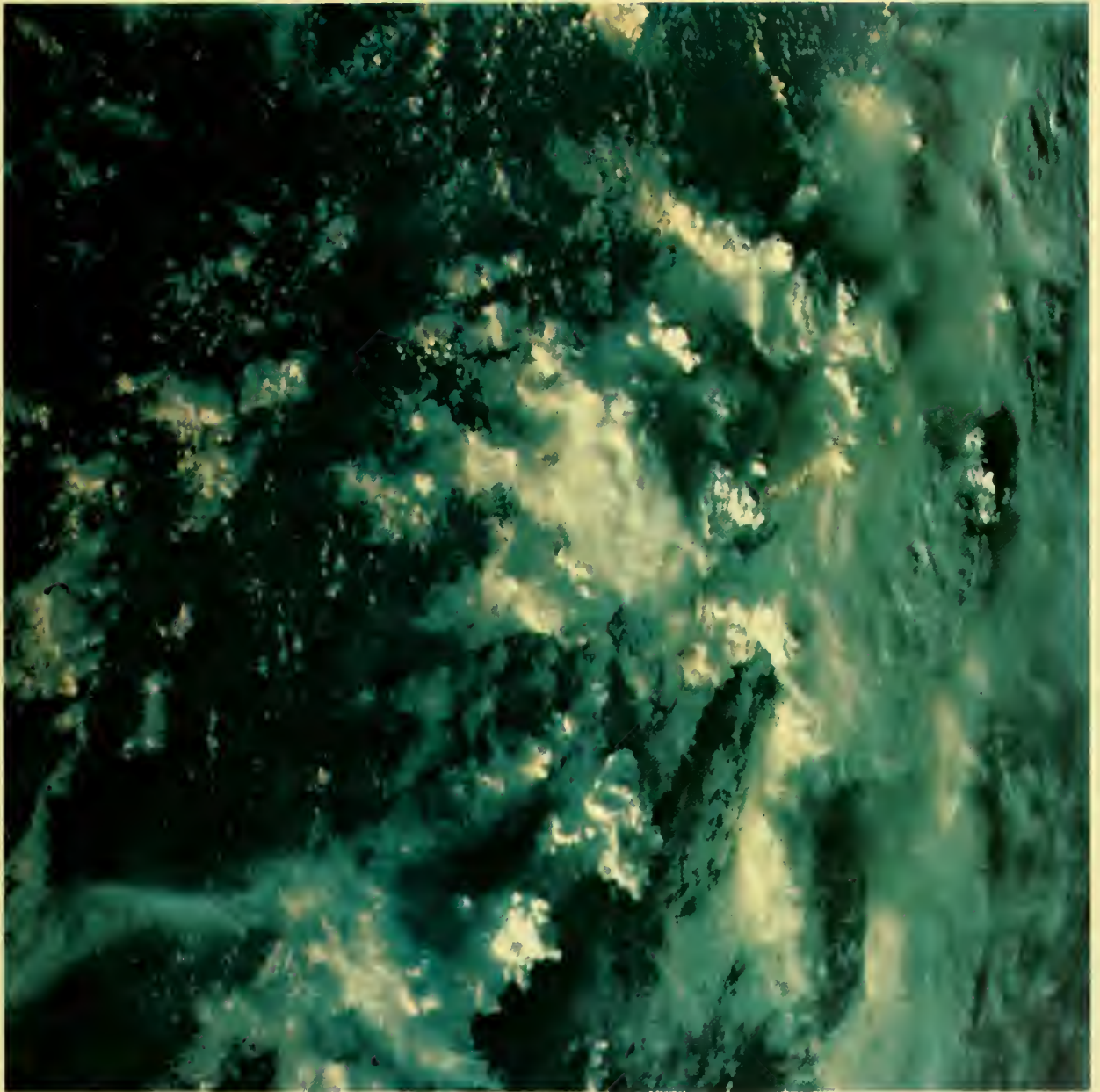
Tropical convective clouds covering the Atlantic Ocean off the coast of French Guiana. The cumulus towers inject water vapor into the upper atmosphere where cirrus clouds of ice crystals form from the vapor.

S-65-45687



This southwesterly view of the Atlantic coastline of South America extends from Cape Raso in northeast Brazil on the left to northeast Surinam on the right. Clouds producing afternoon showers dot the land area.

S-65-45688



The edges of these clouds over the central North Pacific near Wake Island are illuminated by early-morning sunlight. The turretlike tops of some of the clouds to the right indicate that thunderstorms and rainshowers are occurring. S-65-45691

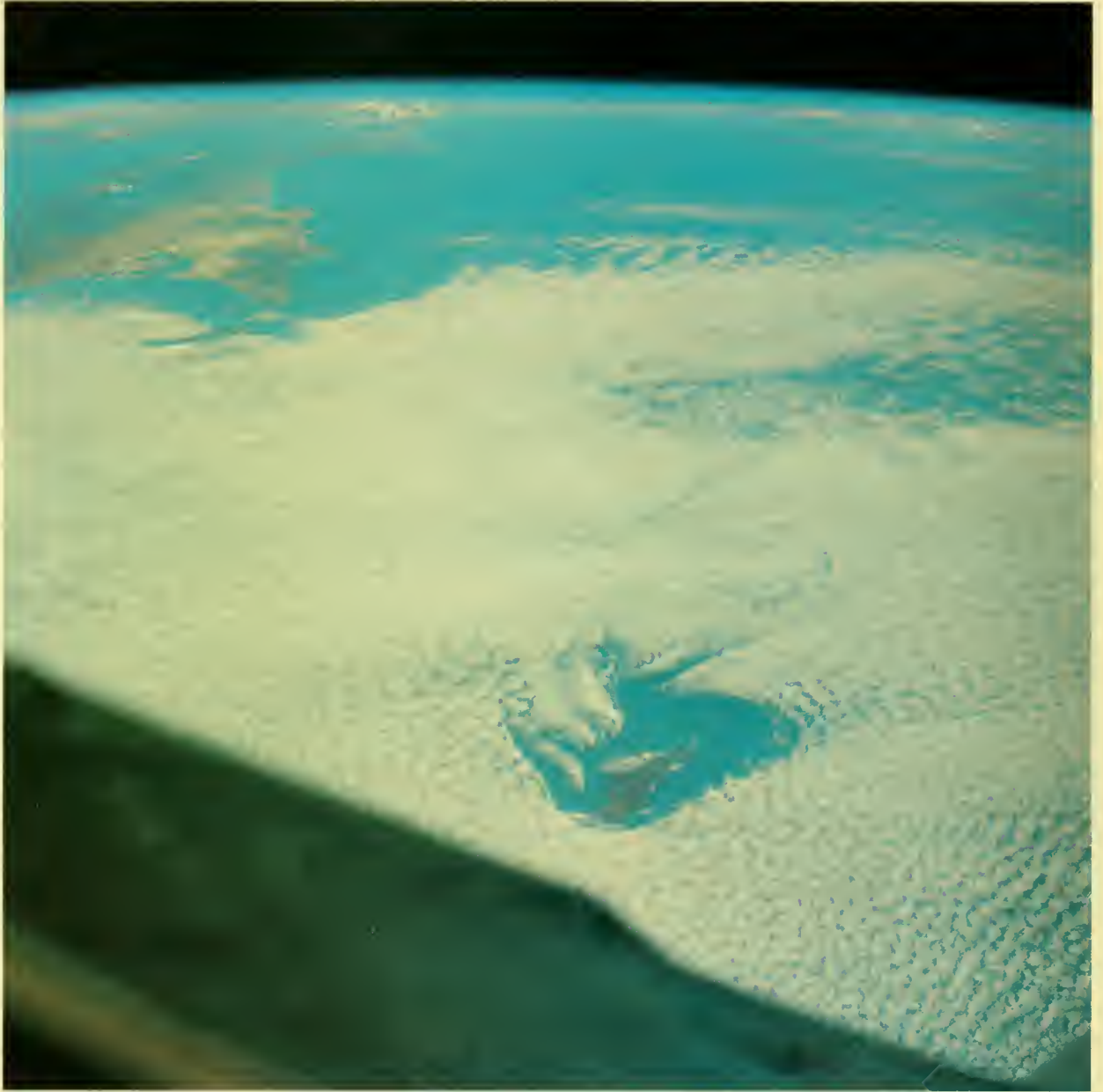


A view of the Pacific Ocean north of the Hawaiian Islands. The wake of a ship is visible in the top center of the photograph. Astronauts Cooper and Conrad sighted the wake and noted it in their log book before taking the photograph. S-65-45695



The Pacific Coast, with the Los Angeles Basin obscured by smog (upper center) and a clear view of Santa Barbara (upper left). The cellular pattern of the stratocumulus cloud cover over the cool, offshore waters is indicative of the inversion layer of warm air, several thousand feet above the ground, which covers the basin a large part of the year.

S-65-45696



Guadalupe Island in the Pacific Ocean seen through an opening in stratocumulus cloud cover. Punta Eugenia, at upper left, is free of clouds while several thunderstorms tower over the southern end of Baja California near the horizon. The cloud patterns around Guadalupe Island reveal the nature of the airflow in its vicinity.

S-65-45697



Another view, looking west, of Guadalupe Island and cloud eddies off Baja California. A V-shaped line resembling a shock wave is seen at the northern end of the island. Farther south, several eddies have formed spirals rotating in opposite directions.

S-65-45698



Punta Eugenia in Baja California with Isla Cedros visible under cloud cover at center right. Sierra Vizcaino, the mountain range south of Punta Eugenia (center) is underlain by Mesozoic metamorphic rock and upper Cretaceous sediments. The Vizcaino Desert lies in the embayed area. The dark area seen at bottom right is underlain by Eocene sedimentary and Mesozoic igneous rock.

S-65-45699



A view across the Gulf of Mexico, showing Baja California and Angel de la Guarda Island to the left. Both areas are underlain by Mesozoic igneous rock, chiefly granitic batholiths. On the lower right, Cape Lobos in Sonora, Mexico, is partially obscured by the spacecraft.

S-65-45700



The coast of Sonora and Tiburon Island, Mexico. The coastal area seen on the right is underlain by Cenozoic intrusive and extrusive igneous rock. Tiburon is composed of Cenozoic volcanic rock. Part of Angel de la Guarda Island and Baja California are visible at top left.

S-65-45701



Seen in this photograph, from left to right, are the Pacific Ocean, Baja California, the islands of Angel de la Guarda and Tiburon in the Gulf of California, and the Sonora coast in Mexico. The Baja California area at lower left is composed of middle Cenozoic volcanic rock; the area to the north is composed of Mesozoic intrusive rock.

S-65-45702



This oblique view of the head of the Gulf of California extends to the Mexico-United States border area with Sonora to the right. At upper center, the dark circle is Cerro del Pinacate, a large volcanic field. The Imperial Valley of California and the Salton Sea are visible above and to the left. The islands in the Gulf are Tiburon and Angel de la Guarda.

S-65-45703



A view along the east coast of the Yucatan Peninsula. The alignment of the cumulus clouds indicates a low-level air flow from the Caribbean Sea. Scattered cumulonimbus clouds are injecting cirrus clouds into the upper region of the troposphere. A section of the main highway west of Chetumal in Quintana Roo, Mexico, is visible near the lower right. Shoal water surrounding many of the offshore islands can be seen clearly.

S-65-45704



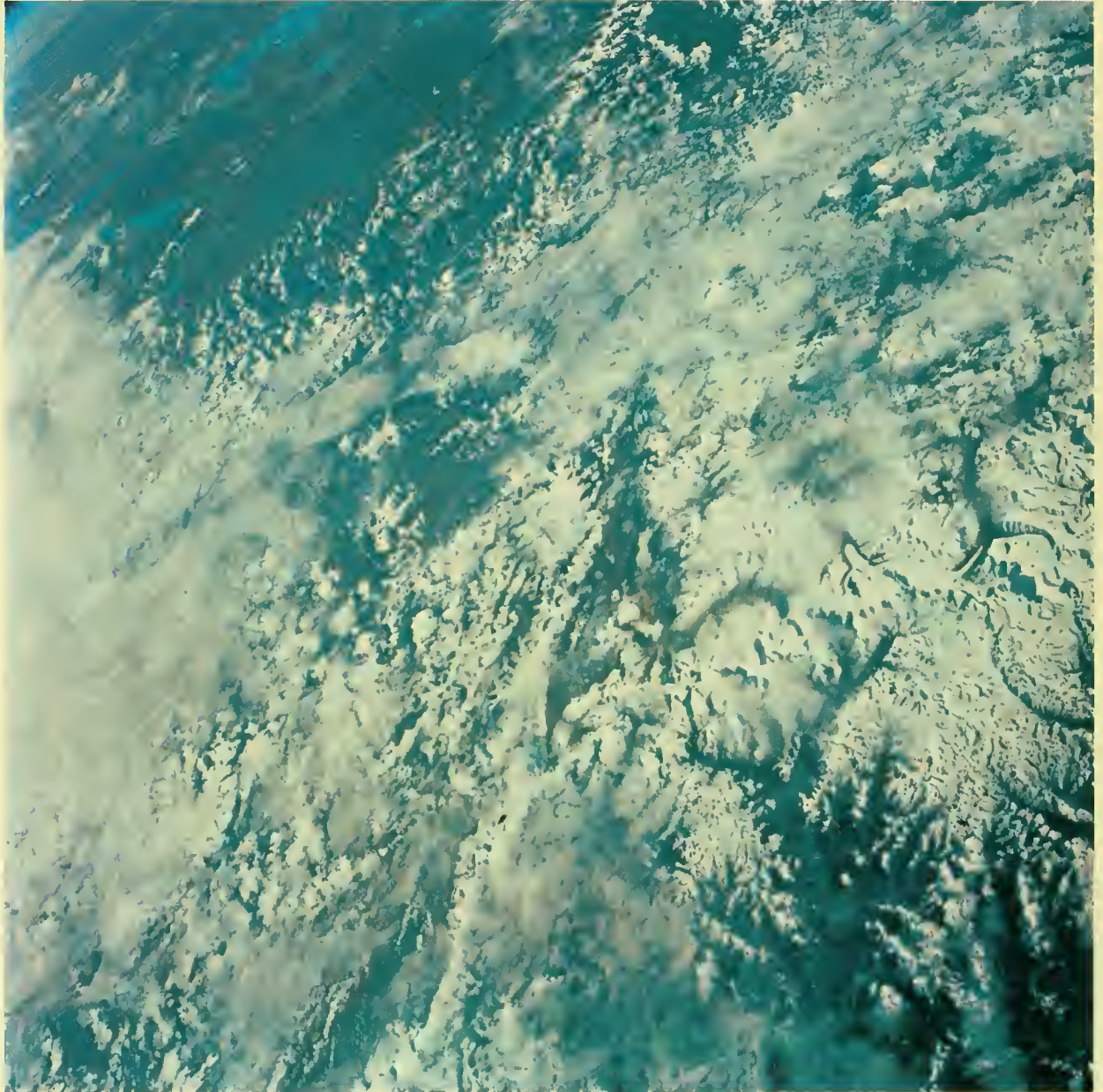
The Caribbean coastline of Honduras and Nicaragua looking southeast. Rio Coco, with its oxbow bends, runs through the center of the picture to Cape Gracias a Dios and forms the boundary between the two countries. Rio Patuca can be seen in the lower right corner. Small, cumulus clouds are prevalent at a lower level of the atmosphere.

S-65-45705



Included in this view of the Himalaya Mountains are parts of Nepal, Tibet, Sikkim, and Bhutan. The Kanchenjunga Massif, 28,208 feet above sea level, is in the center of the photograph near the Nepal-Sikkim border. The city of Darjeeling and the Tista River are near the bottom right corner.

S-65-45709



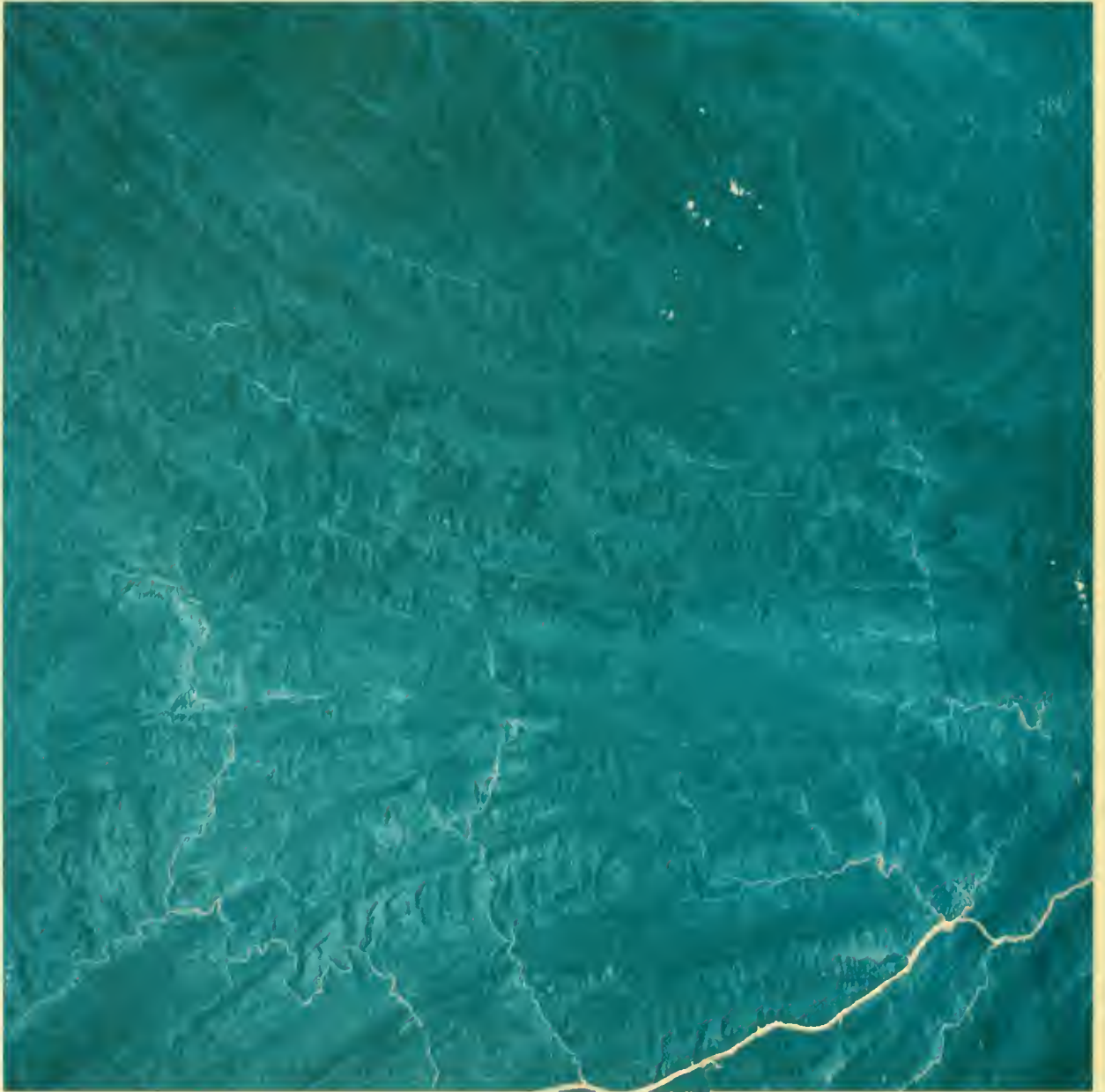
The Great Himalaya Range is in the foreground of this view of Bhutan and Tibet. Part of the Brahmaputra River is visible near the center. The lakes in the background include Kyaring, Natzsong, and Addan.

S-65-45710



The Nyenchen Thanglha Mountain Range of Tibet crosses the center of the picture. Nam Tsho (lake) lies immediately above the range. Below, across the lower portion of the photograph, is the Brahmaputra River. The lakes and highlands of northern Tibet form the background.

S-65-45711



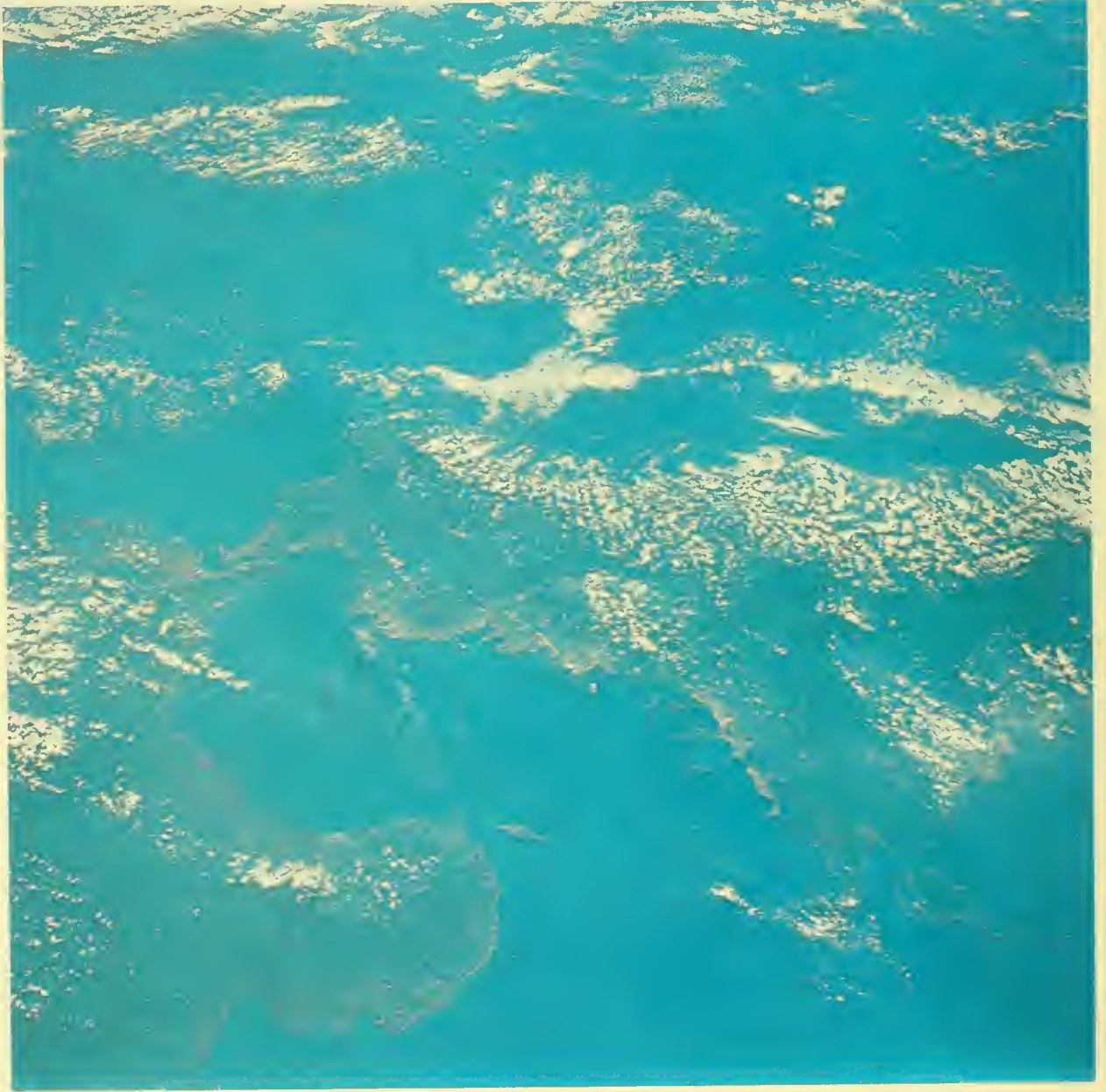
This vertical view covers parts of Szechwan, Hupeh, and Shensi Provinces in mainland China. The Yangtze River is visible to the bottom right of the photograph. The city of Fengchieh is on the far lower right at the confluence of the Yangtze and one of its tributaries. Folded sedimentary rock predominates in the area.

S-65-45713



Shensi Province in mainland China with the Wei (Yellow) River at upper left and the city of Hsian near the center top of the photograph. The Han River system is in the center and lower right.

S-65-45714

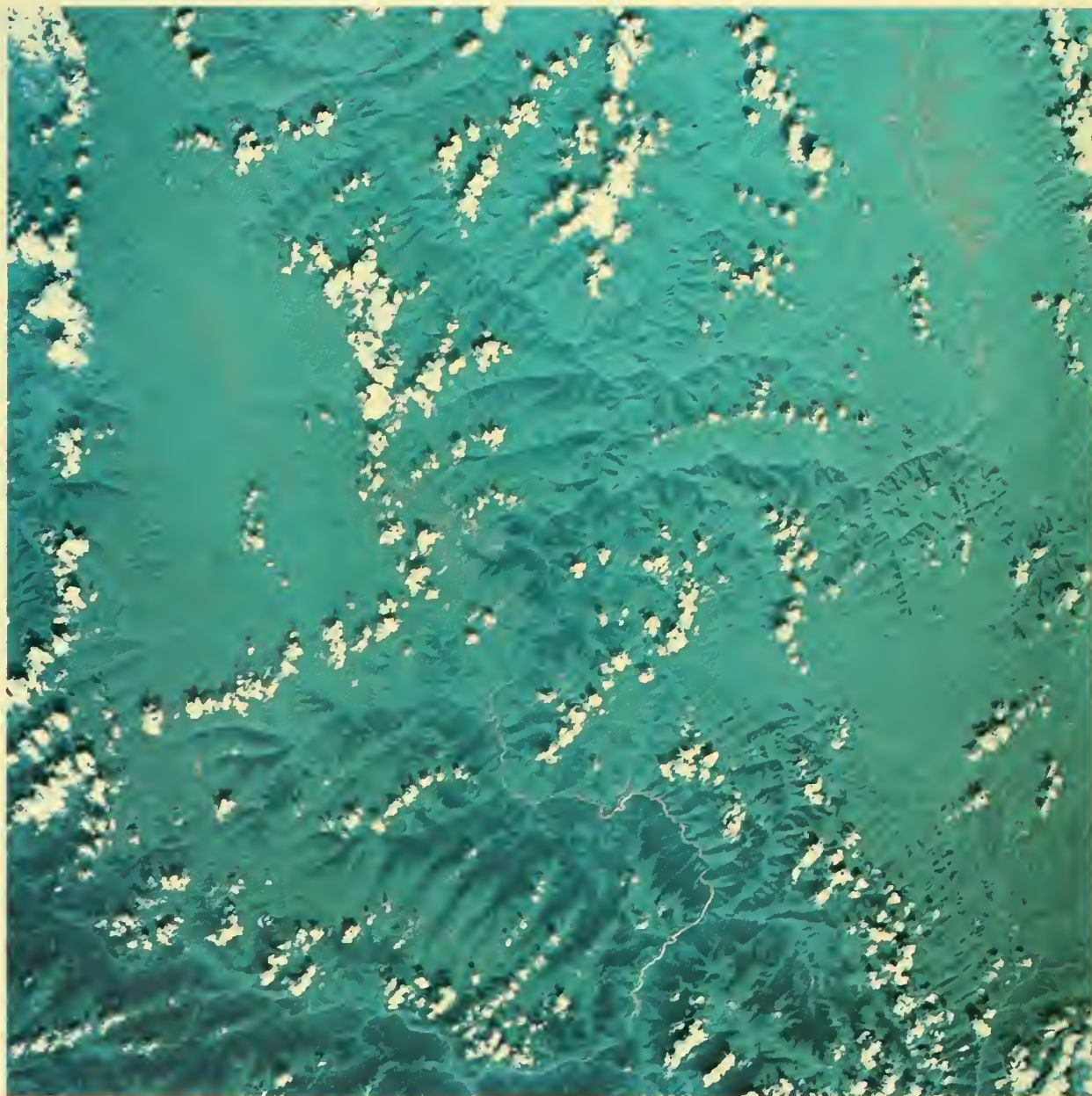


This view of Japan looks across the Eastern Channel of the Korea Straits. Honshu Island is to the right, Kyushu Island to the left, and Tsushima Island in the upper left corner. In the foreground is the Gulf of Suo Nada. S-65-45715



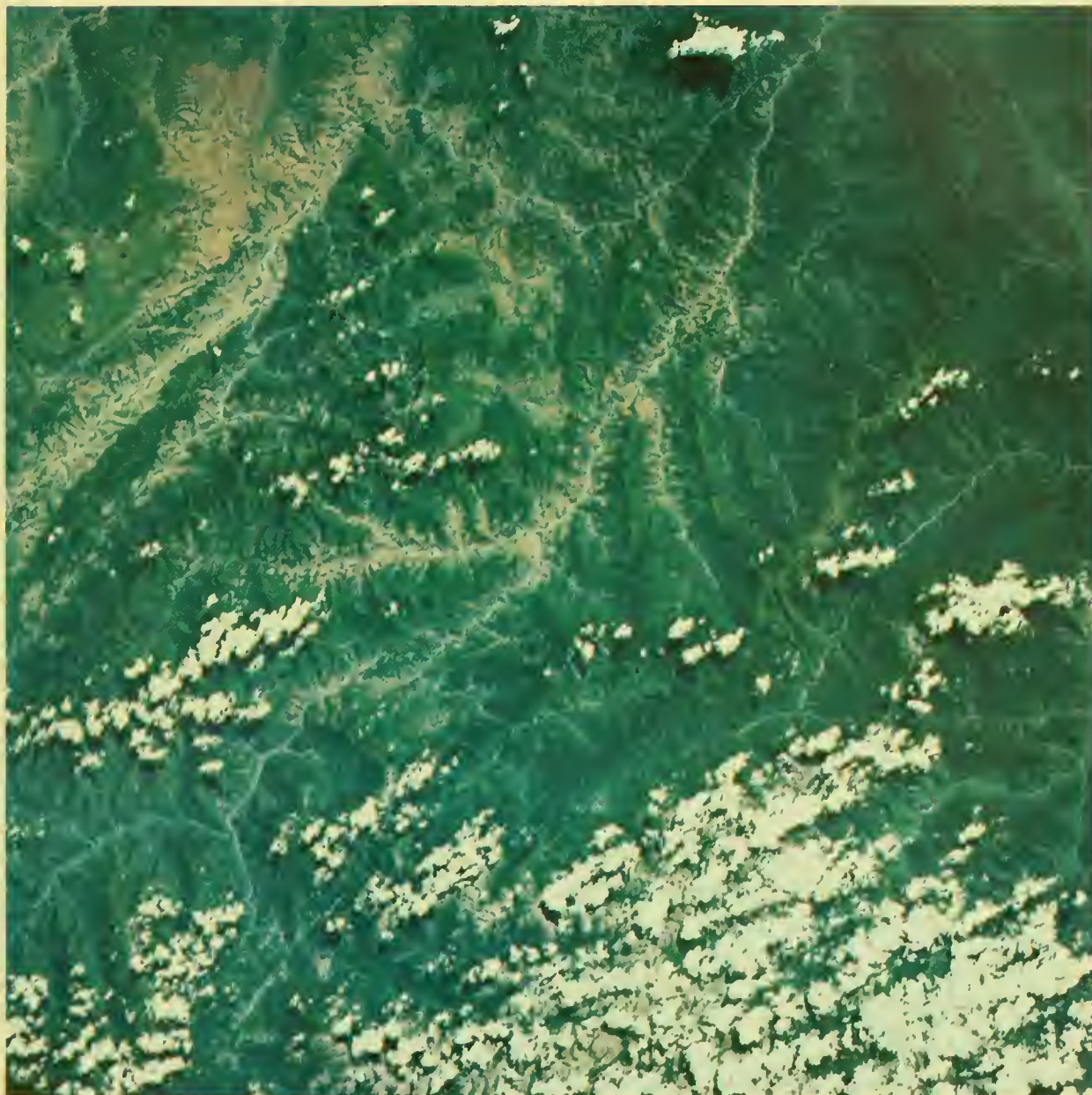
An oblique view of seif dunes in the Empty Quarter area of Saudi Arabia.

S-65-45716

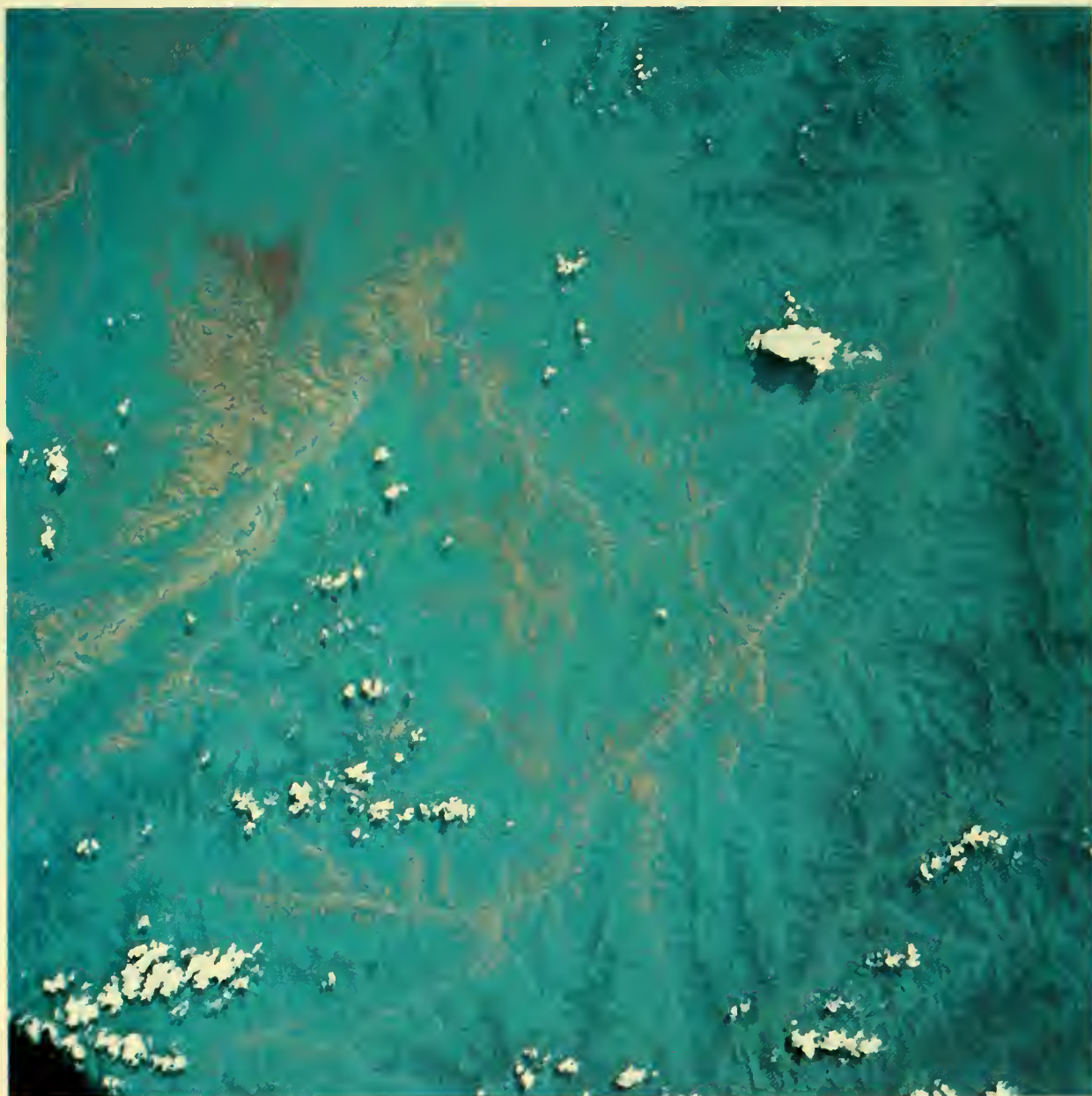


The highest mountains in this part of Szechwan Province, mainland China, rise 15,000 feet above sea level. The cultivated region in the upper right portion of the picture is Ch'iao-ko-a-ma. Prominent in the lower center is the Tachin River, which leads into the Min River.

S-65-45717

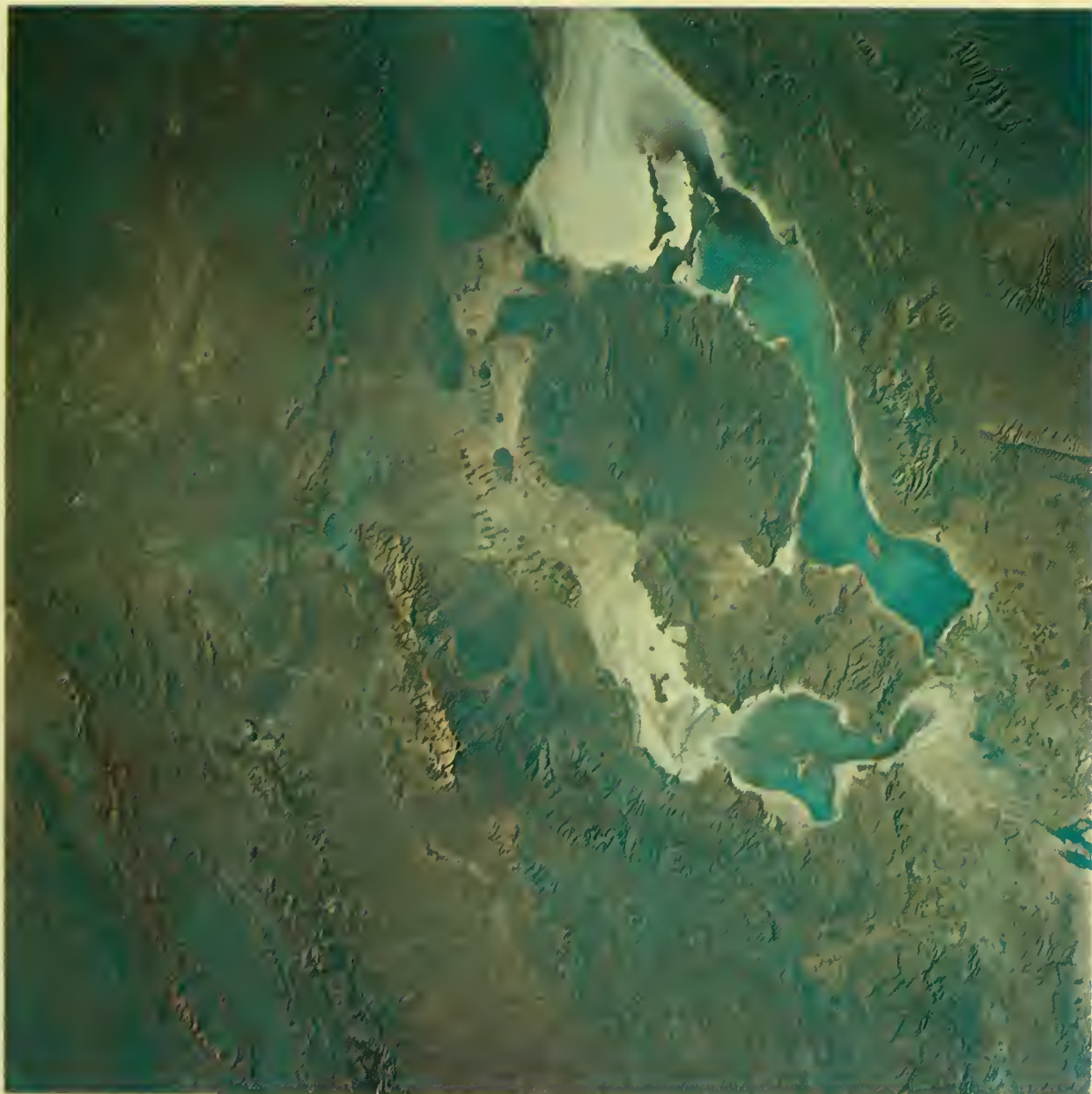


The Pailung Chiang (or Chialing) River in the mainland China Provinces of Szechwan and Kansu winds from left center edge to upper right, where it is joined by the Paishui Chiang. The Yung Feng Shan Mountains are covered by the clouds at lower right. The city of Wutu is in the light-colored valley at upper left. S-65-45718



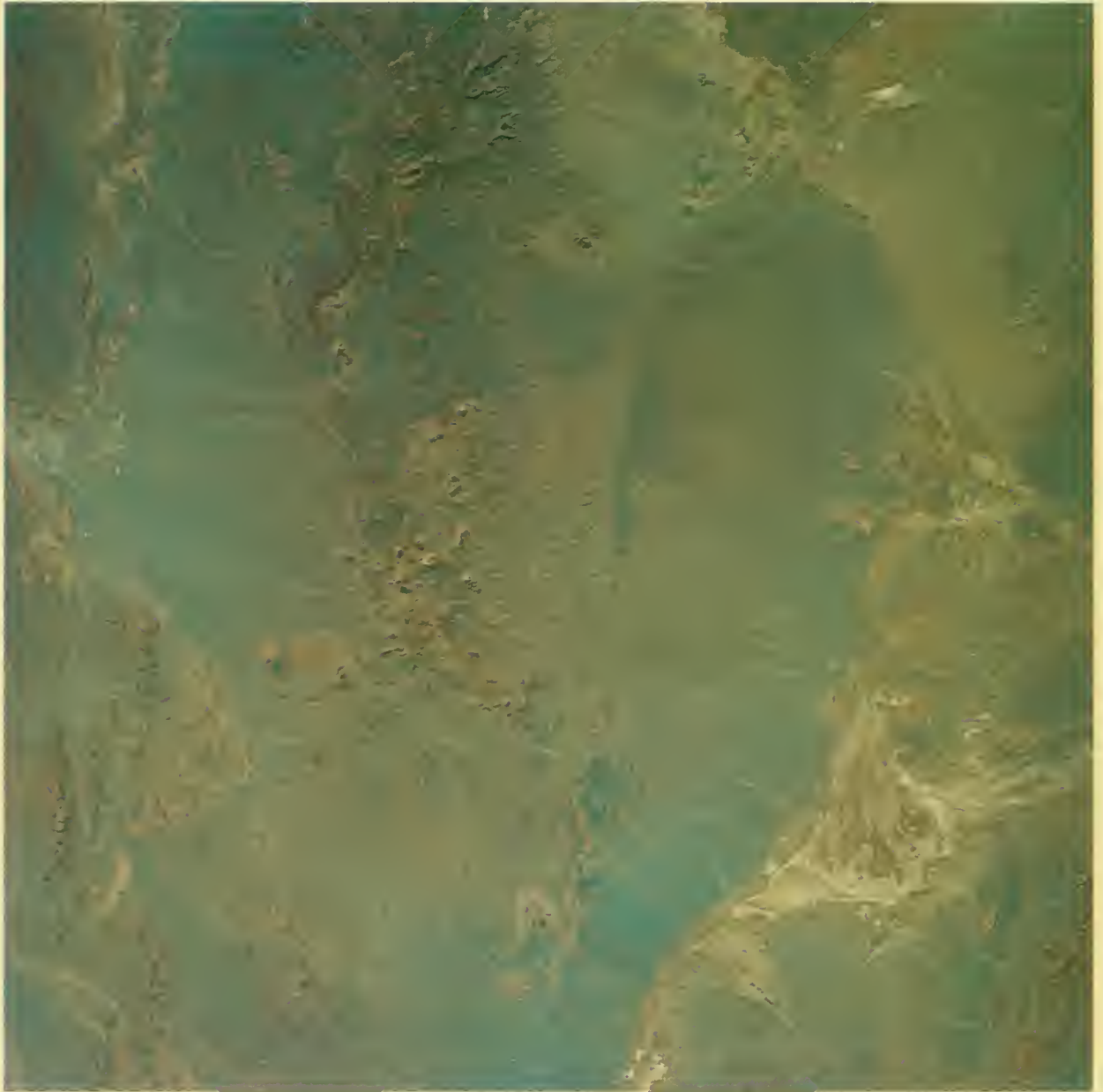
This view of the Szechwan and Kansu Provinces in mainland China largely overlaps the preceding photograph. The Pailung Chiang River is seen from lower left to upper right.

S-65-45 719



The Zagros Mountains in southern Iran, east of Shiraz. Tashk and Bakhtigam salt lakes are clearly delineated. The Persepolis ruins are visible in the lower right corner. Linear ridges consist of folded sedimentary rock; dark areas at top center are igneous rock.

S-65-45720



The town of Saidabad (Sirjan) in southern Iran (right center) with the Aiyub Hills in the background. The linear ridges to the left are folded sedimentary rock.

S-65-45721



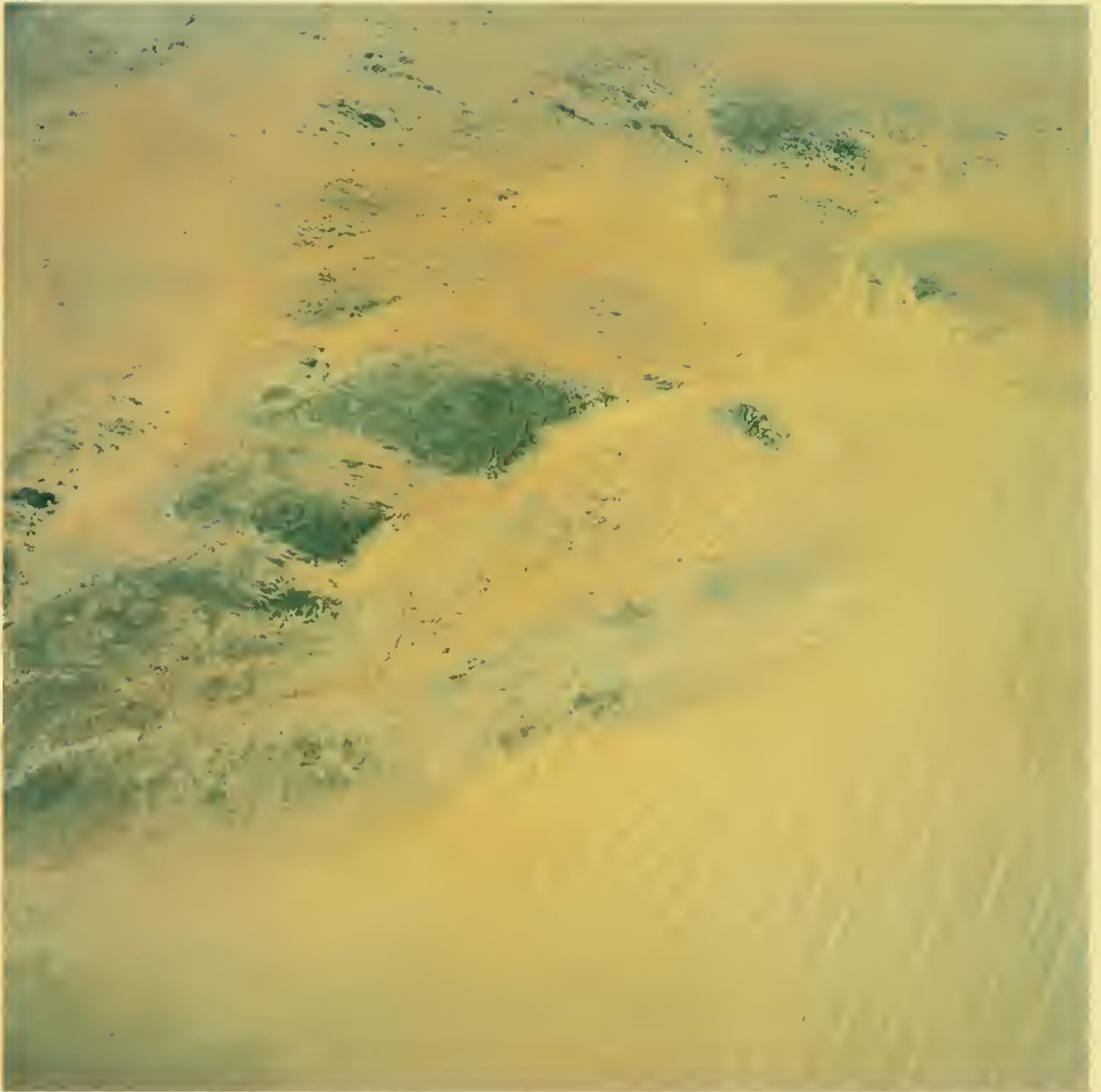
South-central Iran, northwest of Kerman. Plunging anticlines and synclines are seen at lower right. The linear scarp at bottom center is a trace of a fault. S-65-45722



A view of the Dasht-e-Lut Desert in Iran. Namakzar salt lake is at right center, just beyond the sand dunes. This photograph overlaps the preceding one. S-65-45723

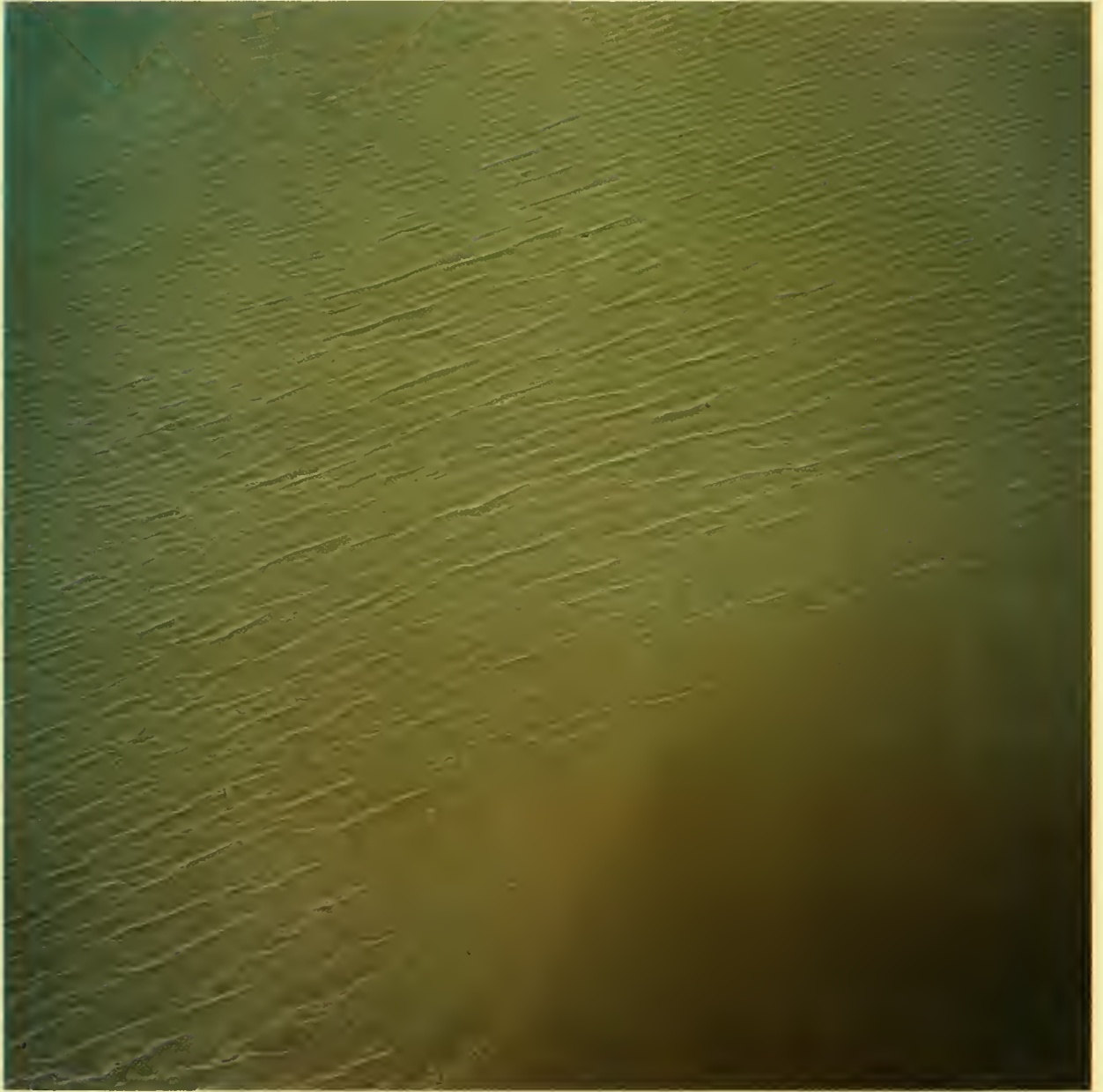


Hunan and Hupeh Provinces in mainland China. The Yangtze River and Lake Tungting are seen at lower left. The Hsiang River is on the right. S-56-45725



The Libyan Desert, north of Al Kufrah, looking southwest. The dark areas above the seif dunes are igneous rock.

S-65-45726



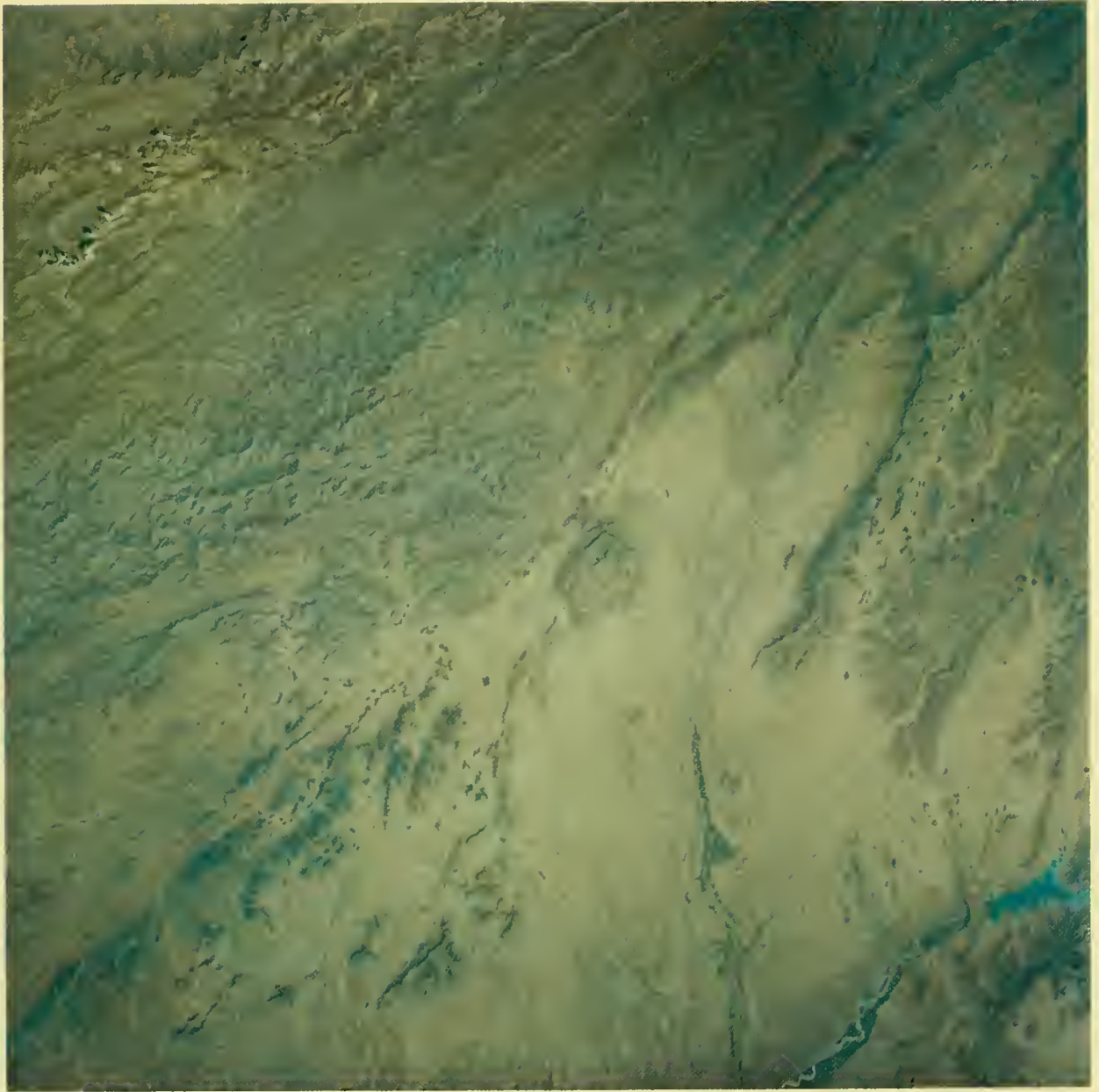
This photograph shows part of the Libyan Desert, an area of extensive sand dunes.

S-65-45727



The Iran-Afghanistan frontier area, west of Farah.

S-65-45728



Central Afghanistan, northwest of Kandahar. The Kajakai Reservoir on the Helmand River is seen at lower right. The linear ridges in the upper left corner consist of folded sedimentary rock.

S-65-45729

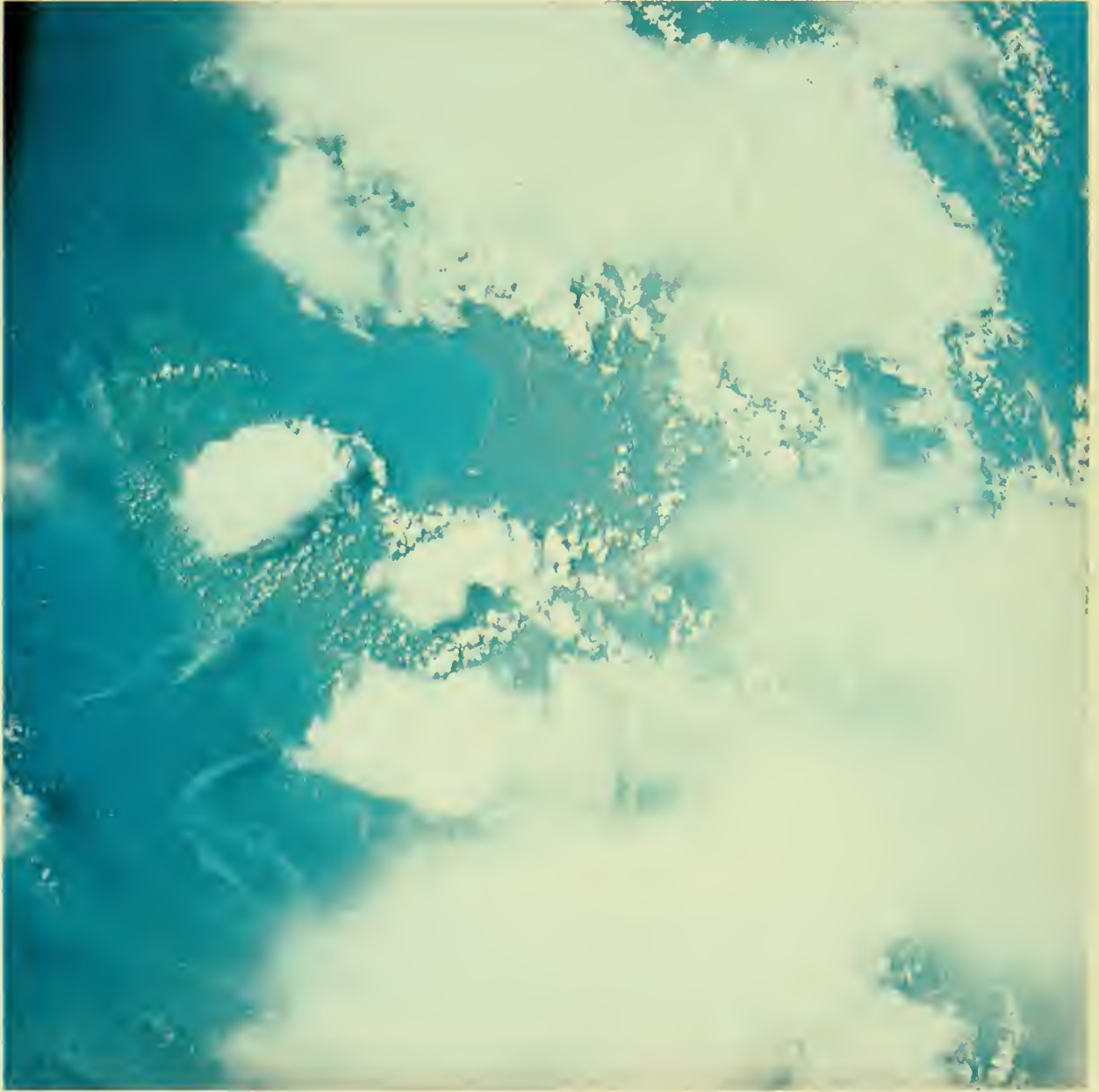


Another view of central Afghanistan, overlapping the previous frame. Areas of cultivated land are seen along the river beds. The Kajakai Reservoir on the Helmand River is on the far left.

S-65-45730



The coast of mainland China in Kwangtung and Kwangsi Provinces. The Gulf of Tonkin is on the right. Above it lies the Leichou Peninsula. S-65-45731

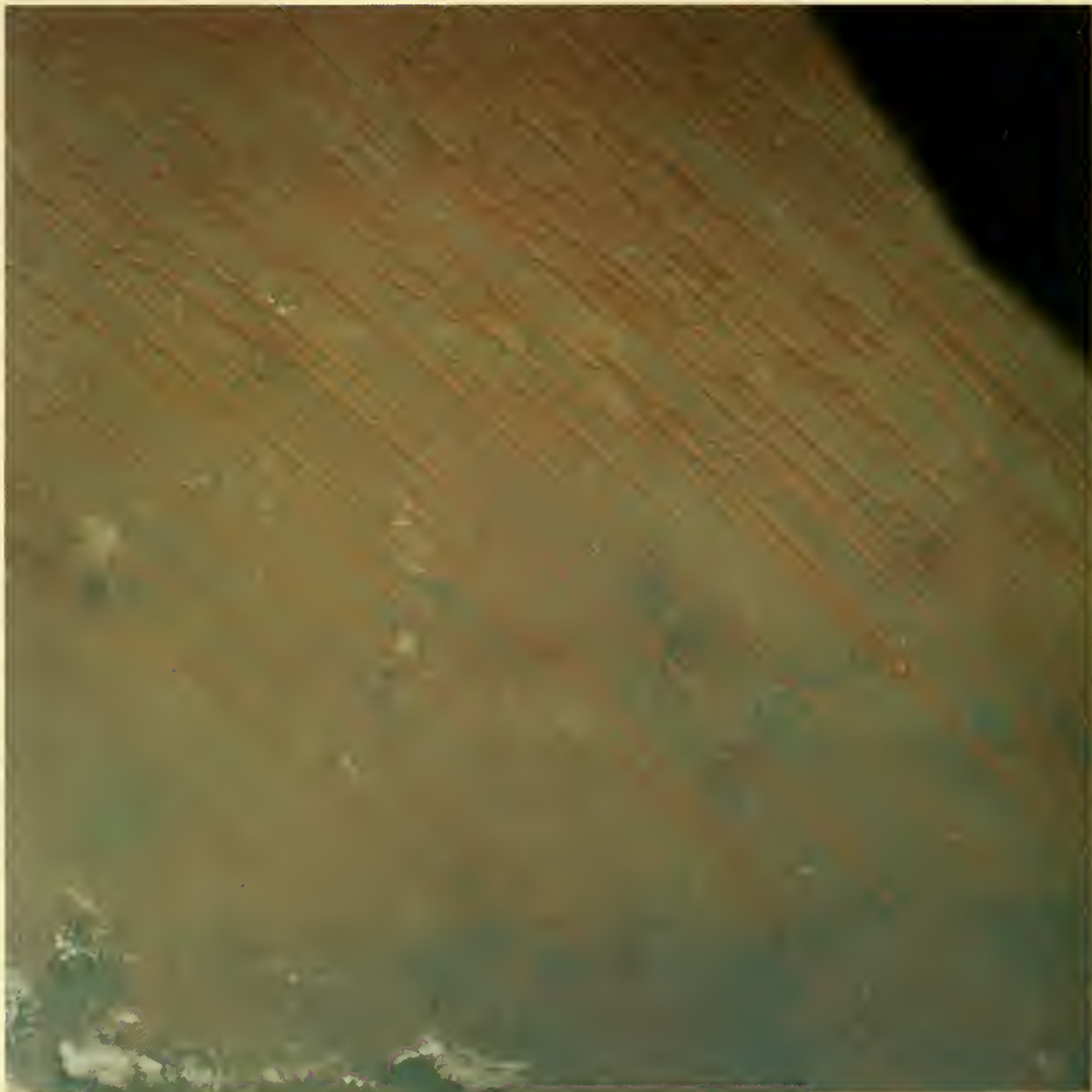


A view of the north end of Luzon Island in the Philippines, showing Cape Bolinao jutting out into the South China Sea (left). Lingayen Gulf is above the cape. Aubarede Point on Luzon's east coast is visible at upper right. S-65-45732



Southern Luzon Island in the Philippines is seen at left center. Cumulus clouds obscure from view mountain peaks 6,000 to 8,000 feet high. Burias Island is in the lower left corner. At the top, across Lagonoy Gulf, is Catanduanes Island. A dense cirrus cloud shield covers Masbate at lower right.

S-65-45733



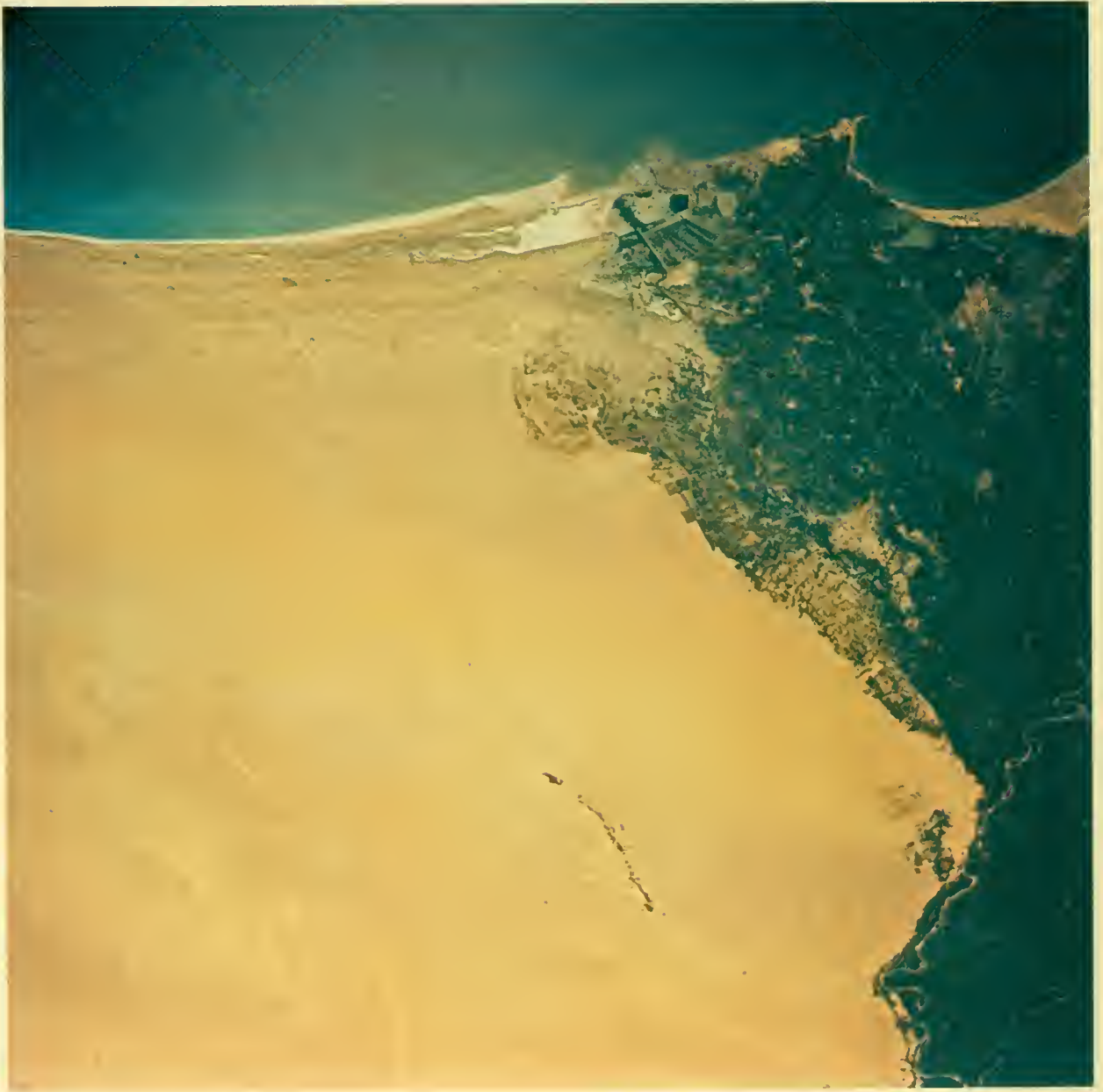
Erg Chech, a large sandy desert in southern Algeria. The photograph was taken northeast of Grizim.

S-65-45734



Fuerteventura Island in the Canary Islands partially covered with clouds aligned in a north-south direction. Below the stratocumulus clouds in the background lies the west coast of Morocco and Spanish Sahara.

S-65-45735



A clear view of the Nile Delta and the city of Alexandria. Wadi el Natrun, a series of salt lakes below sea level, stand out in the desert area at lower center. The Rosetta branch of the Nile River is seen in the lower right corner. S-65-45736



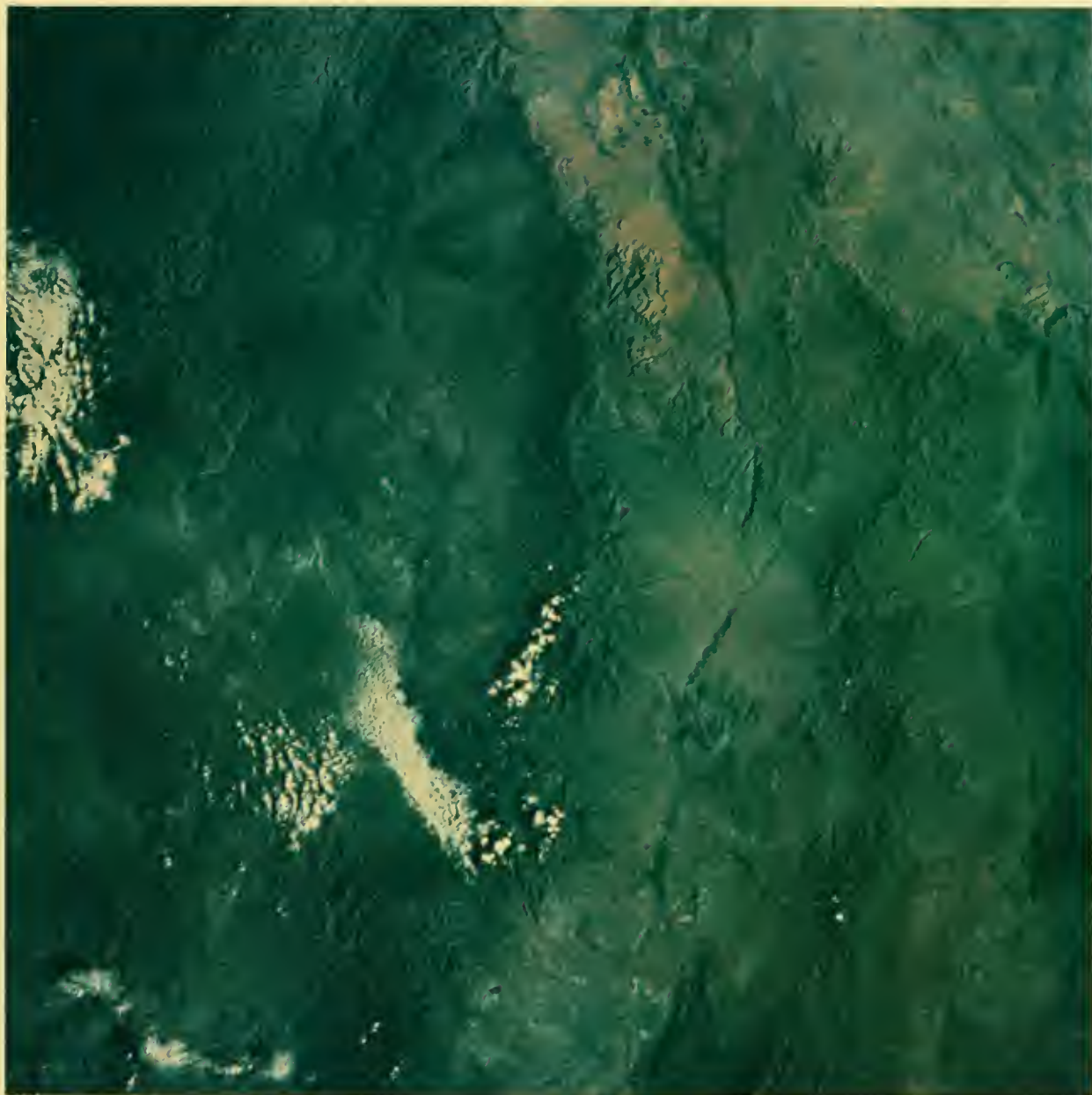
View of the Straits of Gibraltar looking into the Mediterranean. Spain is to the left and the Rif Atlas Mountains of Morocco to the right.

S-65-45737



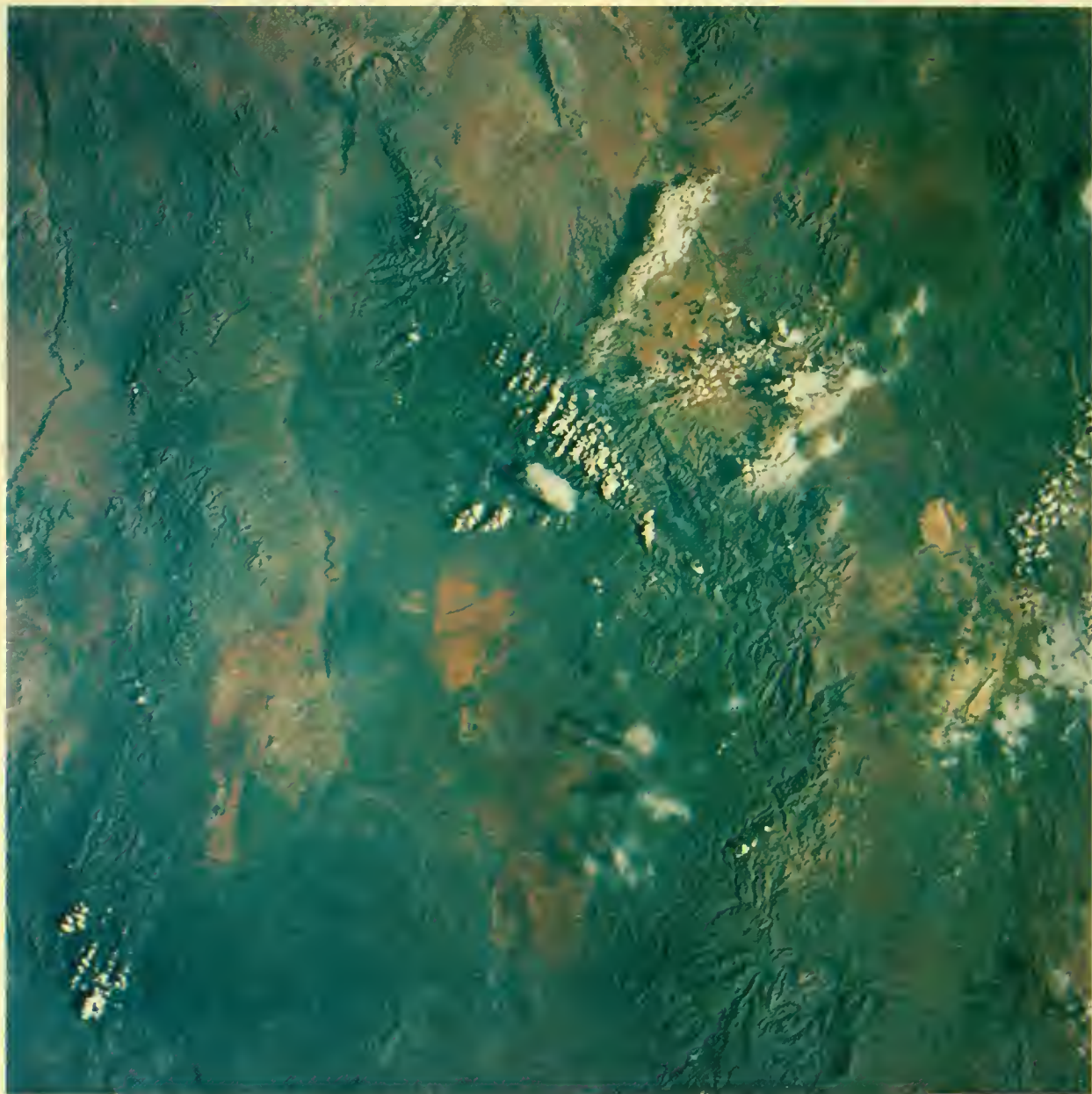
The Atlantic coast of Morocco from Cape Sim, at the top, to south of Agadir. Cape Rhir is in the lower center of the picture. The High Atlas Mountains, of folded sedimentary rock, are to the upper right. Below them is the Oued Sous (river).

S-65-45739



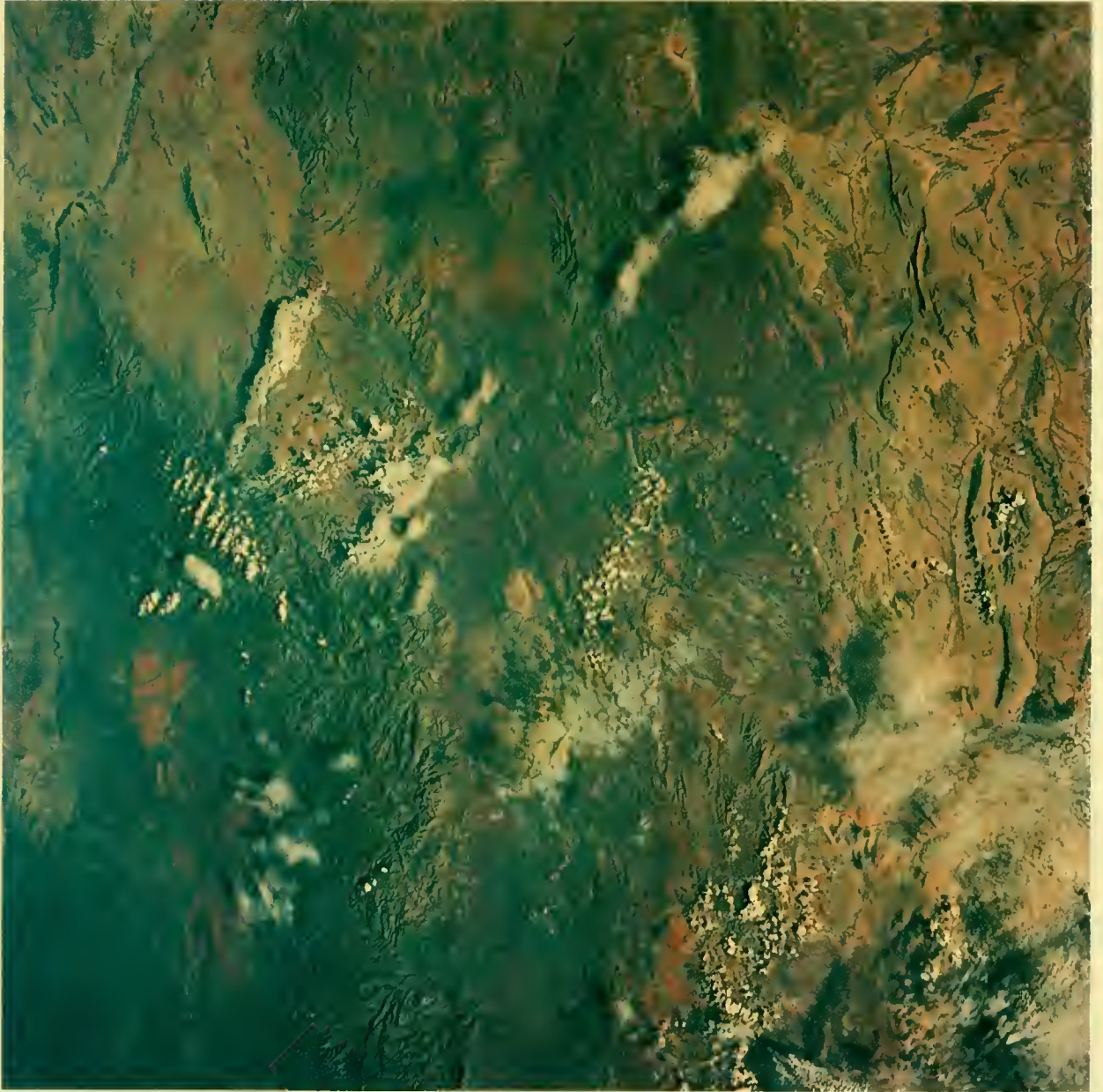
Chihuahua, Mexico, with the Sierra de Babicora in the center and the Sierra Madre Occidental Mountain Range, composed chiefly of volcanic rock, to the left. The Santa Maria River bisects the picture. Sierra de las Tunas and the Santa Clara River are to the right.

S-65-45741



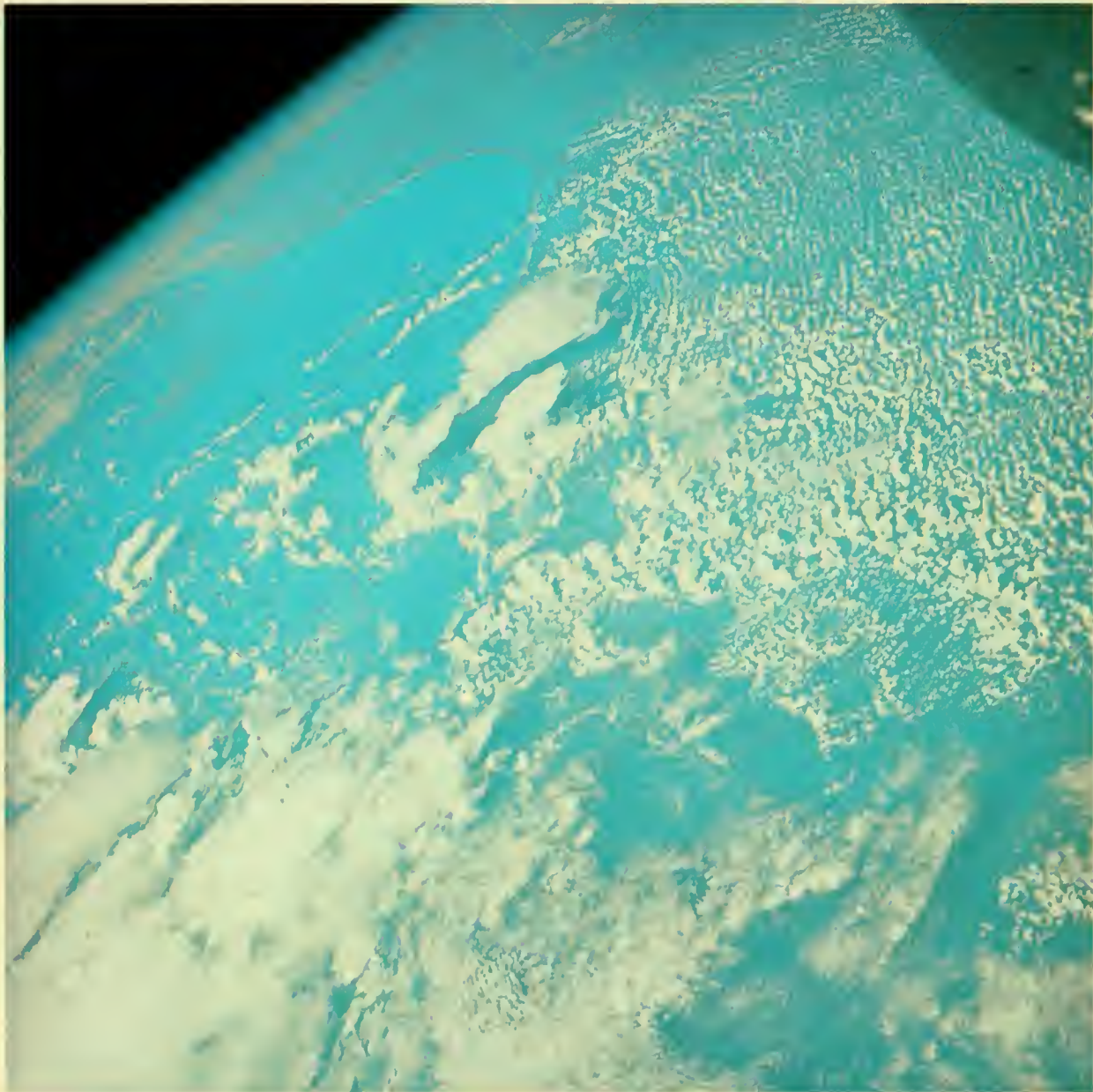
Overlapping the preceding one, this photograph of central Chihuahua shows the Sierra del Nido (center), the Santa Clara River (left), and Laguna de Encinillas (right of center).

S-65-45742



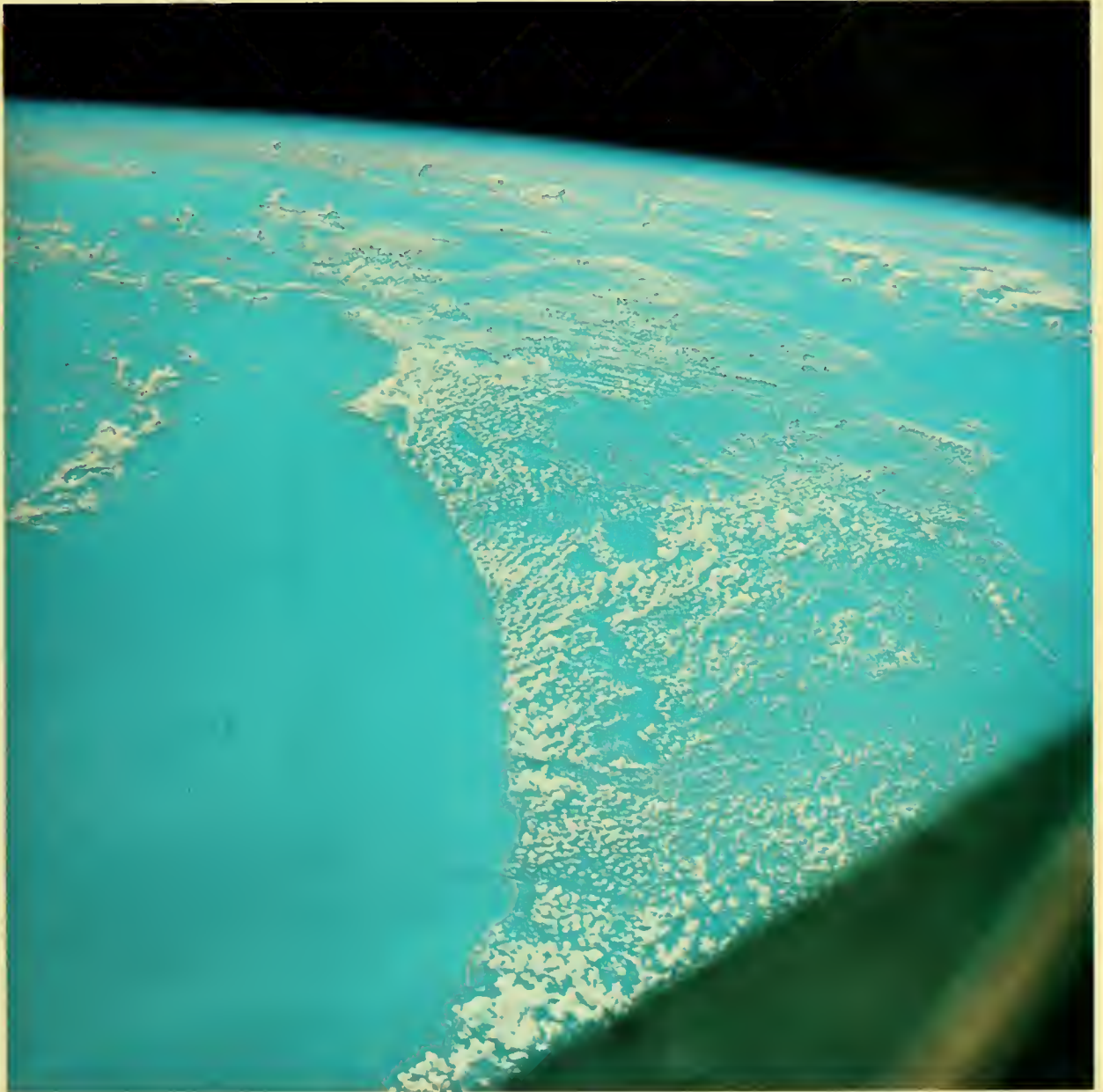
Another view of Chihuahua, Mexico. The three mountain ranges are Sierra del Nido (left), Sierra Magdalena (top right) and Sierra Cascaramusas (right). Laguna de Encinillas is in the center of the photograph.

S-65-45743



View southwestward across Texas and the Gulf of Mexico into Tamaulipas, Mexico. Cloud lines form an arc around thunderstorms near Houston in the center of the picture. Small cloud streets at left center indicate convergence toward towering cumuli building near the Texas-Louisiana border. Altocumulus clouds over western Louisiana at lower right are merging eastward toward the cumulonimbus, overlain with much cirrus cloudiness, in the lower left corner.

S-65-45745



Isolated thunderstorms near the horizon tower in the vicinity of Cuba (left) in this view of Florida. An easterly breeze suppresses cloud development along the coast. Curvature in the cloud lines is evident near Cape Kennedy where development is reaching cumulonimbus stage. The lines across central Florida show the transition in the wind flow from easterly on the Atlantic to southeasterly on the gulf coast. The complex flow pattern is typical for a large peninsula, where sea breezes along both coastlines can influence major mesoscale circulations.

S-65-45746



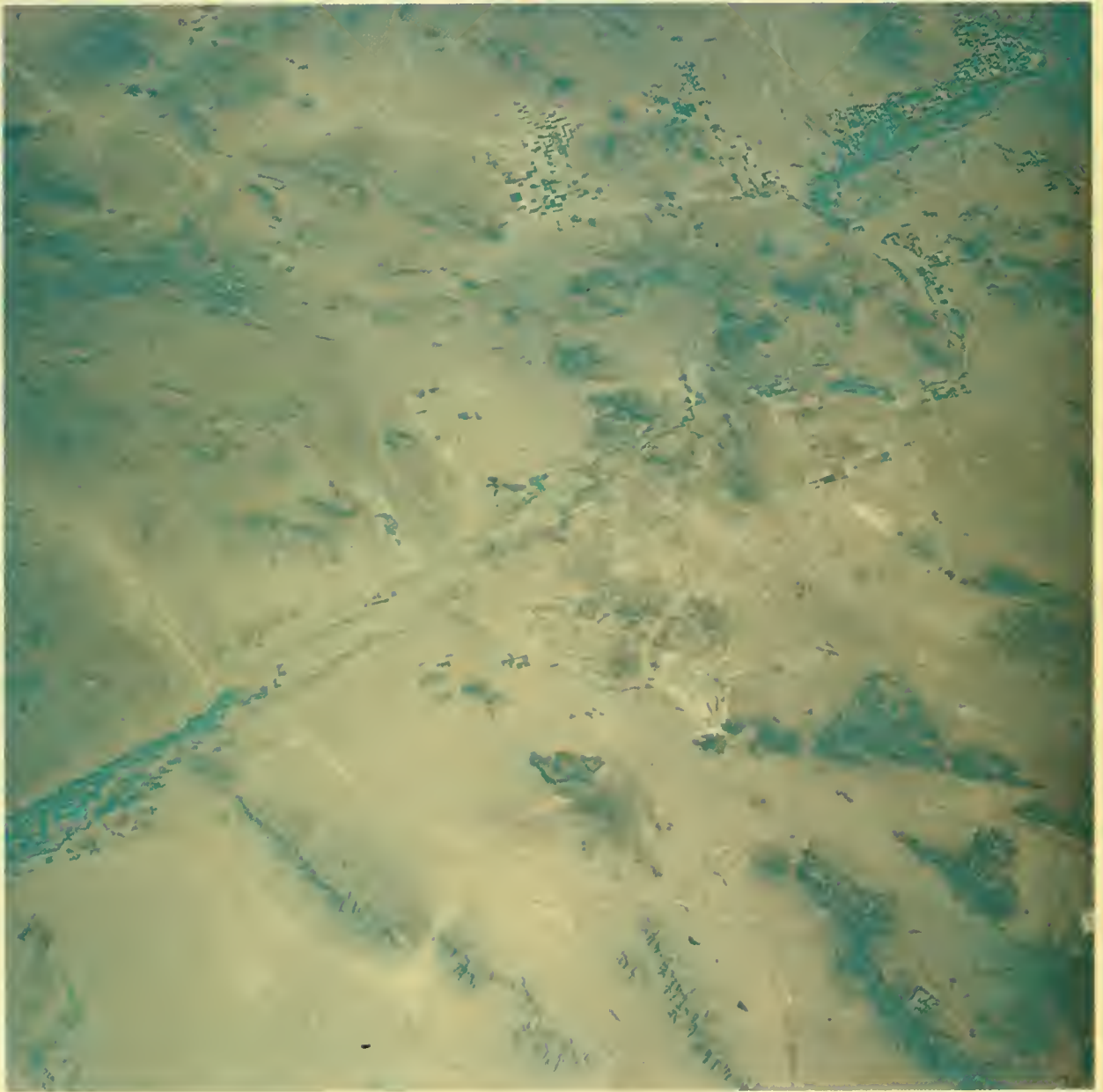
The Imperial Valley of California, with Arizona in the background and the United States-Mexico border to the right. The Joshua Tree National Monument can be seen left of the Salton Sea. Farms are in the foreground.

S-65-45747



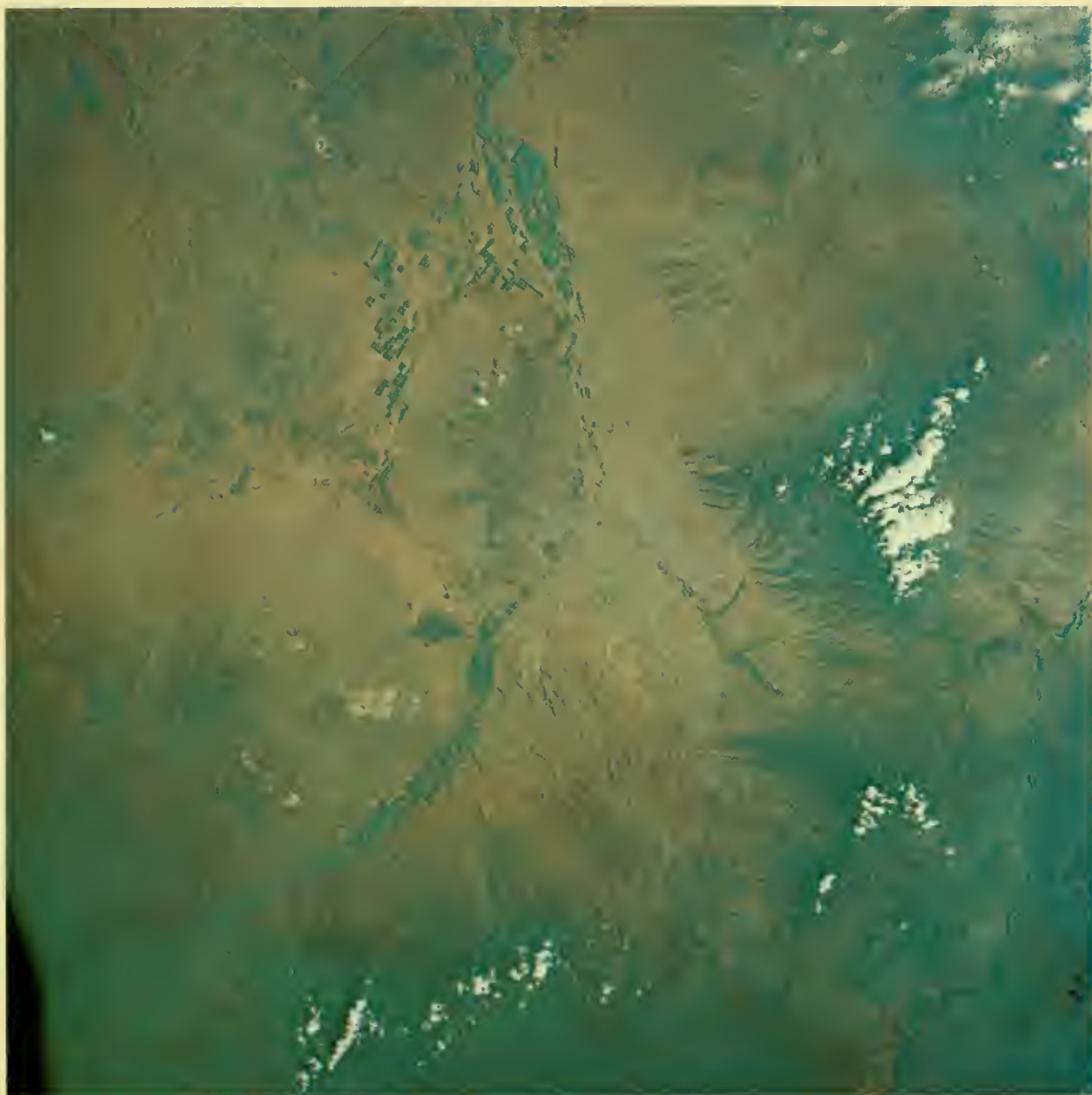
A second photograph of California's Imperial Valley giving a clear view of the Salton Sea. No agreement exists concerning the cause of the gyre seen in the center of the sea.

S-65-45748



The Gila River Valley between Yuma and Phoenix, Arizona. The Mohawk and Growler Mountains are in the foreground and the Gila Bend Mountains at upper right. This picture shows typical physiography of the Basin and Range Province with linear fault block mountains, chiefly composed of igneous rock, and sediment-filled valleys.

S-65-45749

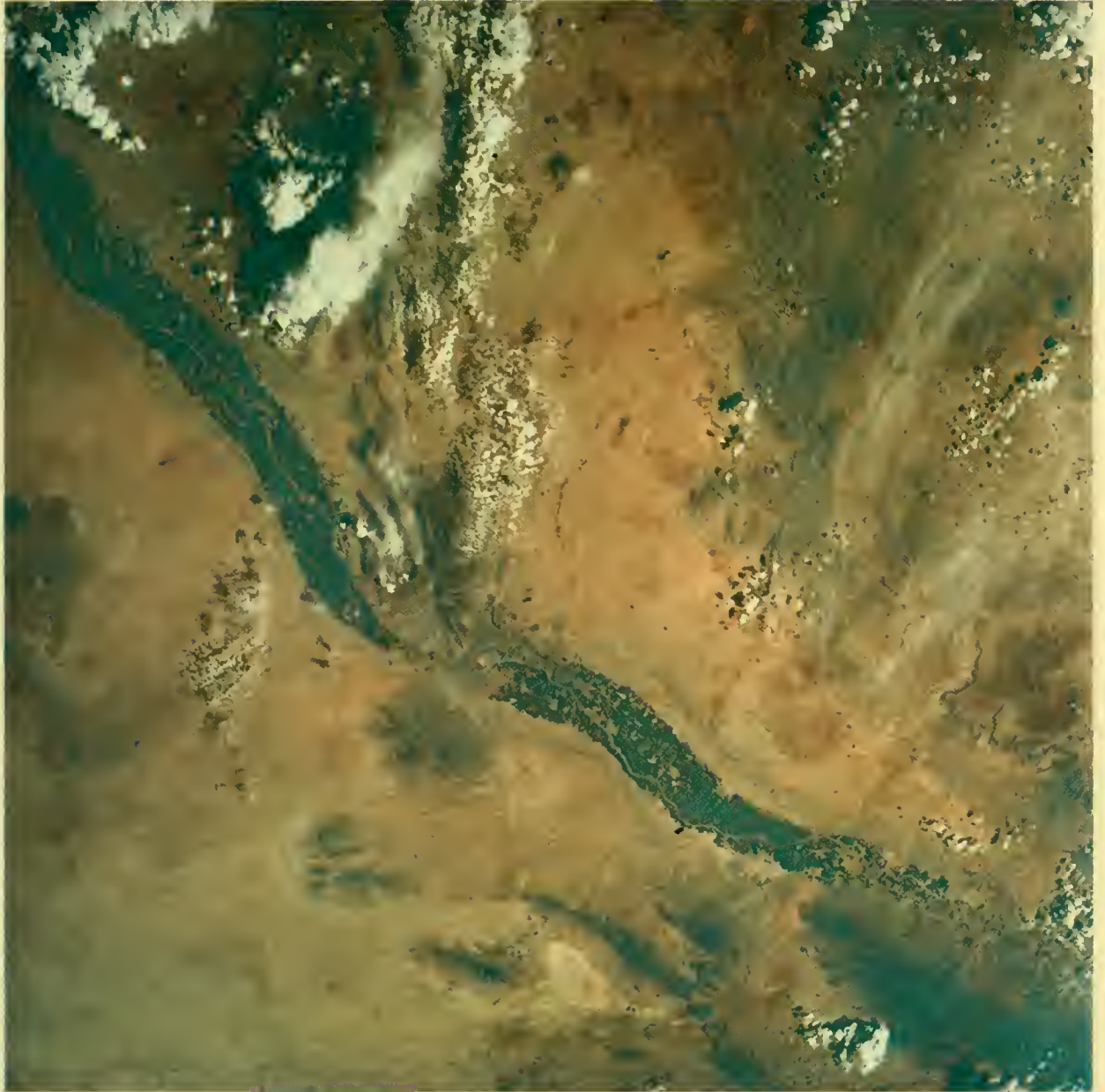


Tucson on the Santa Cruz River lies near the center of this photograph of Arizona. The Saguaro National Monument is toward the lower right. The Tucson Mountains, at left center, are surrounded by a pediment with a few Quaternary lava flows visible. Open pit copper mines can be seen on the pediment. S-65-45750



Southeastern Arizona with the Willcox Dry Lake clearly seen at lower left. From left to right along the upper portion of the picture are the San Pedro River, the Galiuro Mountains, and the Gila River. The Gila Mountains are covered by clouds (upper right corner).

S-65-45751

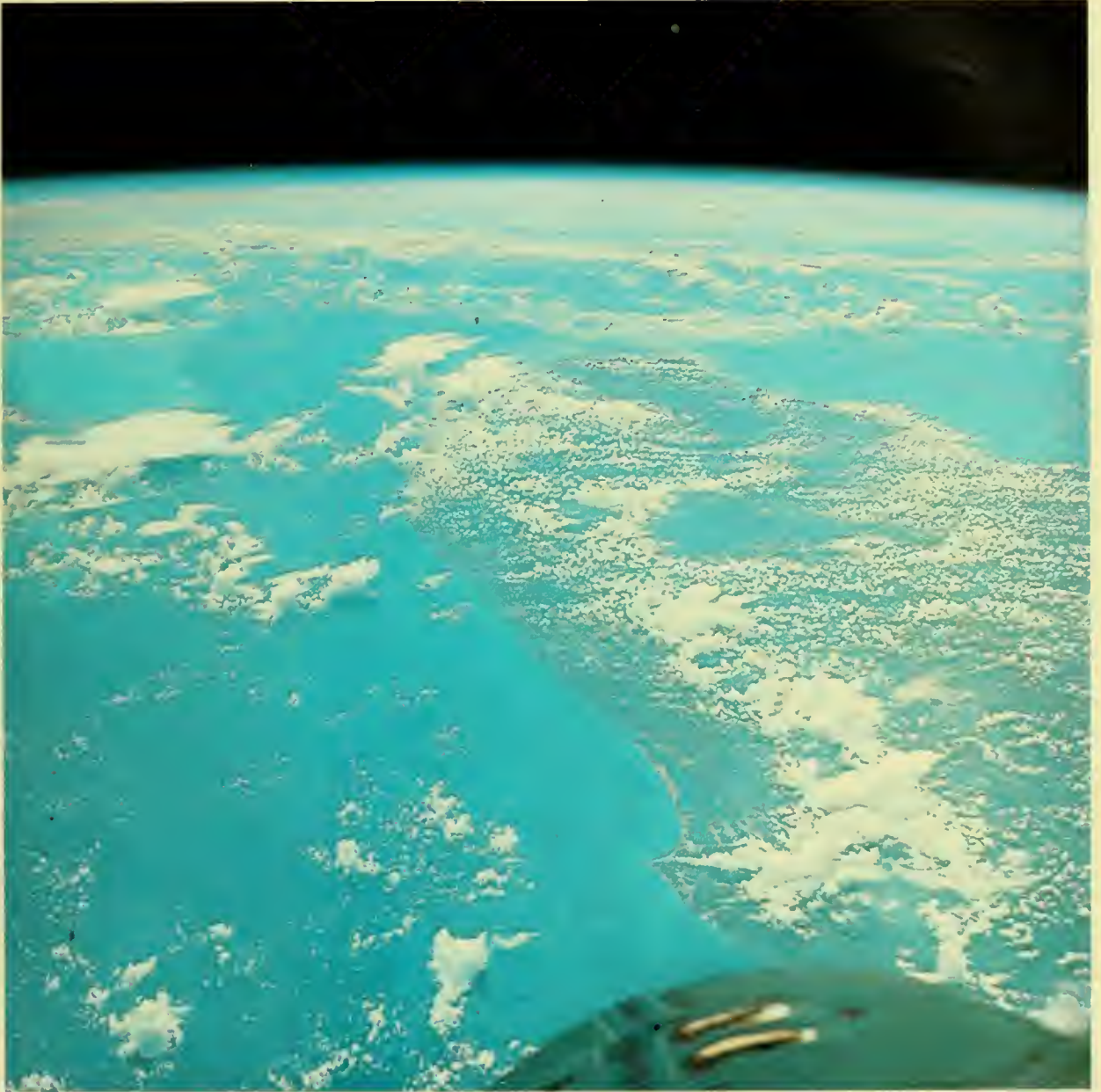


The Rio Grande boundary area between Chihuahua, Mexico (bottom), and the United States (top). El Paso and Ciudad Juarez are near the center of the picture. Kilborne Hole volcano and lava flows of the Potrillo Mountains are visible on the far left.

S-65-45752



Cumulus clouds cover most of the land in this photograph of the Atlantic coast of Florida. The cumulus congestus near Cape Kennedy is developing to the thunderstorm stage. The anvil-topped towers of other thunderstorms are seen over the Miami area and the Bahama Islands (upper left). S-65-45753



A second picture of Florida taken immediately after the preceding one. Both were taken one revolution after the photo on page 163.

S-65-45754



This picture of the Florida peninsula, looking north, was taken on the next revolution, 1½ hours later than the photo on page 170. The cumulus congestus clouds southwest of Cape Kennedy have matured into thunderstorms as indicated by the presence of cirrus clouds being blown westward by the high-altitude winds. The Tamiami Trail, which crosses the Everglades, is visible at the bottom of the picture. S-65-45756



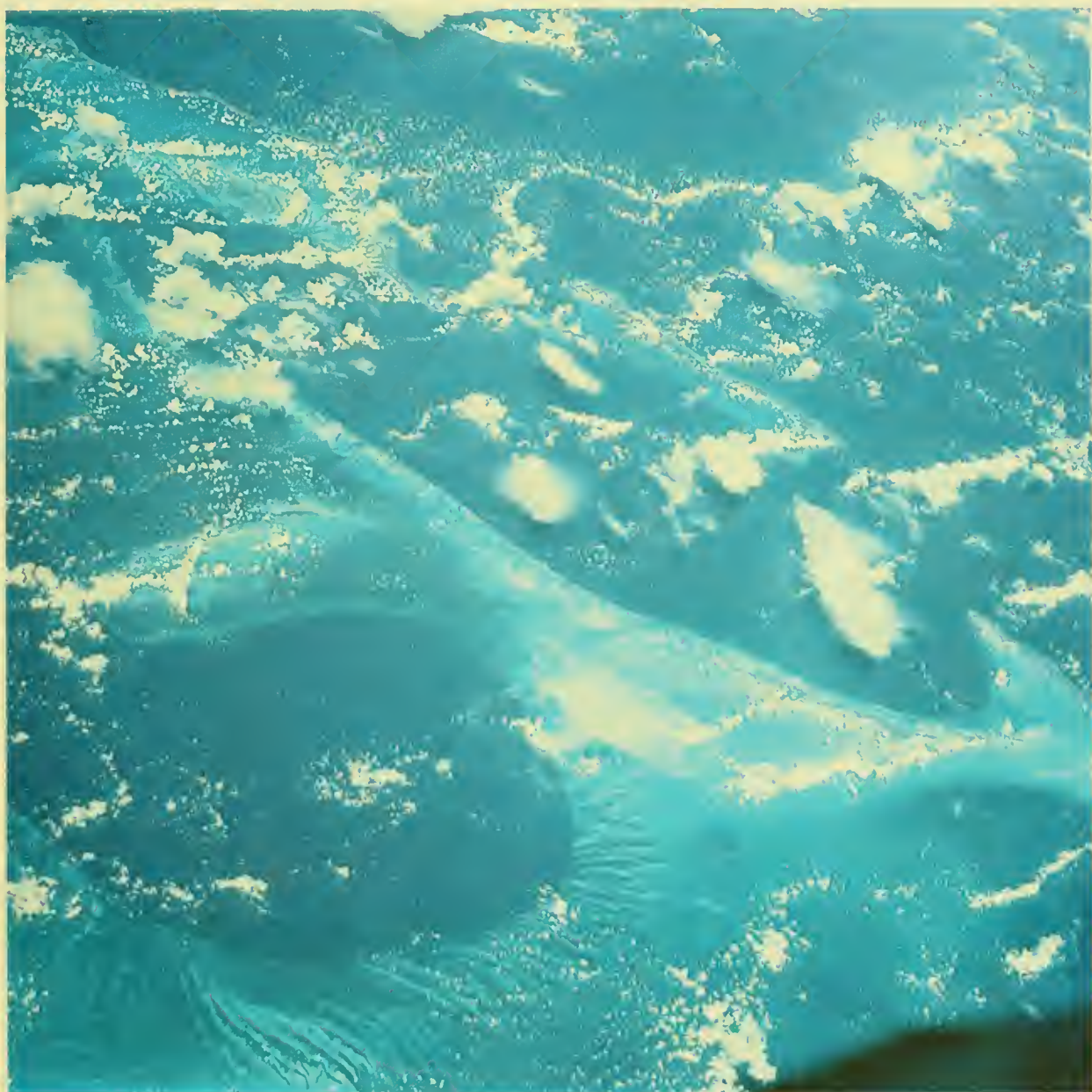
The east coast of Florida from St. Augustine to Florida Bay. Miami is just below the center of the picture. North and South Bimini Islands can be seen at the lower right edge. The cloud mass at the lower left is a complex of thunderstorms. The long lines of cirrus entering from the right side may have originated in the thunderstorms over the Bahamas shown in photo on page 170.

S-65-45758



A view of Andros Island, on the edge of the Tongue of the Ocean, in the Bahamas. The shoal areas surrounding Andros and the northwest edge of the Tongue of the Ocean are seen in the lower portion of the photograph.

S-65-45759



The Great Bahama Bank and the Tongue of the Ocean. The deep blue area in the center is Exuma Sound with depths up to 7,000 feet. Above it is Cat Island; below, Great Exuma Island. A part of Long Island is visible at the far right. The water in the Tongue of the Ocean is over 1 mile deep, while depths on the Banks vary from 6 to 30 feet. Lower left shows bottom topography (sand bores).

S-65-45760



Baja California, Mexico, from Punta San Marcial (bottom right) to Punta Arena on the Gulf of California. The Pacific Ocean is in the upper right corner. Off the coast near Bahia de La Paz are the islands of San Jose (center) and Espiritu Santo (upper right).

S-65-45764



Turbidity caused by offshore currents and sediment movement is shown in this photograph of Laguna de Terminos and Campeche Bay on the Yucatan Peninsula, Mexico. A current from the northeast carries the turbid waters westward along the coast and as far as 3 miles out into the bay. The cumulus cloud pattern is typical of a tropical region. Rio Usumacinta, laden with sediment, is visible in the lower left corner.

S-65-45765



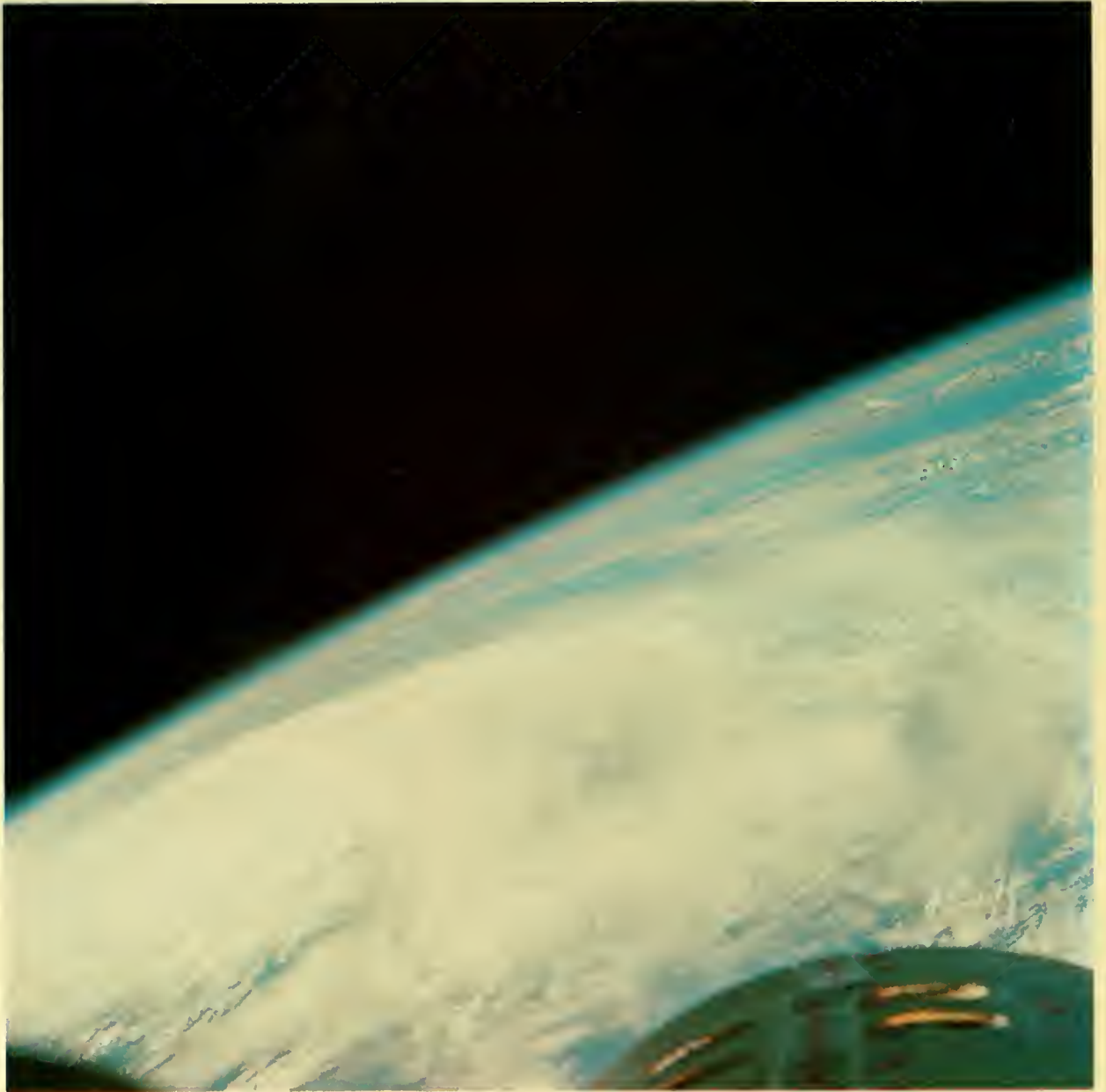
A view of the mouth of the silt-laden Yangtze River on the coast of mainland China, with Shanghai in the lower center of the picture. The river flow pattern and disposition rate seen here can be traced for over 75 miles as the river effluent mixes with the China Sea.

S-65-45768



The southern part of Honshu Island in Japan. Seen at upper left is the port of Nagoya on Ise Wan (bay). Greater Osaka, with a population of 9 million, is at the far left. Kii Suido (straits) and the eastern tip of Shikoku Island are in the lower left corner.

S-65-45769



Typhoon Lucy photographed south of Japan. Extensive cirrus cloudiness covers much of the storm, but some curvature can be seen in the cloud bands, which tend to spiral toward the storm's center.

S-65-45770



This is another view of Typhoon Lucy south of Japan. Some cirrus cloud bands in the lower right corner are oriented radially with the storm's center. All tropical cyclones derive their energy from the latent heat of condensation. Forming in ocean areas having a high surface temperature, usually above 26° C., they die out rapidly on land where surface friction is higher.

S-65-45771



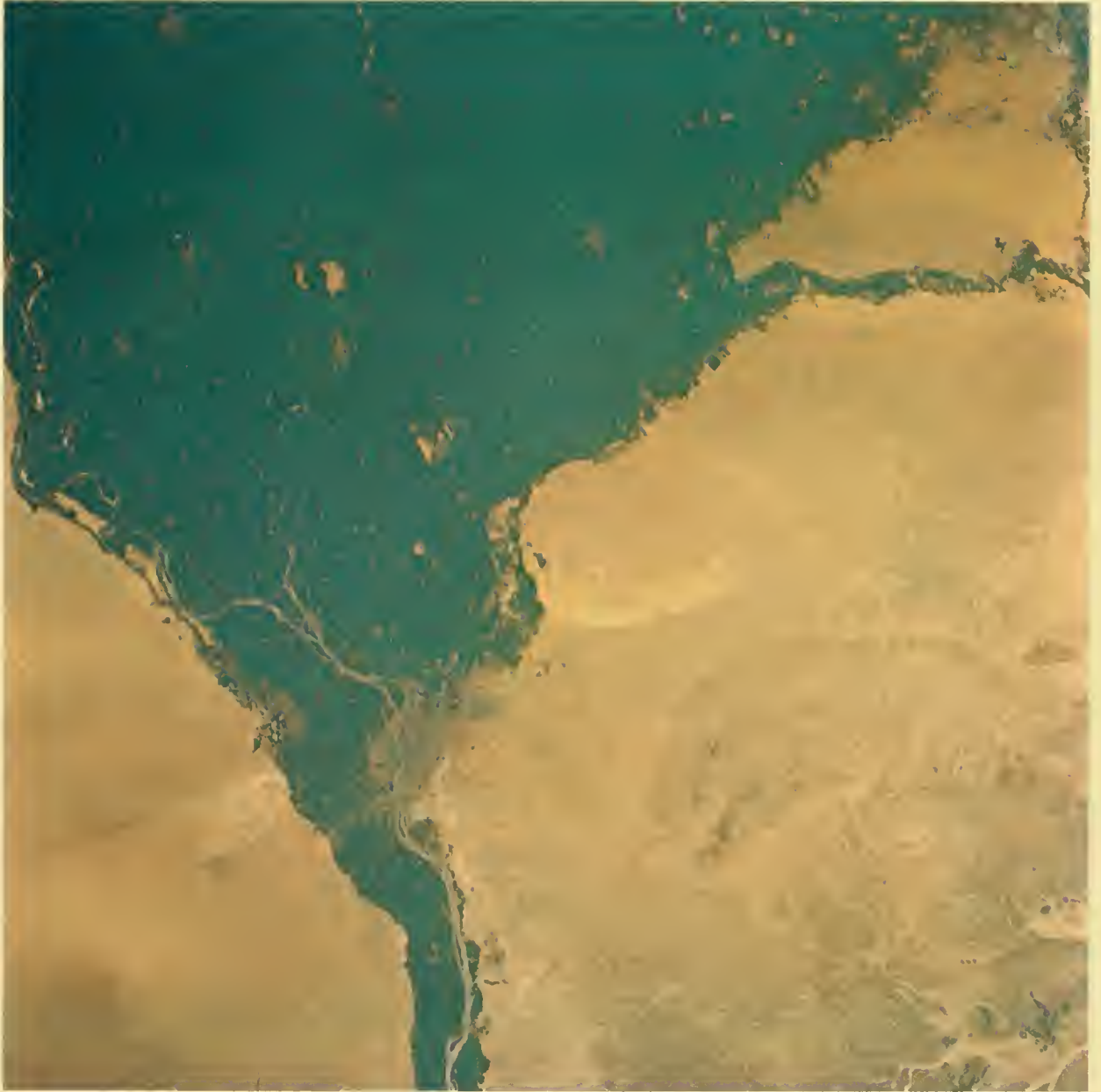
Eastern Afghanistan and northern Pakistan looking northward into mainland China and the U.S.S.R. The Kabul River is in the foreground; the Kunar River, with headwaters in the Hindu Kush Mountains, at right center. The Panjshir River is visible on the far left.

S-65-45773

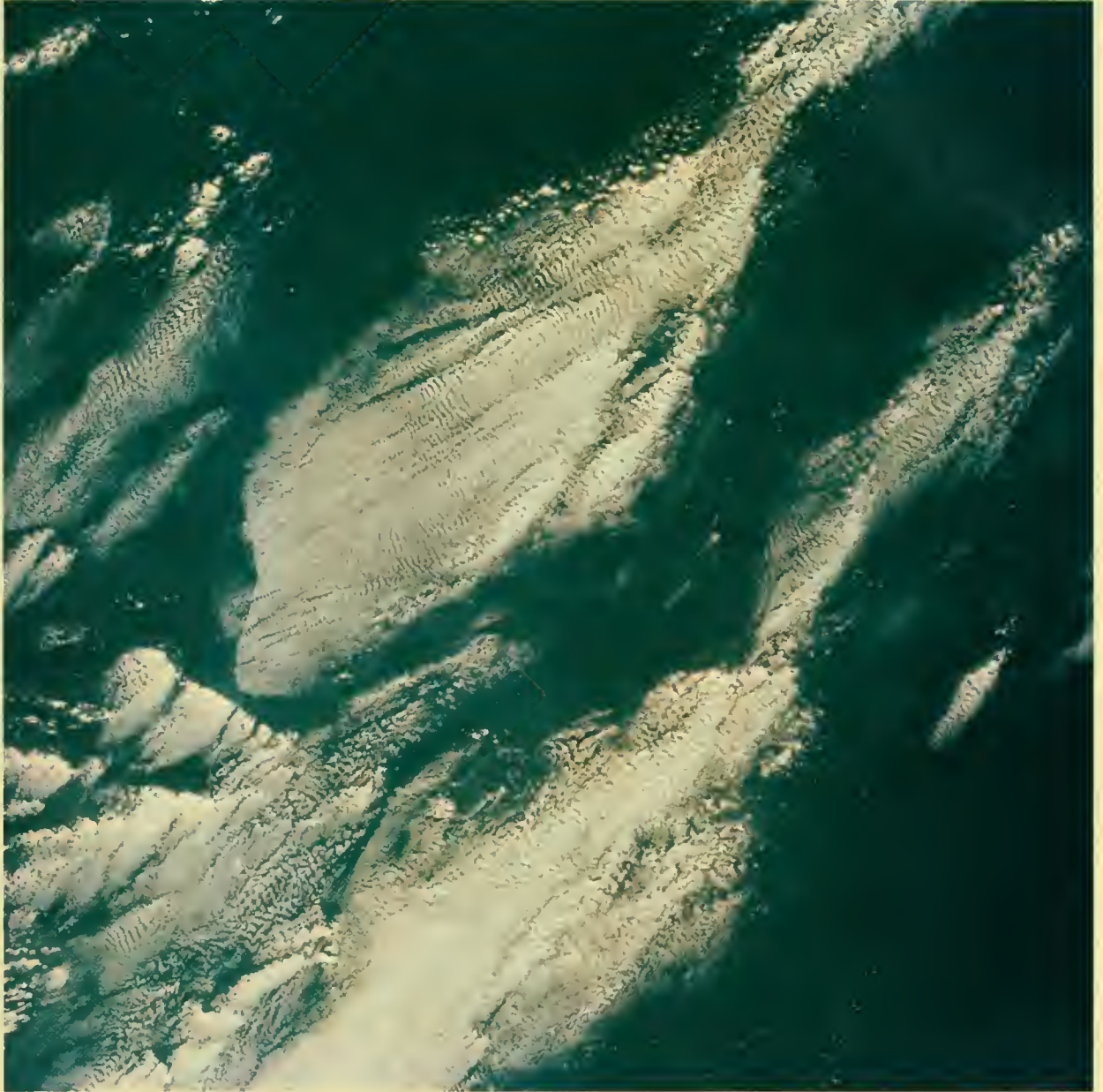


Central Taiwan covered by cumulus clouds. At upper left the cloud streets are aligned north-south over the Pacific Ocean. Some, at upper left, have grown to the cumulonimbus stage. At higher levels the anvil-like tops of cirrus show a northerly wind direction. The rivers in the T'aichung area discharge silt-laden water into the Formosa Straits (foreground), where it is carried northward along the shore.

S-65-45777



The Nile Delta in the United Arab Republic. Branching off north of Cairo (lower center) are the Rosetta Nile (left) and the Damietta Nile. S-65-45778



Band-structured clouds over the Gulf of Guinea off the coast of Africa. The cause of the sharp cloud edge at left center of the picture is unknown. S-65-45781



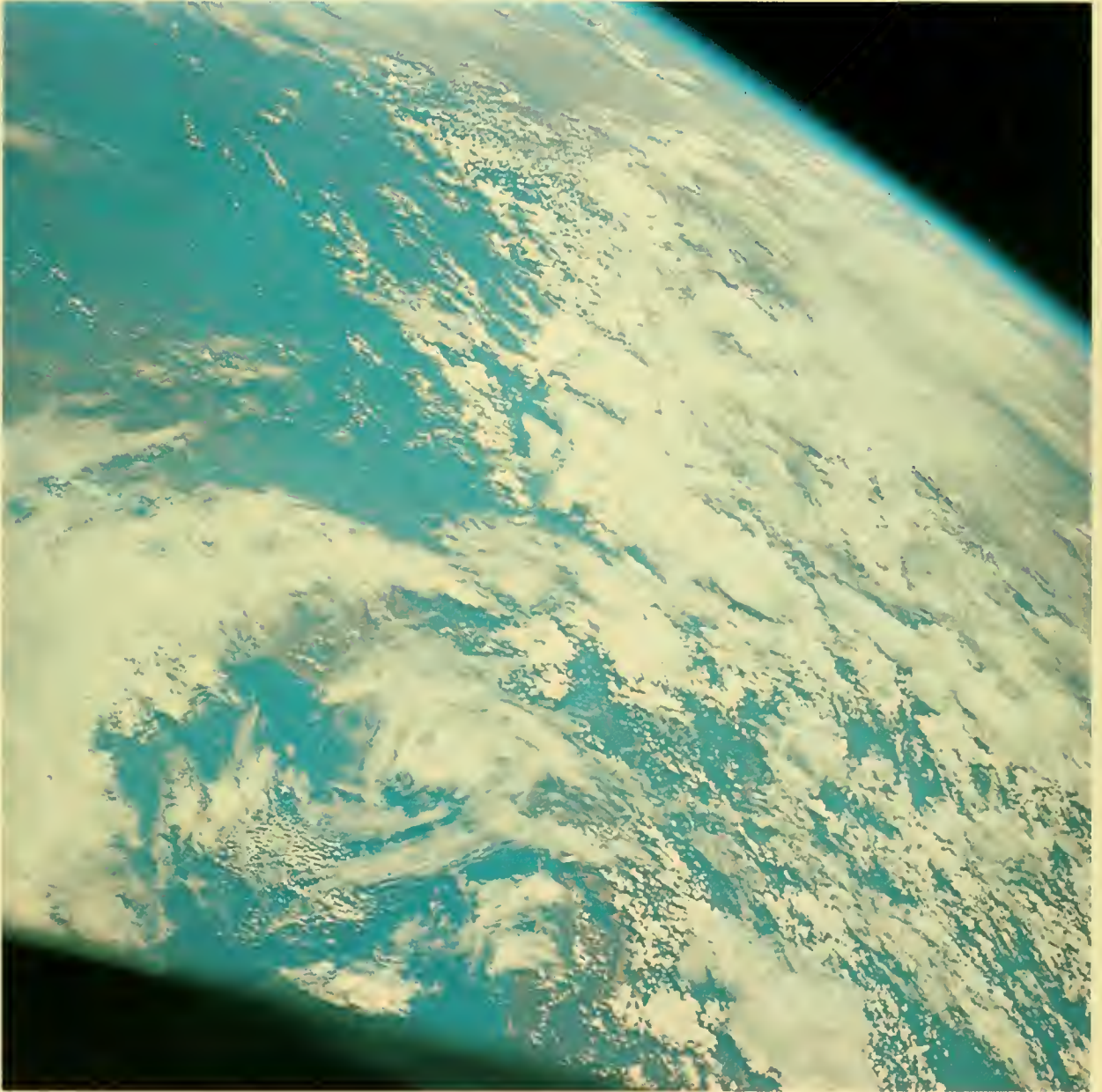
Convective clouds in various stages of development cover Florida and the Southeast in this view looking north. A line showing enhanced cloud growth appears to run from Jacksonville southward across the State to the Cape Sable area. Three thunderstorms in various stages of development are seen at lower left in the Key West region.

S-65-45783



Convective-type clouds dominate this area of central Cuba and several patches of cirrus clouds have been generated by thunderstorms west of Andros Island (upper right) and along the southern coastal region of Cuba. Open, polygon-shaped cloud cells are prominent over the sea north of Cuba. The cell walls, composed of many cumulus elements, may be regions of ascending air while the cloud-free interior may be regions of descending air.

S-65-45785



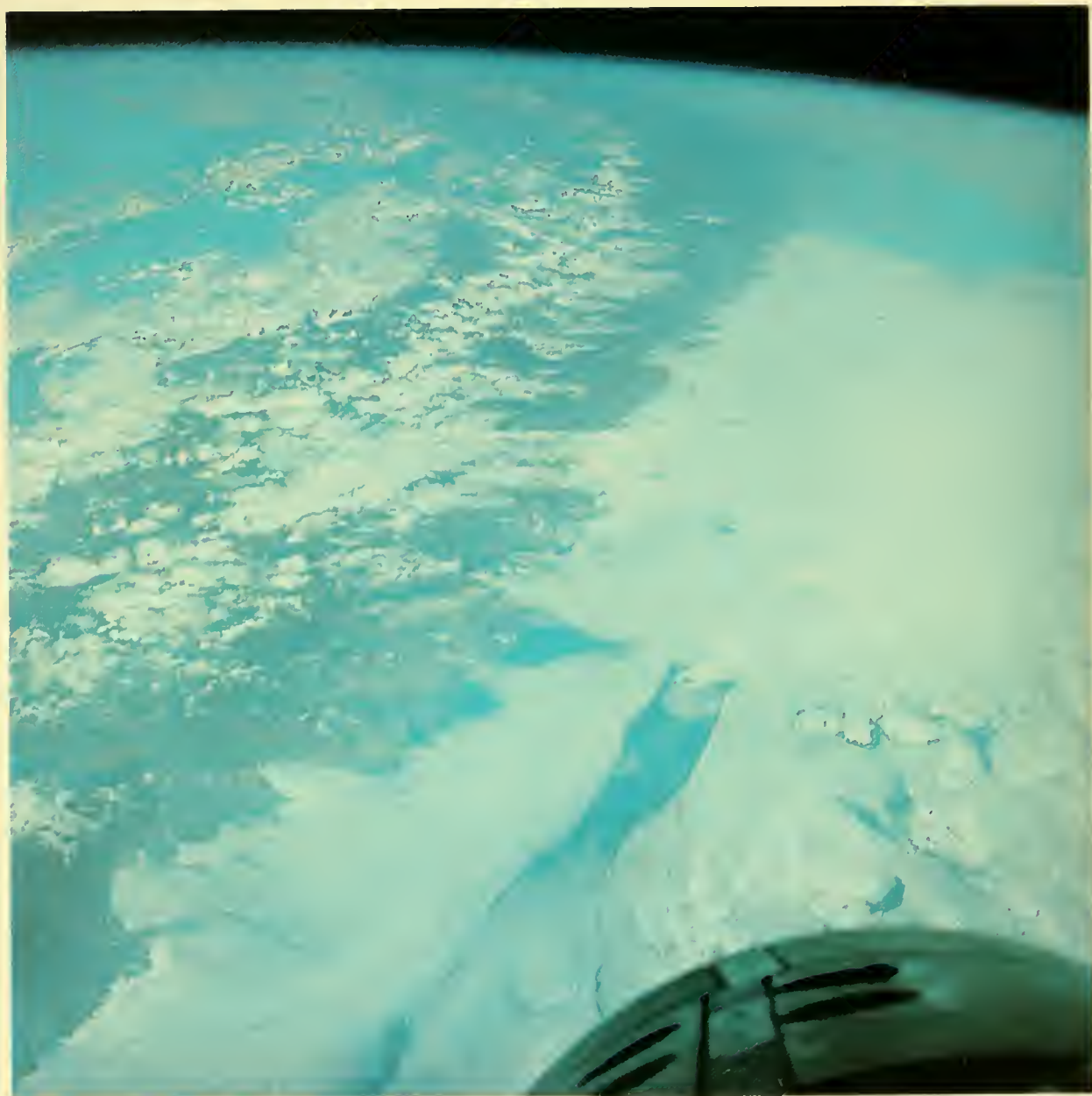
The cirrus cloud eddy in the foreground is located near Navojoa in Sonora, Mexico. It has a diameter of about 40 miles. The view looks across northwest Mexico from the Gulf of California in the foreground to Texas and New Mexico near the horizon. Numerous thunderstorms, each identified by its cirrus cloud top, are scattered throughout the cloudy region.

S-65-45787

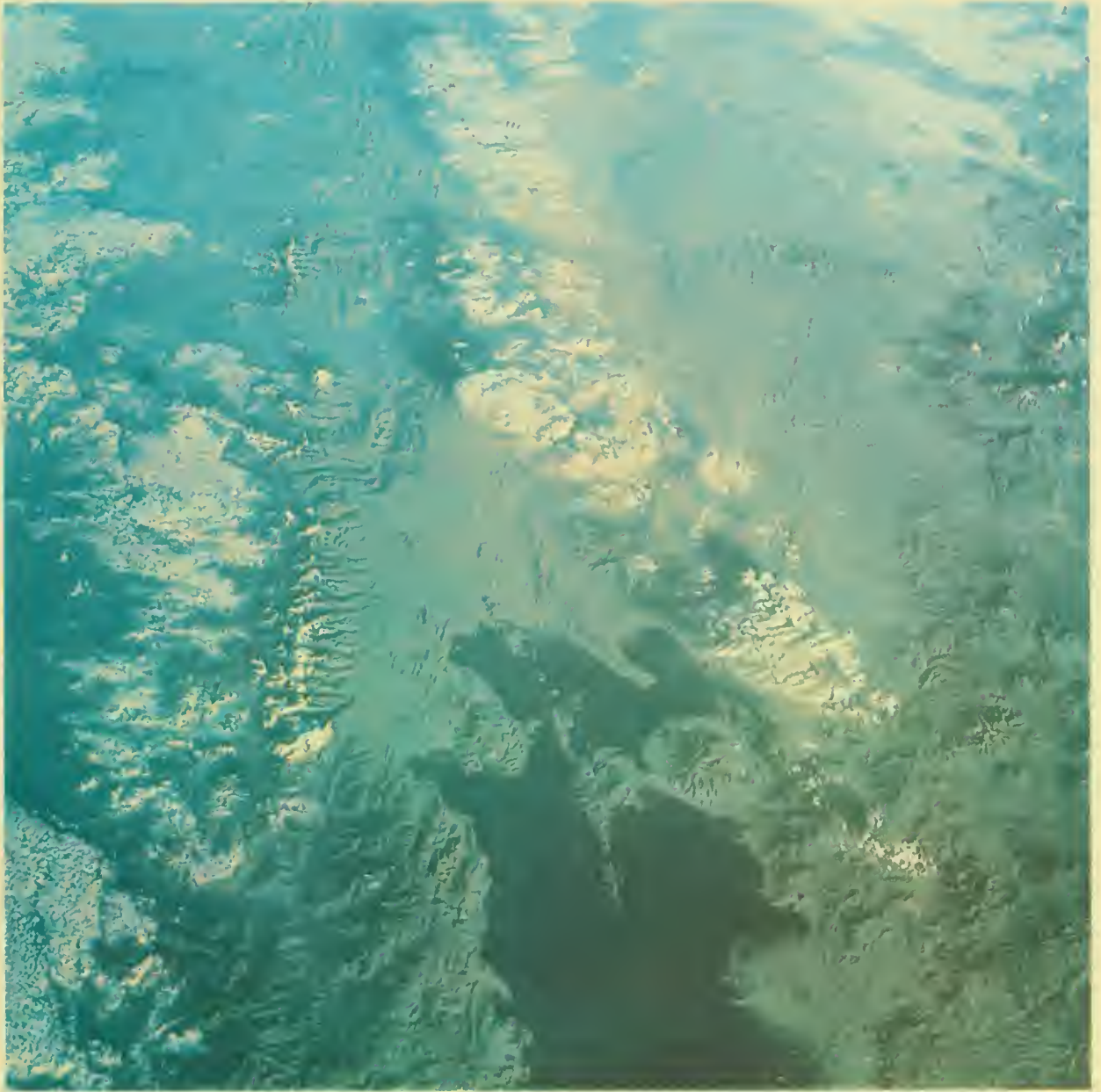


Tropical storm Doreen photographed over the Pacific Ocean between Hawaii and Mexico.

S-65-45790



The coast of Peru near Trujillo, looking south. The cloud-covered Andes Mountain chain stretches south along the left side. Paracus Peninsula is at the top of the coastline, about 100 miles south of Lima. The basin of the Ucayali River, a north-flowing tributary of the Amazon, is the blue area in the upper left. S-65-45791



The border area of Peru and Bolivia with Lake Titicaca and La Paz in center and foreground. Lake Poopo is partially visible at the top of the photograph. Two dry salt lakes, Salar de Corpasa and Salar de Uyuni, are seen in the upper right corner. The snow-covered peaks of the Cordillera Real are to the left. s-65-45792



Another view of Lake Titicaca, which lies 12,506 feet above sea level and is the largest navigable lake in the world at such an altitude. The photograph encompasses parts of Bolivia, Peru, and Chile.

S-65-45794



The Gulf of Kutch on the western coast of India. Above it lies the Rann of Kutch, a swampy area; below is the Kathiawar Peninsula. The city of Jamnagar is located on the Gulf at lower center.

S-65-45603



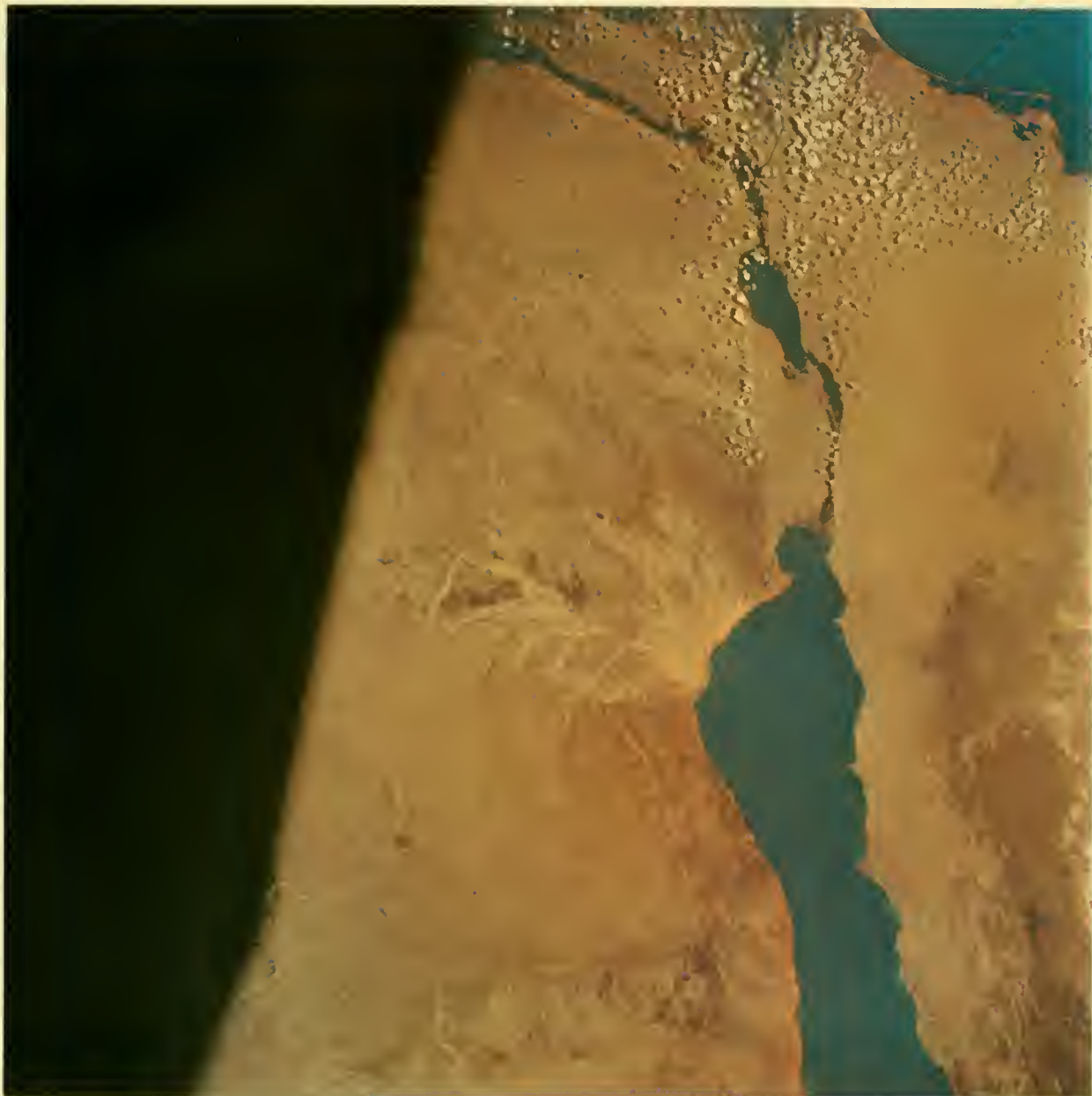
The island-studded sea south of Singapore is seen through a thin layer of cirrus clouds. The Lingga Islands are in the center and Bintan Island is on the far right. A large mushroom-shaped thunderstorm has built up south of the Inderagiri River Delta on the Island of Sumatra.

S-65-45604



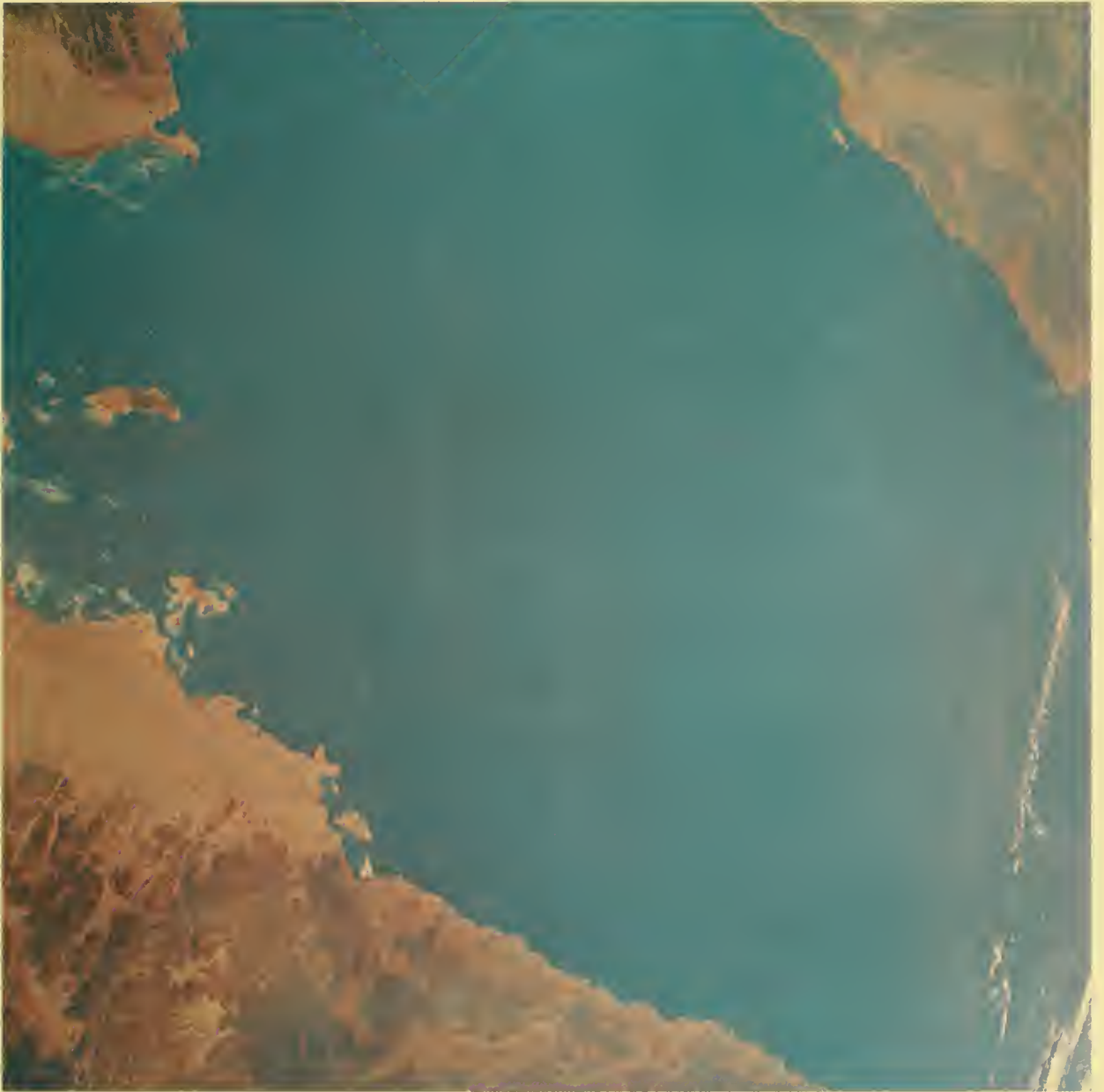
A view of the northern coast of Algeria, looking across the Mediterranean and the Balearic Islands toward Spain, which is visible on the horizon. The city of Algiers is near the center of the picture. Two dry lakes, Rharbi and Chergui, are in the foreground.

S-65-45605



Vertical view of the Suez Canal with the Sinai Peninsula to the right. A part of the Mediterranean Sea is visible in the upper right corner.

S-65-45607



The northern end of the Red Sea dominates this view of the United Arab Republic. The Sinai Peninsula is in the upper left corner and the tip of Saudi Arabia at upper right.

S-65-45608



Four sources of air pollution can be seen in this picture of the Gulf Coast and Mobile Bay, Alabama. A smoke plume bends southeast near Mobile (lower left). Two other plumes being carried by northwest surface winds, appear north of the city. Another is found north of Pensacola, Florida (top). The long line of cumulus clouds running diagonally across the photograph parallels the southwesterly wind flow near 10,000 feet.

S-65-45609



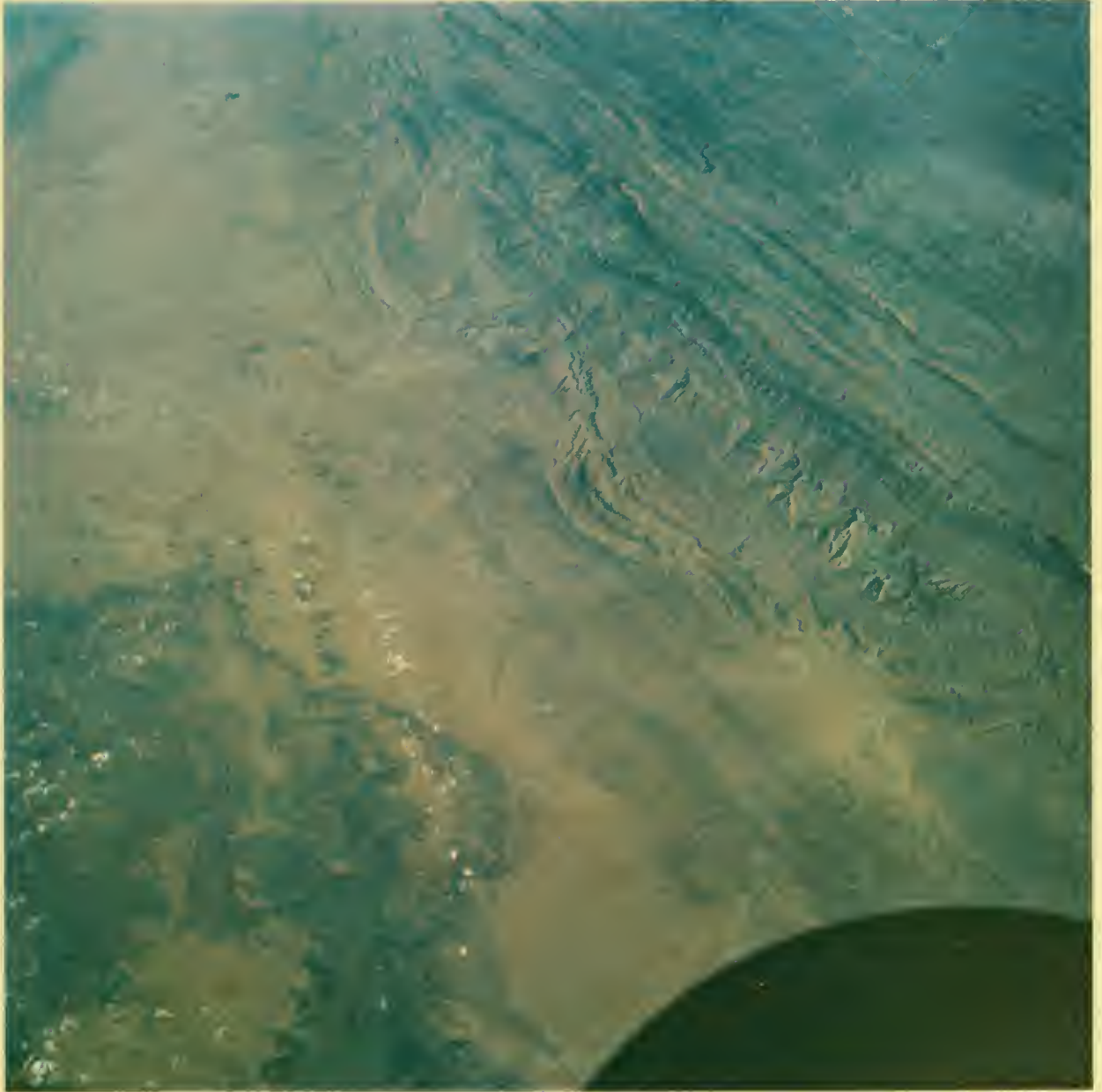
A near-vertical view of Lake Poopo in northwest Bolivia.

S-65-45613



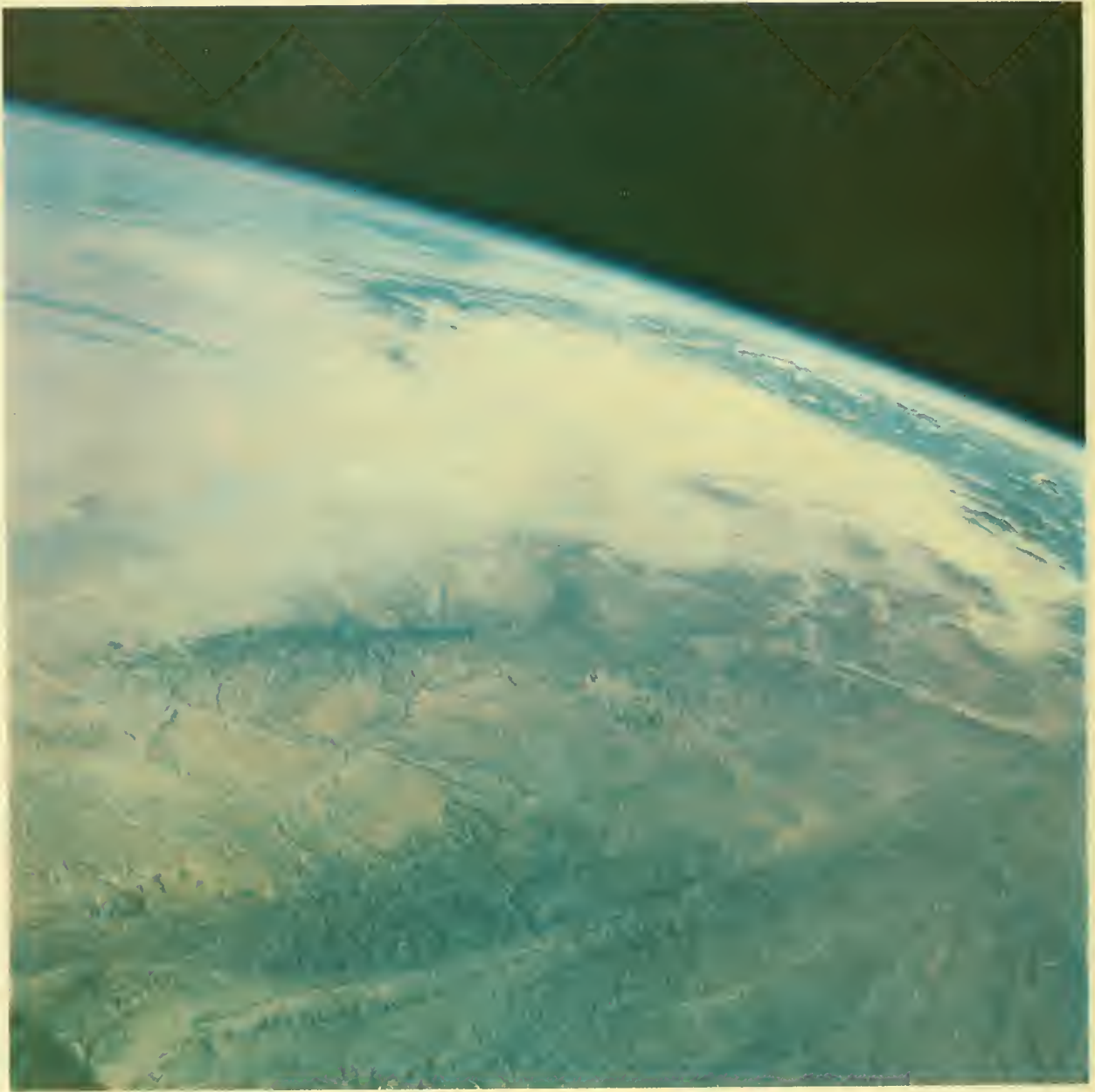
The island of Hawaii with its volcanic peaks of Mauna Loa and Mauna Kea is veiled by graphic clouds. Partly hidden by clouds on the right are the Islands of Maui, Kahoolawe, Lanai, Molokai, and Oahu.

S-65-45616



Southeast Iraq and southwest Iran with Sadiyah Lake and the Tigris River in the foreground. The Kabir Range and Zagros Mountains are seen at upper right.

S-65-45617



Northern Afghanistan near the U.S.S.R. border. The Hari River is in the foreground; the Murghab River and Turkistan Range, at left center. The Amu Dar'ya River and the Zeravshanskiy range in the U.S.S.R. are near the horizon. A large dust storm can be seen clearly to the upper left of the photograph. S-65-45618



Another view of Afghanistan, southwest of Kabul. The Band-i-Amir River is in the top center of the photograph. The Koh-i-Baba Range is at upper right. s-65-45620



Pakistan, southwest of Rawalpindi. The Indus River is in the upper left corner and the Jhelum River at bottom right.

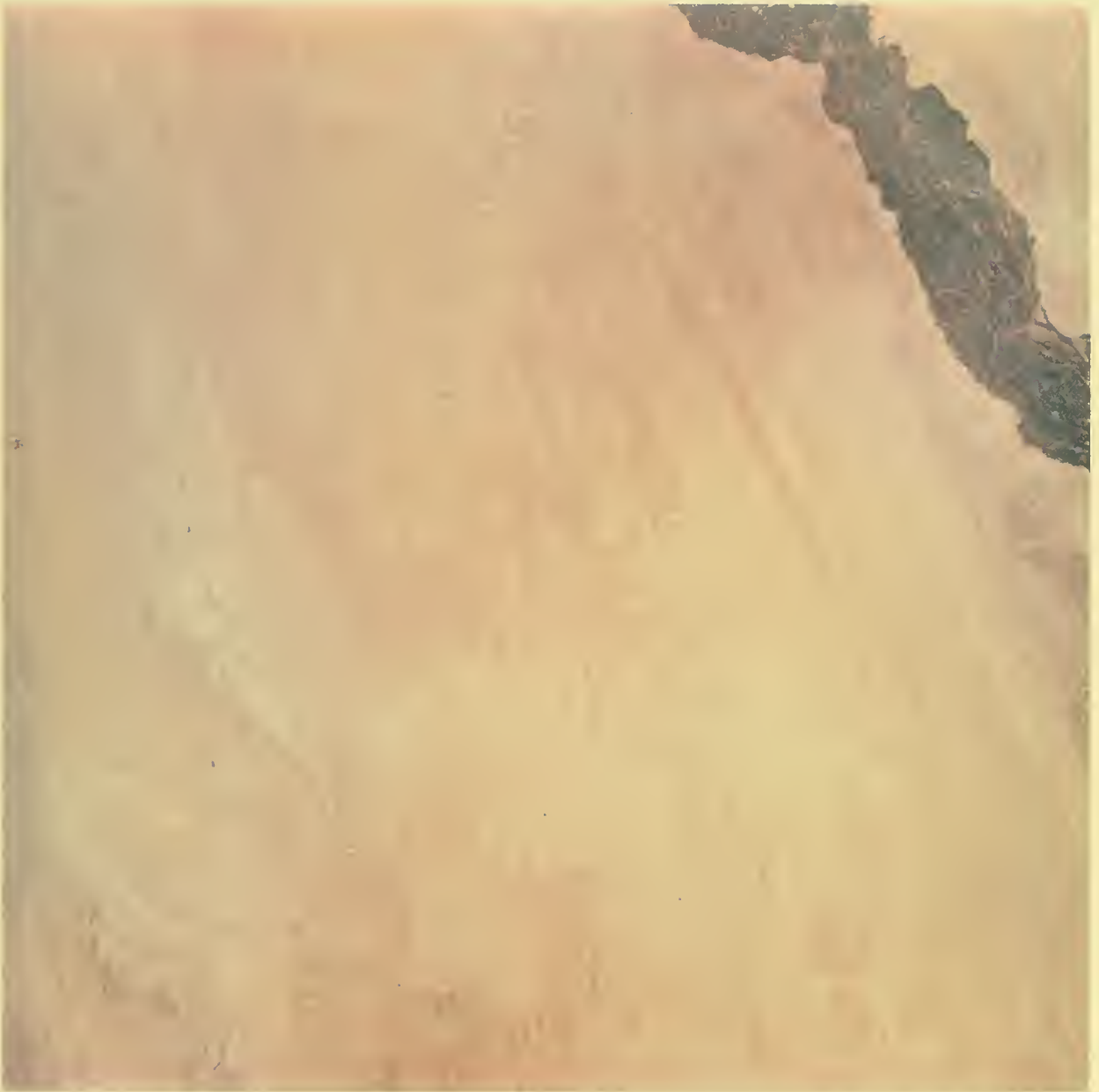
S-65-45621



A view of western Tibet with Lake Nganglaring in the upper left corner. S-65-45624



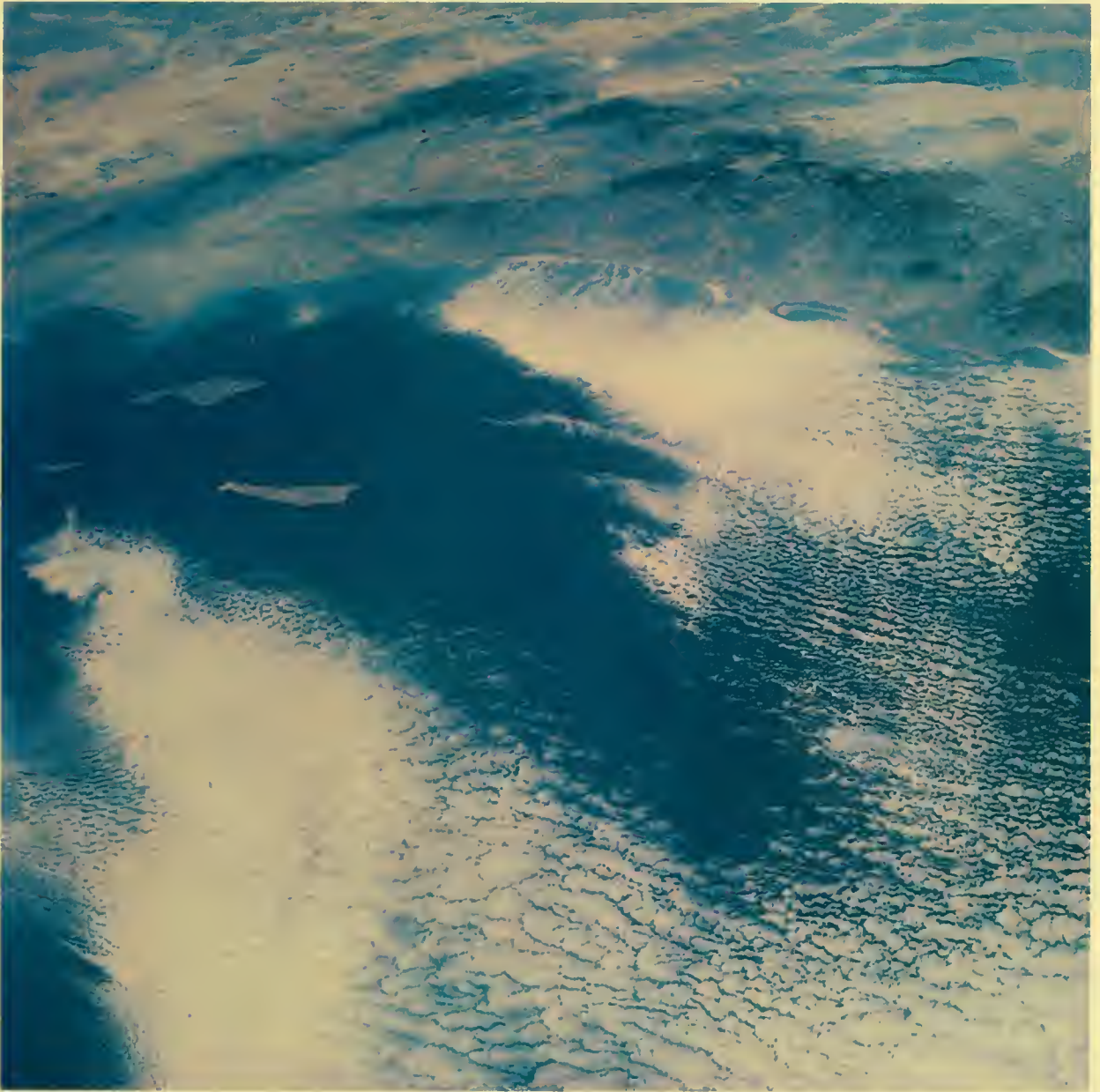
The Kwangtung Province of mainland China, southwest of Canton. Hong Kong is at upper left. The photo shows water-borne sediments from the Chu (Pearl) River being carried into the South China Sea along the coast. S-65-45625



A photograph of contrasts, showing the Western Desert in the United Arab Republic and the city of Asyut in the fertile Nile River Valley (upper right). S-65-45626



Central Cuba, looking southward to the Caribbean Sea. The Great Bahama Bank is in the foreground. The dark blue running across the center of the photograph is the Old Bahama Channel, where depths reach more than 4,000 feet. S-65-45628

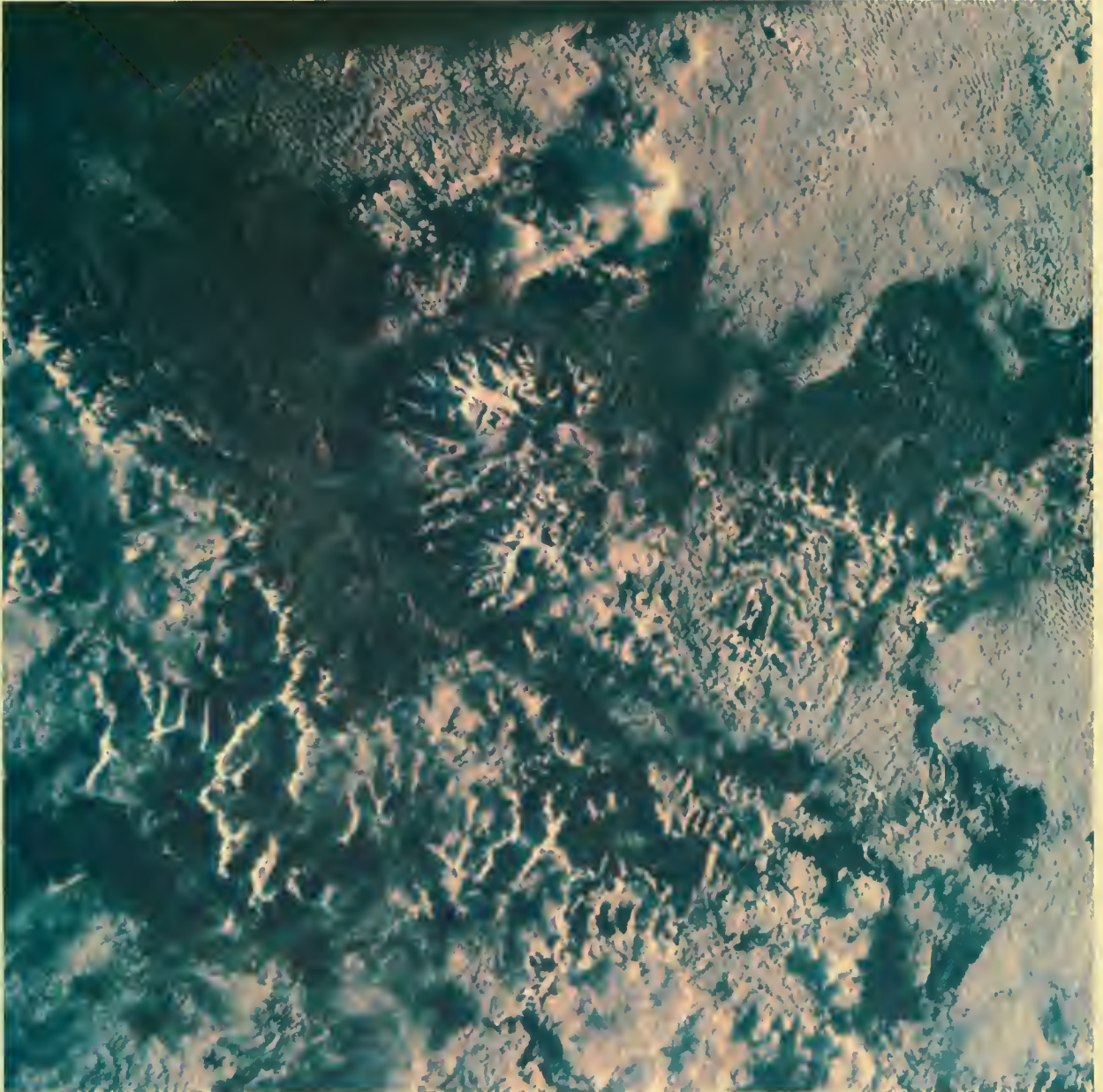


The Pacific coastline of California and Mexico from Los Angeles (left) to Punta Salsipuedes. The islands to the left are San Clemente and Santa Catalina. The Salton Sea in the Imperial Valley of California is visible in the upper right corner.

S-65-45631

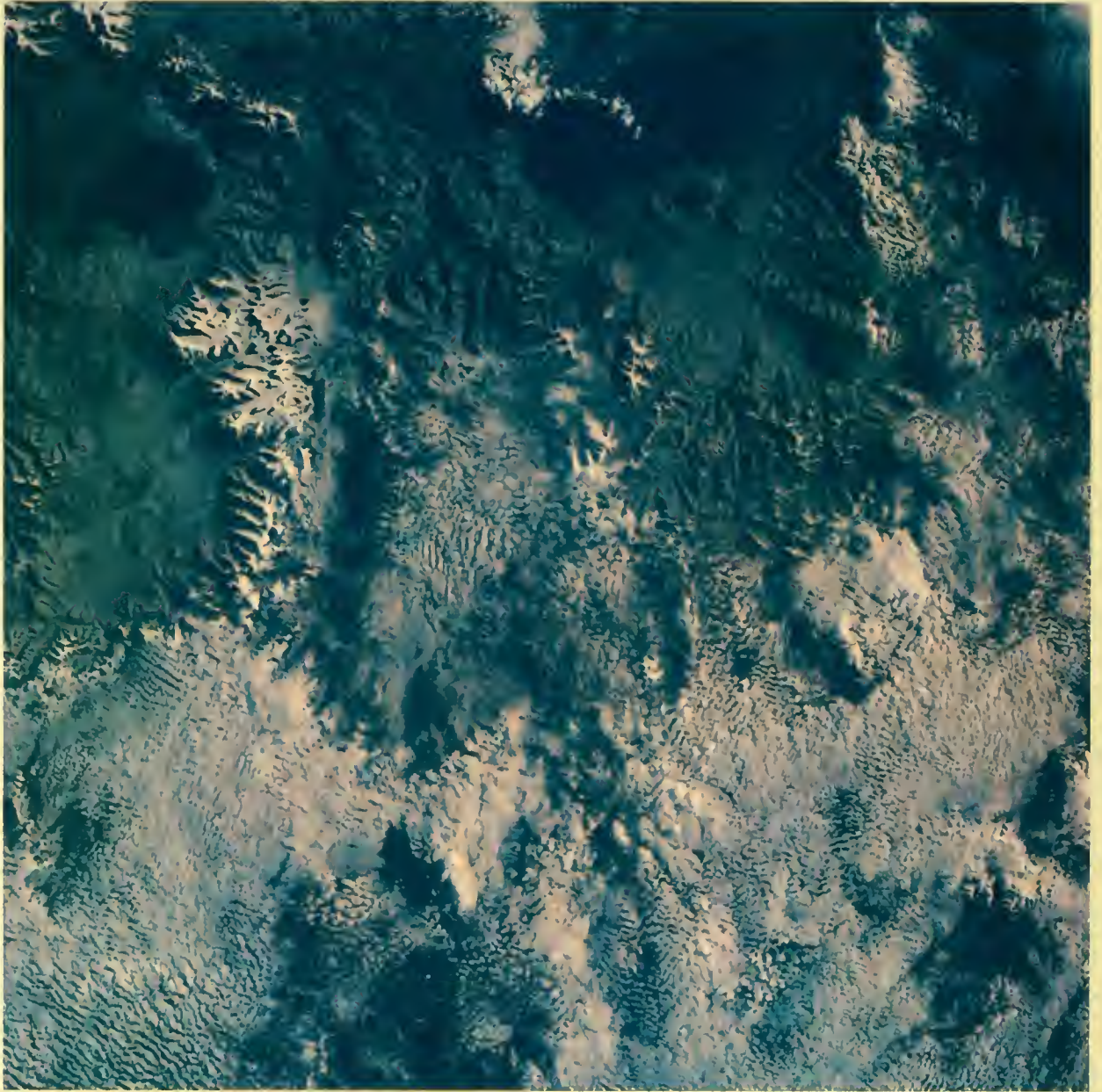


Honshu, the largest of the four major islands of Japan, with the Sea of Japan in the background. The port of Nagoya is located at the upper right edge of Ise Wan (bay) on the Pacific. Osaka is situated to the far left on Osaka Wan. S-65-45641



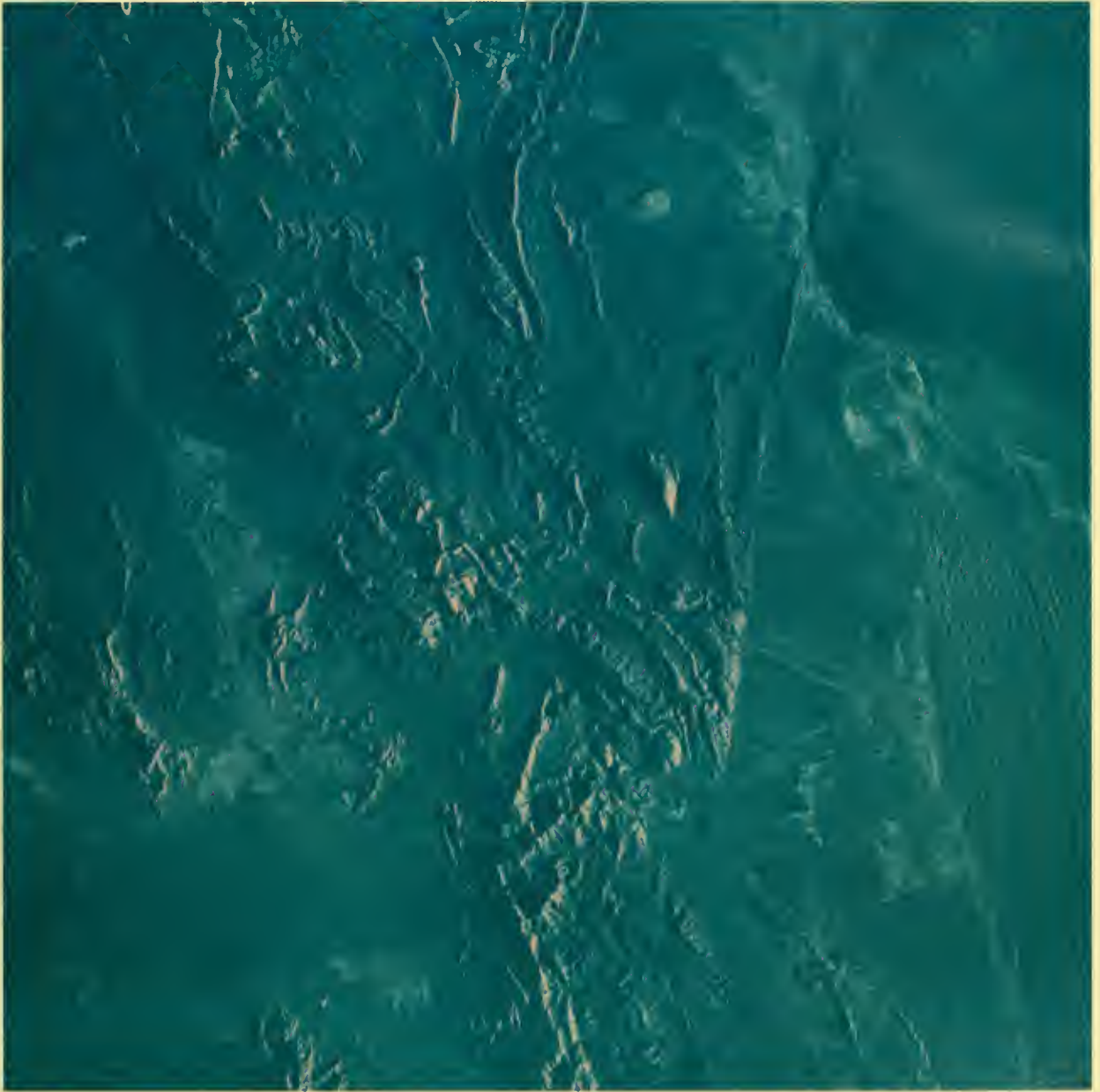
A near-vertical view of the northwestern tip of Nepal and southern Tibet. The peak just above the center of the picture, Gurla Mandhata, lies 25,335 feet above sea level. Glaciers are visible to the right of this area. Rakas and Manasarowar lakes are hidden by clouds to the left. Karnali River is visible in the upper left part of the photograph.

S-65-45644



Tibet in the area between Kebyang and the headwaters of the Brahamaputra River.
Tarok Tsho (lake) is at top center of the photograph.

S-65-45645



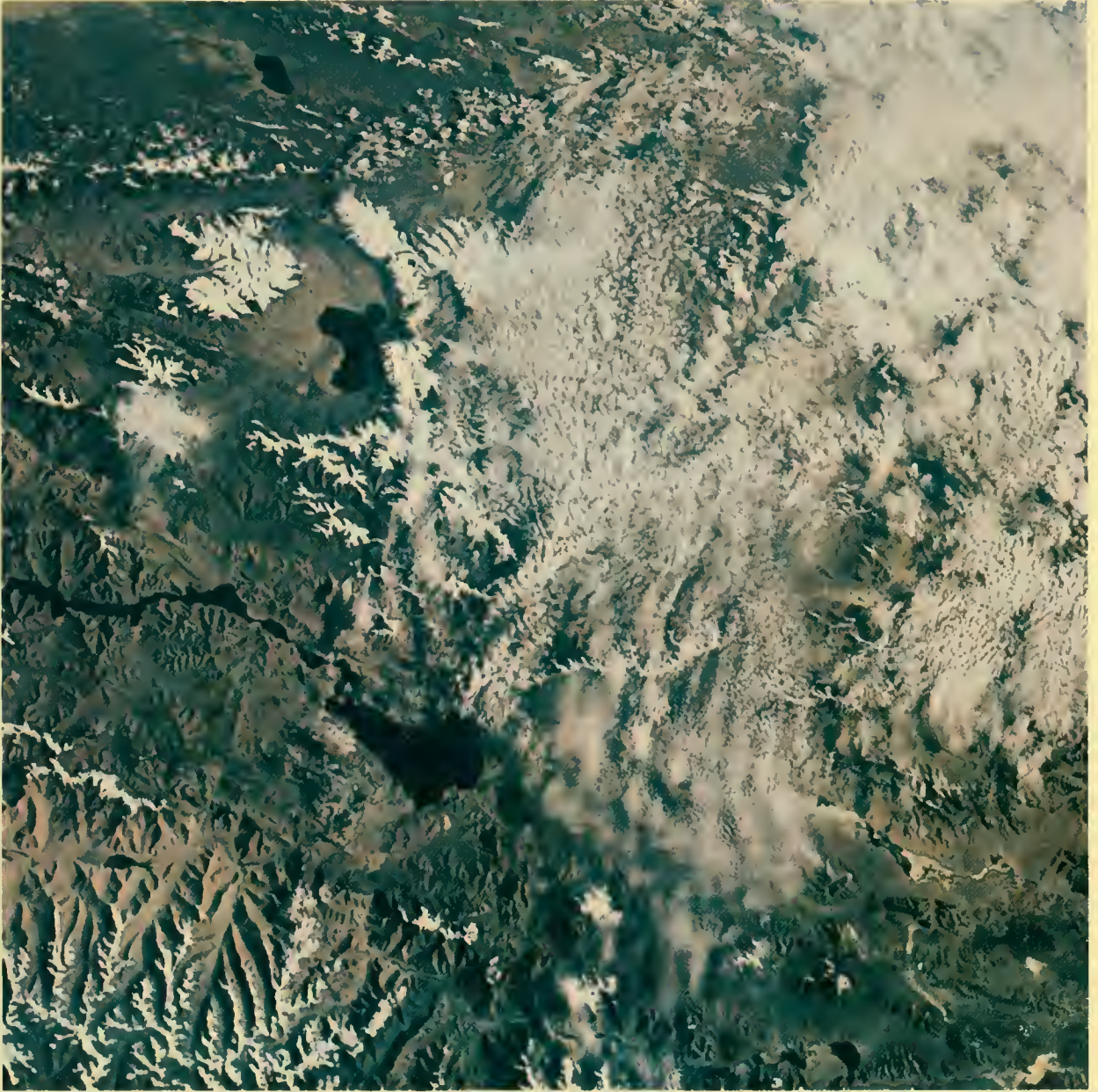
Mountain ranges in central Iran. Kerman City is at left center. In the upper right corner is Namakzas Lake.

S-65-45647



The border area between Kashmir and mainland China. The Shyok River bisects the picture and the Indus River cuts across the lower left corner in the dark valley. The glacier-fed tributary flowing from upper center is the Nubra River. The snow-covered peaks are part of the Karakoram Range.

S-65-45648



The border area of Kashmir and mainland China. Tsho (lake) Ngompa leads from left center into Nyak Tsho near the center. The lake near the upper left edge is Sarigh-yilganing Kol in Kashmir. Dyap Tsho is surrounded by the Chang Chenmo Mountains at upper left. In the left foreground is Shaldat Tsho, amid mountains of the Kailas Range.

S-65-45649



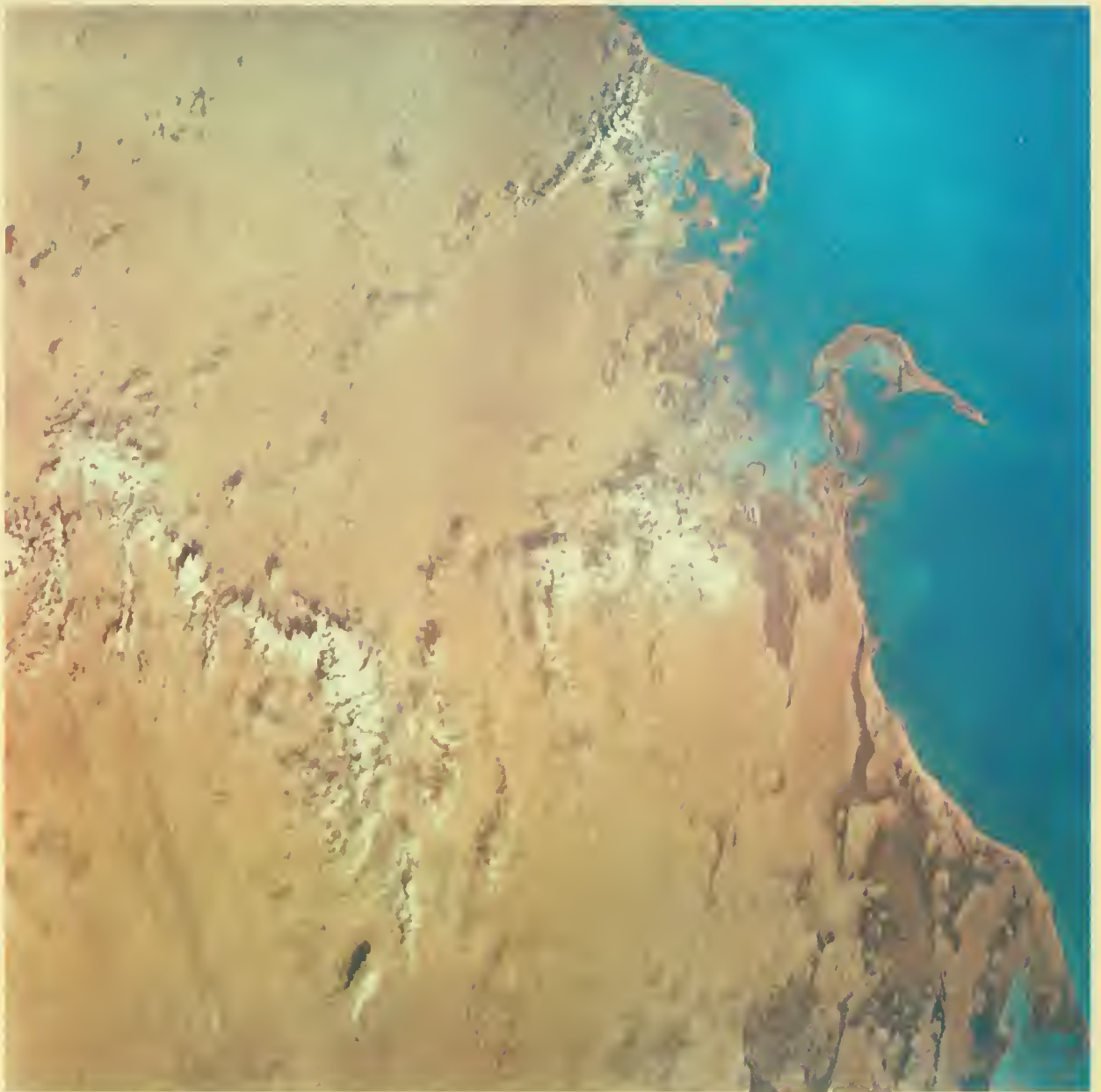
A view of the mainland China coast in Fukien Province. The Futun Min River is in the upper center. The city of Fouchou is located at the mouth of the river, seen in the upper part of the photo. The sun glitter at lower right shows surface detail on the waters of the Formosa Straits.

S-65-45650

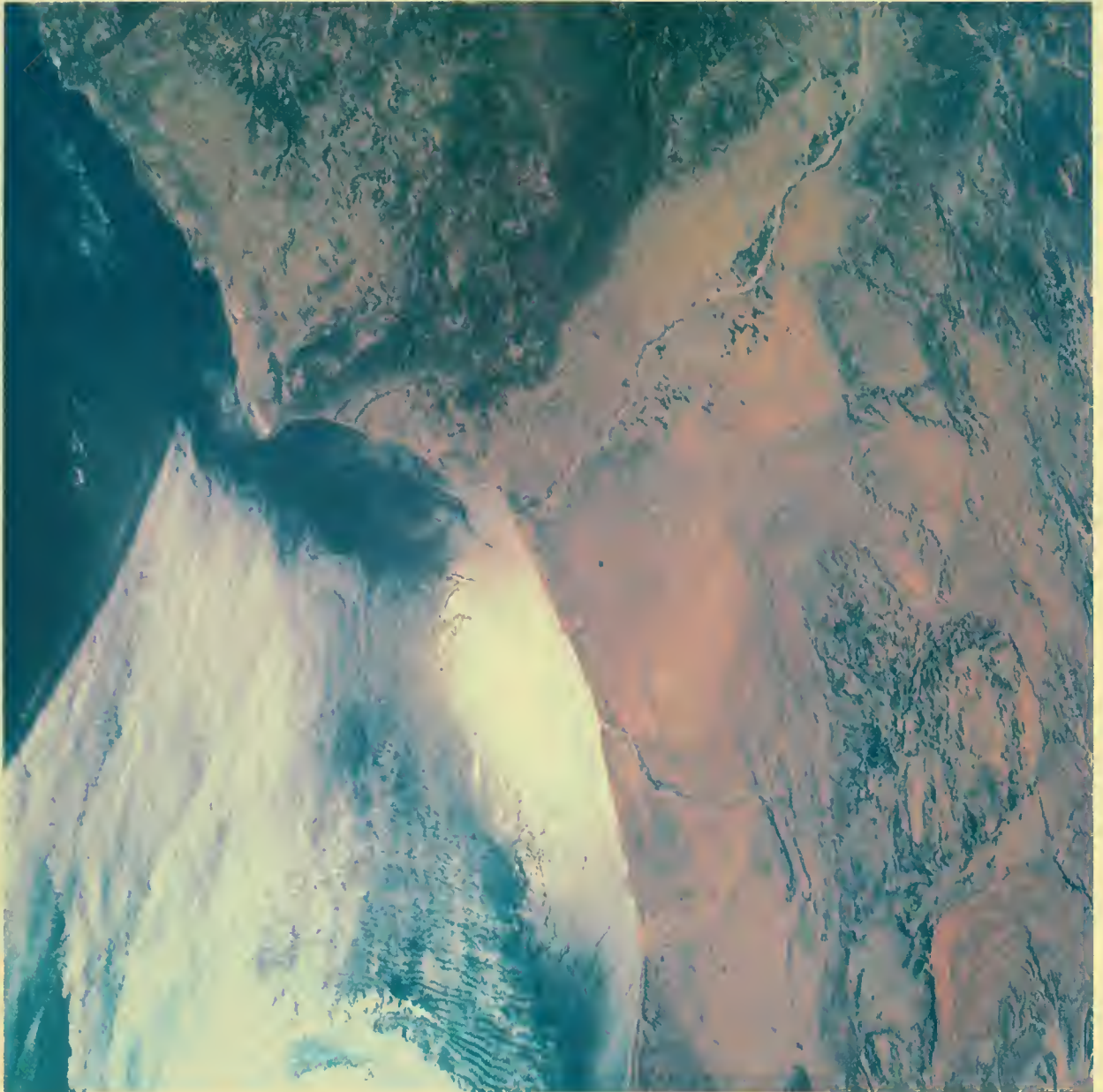


Cape York Peninsula in Queensland, Australia. The Gulf of Carpentaria is to the lower left. The Great Barrier Reef appears as a thin white line running diagonally across the picture. New Guinea, in the upper left corner, is covered by clouds.

S-65-45652

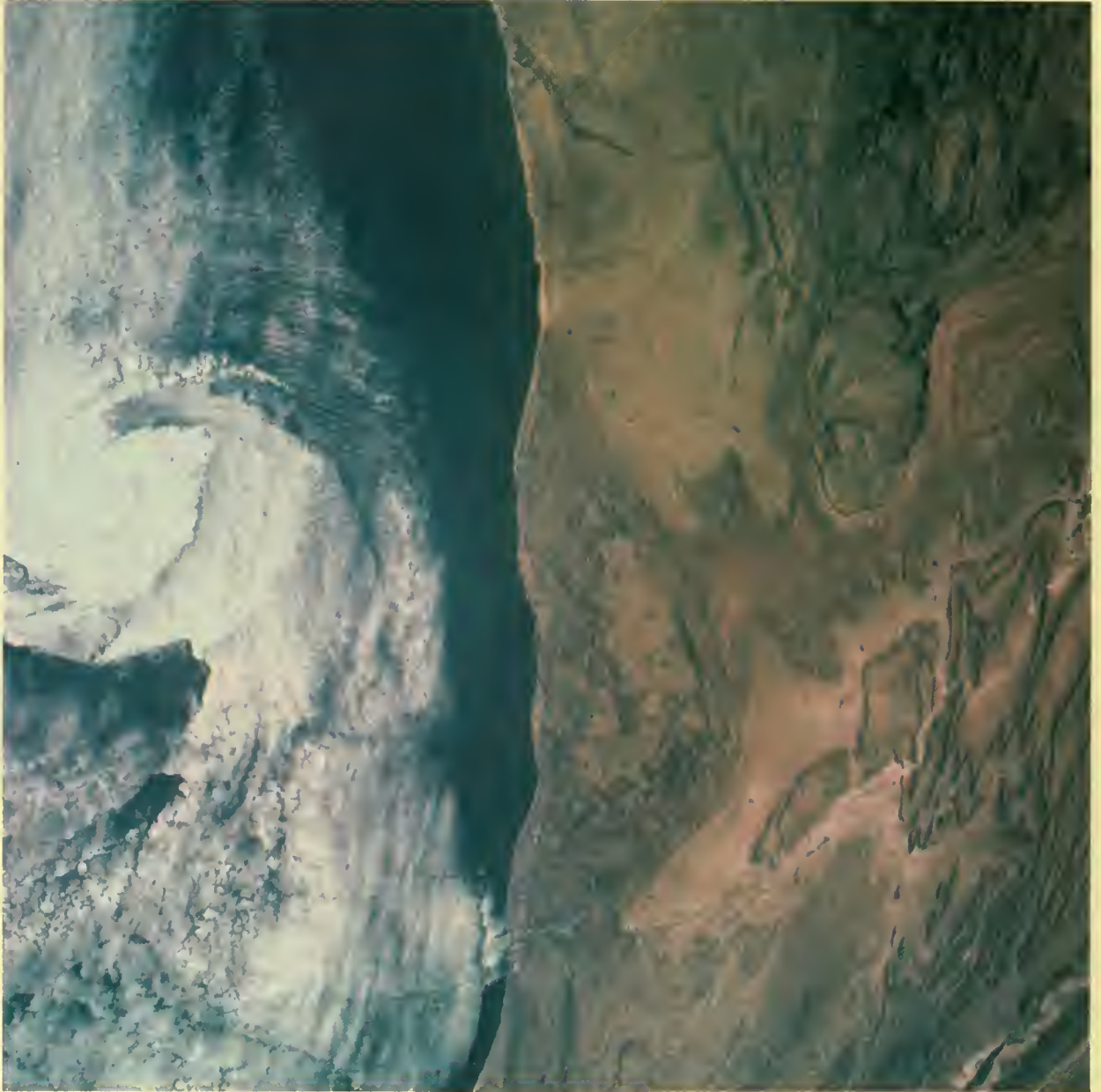


One of the world's major oil producing areas, the El Hasa coast in eastern Saudi Arabia north of Bahrain Island. The Persian Gulf is at upper right. S-65-45662



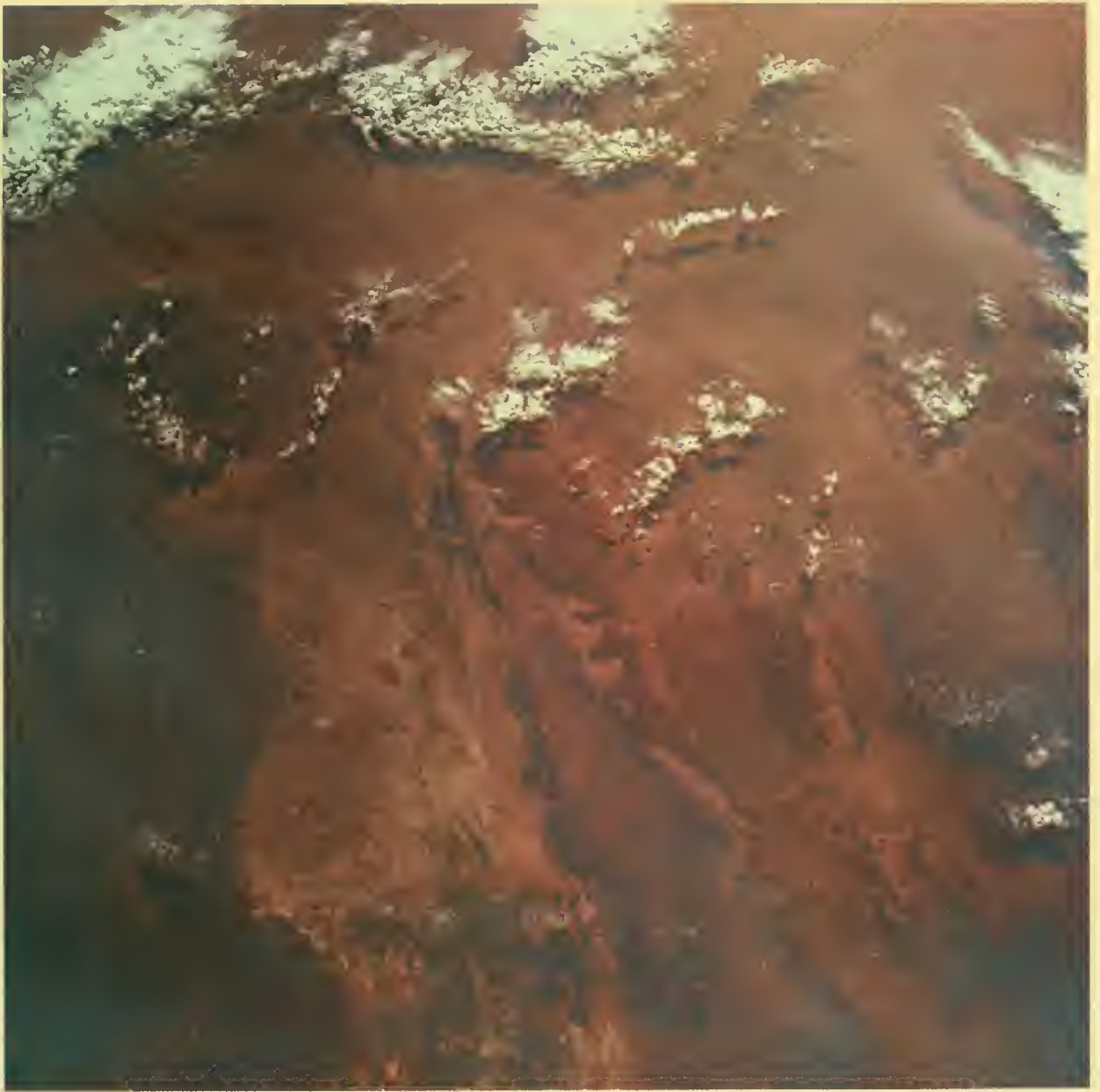
The northwestern African coast near Agadir, Morocco, showing Cape Rhir and the Oued Sous (river). Part of the Anti Atlas Mountains are seen on the right. The intense, localized specular reflection over the water in the center indicates a smooth sea surface and little or no wind. The usual summer Azores anticyclone existed at the time the photograph was taken.

S-65-45664



This view, south of the preceding one, shows the coast of Morocco and Spanish Ifni. The Anti Atlas Mountains, consisting of complex folded sedimentary rock, appear on the right. The clockwise cloud spiral may represent a mesoscale lee eddy induced by the air flow around Cape Rhir (out of view to the north). The Atlas Mountains, with peaks above 10,000 feet, extend to within 100 miles of the Cape and may have some influence on the air flow.

S-65-45665

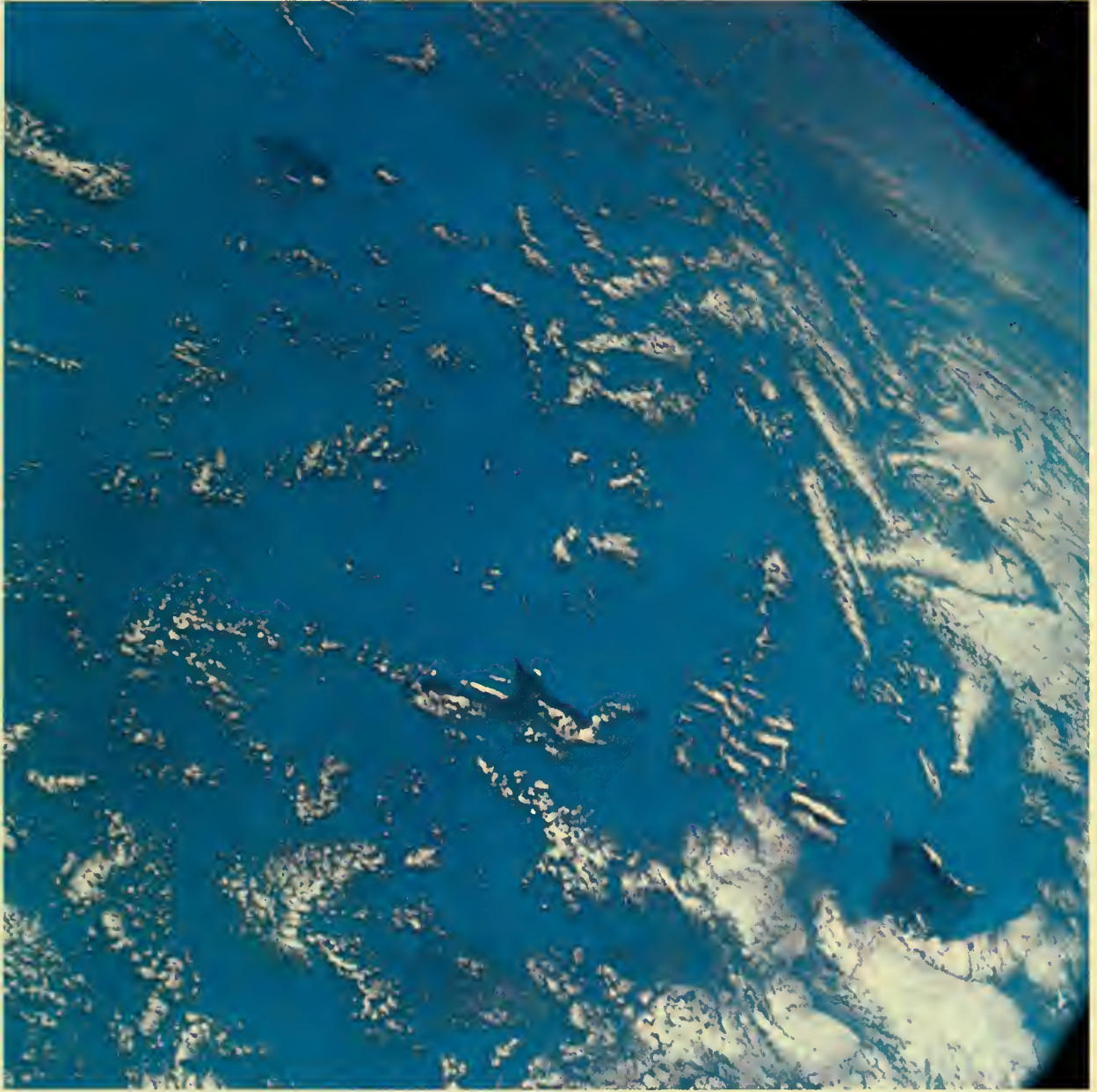


Morocco and Algeria looking to the east. The ridges of the Anti Atlas Mountains are on the left border; the Hamada du Dra (plateau) in the center. S-65-45666

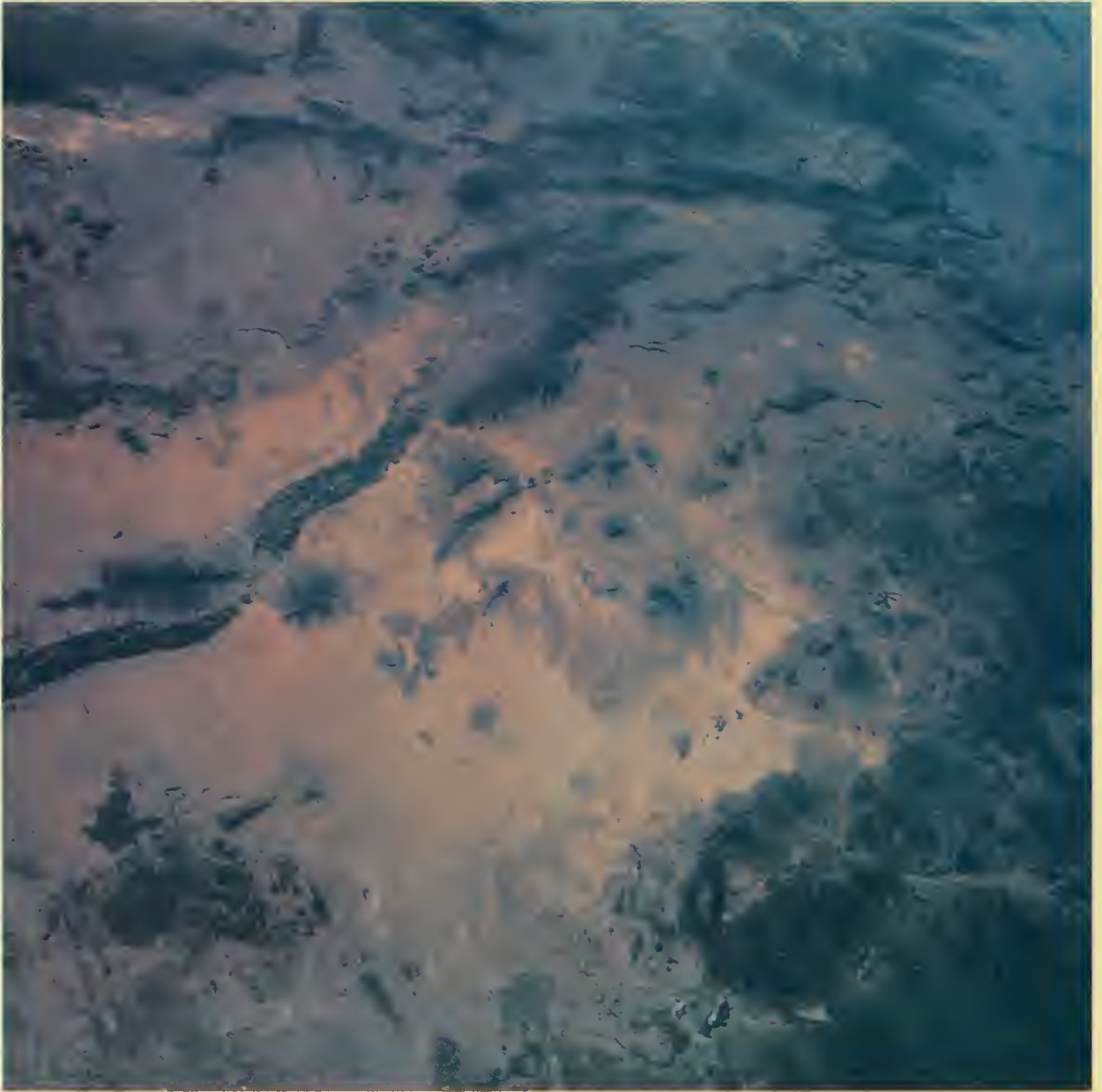


Four of the Cape Verde Islands off Africa's west coast are visible through the strato-cumulus clouds in this view toward the south. The islands, from lower to upper right, are Sal, Boa Vista, Maio, and Sao Tiago. The long line of clouds with clear spaces on both sides, south-southwest of Sal and Boa Vista, is probably the result of air flowing past the 1,300-foot islands under fairly stable conditions in the lower atmosphere.

S-65-45668

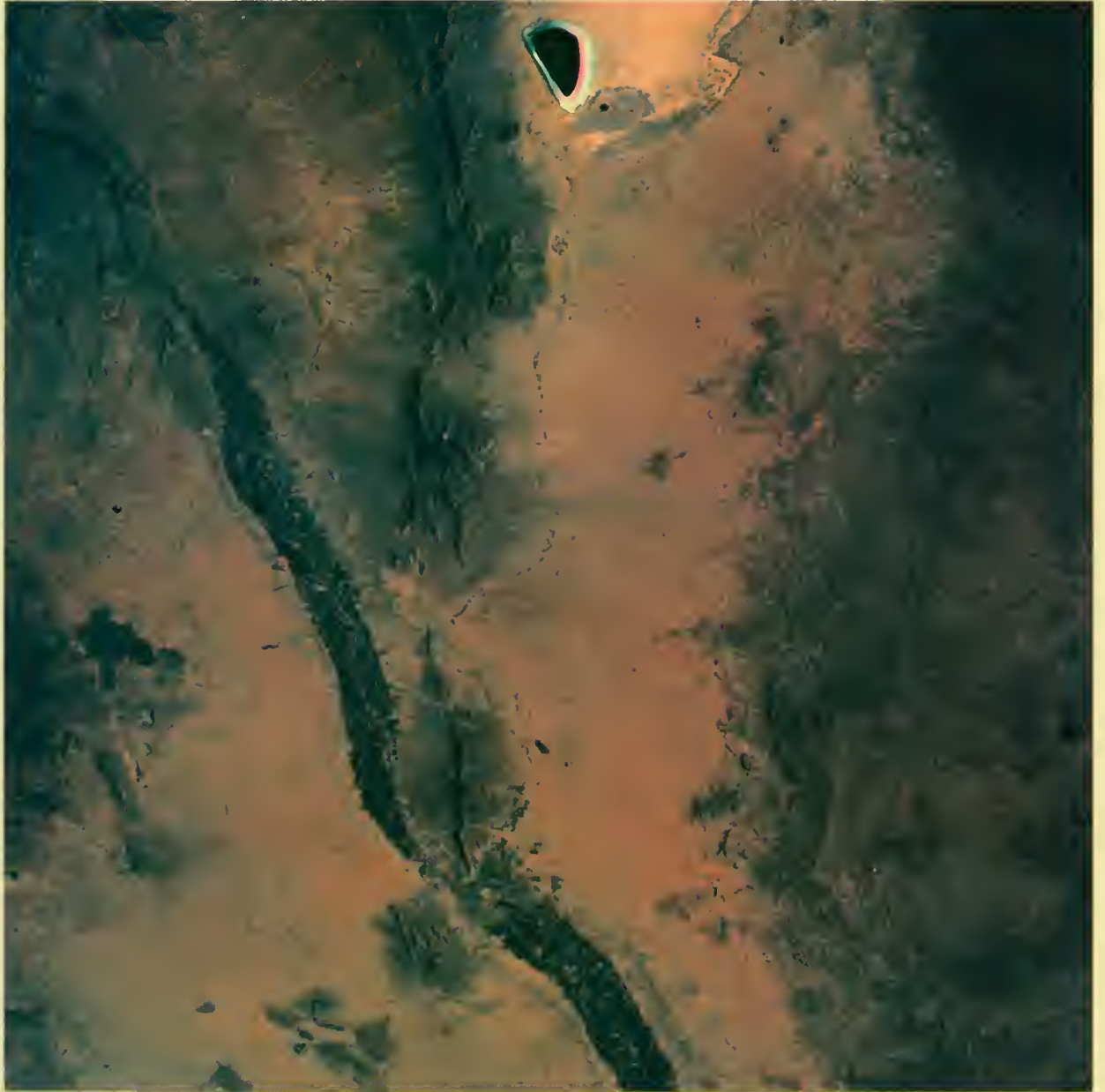


Several large eddies in the stratocumulus clouds are seen on the right in this photograph of the Cape Verde Islands. The islands from the lower center to the right are Sao Nicolau, Santa Luzin, Sao Vicente, and Santo Antao. In the upper left corner, from right to left, are the islands of Brava, Fogo, and Sao Tiago. S-65-45669



El Paso, Texas, and Ciudad Juarez, Mexico, on the Rio Grande (left). The Mexican State of Chihuahua is located to the right. The Potrillo Mountains are at lower left.

S-65-45670



A near-vertical view of the El Paso-Juarez metropolitan area. The valley of the Rio Grande cuts across the picture from upper left to bottom center. The Franklin and Organ Mountains are seen in the center. Near the imperfection in the film, at top center, is the White Sands National Monument.

S-65-45671



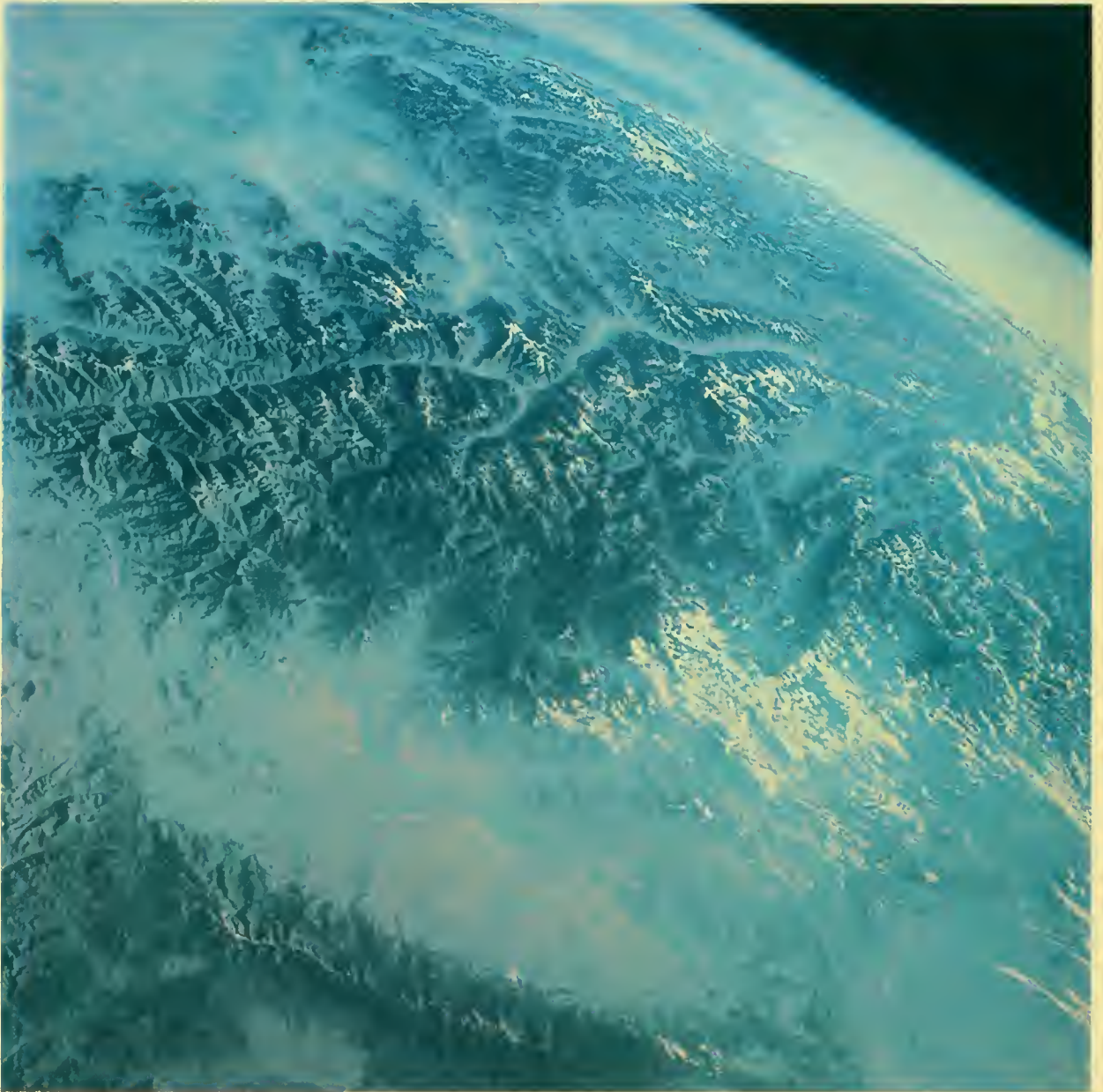
Tropical storm near Ponape Island in the Pacific Ocean. Considerable detail in the cloud structure is shown near the storm's perimeter. The spiral bands are composed of cumulus congestus and cumulonimbus clouds which transport vast amounts of water vapor from the ocean's surface to higher altitudes. Squall lines are found frequently in these bands.

S-65-45548

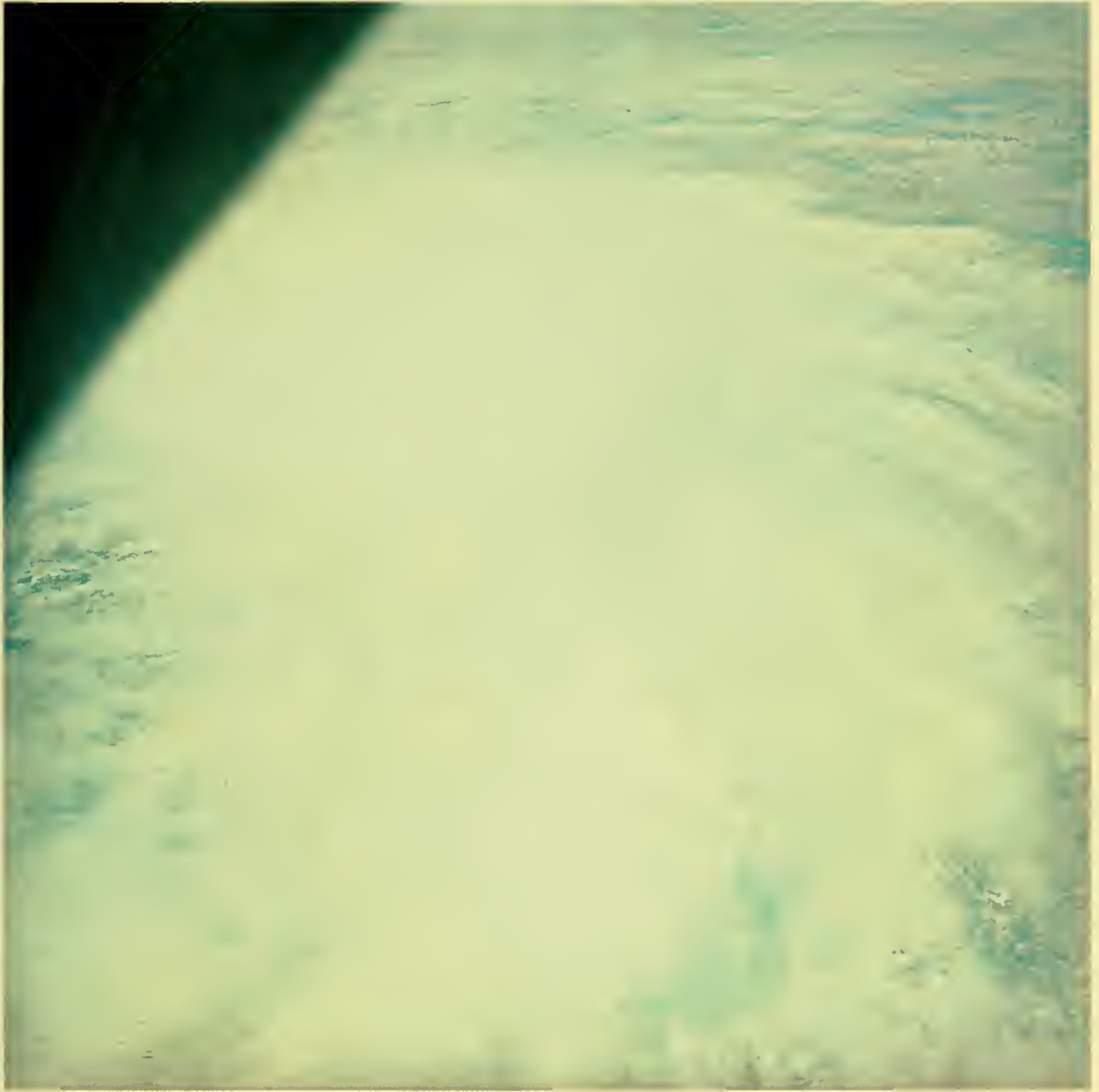


A near-vertical view of Rongelap Atoll in the Marshall Islands of the Pacific. Rongerik Atoll is at the upper edge and Ailinginae Atoll in the foreground. This type of photograph can be used to evaluate the adequacy of existing nautical charts in isolated or remote areas.

S-65-45550



A view of eastern Afghanistan and northern Pakistan with the Kabul River in the foreground. The city of Jalalabad is at the river junction in the lower center. The dark range near the bottom is the Safed Koh (mountains). The Kunar River, under clouds at right, has its headwaters in the Hindu Kush Mountains in the far right center. The Pyandzh River lies in the background. Visible at upper right is the Takla Makan (desert) in Sinkiang Province of mainland China. S-65-45552



This tropical storm was photographed south of the Philippine Islands. Large areas of convective activity are visible through the cirrus cloud cover. The storm center appears to be located at upper left.

S-65-45553



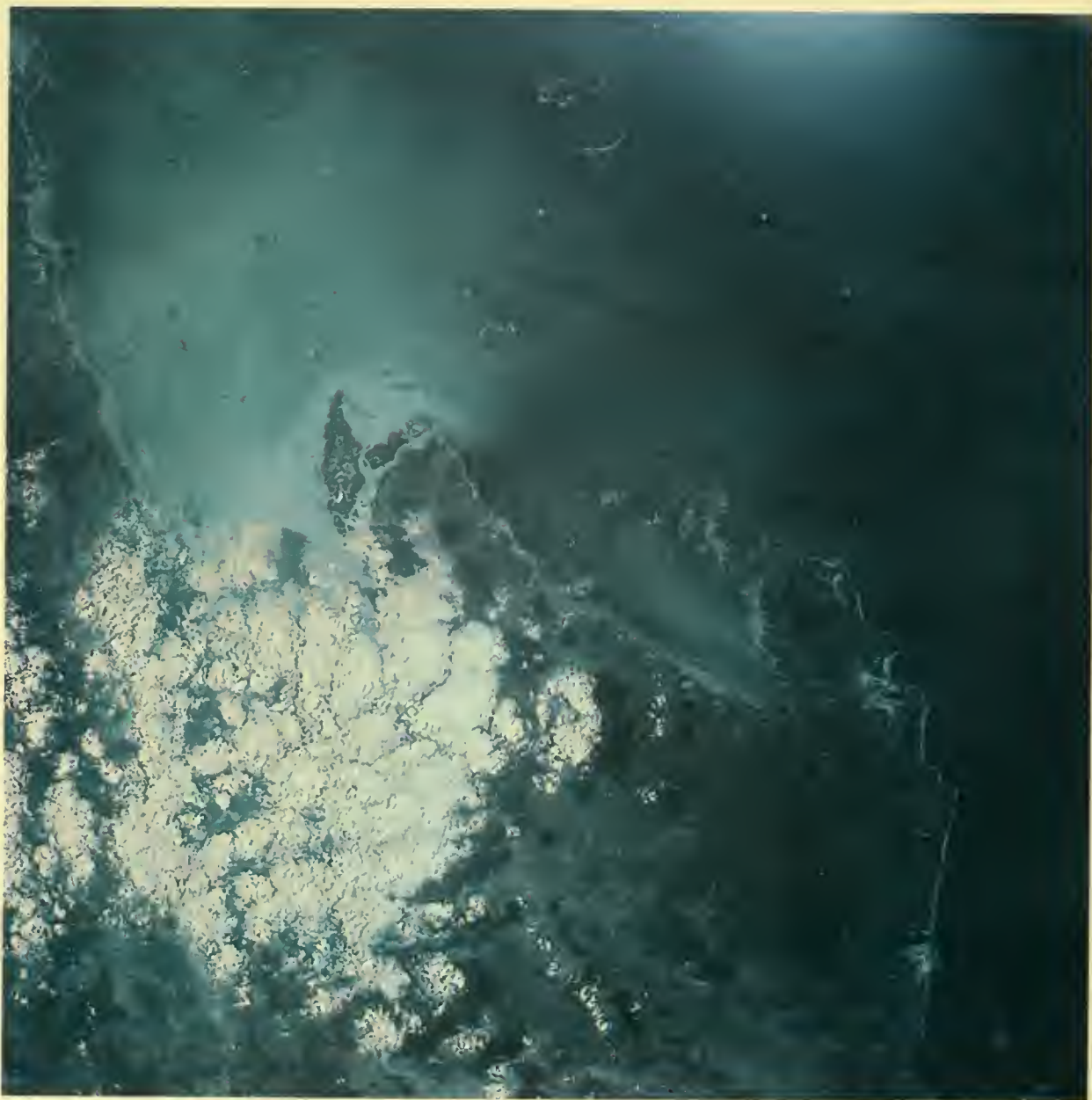
The view looks across the Mediterranean Sea into Turkey. Cyprus is at lower left. The Toros Daglari Mountains run parallel to the Turkish coast. Tuz Golu, a large salt lake, is seen at upper center.

S-65-45556



The coastal area of Northern Territory, Australia, along the Gulf of Carpentaria. The Barkly Tableland is in the upper portion of the photograph. Brush fires at lower left are probably caused by lightning. The McArthur River is seen at lower right.

S-65-45558

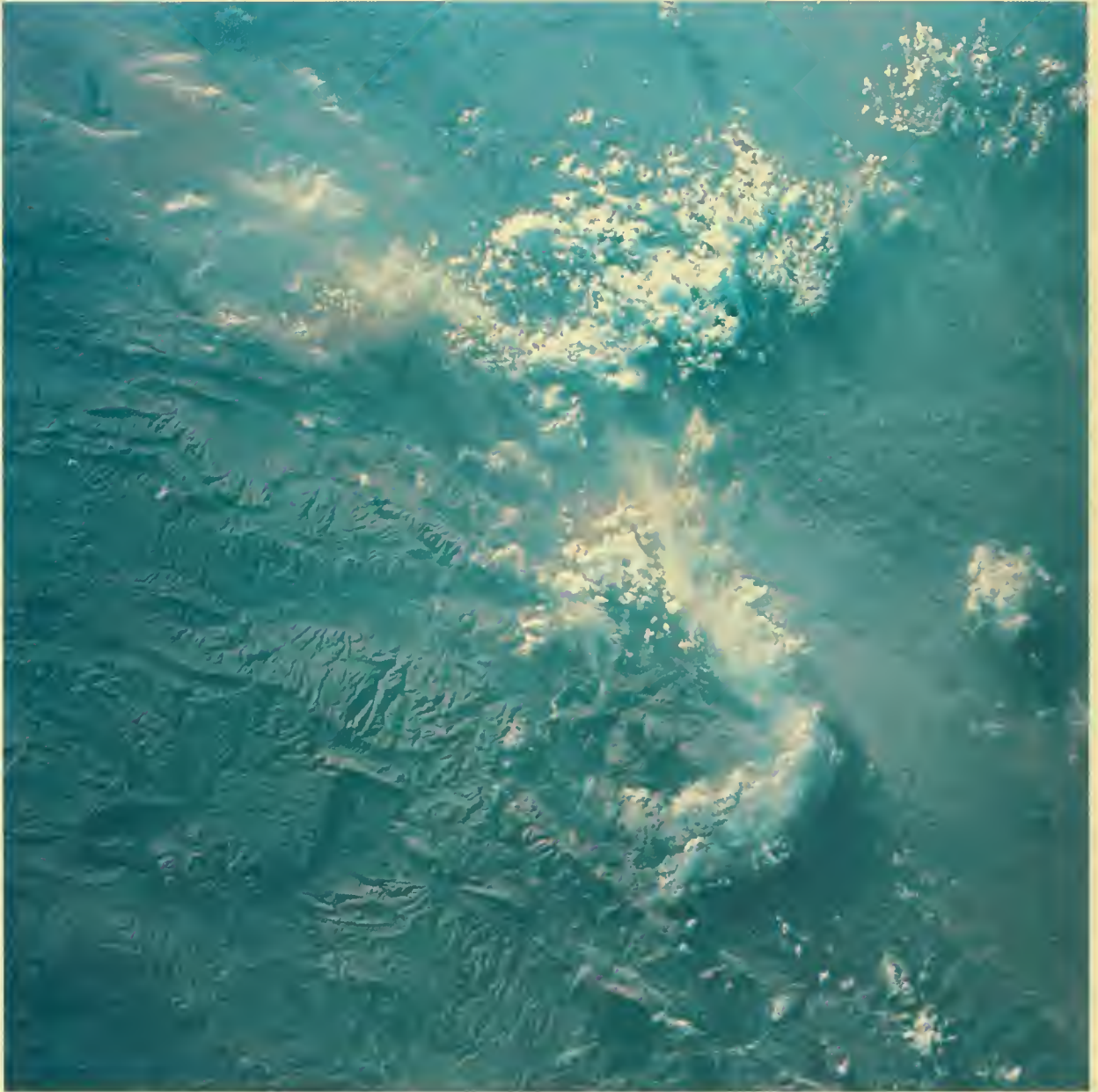


This view of Australia with the Coral Sea to the right shows the eastern coastline of Queensland, north of Rockhampton. Shoalwater Bay is in the center and Broad Sound to the left. The Northumberland Islands are at top center. S-65-45559

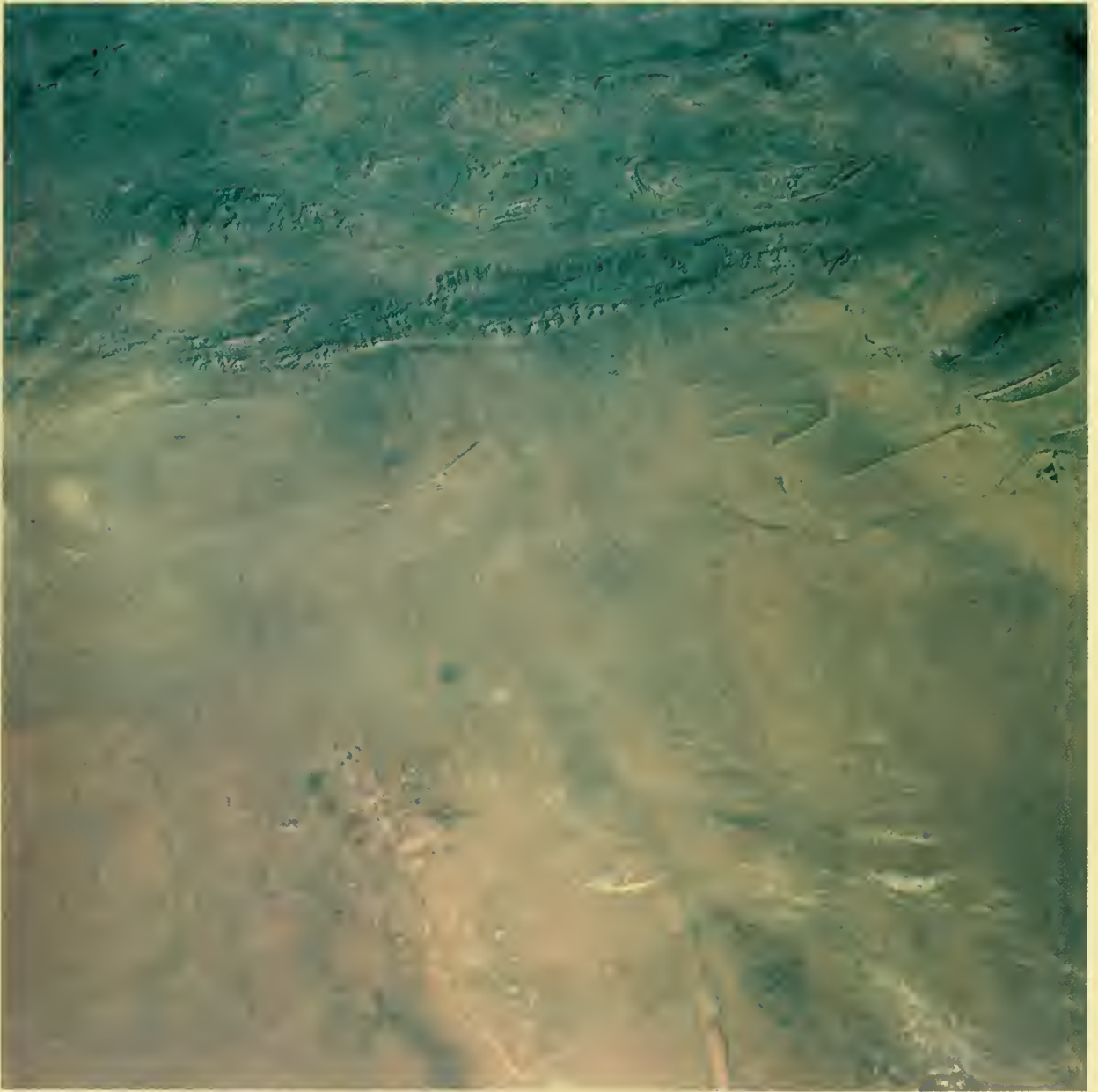


Capricorn and Bunker Islands are visible in this photograph of the Coral Sea and the Australian coast east of Rockhampton, Queensland. The islands, located on the Great Barrier Reef, are coral reefs awash. Only North West Island at the top is above sea level.

S-65-45560



The Atlas Mountains in eastern Morocco east of Marrakech. The mountains are composed of folded Paleozoic sedimentary rock with numerous anticlines and synclines visible. Peaks at lower right are approximately 12,000 feet high. S-65-45561



Northern Algeria. The intensely folded sedimentary rock of the Atlas Saharien Mountains can be seen clearly in the upper half of the photograph. The town of Laghouat is on the far right.

S-65-45562



The Tripolitania area of northern Libya on the Mediterranean Sea. The harbor and breakwater of the port of Tripoli is in the center. The Jabal Nafusah Mountains are at lower right.

S-65-45563



A view of the Saudi Arabian coast on the Red Sea, just below the Gulf of Aqaba. A number of small offshore islands are visible along the coastline. The Al Hijaz Desert and associated igneous outcrops appear as dark areas. S-65-45564

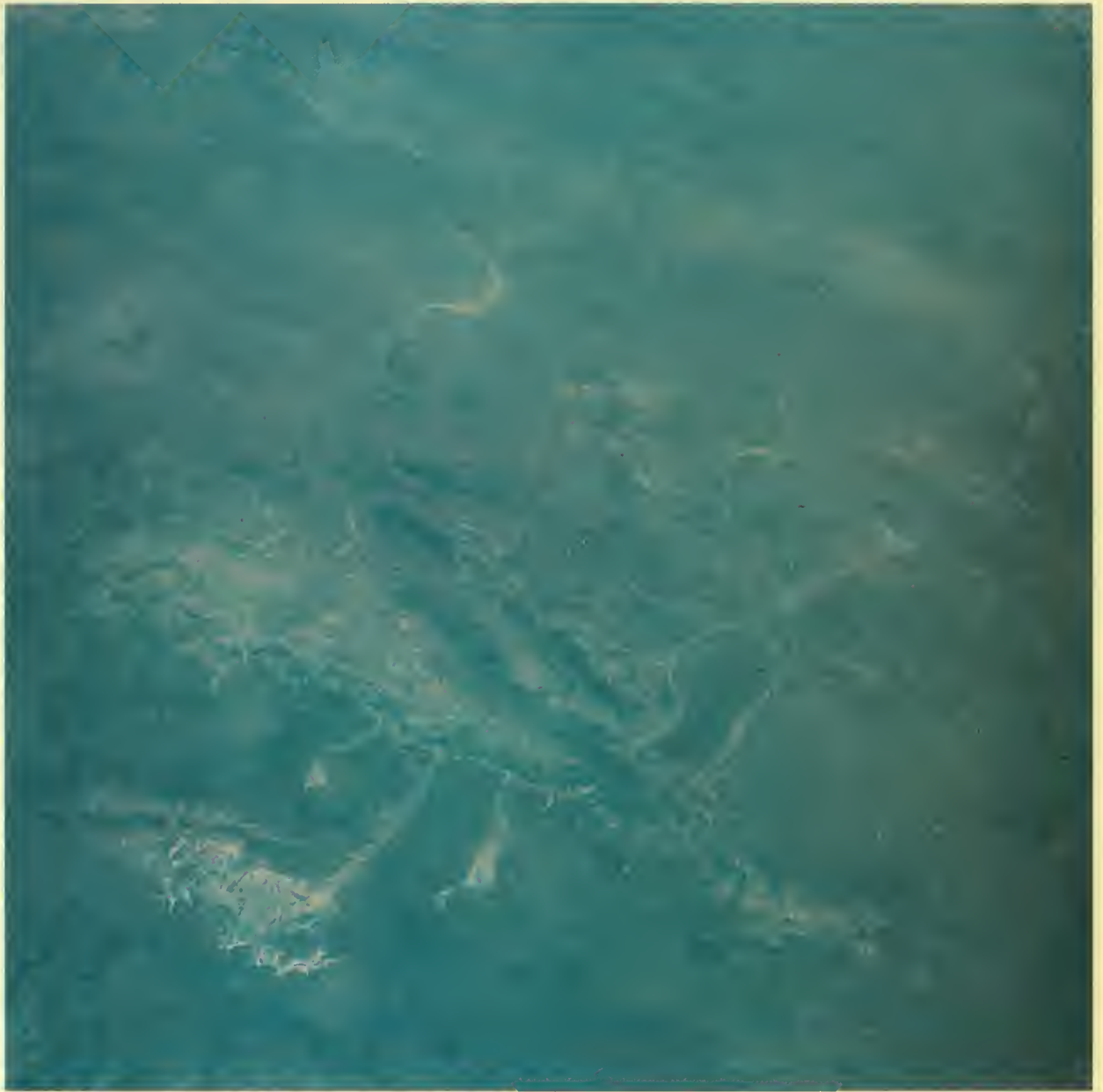


The interior of Saudi Arabia west of the city of Ar Riyad. The Wadi ar Rimah is in the lower left. The photo shows contrast between dark areas of igneous rock and light sandy areas.

S-65-45565



Another view of the Saudi Arabian interior, near Ar Riyad and Al Kharj. The dry streams (wadi) run southeastward toward the Empty Quarter. S-65-45566



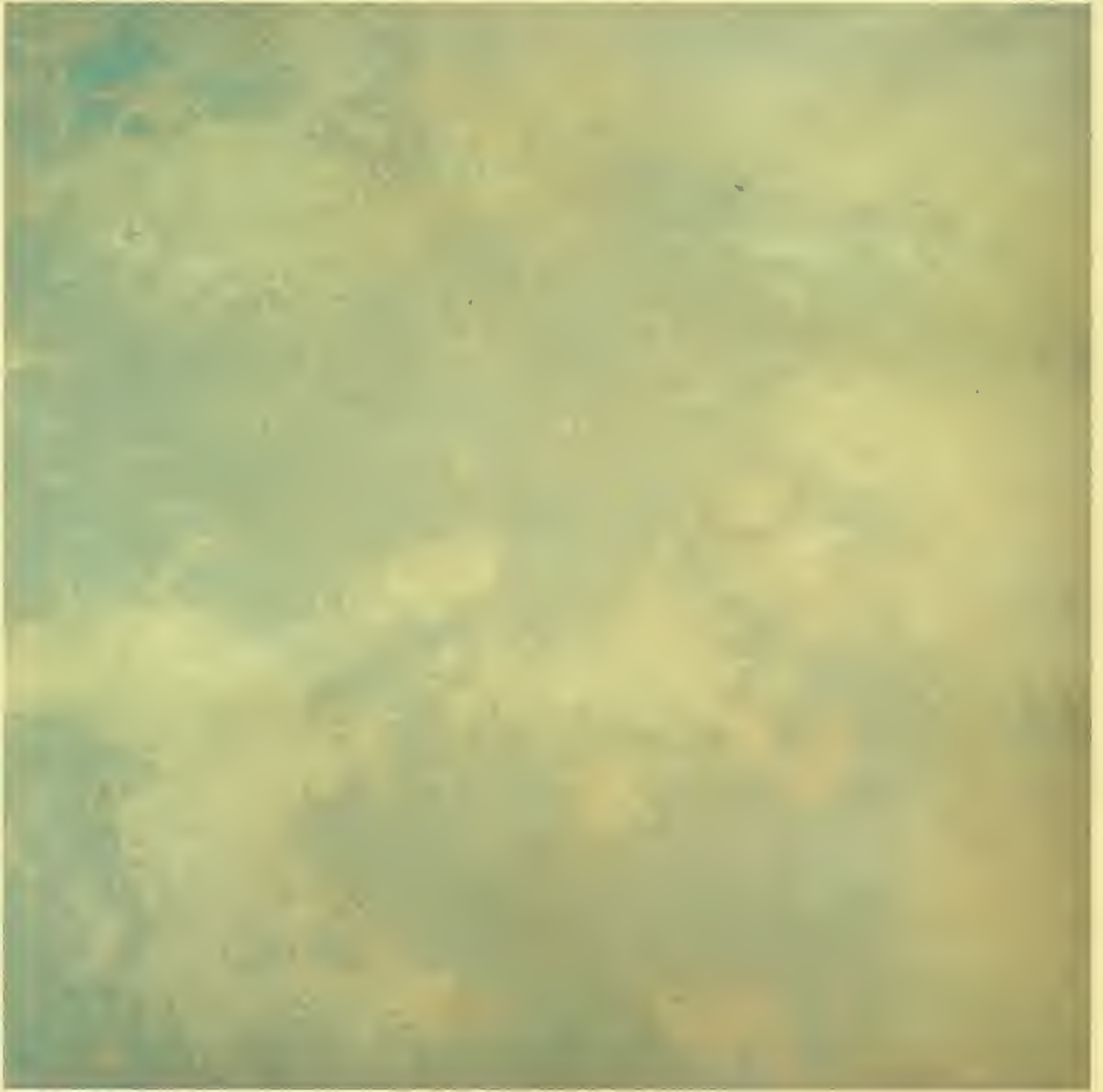
The Northern Territory of Australia near the MacDonnell Range. White meandering lines are dry rivers. An unnamed dry lake is located in the lower left corner just below the Stuart Bluff Range. The Reynolds Range is in the center. The Hanson River is to the right; at upper left, the Lander River. Linear ridges on the left are folded sedimentary rock.

S-65-45567



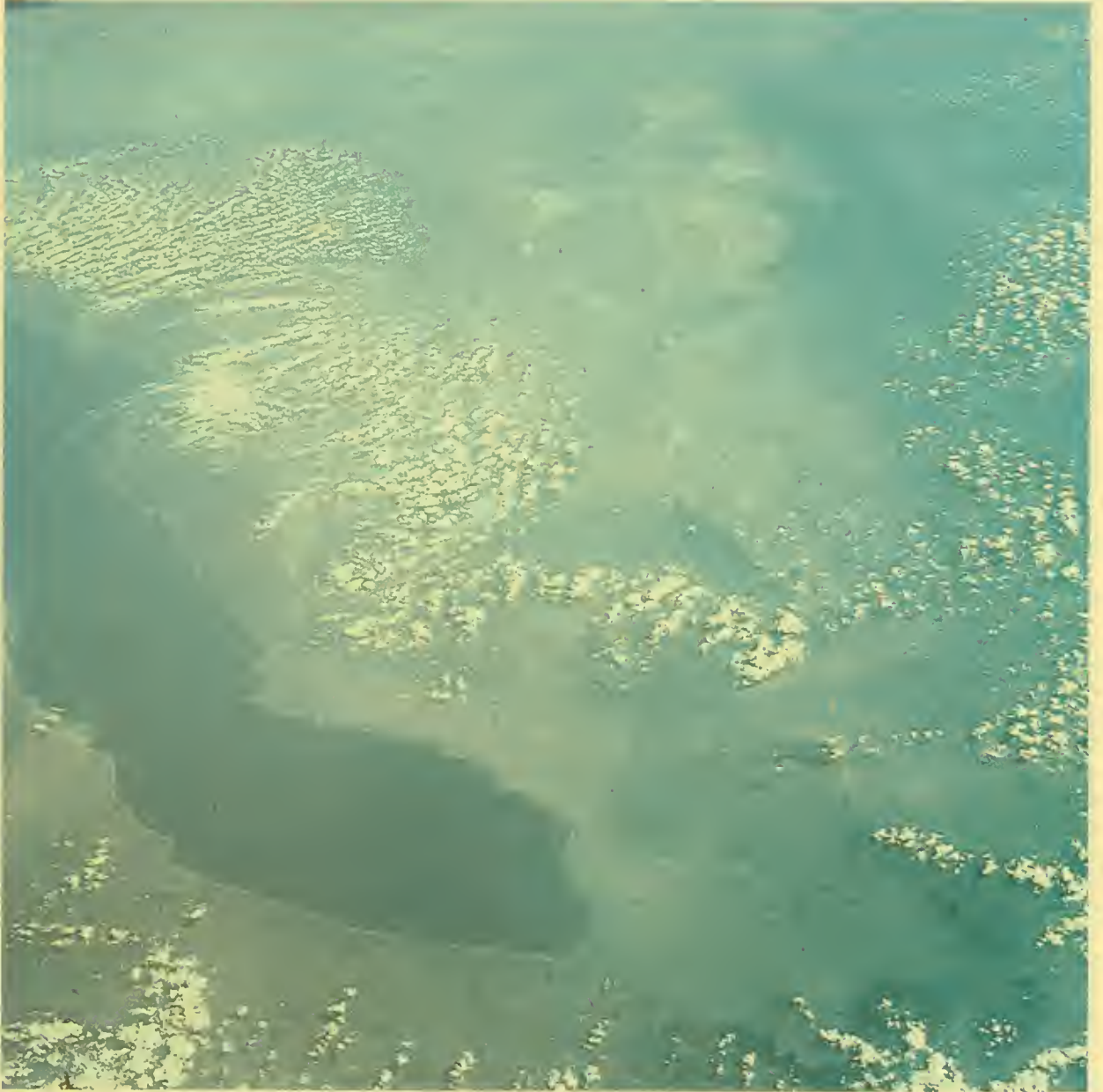
Northern Territory, Australia, in the vicinity of Alice Springs. The Kirchaneff Range is at lower left. Above it, the MacDonnell Range cuts across the lower half of the photograph, exhibiting an appalachian-type structure. The circle on the lower left is Gosses Bluff, a cryptoexplosion structure of possible impact origin. The long dark ellipse at lower right is the Waterhouse Range.

S-65-45568



The Nubian Desert in southern United Arab Republic and northern Sudan. The dark areas are igneous rock; the prominent circular features are ancient craters.

S-65-45569



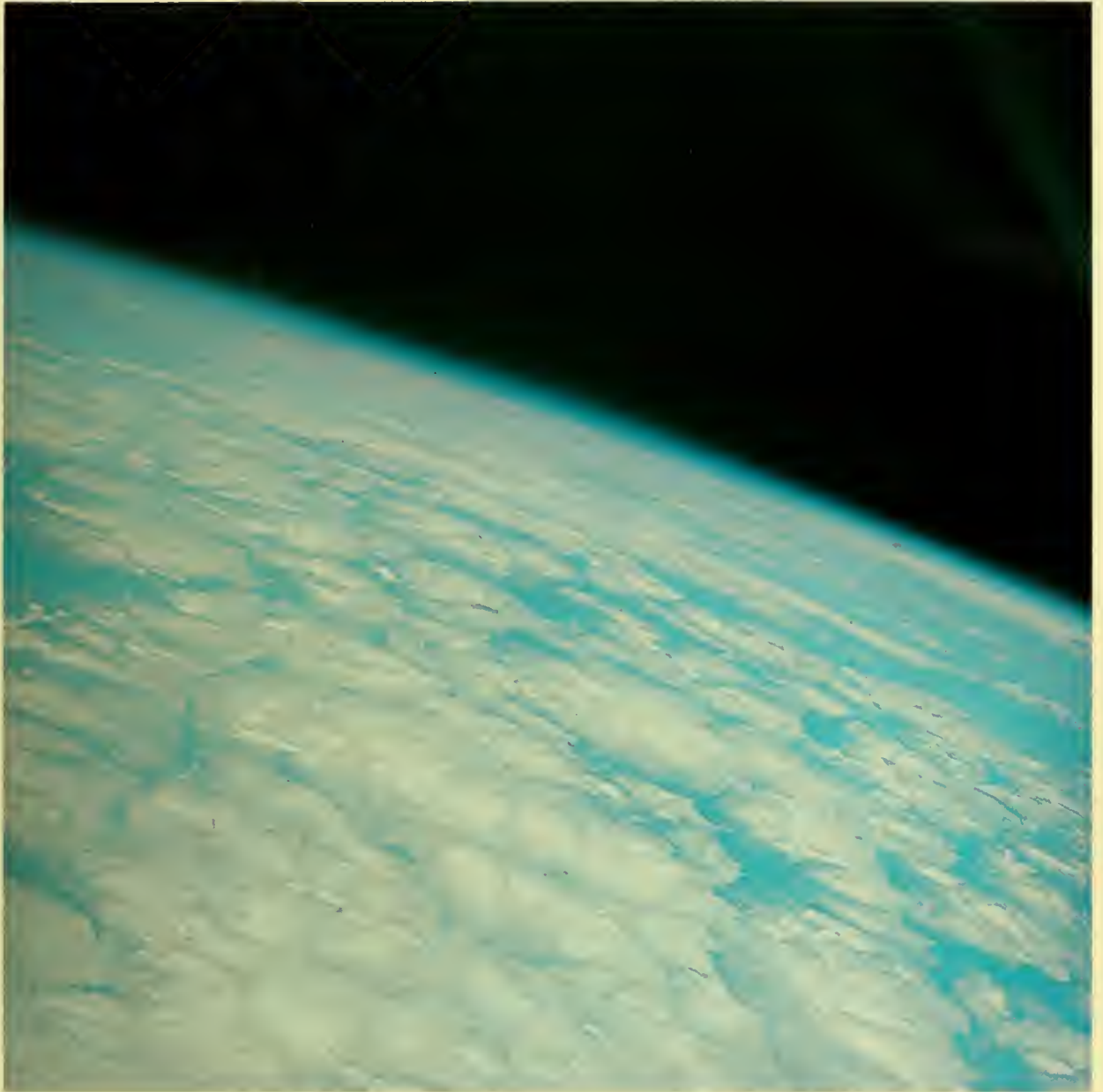
Parts of Tanzania, Zambia, Malawi, and Mozambique in southeastern Africa are visible in this photograph. Lake Nyasa to the left is part of the Great Rift Valley. Forest fires in Zambia are seen at upper left.

S-65-45572



Clouds dot the west coast of Madagascar in this view looking southwest toward the Mozambique Channel. The Mahavavy River is in the lower right corner. The Ikopa River is at bottom left.

S-65-45574



Cells of stratocumulus clouds are located southeast of Madagascar in the Indian Ocean. Similar cell-like structures are seen frequently off the southwest coast of the United States.

S-65-45575



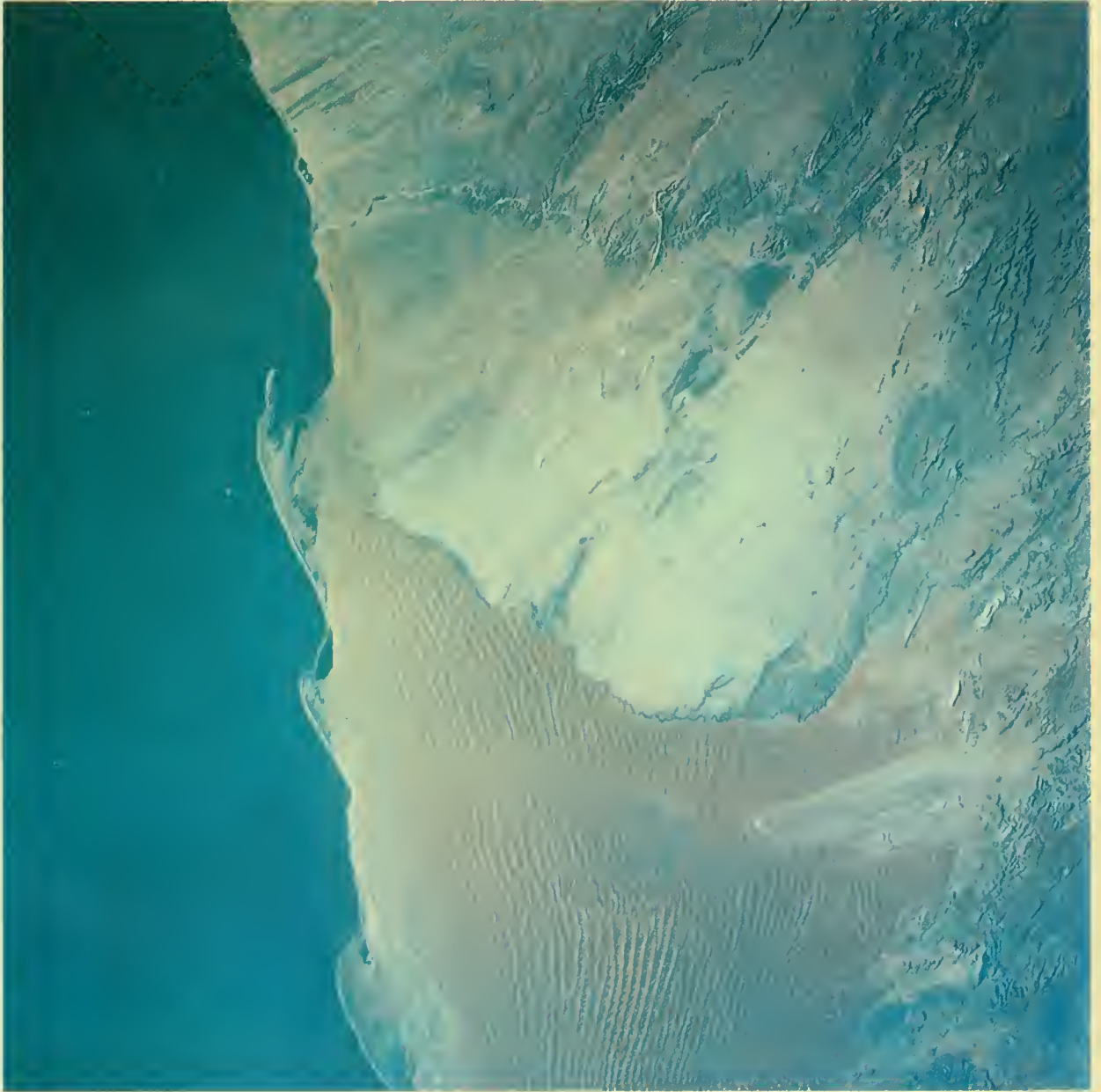
Southeast of Madagascar in the Indian Ocean, an eddy has formed in the strato-cumulus clouds. These eddies appear at times along the perimeter of adjacent cloud cells.

S-65-45576



The Skeleton Coast along South-West Africa with Cape Cross at the far left edge. The photo shows part of the Namib Desert, which is underlain by Precambrian igneous and metamorphic rock. The circular structure in the upper left corner is the Messum intrusive. The Erongo Mountains are at upper right.

S-65-45578



Another view of the South-West African coast. Walvis Bay is the northernmost of the three capes shown here. Longitudinal sand dunes in the lower half of the picture are bounded by the Kuisib River. The capes are formed from sand blown into the ocean and carried northward by the Benguela current.

S-65-45579



South-West Africa in the vicinity of Windhoek, Damaraland. The linear pattern at upper left is the result of erosion along fracture systems in the Precambrian rock.

S-65-45580



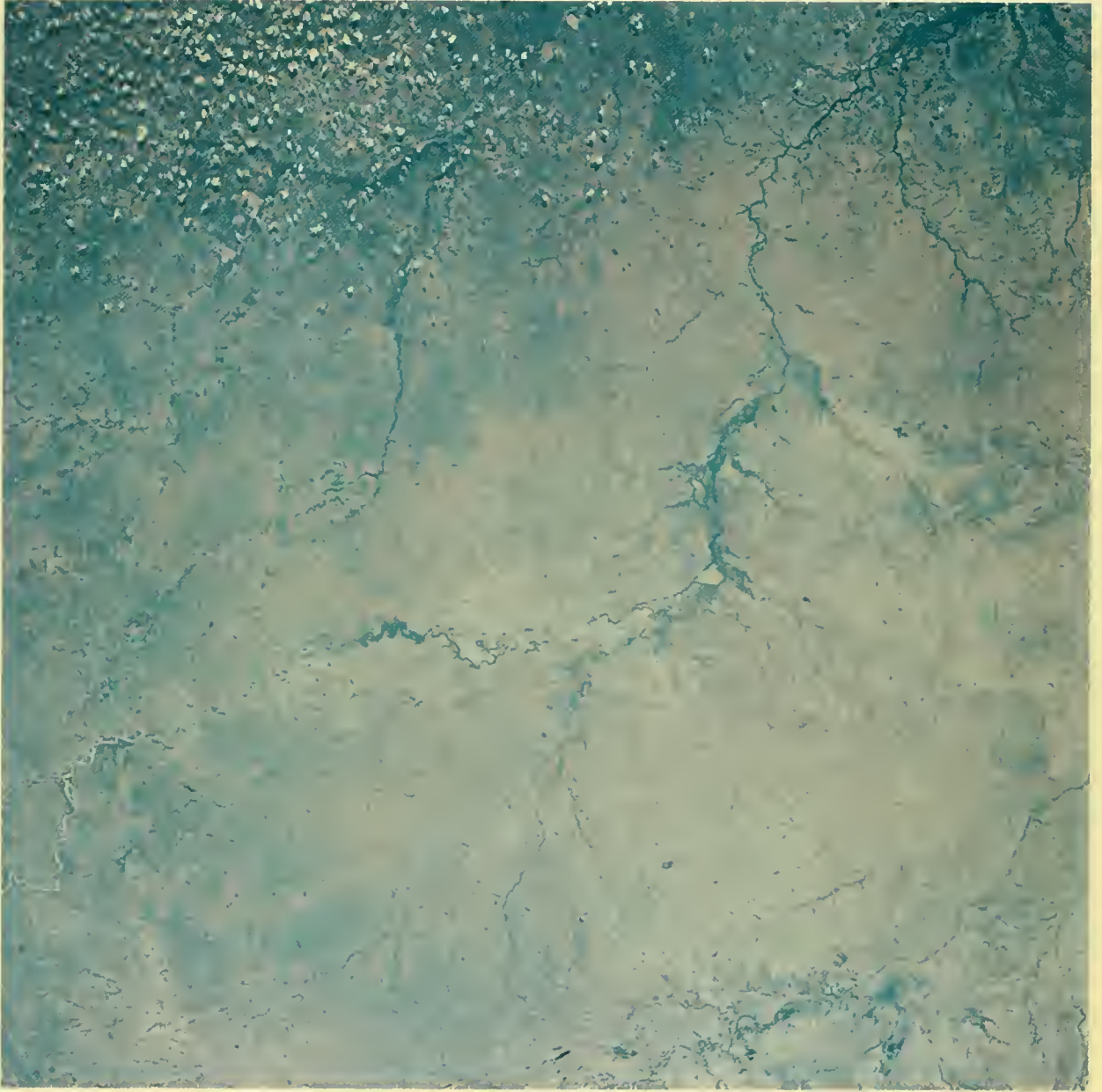
Damaraland in South-West Africa just west of the area shown in the preceding photograph. The linear ridges are folded sedimentary and metasedimentary upper Precambrian rock. White areas in the center and at upper right are salt pans.

S-65-45581



View of Mexico, showing the city of Chihuahua (left center), Laguna Bustillos (far right) and the Sierra Madre Occidental Mountains (upper left), composed of middle Cenozoic volcanic rock. The linear ridges in the foreground are folded sedimentary rock, chiefly of Cretaceous age.

S-65-45582



The Nueces Plains of southern Texas and the Mexican State of Coahuila. The Rio Grande is in the lower right corner at Eagle Pass. The Nueces River runs from the lower left to the upper right of the photograph. The small square patches at far right are targets laid out for a visual acuity experiment performed on this and later flights. The patches are 12 squares of plowed soil 2,000 feet by 2,000 feet arranged in a matrix of four squares deep and three squares wide.

S-65-45583



The Mexican Territory of Baja California Sur on the southern part of the peninsula. The islands in the Gulf of California are Espiritu Santo and Cerralvo. A major fault runs south from Bahia de La Paz (upper left) to the Pacific coast. Dark areas in the foreground are mountains underlain by Cretaceous granitic batholiths.

S-65-45585



False Cape is at the bottom of this photograph of the southernmost tip of the Baja California Peninsula. Bahia de La Paz is in the upper left corner. The north-south trending valley may be fault-controlled.

S-65-45586



Border area of South Africa and South-West Africa, showing Bushmanland and the Orange River, which forms part of the border. The river mouth on the Atlantic is at upper left. The area is underlain chiefly by metamorphic and igneous Proterozoic rock of the Gariep system.

S-65-45600

INDEX

Geographic areas represented in this volume are indexed below by page number. Photographs taken of cloud formations have been listed separately.

AFRICA

Northwestern, 48, 98, 99, 100, 101, 102, 103, 104, 105, 154, 157, 158, 195, 219, 220, 221, 234, 235, 236
Nile Area, 24, 25, 28, 30, 49, 50, 51, 52, 53, 54, 106, 107, 156, 184, 196, 197, 207, 242
Central and Southern, 29, 107, 243, 244, 245, 247, 248, 249, 250, 255

ASIA

Middle East, 18, 19, 20, 21, 22, 23, 26, 46, 47, 137, 146, 147, 197, 201, 218, 230, 237, 238, 239
Southwestern, 27, 131, 132, 133, 141, 142, 143, 144, 148, 149, 150, 182, 193, 194, 201, 202, 203, 204, 205, 211, 212, 213, 228
Southeastern, 55, 56, 134, 135, 138, 139, 140, 145, 151, 178, 183, 206, 214, 215, 216

MEXICO, 7, 8, 13, 42, 162, 164, 177

Baja California, 57, 58, 59, 60, 122, 123, 124, 125, 126, 127, 128, 176, 253, 254
Chihuahua, 72, 75, 76, 77, 78, 79, 80, 81, 82, 83, 159, 160, 161, 169, 224, 225, 251
Sonora, 61, 62, 63, 64, 72, 126, 127, 128, 188

CENTRAL AMERICA, 43

SOUTH AMERICA, 118, 129, 130, 190, 191, 192, 199

UNITED STATES

Southwestern
California, 7, 121, 128, 164, 165, 209

Arizona, 8, 61, 62, 63, 64, 65, 66, 67, 68, 69, 70, 71, 164, 166, 167, 168

New Mexico, 69, 70, 71, 72, 73, 74, 75, 76, 77, 78, 79, 80, 81, 82, 83, 84, 85

Texas, 77, 78, 79, 80, 81, 82, 83, 84, 85, 86, 87, 88, 89, 90, 91, 92, 93, 94, 95, 162, 169, 224, 225, 252

Southeastern

Florida, 33, 96, 97, 108, 113, 163, 170, 171, 172, 173, 186, 198

ATLANTIC OCEAN

Bahamas, Cuba, 34, 35, 36, 174, 175, 187, 208
Canary Islands and Cape Verde Islands, 155, 222, 223

PACIFIC OCEAN, 45, 120

Hawaiian Islands, 200
Marshall Islands, 227
Philippine Islands, 152, 153

AUSTRALIA, 217, 231, 232, 233, 240, 241

JAPAN, 136, 179, 210

CLOUDS, 9, 14, 15, 16, 17, 31, 34, 35, 37, 38, 39, 40, 41, 42, 43, 44, 96, 97, 108, 111, 112, 113, 114, 115, 116, 117, 118, 119, 121, 122, 123, 129, 130, 152, 153, 155, 162, 163, 170, 171, 172, 173, 180, 181, 183, 185, 186, 187, 188, 189, 190, 194, 198, 200, 222, 223, 226, 229, 245, 246

LIMB, 32

APPENDIX

The tabulation below lists every photograph taken on three Gemini flights, in orbital sequence. It also gives the magazine and frame number of the film; the color or black and white print number; the orbit; Greenwich mean time at which the photograph was taken; and geographic location. An asterisk by the frame number denotes a photograph included in this volume. Information about obtaining photographs is discussed in the Introduction.

GEMINI III

<i>Frame</i>	<i>NASA/MSC color No.</i>	<i>NASA/MSC B. & W. No.</i>	<i>Orbit</i>	<i>G.m.t.</i>	<i>Location</i>
MAGAZINE NO. 1					
MARCH 23, 1965					
1	S-65-18737	S-65-18577	1	1556	Mexico (Tamaulipas-Nuevo Leon); Texas.
2	S-65-18738	S-65-18571	2	1602	Clouds; Atlantic Ocean, Bermuda.
3	S-65-18739	S-65-18572	2	1602	Clouds; Atlantic Ocean, near Bermuda.
*4	S-65-18740	S-65-18573	2	1726	Baja California, Mexico; California.
*5	S-65-18741	S-65-18575	2	1726	Baja California and Sonora, Mexico; California; Arizona
6	S-65-18742	S-65-18574	2	1727	Do.
7	S-65-18743	S-65-18570	2	1727	Do.
8	S-65-18744	S-65-18569	3	1804	Clouds over coast of southeastern Africa.
9	S-65-18745	S-65-18508	3	1804	Do.
10	S-65-18746	S-65-18567	3	1804	Do.
11	S-65-18747	S-65-18566	3	1804	Do.
12	S-65-18748	S-65-18564	3	1805	Do.
13	S-65-18749	S-65-18582	3	1805	Do.
14	S-65-18750	S-65-18581	3	1805	Do.
15	S-65-18751	S-65-18580	3	1805	Do.
*16	S-65-18752	S-65-18579	3	1807	Clouds over Madagascar.
17	S-65-18753	S-65-18578	3	1807	Do.
18	S-65-18754	S-65-18588	3	1807	Do.
19	S-65-18755	S-65-18587	3	1807	Do.
20	S-65-18756	S-65-18586	3	1807	Do.
21	S-65-18757	S-65-18585	3	1809	Clouds over Indian Ocean.
22	S-65-18758	S-65-18584	3	1809	Do.
23	S-65-18759	S-65-18583	3	1809	Do.
24	S-65-18760	S-65-18576	3	1809	Do.
25	S-65-18761	S-65-18565	3	1814	Limb sunset over Indian Ocean.

GEMINI IV

<i>Frame</i>	<i>NASA/MSC color No.</i>	<i>NASA/MSC B. & W. No.</i>	<i>Orbit</i>	<i>G.m.t.</i>	<i>Location</i>
MAGAZINE NO. 16					
JUNE 3, 1965					
1	S-65-34630	S-65-32932	1	1643	Eastern Pacific Ocean.
2	S-65-34631	S-65-32933	1	1643	Do.
3	S-65-34632	S-65-32934	1	1646	Sonora and Chihuahua, Mexico.
*4	S-65-34633	S-65-32935	1	1646	Do.
5	S-65-30431	S-65-32928	3	1945	EVA, (extravehicular activity), northeast of Hawaii.
6	S-65-34634	S-65-32929	3	1947	EVA, off coast of California.
7	S-65-30427	S-65-32930	3	1949	Do.
8	S-65-30430	S-65-32931	3	1952	EVA, over southern California.
9	S-65-30433	S-65-32924	3	1954	EVA, over New Mexico.
10			3	1954	Do.
11	S-65-30428	S-65-32926	3		EVA, over El Paso, Texas.
12	S-65-34636	S-65-32927	3		EVA, closeup.
13	S-65-34637	S-65-32920	3		Do.
14	S-65-34638	S-65-32921	3		Do.
15	S-65-34639	S-65-32922	3	1956	EVA, over Texas.
16	S-65-34640	S-65-32923	3		Do.
17	S-65-34641	S-65-32916	3	1958	EVA, over Texas coast.
18	S-65-30429	S-65-32917	3	1959	EVA, over Gulf of Mexico.
19	S-65-30432	S-65-32918	3	1959	Do.
20	S-65-34642	S-65-32919	3	2000	Do.

<i>Frame</i>	<i>NASA/MSC color No.</i>	<i>NASA/MSC B. & W. No.</i>	<i>Orbit</i>	<i>G.m.t.</i>	<i>Locotion</i>
21	S-65-34643	S-65-32912	4	2128	Northern Sonora, Mexico; southern Arizona.
22	S-65-34848	S-65-32913	Limb.
23	S-65-34644	S-65-32914	Clouds.
24	S-65-34645	S-65-32915	Do.
25	Blank.
26	Blank.
27	S-65-34646	S-65-32958	Clouds.
*28	S-65-34647	S-65-32959	8	0317	Cold front southeast of Japan.
JUNE 4, 1965					
29	S-65-34648	S-65-32960	8	0317	Cold front southeast of Japan.
30	S-65-34649	S-65-32961	8	0318	Do.
31	Blank.
*32	S-65-34650	S-65-32954	8	0319	Cloud front southeast of Japan.
*33	S-65-34651	S-65-32955	8	0325	Pacific Ocean east of Wake Island.
*34	S-65-34652	S-65-32956	8	0326	Do.
35	S-65-34653	S-65-32957	8	0326	Do.
36	S-65-34654	S-65-32950	8	0326	Do.
37	S-65-34655	S-65-32951	8	0333	Pacific Ocean southwest of Hawaii.
*38	S-65-34656	S-65-32952	9	0430	South Arabia; Gulf of Aden; Yemen.
*39	S-65-34657	S-65-32953	9	0430	South Arabia; Gulf of Aden; Somali Republic.
*40	S-65-34658	S-65-32946	9	0431	South Arabia; Gulf of Aden; Wadi Hadramawt.
*41	S-65-34659	S-65-32947	9	0431	South Arabia; Gulf of Aden; Ras Asir.
*42	S-65-34660	S-65-32948	9	0434	Southern Saudi Arabia; Muscat and Oman.
*43	S-65-34661	S-65-32949	9	0435	Sultanate of Muscat and Oman; Ras Al Hadd.
44	S-65-34662	S-65-32942	9	0512	Pacific Ocean southeast of Canton Island.
*45	S-65-34663	S-65-32943	10	0602	Sahara Desert; northern Sudan.
*46	S-65-34664	S-65-32944	10	0603	United Arab Republic; Red Sea; Foul Bay; Eastern Desert.
*47	S-65-34665	S-65-32945	10	0606	United Arab Republic; Saudi Arabia north of Medina.
48	S-65-34667	S-65-32939	10	0606	Central Saudi Arabia; Qatar Peninsula; Bahrain Island.
*49	S-65-34666	S-65-32940	10	0608	Persian Gulf; Iran coast; Qatar Peninsula.
*50	S-65-34668	S-65-32941	11	0734	Nile Delta; El Faiyum Depression.
51
52	S-65-34669	S-65-32937	12	0854	Atlantic Ocean.
*53	S-65-34670	S-65-32938	12	0901	Richat Structure; Mauritania.

End of roll.

MAGAZINE NO. 7

*1	S-65-34776	S-65-32752	12	0910	Nile Delta; Suez Canal; Sinai Peninsula.
2	S-65-34775	S-65-32751	13	1150	Pacific Ocean southwest of Panama.
3	S-65-34774	S-65-34750	13	1150	Do.
*4	S-65-34773	S-65-32749	13	1151	Do.
5	S-65-34772	S-65-32756	Limb.
*6	S-65-34771	S-65-32755	Do.
7	Blank.
8	Blank.
9	S-65-34770	S-65-32760	Limb (not apparent on photo).
10	S-65-34769	S-65-32759	Limb.
11	S-65-34768	S-65-32758	18	1834	Southeast Atlantic Ocean off Congo coast.
12	S-65-34767	S-65-32757	18	1834	Do.
*13	S-65-34766	S-65-32764	18-19	1943	Florida Keys; Cape Sable; Everglades National Park.
14	S-65-34764	S-65-32763	19	1944	Florida Straits; Grand Bahama Bank.
*15	S-65-34763	S-65-32762	19	1944	Andros Island, Bahamas.
*16	S-65-34762	S-65-32761	19	1945	Great Exuma Island, Bahamas.
*17	S-65-34761	S-65-32765	19	1945	Acklins and Crooked Island, Bahamas.
18	S-65-34760	S-65-32766	Clouds.
19	Blank.
20	S-65-34759	S-65-32767	Clouds.
21	S-65-34758	S-65-32768	20	2224	Pacific Ocean north of Marcus Island.
22	S-65-34757	S-65-32769	20	2225	Do.
23	S-65-34756	S-65-32770	20	2225	Do.
24	S-65-34755	S-65-32771	20	2226	Do.
*25	S-65-34754	S-65-32772	20	2226	Do.
*26	S-65-34753	S-65-32773	20	2227	Do.
*27	S-65-34752	S-65-32774	20	2227	Do.
*28	S-65-34751	S-65-32775	20	2228	Do.
*29	S-65-34750	S-65-32776	20	2228	Do.
*30	S-65-34749	S-65-32777	20	2247	Coast of Mexico (Jalisco-Colima).
31	S-65-34748	S-65-32778	20	2247	Coast of Mexico (Manzanillo to Acapulco).
*32	S-65-34747	S-65-32779	20	2249	Coast of Central America and Mexico.

Frame	NASA/MSC color No.	NASA/MSC B. & W. No.	Orbit	G.m.t.	Location
JUNE 5, 1965					
33	S-65-34746	S-65-32780	21	0012	Pacific Ocean east of Hawaii.
34	S-65-34745	S-65-32781	21	0013	Pacific Ocean southeast of Hawaii.
35	S-65-34744	S-65-32782	21	0013	Do.
*36	S-65-34743	S-65-32783	21	0014	Do.
37	S-65-34742	S-65-32784	21	0015	Do.
38	S-65-34741	S-65-32785	21	0015	Do.
39	S-65-34740	S-65-32786	21	0016	Do.
40	S-65-34738	S-65-32787	21	0017	Pacific Ocean off Mexico; storm Victoria.
41	S-65-34736	S-65-32788	21	0018	Do.
42	S-65-34739	S-65-32789	21	0019	Pacific Ocean west of Galapagos Islands.
43	S-65-34735	S-65-32790	21	0019	Do.
*44	S-65-34737	S-65-32791	21	0020	Do.
45					Blank.
46	S-65-34734	S-65-32792			Clouds.
47	S-65-34733	S-65-32793			Do.
48	S-65-34732	S-65-32794	23	0252	Himalaya Mountains, Tibet; Burma.
49	S-65-34731	S-65-32795	23	0259	Typhoon Carla off Japan.
50	S-65-34730	S-65-32796	23	0309	Pacific Ocean east of Wake Island.
51	S-65-34729	S-65-32797	23	0310	Do.
52	S-65-34728	S-65-32798	23	0311	Do.
53	S-65-34727	S-65-32799	23	0412	Do.
*54	S-65-34726	S-65-32800	24	0413	Southwest Saudi Arabia; Yeman.
55	S-65-34847	S-65-32801	24	0414	Southwest Saudi Arabia, seif dunes.
*56	S-65-34765	S-65-32802	24	0415	Do.

End of roll.

MAGAZINE NO. 6

*1	S-65-34778	S-65-32814	25	0524	Chad and Libya; Plateau D'Erdebe area.
*2	S-65-34779	S-65-32813	25	0544	Nile River; Sudan; Wadi Halfa area.
*3	S-65-34780	S-65-32812	25	0544	Nile River; United Arab Republic; Sudan.
*4	S-65-34781	S-65-32811	25	0545	Southeast United Arab Republic; Eastern Desert.
*5	S-65-34782	S-65-32810	25	0545	Do.
*6	S-65-34783	S-65-32809	25	0545	Southeast United Arab Republic; Red Sea.
*7	S-65-34784	S-65-32808	25	0546	Southeast United Arab Republic; Red Sea; Ras Banas.
8	S-65-34785	S-65-32807	25	0548	Saudi Arabia and Iraq.
*9	S-65-34786	S-65-32806	25		Mainland China, Hunan Province; Hsiang River.
*10	S-65-34787	S-65-32805	25		Mainland China, Southeast Hunan Province.
11					Blank.
12					Blank.

End of roll (camera magazine jammed).

MAGAZINE NO. 8

*1	S-65-34671	S-65-32908	32	1741	Baja California, Mexico; Todos Santos Bay.
*2	S-65-34672	S-65-32909	32	1741	Northern Baja California; Colorado River.
*3	S-65-34673	S-65-32910	32	1741	Baja California; mouth of Colorado River; Sonora Desert.
*4	S-65-34674	S-65-32911	32	1741	Sonora Desert; mouth of Colorado River.
*5	S-65-34675	S-65-32904	32	1742	Cerro del Pinacate; Sonora, Mexico.
*6	S-65-34676	S-65-32905	32	1742	Do.
*7	S-65-34677	S-65-32906	32	1742	Sonora, Mexico; Arizona.
*8	S-65-34678	S-65-32907	32	1742	Kitt Peak Observatory, Arizona.
*9	S-65-34679	S-65-32900	32	1742	Southern Arizona.
*10	S-65-34680	S-65-32901	32	1742	Do.
*11	S-65-34681	S-65-32902	32	1742	San Pedro Valley, Arizona.
*12	S-65-34682	S-65-32903	32	1742	Willcox Dry Lake, southeast Arizona.
*13	S-65-34683	S-65-32896	32	1743	Willcox Dry Lake, Chiracahua Mountains, Arizona.
*14	S-65-34684	S-65-32897	32	1743	Arizona; New Mexico.
*15	S-65-34685	S-65-32898	32	1743	Do.
*16	S-65-34686	S-65-32899	32	1743	Southwestern New Mexico; northern Chihuahua.
*17	S-65-34687	S-65-32892	32	1743	Do.
*18	S-65-34688	S-65-32893	32	1743	Southern New Mexico; northern Chihuahua.
*19	S-65-34689	S-65-32894	32	1743	South central New Mexico; northern Chihuahua.
*20	S-65-34690	S-65-32895	32	1743	South New Mexico; Chihuahua.
*21	S-65-34691	S-65-32888	32	1743	South New Mexico; El Paso, Texas; Chihuahua.
*22	S-65-34692	S-65-32889	32	1744	South New Mexico; west Texas; Chihuahua.
*23	S-65-34693	S-65-32890	32	1744	Do.
*24	S-65-34694	S-65-32891	32	1744	Do.
*25	S-65-34695	S-65-32884	32	1744	Do.
*26	S-65-34696	S-65-32885	32	1744	Do.
*27	S-65-34697	S-65-32886	32	1744	New Mexico; Texas; Chihuahua.
*28	S-65-34698	S-65-32887	32	1744	Texas, Rio Grande and Pecos River Valley.

Frame	NASA/MSC color No.	NASA/MSC B. & W. No.	Orbit	G.m.t.	Location
*29	S-65-34699	S-65-32880	32	1744	Texas, Red Bluff Lake.
*30	S-65-34700	S-65-32881	32	1744	Texas, Toyah Basin.
*31	S-65-34701	S-65-32882	32	1745	West Texas, Permian Basin.
*32	S-65-34702	S-65-32883	32	1745	Texas, Midland-Odessa area.
*33	S-65-34703	S-65-32876	32	1745	Do.
*34	S-65-34704	S-65-32877	32	1745	Do.
*35	S-65-34705	S-65-32878	32	1745	Texas, Edwards Plateau.
*36	S-65-34706	S-65-32879	32	1745	Do.
*37	S-65-34707	S-65-32872	32	1745	San Angelo, Texas.
*38	S-65-34708	S-65-32873	32	1745	Texas, San Angelo-Sweetwater area.
*39	S-65-34709	S-65-32874	32	1745	Texas, Abilene.
40	S-65-34710	S-65-32875	32	1748	West Florida; south Alabama.
41	S-65-34711	S-65-32868	32	1748	Do.
*42	S-65-34712	S-65-32869	32	1748	West Florida; Alabama; Georgia.
43	S-65-34713	S-65-32870	32	1749	West Florida; Gulf of Mexico.
44	S-65-34714	S-65-32871	32-33	1749	Northeast Florida, Jacksonville.
45	S-65-34715	S-65-32864	33	1750	Central Florida, Cape Kennedy.
46	S-65-34716	S-65-32865	33	1750	Do.
*47	S-65-34717	S-65-32866	33	1750	Do.
48	S-65-34718	S-65-32867	33	1750	North Florida along Gulf Coast.
49	S-65-34719	S-65-32860	33	1751	Do.
50	S-65-34720	S-65-32861	33	1751	South Florida; Bahamas; Cuba.
51	S-65-34721	S-65-32862	33	1751	North Florida along Gulf Coast.
52	S-65-34722	S-65-32863	33	1752	South tip of Florida; Bahamas; Cuba.
53	S-65-34723	S-65-32857	33	1752	Bahamas; Cuba.
54	S-65-34724	S-65-32858	33	1752	Do.
55	S-65-34725	S-65-32859	33	1752	Atlantic Ocean east of Bahamas.

End of roll.

MAGAZINE NO. 9

JUNE 6, 1965

1	S-65-34827	S-65-32854	40	0526	Kuwait; Iraq; Iran.
2	S-65-34826	S-65-32855	40		Underexposed.
3					Blank.
4	S-65-34825	S-65-32856	40		Overexposed.
5	S-65-34824	S-65-32850	40		Limb.
6	S-65-34823	S-65-32851	40		Do.
7	S-65-34822	S-65-32852	40		Tibet, northeast of Lhasa.
8	S-65-34821	S-65-32853	40		Clouds.
9					Blank.
10	S-65-34820	S-65-32846	41		Clouds.
11	S-65-34819	S-65-32847	41		Underexposed.
12	S-65-34818	S-65-32848	41		Libyan Desert of Chad, Sudan, and Libya.
13	S-65-34817	S-65-32849			Limb.
14	S-65-34816	S-65-32842			Do.
15	S-65-34815	S-65-32843			Do.
16	S-65-34814	S-65-32844			Limb and sunrise.
17	S-65-34813	S-65-32845	44	1124	Off west coast of North Africa.
18	S-65-34812	S-65-32838	44	1124	Do.
19	S-65-34811	S-65-32839	44	1124	Do.
*20	S-65-34810	S-65-32840	44	1127	Morocco; Hamada du Dra area.
*21	S-65-34809	S-65-32841	44	1127	Morocco; Algeria; Hamada du Dra area.
22	S-65-34808	S-65-32834	44	1127	Do.
*23	S-65-34807	S-65-32835	44	1128	Southwest Algeria; Sahara Desert.
*24	S-65-34806	S-65-32837	44	1128	Southwest Algeria; Northern Mauritania.
25	S-65-34805	S-65-32838	44	1128	Central Algeria; Sahara Desert.
26	S-65-34804	S-65-32831	44	1128	Central Algeria; Grand Erg Occidental.
*27	S-65-34803	S-65-32832	44	1128	Central Algeria; Assedjrad Escarpment.
*28	S-65-34802	S-65-32833	44	1128	Eastern Algeria; Grand Erg Oriental.
*29	S-65-34801	S-65-32834	44	1130	South central Algeria; Erg Afarag.
30	S-65-34800	S-65-32826	44	1130	South central Algeria; Sahara Desert.
*31	S-65-34799	S-65-32827	44	1130	South central Algeria; Ahaggar massif.
32	S-65-34798	S-65-32828	45	1311	South Sudan; Equatorial Province.
33	S-65-34797	S-65-32829	45	1313	Sudan; Ethiopia; Kenya; Lake Rudolph.
*34	S-65-34796	S-65-32822	45	1313	Do.
35	S-65-34795	S-65-32823	45	1315	Somali Republic coast north of Mogadishu.
36	S-65-34794	S-65-32824	45		Clouds.
37	S-65-34793	S-65-32825	45		Do.
38	S-65-34792	S-65-32818	45	1415	North Florida; south Georgia.
*39	S-65-34791	S-65-32819	45	1416	Georgia; South Carolina coast.
40	S-65-34790	S-65-32820	46	1417	Do.
41	S-65-34789	S-65-32821	46	1418	Carolina coast; Cape Lookout Cape Fear.
42	S-65-36153	S-65-32816	46	1434	Richat Structure; Mauritania (overexposed).
43	S-65-36154	S-65-32817	46	1434	Do.

End of roll.

GEMINI V

Frame	NASA/MSC color No.	NASA/MSC B. & W. No.	Orbit	G.m.t.	Location
MAGAZINE NO. 3					
1	S-65-45672		1	Radar Evaluation Pod.
2	S-65-45673		1	Do.
*3	S-65-45674	S-65-45432	2	1702	Clouds off coast of Baja California.
4	S-65-45675	S-65-45433	2	1703	Clouds off coast of Baja California; Isla Cedros.
*5	S-65-45676	S-65-45434	2	1703	Baja California, Mexico; Gulf of California.
6	S-65-45677	S-65-45435	2	1705	Clouds; New Mexico.
7	S-65-45678	S-65-45436	2	1711	Clouds; Gulf Coast area.
*8	S-65-45679	S-65-45437	2	1711	Do.
9	S-65-45680	S-65-45438	2	1712	Florida.
*10	S-65-45681	S-65-45439	3	1717	Thunderstorms southeast of Bermuda.
*11	S-65-45682	S-65-45440	3	1718	Clouds southeast of Bermuda.
12	S-65-45683	S-65-45441	Astronaut C. Conrad (inside spacecraft).
13	S-65-45684	S-65-45442	Overexposed.
14	S-65-45685	S-65-45443	4	1851	East end of Hispaniola (Dominican Republic).
*15	S-65-45686	S-65-45444	4	1855	Clouds over Atlantic east of Lesser Antilles.
*16	S-65-45687	S-65-45445	4	1856	Clouds off coast of French Guiana.
*17	S-65-45688	S-65-45446	4	1856	French Guiana.
18	S-65-45689	S-65-45447	4	1857	Brazil; French Guiana.
19	S-65-45690	S-65-45448	4	1908	Limb off west coast of Africa.
*20	S-65-45691	S-65-45449	4	1954	Clouds near Wake Island.
21	S-65-45692	S-65-45450	4	1954	Do.
22	S-65-45693	S-65-45451	4	1955	Do.
23	S-65-45694	S-65-45452	4	2004	Do.
*24	S-65-45695	S-65-45453	4	2005	Pacific Ocean north of Hawaii; wake of ship.
*25	S-65-45696	S-65-45454	4	2012	Coast of California; San Luis Obispo.
*26	S-65-45697	S-65-45455	4	2014	Clouds near Baja California, Mexico; Guadalupe Island.
*27	S-65-45698	S-65-45456	4	2014	Do.
*28	S-65-45699	S-65-45457	4	2015	Baja California, Mexico; Point Eugenia.
*29	S-65-45700	S-65-45458	4	2015	Gulf of California; Angel de la Guarda Island.
*30	S-65-45701	S-65-45459	4	2015	Gulf of California; Sonora Coast; Tiburon Island.
*31	S-65-45702	S-65-45460	4	2015	Do.
*32	S-65-45703	S-65-45461	4	2016	Baja California and Sonora, Mexico.
*33	S-65-45704	S-65-45462	4	2021	Yucatan Peninsula; Gulf of Honduras.
*34	S-65-45705	S-65-45463	4	2022	Honduras-Nicaragua; Cape Gracias a Dios.
AUGUST 22, 1965					
35	S-65-45706	S-65-45464	6	0047	Limb; sunrise south of India.
36	S-65-45707	S-65-45465	6	0055	North end of Luzon, Philippines.
37	S-65-45708	S-65-45466	6	0055	Do.
*38	S-65-45709	S-65-45467	8	0157	Himalaya Mountains; Tibet; Nepal; Bhutan; Sikkim.
*39	S-65-45710	S-65-45468	8	0158	Himalaya Mountains; Tibet; Bhutan.
*40	S-65-45711	S-65-45469	8	0158	Tibet; Nam Tsho (lake) in center.
41	S-65-45712	S-65-45470	8	0159	Tibet; Tsinghai Province.
*42	S-65-45713	S-65-45471	8	0200	Mainland China, Szechwan, Shensi, and Hupeh Provinces.
*43	S-65-45714	S-65-45472	8	0203	Mainland China, Shensi Province near Hsian.
*44	S-65-45715	S-65-45473	8	0208	Japan, Honshu and Kyushu Islands.
*45	S-65-45716	S-65-45474	9	0330	Saudi Arabia, Empty Quarter, seif dunes.
*46	S-65-45717	S-65-45475	9	0441	Mainland China, Szechwan Province.
*47	S-65-45718	S-65-45476	9	0441	Do.
*48	S-65-45719	S-65-45477	9	0441	Do.
*49	S-65-45720	S-65-45478	10	0459	Iran, east of Shiraz; Persepolis ruins.
*50	S-65-45721	S-65-45479	10	0459	Iran, east of Shiraz, near Saidabad.
*51	S-65-45722	S-65-45480	10	0500	Iran, north of Kerman.
*52	S-65-45723	S-65-45481	10	0501	Iran, Dasht-e-Lut Desert.
53	S-65-45724	S-65-45482	10	0506	Tibet; clouds.
*54	S-65-45725	S-65-45483	10	0512	Mainland China, Hupah and Hunan Provinces.
*55	S-65-45726	S-65-45484	11	0628	Libyan Desert.
*56	S-65-45727	S-65-45485	11	0628	Do.
*57	S-65-45728	S-65-45486	11	0635	Afghanistan-Iran frontier area.
*58	S-65-45729	S-65-45487	11	0636	Afghanistan, Kajaki Reservoir.
*59	S-65-45730	S-65-45488	11	0647	Do.
*60	S-65-45731	S-65-45489	11	0649	Mainland China, Kwangtung-Kwangsi Provinces.
*61	S-65-45732	S-65-45490	11	0651	Luzon Island, Philippines; Lingayen Gulf.
*62	S-65-45733	S-65-45491	12	0756	Southern Luzon Island.
*63	S-65-45734	S-65-45492	12	0758	Southern Algeria, Erg Chech.

End of roll.

<i>Frome</i>	<i>NASA/MSC color No.</i>	<i>NASA/MSC B. & W. No.</i>	<i>Orbit</i>	<i>G.m.t.</i>	<i>Location</i>
MAGAZINE NO. 1					
*1	S-65-45735	S-65-45370	13	0927	Canary Islands; Fuerteventura Island.
*2	S-65-45736	S-65-45371	13	0937	Alexandria; Nile Delta.
*3	S-65-45737	S-65-45372	14	1103	Straits of Gibraltar; Morocco; Spain.
4	S-65-45738	S-65-45373	14	1106	Coast of Libya; Tunisia.
*5	S-65-45739	S-65-45374	15	1238	Morocco; Ras Rhir; Agadir.
6	S-65-45740	S-65-45375	15	1238	Do.
*7	S-65-45741	S-65-45376	16	1525	Chihuahua, Mexico.
*8	S-65-45742	S-65-45377	16	1525	Chihuahua, Mexico; Laguna de Encinillas.
*9	S-65-45743	S-65-45378	16	1526	Do.
10	S-65-45744	S-65-45379	16	1526	Chihuahua, Mexico.
*11	S-65-45745	S-65-45380	16	1527	Gulf of Mexico; Texas; Tamulipas.
*12	S-65-45746	S-65-45381	17	1531	Florida.
*13	S-65-45747	S-65-45382	17	1659	California; Salton Sea; Imperial Valley.
*14	S-65-45748	S-65-45383	17	1659	Do.
*15	S-65-45749	S-65-45384	17	1700	Arizona; Gila River Valley.
*16	S-65-45750	S-65-45385	17	1701	Arizona; Tucson vicinity.
*17	S-65-45751	S-65-45386	17	1701	Arizona; New Mexico; Willcox Dry Lake.
*18	S-65-45752	S-65-45387	17	1702	Texas; New Mexico; Chihuahua, Mexico.
*19	S-65-45753	S-65-45388	18	1707	Clouds over Florida.
*20	S-65-45754	S-65-45389	18	1707	Do.
21	S-65-45755	S-65-45390	18	1712	Clouds, southeast of Bermuda.
*22	S-65-45756	S-65-45391	18	1838	Florida, Cape Kennedy.
23	S-65-45757	S-65-45392	18	1838	Miami and eastern Florida.
*24	S-65-45758	S-65-45393	19	1838	St. Augustine and Miami, Florida.
*25	S-65-45759	S-65-45394	19	1839	Andros Island, Bahamas.
*26	S-65-45760	S-65-45395	19	1839	Great Bahama Bank; Tongue of the Ocean.
27	S-65-45761	S-65-45396	19	1839	Bahama Islands, Crooked, Acklins, and Long Islands.
28	S-65-45762	S-65-45397	19	1840	Bahama Islands, Grand Turk; Caicos group.
29	S-65-45763	S-65-45398	19	2004	Baja California, Mexico.
*30	S-65-45764	S-65-45399	19	2004	Do.
*31	S-65-45765	S-65-45400	19	2009	Campeche, Mexico; Laguna de Terminos.
32	S-65-45766	S-65-45401	19	2009	British Honduras; Gulf of Honduras.
33	S-65-45767	S-65-45402	20	2016	Clouds over Caribbean Sea.

AUGUST 23, 1965

*34	S-65-45768	S-65-45403	23	0158	Mainland China, mouth of Yangtze River.
*35	S-65-45769	S-65-45404	23	0159	Japan, Honshu Island.
*36	S-65-45770	S-65-45405	23	0201	Typhoon Lucy near Japan.
*37	S-65-45771	S-65-45406	23	0201	Do.
38	S-65-45772	S-65-45407	25	0449	Afghanistan; Pakistan.
*39	S-65-45773	S-65-45408	25	0449	Do.
40	S-65-45774	S-65-45409	25	0458	Mainland China; Tibet Highlands.
41	S-65-45775	S-65-45410	25	0458	Mainland China; Tibet Highlands; Himalayas.
42	S-65-45776	S-65-45411	25	0458	Do.
*43	S-65-45777	S-65-45412	25	0505	Taiwan; Formosa Straits.
*44	S-65-45778	S-65-45413	28	0929	United Arab Republic; Nile Delta; Cairo.
45	S-65-45779	S-65-45414	32	1543	Clouds over Gulf of Guinea.
46	S-65-45780	S-65-45415	32	1543	Do.
*47	S-65-45781	S-65-45416	32	1543	Do.
48	S-65-45782	S-65-45417	33	1822	Texas, between Laredo and Uvalde.
*49	S-65-45783	S-65-45418	33	1826	Florida, Jacksonville to Key West.
50	S-65-45784	S-65-45419	34	1827	Cuba, Camaguey Province.
*51	S-65-45785	S-65-45420	34	1827	Do.
52	S-65-45786	S-65-45421	34	1828	Cuba, Oriente Province.
*53	S-65-45787	S-65-45422	34	1958	Sonora, Mexico; Gulf of California.
54	S-65-45788	S-65-45423	34	2001	Gulf of Mexico; Texas; Tamaulipas, Mexico.
55	S-65-45789	S-65-45424	35	2133	Tropical storm Doreen in Pacific.
*56	S-65-45790	S-65-45425	35	2133	Do.
*57	S-65-45791	S-65-45426	35	2147	Coast of Peru; Paracus Peninsula.
*58	S-65-45792	S-65-45427	36	2150	Bolivia-Peru; Lake Titicaca.
59	S-65-45793	S-65-45428	36	2150	Do.
*60	S-65-45794	S-65-45429	36	2150	Do.

AUGUST 24, 1965

61	S-65-45795	S-65-45430	41	0625	Iran; Iraq.
62	S-65-45796	S-65-45431	41	0625	Clouds over Mainland China.

End of roll.

Frame	NASA/MSC color No.	NASA/MSC B. & W. No.	Orbit	G.m.t.	Location
MAGAZINE NO. 4					
*1	S-65-45603	S-65-45301	42	0749	India; Gulf of Kutch; City of Jamnagar.
*2	S-65-45604	S-65-45302	42	0758	Sumatra; Lingga and Bintan Islands.
*3	S-65-45605	S-65-45303	43	0913	Algeria; Mediterranean Sea; Balearic Islands.
4	S-65-45606	S-65-45304	43	0920	United Arab Republic; Nile Delta; Suez Canal.
*5	S-65-45607	S-65-45305	43	0920	United Arab Republic; Nile Delta.
*6	S-65-45608	S-65-45306	43	0921	United Arab Republic; Red Sea; Saudi Arabia.
*7	S-65-45609	S-65-45307	45	1336	Pensacola-Mobile area.
8	S-65-45610	S-65-45308			Inside Gemini V spacecraft.
9	S-65-45611	S-65-45309			Out of focus.
10	S-65-45612	S-65-45310	46	2135	Bolivia; Lake Poopo.
*11	S-65-45613	S-65-45311	46	2135	Do.
12	S-65-45614	S-65-45312	51	2243	Clouds.
13	S-65-45615	S-65-45313	51	2248	Clouds over the Hawaiian Islands.
*14	S-65-45616	S-65-45314	51	2248	Hawaiian Islands.

AUGUST 25, 1965

*15	S-65-45617	S-65-45315	55	0431	Iran; Iraq; Valley of Tigris River.
*16	S-65-45618	S-65-45316	55	0433	Northern Afghanistan (dust storm).
17	S-65-45619	S-65-45317	55	0433	Do.
*18	S-65-45620	S-65-45318	55	0434	Afghanistan; Band-i-Amir River.
*19	S-65-45621	S-65-45319	55	0436	Pakistan, south of Rawalpindi.
20	S-65-45622	S-65-45320	55	0437	India; Tibet; Himalaya Mountains.
21	S-65-45623	S-65-45321	55	0439	Tibet, southwest of Lhasa; Himalaya Mountains.
*22	S-65-45624	S-65-45322	55	0439	Do.
*23	S-65-45625	S-65-45323	55	0446	Mainland China, Kwangtung Province; Hong Kong.
*24	S-65-45626	S-65-45324	58	0918	United Arab Republic; Nile Valley.
25	S-65-45627	S-65-45325	62	1637	Florida.
*26	S-65-45628	S-65-45326	63	1639	Cuba, Camaguey Province; Caribbean Sea.
27	S-65-45629	S-65-45327	63	1639	Bahamas, Great Exuma and Long Islands.
28	S-65-45630	S-65-45328	63	1640	Cuba, Oriente Province; Jamaica; Hispaniola.
*29	S-65-45631	S-65-45329	63	1803	California, Los Angeles; Salton Sea.
30	S-65-45632	S-65-45330	63	1811	Mexico; Yucatan; Gulf of Mexico.
31	S-65-45633	S-65-45331	63	1812	Mexico; Yucatan; British Honduras.
32	S-65-45634	S-65-45332	63	1814	Honduras; Nicaragua; Caribbean coast.
33	S-65-45635	S-65-45333	65	2056	Inside spacecraft (out of focus).
34	S-65-45636	S-65-45334	65	2109	Out of focus—storm.
35	S-65-45637	S-65-45335	65	2110	Do.
36	S-65-45638	S-65-45336	66	2130	Out of focus.
37	S-65-45639	S-65-45337	66	2130	Double exposure.
38	S-65-45640	S-65-45338	66	2225	Japan, Kyushu and Honshu Islands.
*39	S-65-45641	S-65-45339	67	2359	Japan, Ise Wan; Port of Nagoya.
40	S-65-45642	S-65-45340	67	2359	Do.

AUGUST 26, 1965

41	S-65-45643	S-65-45341	68	0121	India; Tibet; Zaskar Range; northeast of Dehra-Dun.
*42	S-65-45644	S-65-45342	68	0121	India; Tibet; Nepal.
*43	S-65-45645	S-65-45343	68	0122	Tibet; headwaters of Brahmaputra River.
44	S-65-45646	S-65-45344	68	0122	Tibet; Nepal.
*45	S-65-45647	S-65-45345	69	0249	Iran; Dasht-e-Lut Desert; Kerman City.
*46	S-65-45648	S-65-45346	69	0250	Mainland China; India; Kashmir; Pakistan.
*47	S-65-45649	S-65-45347	69	0250	Tibet and Kashmir; Chang Chenmo Range.
*48	S-65-45650	S-65-45348	69	0303	Mainland China coast, Fukien Province; Futun-Min River.
49	S-65-45651	S-65-45349	70	0435	Northeast New Guinea; Bismarck Sea.
*50	S-65-45652	S-65-45350	71	0624	Cape York Peninsula, Australia.
51	S-65-45653	S-65-45351	71	0624	Do.
52	S-65-45654	S-65-45352	71	0625	Do.
53	S-65-45655	S-65-45353	71	0625	Do.
54	S-65-45656	S-65-45354	71	0626	Do.
55	S-65-45657	S-65-45355	71	0626	Do.
56	S-65-45658	S-65-45356	71	0626	Do.
57	S-65-45659	S-65-45357			Underexposed—Sunset on clouds.
58	S-65-45660	S-65-45358			Do.
59	S-65-45661	S-65-45359	72	0729	Crete; Turkey; Greece.
*60	S-65-45662	S-65-45360	72	0731	Saudi Arabia; Persian Gulf.
61	S-65-45663	S-65-45361	72	0757	Underexposed.
*62	S-65-45664	S-65-45362	74	1025	Morocco; Cape Rhir; Agadir.
*63	S-65-45665	S-65-45363	74	1025	Morocco south of Agadir; Spanish Ifni.
*64	S-65-45666	S-65-45364	74	1027	Sahara Desert; border of Morocco and Algeria.

Frame	NASA/MSC color No.	NASA/MSC B. & W. No.	Orbit	G.m.t.	Location
65	S-65-45667	S-65-45365	74	1027	Algeria; Sahara Desert.
*66	S-65-45668	S-65-45366	76	1334	Cape Verde Islands.
*67	S-65-45669	S-65-45367	76	1334	Do.
*68	S-65-45670	S-65-45368	77	1614	Rio Grande; El Paso, Texas; Juarez, Mexico.
*69	S-65-45671	S-65-45369	77	1614	Do.

End of roll.

MAGAZINE NO. 2

1	S-65-45547	S-65-45493	81	2234	Clouds near Hawaii.
---	------------	------------	----	------	---------------------

AUGUST 27, 1965

*2	S-65-45548	S-65-45493	83	0125	Tropical storm near Ponape Island.
3	S-65-45549	S-65-45494	83	0131	Bikini Atoll in the Marshall Islands.
*4	S-65-45550	S-65-45496	83	0131	Rongelap Atoll in the Marshall Islands.
5	S-65-45551	S-65-45497	83	0148	Urine Drop.
*6	S-65-45552	S-65-45497	84	0220	Afghanistan; Pakistan.
*7	S-65-45553	S-65-45498	85	0418	Storm south of Philippine Islands.
8	S-65-45554	S-65-45499	85	0525	Crete; Rhodes; Turkey; Greece.
9	S-65-45555	S-65-45500	86	0526	Cyprus; Turkey in background.
*10	S-65-45556	S-65-45501	86	0526	Cyprus; Turkey; Syria.
11	S-65-45557	S-65-45502	86	0612	Northern Territory, Australia; Gulf of Carpentaria.
*12	S-65-45558	S-65-45503	86	0612	Queensland, Australia; Gulf of Carpentaria.
*13	S-65-45559	S-65-45504	86	0614	Queensland, Australia; Shoalwater Bay.
*14	S-65-45560	S-65-45505	86	0615	Queensland, Australia; Capricorn Island.
*15	S-65-45561	S-65-45506	87	0654	Morocco; Atlas Mountains.
*16	S-65-45562	S-65-45507	87	0656	Northern Algeria.
*17	S-65-45563	S-65-45508	87	0658	Libya; Tripoli.
*18	S-65-45564	S-65-45509	87	0710	Red Sea; Saudi Arabia.
*19	S-65-45565	S-65-45510	87	0710	Saudi Arabia interior.
*20	S-65-45566	S-65-45511	87	0711	Do.
*21	S-65-45567	S-65-45512	87	0745	Northern Territory; Australia; McDonnell Range.
*22	S-65-45568	S-65-45513	87	0747	Do.
*23	S-65-45569	S-65-45514	88	0852	Sahara Desert; Chad; Sudan; United Arab Republic.
24	S-65-45570	S-65-45515	90	1204	Tanzania; Lake Tanganyika.
25	S-65-45571	S-65-45516	90	1205	Tanzania; Zambia; Lake Tanganyika.
*26	S-65-45572	S-65-45517	90	1205	Tanzania; Zambia; Malawi.
27	S-65-45573	S-65-45518	90	1207	Mozambique coast.
*28	S-65-45574	S-65-45519	90	1210	Madagascar west coast.
*29	S-65-45575	S-65-45520	90	1215	Clouds southeast of Madagascar.
*30	S-65-45576	S-65-45521	90	1215	Do.
31	S-65-45577	S-65-45522	90	1310	Jacksonville, Florida; Georgia.
*32	S-65-45578	S-65-45523	92	1510	South-West Africa; Cape Cross.
*33	S-65-45579	S-65-45524	92	1510	South-West Africa; Walvis Bay.
*34	S-65-45580	S-65-45525	92	1511	South-West Africa; Windhoek area.
*35	S-65-45581	S-65-45526	92	1511	Do.
*36	S-65-45582	S-65-45527	92	1551	Mexico, Chihuahua; Sonora.
*37	S-65-45583	S-65-45528	92	1553	Texas; Laredo-Uvalde area.
38	S-65-45584	S-65-45529	92	1554	Texas; Gulf Coast.
*39	S-65-45585	S-65-45530	93	1743	Baja California, Mexico; Gulf of California.
*40	S-65-45586	S-65-45531	93	1743	Baja California, Mexico.
41	S-65-45587	S-65-45532	93	1749	Zodiacal light study.
42	S-65-45588				Overexposed.
43	S-65-45589				Do.
44	S-65-45590				Do.
45	S-65-45591				Do.
46	S-65-45592				Do.

AUGUST 28, 1965

47	S-65-45593	S-65-45537	106	1300	Angola; Tandave River.
48	S-65-45594	S-65-45538	106	1300	Angola; Cuito River.
49	S-65-45595	S-65-45539	106	1300	Angola; western Zambia.
50	S-65-45596	S-65-45540	106	1301	Do.
51	S-65-45597	S-65-45541	106	1301	Western Zambia; Southern Rhodesia.
52	S-65-45598	S-65-45542	106	1301	Zambia; Rhodesia; Mozambique.
53	S-65-45599	S-65-45543	106	1404	Cape Kennedy, Florida.
*54	S-65-45600	S-65-45544	107	1432	South Africa; South-West Africa.
55	S-65-45601	S-65-45545	107	1434	South Africa.
56	S-65-45602	S-65-45546			Sky study; moon.

End of roll.

